0269

EASTERN OFFICER BASIN

GEOLOGY AND HYDROCARBON POTENTIAL

D.I. Gravestock & A. Sansome

South Australian Department of Mines & Energy

VOLUME 1

TEXT

July 1994

Envelope 8591

NEOPROTE.ROZ

CONTENTS

CONTENTS VOLUME 2

Figures

Tables

Enclosures

CONTENTS VOLUME 3

Appendices

EASTERN OFFICER BASIN GEOLOGY AND HYDROCARBON POTENTIAL

Introduction

During the 1960s the hydrocarbon potential of the 300 000 km^2 Officer Basin (100 000 km^2 in South Australia, Fig. 1) was compared favourably with the gas-productive Amadeus Basin in the Northern Territory (Logan, 1965; Webb, 1965). However this early optimism was followed by *fifteen years* of inactivity following the unsuccessful drilling of three wildcat wells.

Reasons for this astonishing oversight include:

- Devonian and older rocks which make up the Officer Basin had low perceived hydrocarbon potential despite Early Palaeozoic giant gas discoveries in the USSR (e.g. Markovo);
- gas discoveries in the Permian Cooper Basin in 1963 were sufficient to satisfy South Australian demand;
- oil discovered in the Cooper Basin in 1970 (600 km N of Adelaide) remained shut-in to 1983 awaiting favourable return on infrastructure investment;
- the Officer Basin is at least 1000 km northwest of Adelaide with restricted road access and scarce water supply;
- most of the Officer Basin in South Australia is within Aboriginal Lands, other parts are covered by conservation parks or are under Commonwealth control (former atomic test areas), compounding perceived access problems;
- exploration had been unsuccessful and,
- since 1986 the oil price has been unfavourable.
- 100 000 km^2 of sedimentary basin is 'too big' to explore from grass-roots level.

The observation by Devine (1975) that 'knowledge of the Officer Basin geology is still ~~to~~ so sketchy that any assessment of its petroleum potential must be more than usually speculative' remained valid until Comalco's exploration for the mineral trona and petroleum shed light on the easternmost part of the basin. Even today, however, large tracts remain unexplored. Comalco's initial mineral exploration effort and subsequently its petroleum search (1981-88) followed the discovery in 1979 of trona/shortite evaporite pseudomorphs and oil bleeds from vugs and fractures in stratigraphic well Byilkaoora-1 (Pitt *et al.*, 1980; McKirdy & Kantsler, 1980). Prior to 1980 only 2260 km of seismic recording and six wells (Emu-1, Birksgate-1, Munyarai-1, Officer-1, Wilkinson-1, Byilkaoora-1) made up the petroleum exploration effort in the east Officer Basin. Munyarai-1 was the only on-structure test and the drilled section to total depth (2899 m) was mistakenly thought to be Devonian.

Comalco and Amoco exploration in the 1980s clarified the stratigraphic position by confirming that the basin was filled primarily with Neoproterozoic to Ordovician sediments overlain in the Munyarai Trough by up to 2.5 km of Devonian (1000 m in Munyarai-1) and a thin veneer of Permian or Mesozoic (Brewer *et al.*, 1987; Womer *et al.*, 1987; Stainton *et al.*, 1988). Devine's (1975) suggestion that structures in the basin (including detachment due to salt flowage) could be analogous to those in the Amadeus Basin was proved (e.g. Stainton *et al.*, 1988; Thomas, 1990). The Amadeus Basin analogue led the Australian Geological Survey Organisation (AGSO) to record a seismic survey in the central and southern Officer Basin (Leven & Lindsay, 1992; Lindsay *et al.*, 1992; Gravestock & Lindsay, 1994) but no major anticlines were found. The survey nevertheless demonstrated that petroleum exploration could be resumed in both the Pitjantjatjara and Maralinga Aboriginal Land; it extended subsurface correlations and further defined salt and thrust structures. The extent of overthrusting near the eastern margin of the basin was not fully appreciated prior to a seismic survey by the South Australian Department of Mines and Energy (MESA) in 1993 (Mackie & Gravestock, 1993; Mackie, 1994), but it is now known that a number of thrust fronts extend for up to 100 km, striking northeast-southwest.

Following the allocation in 1992 of AUD 2 million to MESA for petroleum exploration a seismic survey of 378 km was recorded and processed, 140 km of existing seismic were reprocessed, and comprehensive geological reinterpretation of existing data were completed in 1993. This report is a presentation of geological information obtained to date.

GEOLOGICAL DATABASE

Separate reports

A number of studies have been completed; others are ongoing. Separate reports available from MESA are seismic interpretation (Thomas, 1990; Mackie & Gravestock, 1993; Mackie, 1994), preliminary burial history analysis (Moussavi-Harami, 1994), acritarch biostratigraphy (Zang, 1993 - see Appendix 3) and Devonian geology (Tucker, 1994).

Ongoing studies scheduled for completion in December 1994 include a source rock geochemical review (McKirdy, in prep.), apatite fission track paleothermometry and a comprehensive geohistory analysis (Moussavi-Harami, in prep.). The latter includes comprehensive listings of formation tops from water bores, petroleum, stratigraphic and mineral drillholes and seismic upholes. Two PhD theses (seismic analysis; source and reservoir potential of Ouldburra Formation) are being undertaken at the National Centre for Petroleum Geology & Geophysics in Adelaide. All company data (well completion reports, seismic sections) are open file and available from the Document Storage Centre at MESA. An aeromagnetic interpretation is being marketed by World Geoscience Corporation.

Data in this report

This report is in three volumes. The first contains the text, volume two includes figures, tables and enclosures; appendices are in volume three. Formation tops for all significant wells are listed in Table 1; well locations and seismic lines are shown on Enclosure 1A-D. Enclosures 2 to 12 display wireline logs from selected intervals in 18 wells. The logs include Gamma Ray (GR), Sonic (DT), Bulk Density (RHOB) and Neutron (NEUT in either limestone porosity units or counts per second). The location and number of core analysis, source rock, acritarch and XRD samples are also listed on each enclosure in 10 metre interval groupings. The actual depth (driller) for each sample is listed with the raw data in Appendices 1 and 2. A preprint of acritarch studies of the Alinya Formation is provided in Appendix 3. Acritarchs from other formations indicated on Enclosures 2 to 12 form the basis for a biostratigraphic zonation (Zang, 1993, in prep.) which is incorporated in the correlations used in the text.

NEOPROTEROZOIC COVER SEQUENCES

Neoproterozoic cover above crystalline basement in the central and eastern Officer Basin forms a northwest thickening sedimentary prism which is tectonically truncated at the northern basin margin by Devonian thrust faults. The succession comprises several sequence sets (supersequences) which can be correlated with those in the Adelaide fold belt, although they are thicker and more complete in the latter region. The sequence set nomenclature introduced for the Adelaide Geosyncline by Preiss (1993) is followed here to highlight correlated units and to indicate where major breaks in the stratigraphic succession occur. Rock units in the eastern Officer Basin are shown in Figure 2.

Sequence set I: Willouran

Basal cover rocks in the Officer Basin comprise the Willouran **Pindyin Sandstone** and **Alinya Formation.** These units outcrop in the Streich Hills and North and South Pindyin Hills, close to the northern basin margin and have been intersected in Giles-1, 300 km southeast on the Murnaroo Platform (Fig. 1).

Equivalents in the Western Officer Basin are the Townsend Quartzite, Lefroy and Browne beds (Townson, 1985); in the Amadeus Basin - the Heavitree Quartzite and Bitter Springs Formation. Presumed correlatives in the basal Neoproterozoic (Willouran) rift zone in the Peake and Denison Inliers are the Younghusband Conglomerate and Coominaree Dolomite (Ambrose *et al.*, 1981; Preiss, 1993). The Coominaree Dolomite is overlain by basalts, redbeds and pyroclastics of the Cadlareena Volcanics. Part of this succession (volcanics underlain by evaporitic redbeds and stromatolitic dolomite) was intersected in Manya 5 on the eastern edge of the Marla Overthrust Zone. Amygdaloidal basalt and redbeds in Mallabie-1 in the far south of the basin may also correlate with this basal cover sequence. Tholeiitic basalts are also known from the Bitter Springs Formation.

The facies, reservoir and source rock characteristics of the Pindyin Sandstone and Alinya Formation are described in later sections. This basal clastic cover sequence appears to be widespread in the subsurface on seismic evidence. It forms the major detachment for the propagation of thrust faults and is the source of salt in halokinetic structures. Facies changes from clastic source and reservoir units to tight carbonates and volcanics is presumed to be restricted to the region east of the Marla Overthrust Zone. Zang (in prep.), however, considers this volcanic and carbonate succession to be older than the Pindyin Sandstone and Alinya Formation which he assigns to the Torrensian.

Sequence sets II to VI: Torrensian

Throughout most of the Officer Basin there is a major disconformity between sequence set I (Willouran) and sequence set XI (Marinoan). Only in the northeastern and eastern basin regions are there any presumed remnants of Torrensian rocks. Interbedded sandstone and siltstone between 712 m and 814.5 m (T.D.) in Nicholson-2, east of the Marla Overthrust Zone, is presumed to be an equivalent of the Nilpinna beds and/or War Loan beds which outcrop in the Peake and Denison Inliers (Ambrose *et al.* 1981). A partly disrupted (?diapiric) succession in Nicholson-1A probably represents the same interval. The Hussar-Kanpa-Steptoe sequence in the western Officer Basin may be correlative (Townson, 1985).

Sequence set VII: Sturtian

Neoproterozoic glacigene sediments of the **Chambers Bluff Tillite** occur in fault-bounded outcrops in the Chambers Bluff, Wantapella Anticline and Granite Downs areas on the northern overthrust margin of the basin (Wilson, 1952; Krieg, 1973; Preiss, 1993). Fresh basalt erratics in the glaciofluvial diamictite may be from eroded Cadlareena Volcanics of sequence set I, but black oolitic chert pebbles attributed by Major (1973a) to the Pindyin Sandstone and Wright Hill beds (see below) are most likely to have come from eroded remnants of Torrensian rocks which reach several kilometres thickness in the Peake and Denison Inliers 480 km to the southeast.

Glaciofluvial sandstone, glaciolacustrine sand and siltstone, and diamictite in Nicholson 2 correlate with the Chambers Bluff Tillite and its equivalent the Calthorinna Tillite/Unnamed sandstone interval in the Peake and Denison Inliers (Ambrose *et al.*, 1981; Preiss, 1993). Western Officer Basin equivalents are the Lupton and Turkey Hill beds which also unconformably overlie Torrensian or older rocks (Townson, 1985).

Sturtian glacigene rocks in the Adelaide Geosyncline have been studied intensively (e.g. Preiss, 1987); equivalent strata in the Amadeus Basin comprise the Areyonga Formation and equivalents which unconformably overlie the Bitter Springs Formation.

The unconformity between Sturtian glacials and rift-related Torrensian/Willouran rocks is not restricted to the Officer Basin but appears sufficiently widespread to indicate major continental uplift - which also probably triggered glaciation. As a consequence the rocks of the basal sequence I have not been so deeply buried that their source and reservoir potential on the Murnaroo Platform can be dismissed.

Sequence sets VIII to X: upper Sturtian-basal Marinoan

With two possible exceptions, sedimentary rocks in this part of the succession are either not represented or not recognised in the Officer Basin. The first is a 3.9 m thick granule sandstone (Whyalla Sandstone equivalent, ? sequence set X) which has only been intersected to date in Giles-1 on the Murnaroo Platform (Stainton *et al.*, 1988; Preiss, 1993). This fluvial sandstone is interpreted by Sukanta (1993) as an incised valley fill and it may thus belong at the base of the overlying sequence set.

The second exception is the **Wantapella Volcanics,** a fault-bounded tholeiitic basalt suite 190 m thick at Chambers Bluff and in the Wantapella anticline (Krieg, 1973; Preiss, 1993). The volcanics occur above the Chambers Bluff Tillite and beneath shale and sandstone of presumed Marinoan age.

Sequence set XI: early-middle Marinoan

For the first time in the Neoproterozoic an alluvial clastic apron spread across the Murnaroo Platform signalling the onset of more or less continuous subsidence. Braided fluvial clastics of the **Tarlina Sandstone** and equivalent coarse gravelly sandstones accumulated on the Murnaroo Platform, reaching a thickness of 167 m in Giles-1; they have been intersected in Lake Maurice West-1 and Lake Maurice East-1, 160 km southwest of Giles-1. In the southern region equivalents of the Tarlina Sandstone unconformably overlie crystalline basement (Sukanta, 1993; Sukanta *et al.*, in prep. 1994a).

A relatively thick (192 m) wedge of **Meramangye Formation** overlies the Tarlina Sandstone conformably in Giles-1. This unit intertongues with the lower Murnaroo Formation to the southwest and presumably thickens into the Munyarai Trough. Marla-9 reached total depth in the Meramangye Formation confirming the presence of this unit in the Marla Overthrust Zone.

The Meramangye Formation was deposited in the highstand of the first major marine transgression into the Officer Basin. Its equivalent in the Adelaide fold belt is the Brachina Formation. The name Meramangye Formation replaces 'Giles Mudstone' used by Sukanta (1993).

The Murnaroo Formation conformably overlies Meramangye Formation on the basinward margin of the Murnaroo Platform; further south the formation intertongues with and replaces the Meramangye, and rests directly on the Tarlina Sandstone (Gatehouse *et al.*, 1986; Brewer *et al.*, 1987; Sukanta, 1993). The thickest intersection of the Murnaroo Formation is 581 m in Lake Maurice East-1 on the southern Murnaroo Platform. In Giles-1, 150 km to the northeast the formation is 186 m thick as it is partly replaced by Meramangye Formation.

In the Marla Overthrust Zone the Murnaroo Formation is represented by a 4.3 m interval in Marla-9 and possibly by more than 600 m of cross-bedded sandstone which unconformably overlies the Cadlareena Volcanics (sequence set I) in Manya-5.

Acritarchs recovered in outcrop and in Birksgate-1 from the upper **Wright Hill beds** suggest, by superposition, that the lower Wright Hill beds in the Birksgate sub-basin correlate with the Tarlina Sandstone, Meramangye and Murnaroo Formations (Zang, 1993). The 3400 m thick Wright Hill beds (Major, 1973b) are presumed to overlie the Alinya Formation disconformably (contact covered) and to?onlap (?low angle thrust) crystalline basement west of the Purndu Hills. Zang considers the basal 3 units (basal 900 m) to correspond more or less to the Tarlina Sandstone-Murnaroo Formation sequence. Birksgate-1 terminated before these beds were reached.

Formations of sequence set XI in the central and eastern Officer Basin were connected across the Stuart Shelf to the Adelaide Geosyncline (lower Wilpena Group) for the first time, initiating what was to become a nearly continuous terminal Proterozoic succession. However a stratigraphic break is still evident in the Peake and Denison Inliers (Ambrose *et al.*, 1981) and the western Officer Basin (Townson, 1985).

Sequence set XII: late Marinoan (Ediacaran)

Marine sedimentation characterises the late Marinoan sequences. Seismic stratigraphy, acritarchs and two major geological events - the Acraman meteorite impact and submarine canyon incision - provide firm correlations with the Stuart Shelf and Adelaide Geosyncline (Stainton *et al.*, 1988; Thomas, 1990; Wallace *et al.*, 1990, Sukanta *et al.*, 1991; Zang, in prep.).

Stratigraphic nomenclature varies with locality based on the density of outcrop, drillhole and seismic data. Comalco seismic and drilling on the Murnaroo Platform provide the best control; nomenclature in this region follows Sukanta (1993) and Sukanta *et al.* (in prep.b) with an additional unit recognised by Zang (pers. comm., 1994).

The lower **Ungoolya Group** comprises formations which pre-date the canyon forming event. The basal unit, **Dey-Dey Mudstone**, unconformably overlies the Murnaroo Formation and reaches a thickness of 290 m in Munta-1 on the northern Murnaroo Platform. It thins southward but is still present in Lake Maurice West-1 (147 m), and drillhole OBD-12 (23 m) in the Tallaringa Trough. The meteorite impact layer occurs in this unit in Lake Maurice West-1, Observatory Hill-1 and in Marla-9. **Dey-Dey Mudstone** is equivalent to the Bunyeroo Formation in the Adelaide Geosyncline and Unit 4 of the Wright Hill beds.

The conformably overlying **Karlaya Limestone**, 13-110 m thick, can be traced north seismically to Munyarai-1 (2580-2645 m, logger) in the Munyarai Trough, and northeast into the Manya Trough where it has not yet been drilled. It is overlain by **Wilari Dolomite**, restricted to the southern Murnaroo Platform and by **Leemurra Mudstone** which extends north and northeast into the Munyarai and Manya Troughs. Thickness of the Leemurra Mudstone ranges from 63 m to 337 m in drillholes but the unit is incomplete on the Murnaroo Platform, being overlain by either the canyon erosion surface or by Cambrian sediments. The deepest known canyon incision northeast of Giles-1 has cut down to the level of the Meramangye Formation.

Several carbonates are interbedded with the **Leemurra Mudstone** in Marla-9, Munta-1 and Munyarai-1. In these drillholes this succession is referred to here as 'Leemurra Mudstone/Karlaya Limestone equivalent'. The succession correlates with Units 5 and 6 of the Wright Hill beds and with the Wonoka Formation in the Adelaide Geosyncline.

Zang (in prep.) has recognised an additional unit at the top of the lower Ungoolya Group, above Leemurra Mudstone/Karlaya Limestone equivalent and below the canyon unconformity. This informally named **'Munyarai Unit'** has been intersected only in Munyarai-1 (1707-2155m) but is widespread on seismic sections and is locally incised by channels.

The Munyarai Unit comprises muddy siltstone and appears to be a fine-grained equivalent of the sandy Unit 7 of the Wright Hill beds.

The upper Ungoolya group comprises the submarine canyon fill and two other units. The deepest canyon incision is interpreted to locally downcut over 600 m (seismic line 84-0190; Sukanta *et al.*, 1991). It is one of a canyon pair situated 15 to 30 km northeast of Giles-1. Another canyon pair is mapped 15-20 km north of Munta-1; all four canyons define a northwest paleoslope into the Munyarai Trough (Thomas, 1990). The canyon fill was fully cored in Munta-1, Karlaya-1 and Ungoolya-1, while Lairu-1 reached total depth within the canyon fill. Sukanta (1993) has described two canyon fill sequences separated by an exposure surface.

The **lower canyon sequence** comprises sand-matrix conglomerate (clasts chaotic to imbricated, of mudstone, sandstone, micritic and oolitic limestone), sandstone and mudstone in varying proportions in different drillholes. The top of the lower sequence was deposited in a tidal flat environment.

The **upper canyon sequence** is composed of transgressive to highstand deeper water turbidite mudstone and interbedded shelf limestone and mudstone in varying proportions between wells. The conformably overlying **Munta Limestone** and **Mena Mudstone** onlap the canyon margins and reach their greatest preserved thickness in Ungoolya-1 and Lairu-1. The upper Ungoolya Group is absent due to non-deposition or uplift and erosion from Giles-1 southward.

Historically the term **Rodda beds** has been applied to outcropping equivalents in the northeastern Officer Basin (Krieg, 1973). The Rodda beds are at least 3.7 km thick (outcrop and drillhole) at the type section 10 km northwest of Mount Johns, and have been slightly metamorphosed (Preiss & Krieg, 1992). Although slumped units with abundant carbonate blocks indicate slope deposition, there is no direct correlation with Ungoolya Group canyons owing to the fault bounded Rodda type locality and lack of seismic tie. The Rodda beds are essentially caught up in the Marla Overthrust Zone and correlation with the Munyarai Trough and Murnaroo Platform requires additional seismic or reprocessing of poor quality 1970s data.

In the Birksgate sub-basin, the Ungoolya Group equivalents comprise the outcropping upper Wright Hill beds and the **Punkerri Sandstone** which contains Ediacaran metazoan impressions (Major, 1974). The upper Wright Hill and possibly the Punkerri Sandstone were intersected in Birksgate-1 (Zang, in prep.). An earlier correlation of the Birksgate intersection with the Cambrian (Gravestock & Hibburt, 1991) is incorrect.

The Ungoolya Group correlates with the upper Wilpena Group in the Adelaide Geosyncline (Sukanta *et al.*, 1991) and possibly in part with the Babbagoola beds in the western Officer Basin (Townson, 1985). Ediacaran fossil remains from the Stirling Range Formation north of Albany (Cruse *et al.*, 1993) indicate correlation with the Punkerri Sandstone and also suggest that equivalent units may be widespread in the subsurface of the central Officer Basin. The upper Ungoolya Group and its lateral equivalents comprise the youngest Precambrian sequence in the Officer Basin.

NEOPROTEROZOIC BASIN ARCHITECTURE

Studies in the past six years (Stainton *et al.*, 1988; Thomas, 1990; Sukanta, 1993; Sukanta *et al.*, 1991; Zang, 1993; in prep.; Zang & McKirdy, 1993) have transformed Neoproterozoic geology of the Officer Basin such that data can be integrated into a sketch of key elements of basin architecture. Thomas (1990) proposed four stages of basin evolution, his fourth and final stage being structural deformation of the Neoproterozoic during the Alice Springs Orogeny. Thomas envisaged the first stage to be the depositional phase of a sedimentary section of more or less uniform thickness. Stage 1 refers to deposition of the Willouran Pindyin Sandstone and Alinya Formation in the (present day) southern reaches of the Centralian Superbasin (Walter *et al.*, 1993). The Centralian Superbasin comprised the Officer, Amadeus, Ngalia, Georgina and Savory Basins before they were separated in the Ediacaran by the Petermann Ranges Orogeny.

However, as Torrensian and Sturtian rocks also occur on the north and east structural margins of the Officer Basin, there were several geologically significant events, which are poorly known, between Stage 1 and Stage 2. Stage 2 resulted from collapse of the sedimentary cover (Tarlina, Giles, Murnaroo units) above Alinya evaporites as a north-steepening gradient drove salt basinward. His stage 3 was related to growth of salt diapirs and creation of peripheral sinks. The conclusions of Thomas (1990) and Sukanta (1993) were based largely on study of the Comalco seismic grid and drillholes on the Murnaroo Platform and adjacent slope to Munyarai-1 in the basin. However, salt-related structures are confined to the area around Munta-1, Karlaya-1 and Ungoolya-1 and, although important, are localised features (S. Mackie, pers. comm., 1994).

Important questions e.g. Why are there submarine canyons? How did the Petermann Ranges Orogeny affect the basin? How did Neoproterozoic basin architecture control Cambrian deposition, require answers. At the present state of knowledge, the answers suggested here are speculative, but we can take a guess at the amount of sedimentary accommodation, and loss by erosion, in order to perform preliminary burial history analysis (Moussavi-Harami, 1994). Some general features of the basin and three stages of basin architecture are described below.

General features

The Willouran stage 1 sediments (Pindyin-Alinya) extend west to the Yowalga sub-basin and were very widespread (Figure 3). The Marinoan Officer Basin (stages 2 and 3) does not thicken north but thickens northwest. It is situated over the Fraser-Musgrave Orogen and has two margins (Appendix 3, fig. 2). The southeast margin borders the Gawler Craton. The northwest margin is ill-defined but is presumably a broad shelf reaching east from the Yilgarn Block to the Yowalga sub-basin where no thick Marinoan sequences are recorded.

The Musgrave Block was not elevated until the Petermann Ranges Orogeny and is not an element of basin architecture. Similarly the Nurrai Ridge between the Birksgate sub-basin and Munyarai Trough appears to have no topographic expression in the Neoproterozoic - at least near its southern limit where it was crossed by AGSO seismic line 4 (J. Leven, AGSO, pers. comm., 1993).

The Marinoan (stage 2 and 3) sedimentary fill is polarised. Sediments in the east (Munyarai Trough, Murnaroo Platform margin) are mudrocks with minor limestone and sandstone; those in the Birksgate sub-basin are sandstone and siltstone dominated with lesser mudstone and limestone.

Stage 1

As Thomas (1990) has shown, stage 1 deposition is characterised by only slight thickening from the Murnaroo Platform into the (not yet formed) Munyarai Trough. It is composed of two unconformity bounded sequences: the Pindyin-Alinya and Tarlina-Murnaroo sequences, separated by a break of about 110 My, partly represented by the Sturtian glacials and Torrensian shallow marine clastics and carbonates in the Peake and Denison Inliers (Fig. 2).

Since sediment thickness did not vary dramatically in either sequence (approx. 600 to 1200m) basin architecture was controlled by depositional facies rather than tectonic subsidence. The Officer was at that time a component of the Centralian Superbasin which also incorporated the Amadeus, Ngalia, Savory and Georgina Basins (Walter *et al.*, 1993).

Zang (Appendix 3) interprets the basal Pindyin-Alinya sequence as part of a saline supergiant with considerable source and reservoir potential. Sukanta's (1993) reconstructions of the overlying Tarlina-Murnaroo sequence incorporate an alluvial basal clastic wedge which passed into deltaic and marine transgressive muds and culminated in the Murnaroo Formation. Both stage 1 sequences are extensively faulted in the Munta area due to salt movement. This is expressed as an angular unconformity at the base of stage 2 (horizon F5, Thomas, 1990).

Stage 2

Extension related subsidence close to the Gawler Craton (Fig. 4A) led to differentiation of the Murnaroo Platform and Munyarai 'Deep' across the Ungoolya Hinge. The expression Munyarai 'Deep' is used to denote the basin's depocentre (the Munyarai Trough is a structural low imposed by the Alice Springs Orogeny). Nearly 1200m of lower (pre-canyon) Ungoolya Group sediments were intersected in Munyarai-1 which reached total depth without penetrating this sequence. More than 1000m were intersected in Munta-1, but only 935m of Ungoolya Group equivalents (Wright Hill beds, units 4 and 5) outcrop in the Birksgate sub-basin (Zang, 1993), thus the Basin is suggested to shelve in a northwest direction.

Water depth is difficult to gauge because of eustatic sea-level fluctuations (melting of Marinoan ice sheets), but the presence of siltstone and sandstone in the Birksgate sub-basin, and limestone and dolomite on the Murnaroo Platform, suggest shallow depths on the southeastern and northwestern margins and greater water depths in the Munyarai 'Deep' where mudstones dominate.

Stage 3

Reconstruction of Stage 3 basin architecture requires much guess work due to erosional loss of section during the Petermann Ranges Orogeny (see below). A current best guess is shown in Figure 4B. The extensional regime of stage 2 is replaced by one of mild but increasing compression leading to structural differentiation of the Murnaroo Platform into an inner shelf, mid-shelf ridge and outer shelf, and a westward shift of the depocentre to the Birksgate sub-basin.

Differentiation of the Murnaroo Platform

Thomas (1990) mapped two canyon pairs (Fig. 5): one pair east of Ungoolya-1 and a second pair between Munta-1 and Karlaya-1. Both pairs indicate a basinward paleoslope to the northwest suggesting the presence of two bathymetric levels - inner shelf and outer shelf. Incision of one of the inner canyon pairs exceeds 600m (Sukanta *et al.*, 1991) and both are considerably larger than the outer canyons. The inner and outer shelves strike northeast, parallel to the underlying Fraser-Musgrave Orogen. This being so, it is plausible to suggest that Rodda-2 intersected a canyon on the outer shelf, explaining the 760m of slump-folded siltstones in that drillhole (Preiss & Krieg, 1992). It is not known whether the 2700+m of additional, overlying Rodda beds in outcrop have been tectonically thickened. Preiss & Krieg (1992) suggest that upward coarsening reflects the impending Petermann Ranges Orogeny.

The great inner canyon incision, locally penetrating the entire lower Ungoolya Group and Murnaroo Formation points clearly to tectonic as well as eustatic control i.e. the inner shelf margin was uplifted. A mid-shelf ridge composed of keystone or pop-up structures is interpreted to have caused local uplifts of up to 1100m. Support for this value comes from Meramangye-1 in which the Cambrian Relief Sandstone unconformably overlies Meramangye Formation (Fig. 3).

Guesstimated restoration of section removed during the Petermann Ranges Orogeny amounts to 1000m in Munta-1 and 1200m in Giles-1, but Meramangye-1, between these drillholes, requires 2200m of section loss to account for the missing stratigraphy. This is too great to be accounted for by fault block rotation during salt withdrawal or by subsequent orogenesis. If 1100m are assigned to the Petermann Ranges Orogeny (reasonable given the position of Meramangye-1 between Giles-1 and Munta-1), then the remaining 1100m can most simply be ascribed to uplift which caused the canyon cutting event (N.B. some canyons at a slightly lower stratigraphic level in the northern Adelaide Geosyncline are more than 1 km deep, Christie-Blick *et al.*, 1990). Meramangye-1 is thus placed on a pop-up structure. Marla-9 similarly encountered thin, glauconitic, condensed sandstones of the Murnaroo Formation beneath the middle or upper Rodda beds, suggesting some form of long-lived structural elevation in that region. The positions of the Rodda-2 canyon and Marla-9 structure are shown 30 km northwest of present well positions on Figure 5 to account for later tectonic transport during the Alice Springs Orogeny.

Structures crossing the Manya Trough evident from gravity and the OF93 seismic data suggest additional uplifts on the mid-shelf ridge.

Shift of depocentre

Acritarchs and Ediacaran fossils (Major, 1974; Zang, 1993) permit correlation of younger sediments in the Birksgate sub-basin with the Wonoka Formation and Pound Subgroup of the Flinders Ranges. This correlation allows the thickness and nature of sediments formerly deposited in the upper Ungoolya Group (but lost during the Petermann Ranges Orogeny) to be estimated. A maximum erosional loss of 1 400 m is shown on Figure 4B but this is approximate. Moussavi-Harami (1994) has assumed a loss of 1 500 m for Munyarai-1 and 1000m for Giles-1 in his burial history analysis.

At least the upper part of the missing section is assumed to be sandstone by analogy with the more complete succession in the Birksgate sub-basin. Outcropping upper Wright Hill beds (units 6, 7) comprise 1565m of interbedded sandstone and limestone (Major, 1973b); in Birksgate-1, 794m of sandstone and limestone were drilled (Figs. 6,7). Above these beds are at least 1200m of Punkerri Sandstone with Ediacaran fossil impressions near the top (Major, 1974). Aggregate thickness exceeds 2800m, indicating clearly that the greatest subsidence in Stage 3 was in the Birksgate sub-basin (Fig. 4B).

Limestone in the upper Wright Hill beds is partly oolitic (mistaken for an Early Cambrian (C2.2) transgression by Gravestock & Hibburt, 1991); the Punkerri Sandstone is characterised by scour surfaces, current lineations, ripple marks and mudstone intraclasts, pointing to a shallow marine, high energy depositional environment.

The equivalent Pound Subgroup in the Adelaide Geosyncline passes distally into muddy Billy Springs Formation (e.g. Pell *et al.*, 1993). If we assume a sandy to muddy, proximal-distal relationship between the Punkerri Sandstone and restored upper Ungoolya Group, it is reasonable to assume that the greatest water depth was in the vicinity of basin floor fans at the mouths of submarine canyons. Although no paleocurrent measurements have been recorded, the likely source of Punkerri Sandstone was from the west. Thus the Birksgate (? and Waigen) sub-basin was a depocentre for shallow marine sandstone and the Munyarai 'Deep' accommodated muddy, deeper marine sediments.

Petermann Ranges Orogeny

An idea of how little is known of the effects of the Petermann Ranges Orogeny in South Australia can be gauged from Drexel *et al.* (1993) The Geology of South Australia. Volume 1, The Precambrian. The index devotes 3 page references to the Petermann Ranges Orogeny compared with 48 page references to the Delamerian Orogeny; the latter to be described in Volume 2, The Phanerozoic. With reference to the Adelaide Geosyncline, Parker (*in* Drexel *et al.*, 1993, p.21) states:

'Cambrian sedimentation was separated from Adelaidean sedimentation by a widespread hiatus. This disconformity, and breaks within the Cambrian succession, record sea-level falls and, possibly, minor epeirogenic movements, but no significant changes in deformation or basin structure'.

In contrast, the Gondwanan significance of the same hiatus, i.e. the Petermann Ranges Orogeny, is concisely summed up by Powell *et al.* (1993, p.32):

'After the Marinoan glaciation in Australia, dextral shear between northern and southern Australia along the Paterson-Petermann Ranges Orogen between 600 and 550Ma, broke-up the continuity of the Central Australian basins and led, at the beginning of the Ediacaran, to renewed rifting, possibly reflecting the latest Neoproterozoic continental breakup that formed the eastern margin of Laurentia'.

It is true that Cambrian architecture in the Adelaide Geosyncline was inherited from its Marinoan precursor (Gravestock & Hibburt, 1991); likewise, Cambrian architecture of the Officer Basin is also inherited (see below). It is also true that no major folding or metamorphic events are recorded in the cover rocks, thus the first statement is largely correct. However, the tectonic movements in the Officer Basin and Adelaide Geosyncline are of greater than minor magnitude because they caused partial basin inversion, removed up to 1.5 km of sedimentary rock and produced early structures capable of trapping hydrocarbons.

An estimate of the geometry and severity of Officer Basin uplift in the late Ediacaran is shown on Figure 8. Using the dextral shear along the Paterson-Petermann Ranges Orogen as a guide, two centres of maximum uplift in a strike-slip **Z** configuration are centred on the Musgrave Block in the north and the Coompana Block-west Gawler Craton in the south. Two kilometres or more of Neoproterozoic strata may have been removed at these centres. An offset on the Musgrave Block along the Ferdinand Fault is suggested from observations of Petermann Ranges reactivation by Major and Conor (*in* Drexel *et al.*, 1993). East-west faults and shear zones e.g. Mann, Hinckley, Wintiginnia, the Levenger and Moorilyanna 'Grabens' (Major & Conor, 1993, fig. 5.30), and the Bitchera Ridge, control the architecture on the northern arm of the **Z**. Effects on the southern arm are impossible to gauge in the Officer Basin but the more distant Polda Trough on the southern Gawler Craton has an east-west geometry and may be a product of this shear (Nelson *et al.*, 1986).

Uplift of the sedimentary cover appears to have ranged from less than 500m to more than 1000m along the 'shank' of the **Z**, parallel to the main basin trend. The dextral strike-slip configuration of the Petermann Ranges orogenic uplift in the Officer Basin is a local aspect of Veevers' (1984) 'epi-Adelaidean shear' which also shaped the Amadeus and Ngalia Basins. The geometry of uplifts in the Adelaide Geosyncline, evident on seismic sections, has yet to be determined.

The Petermann Ranges Orogeny was probably heralded by the early uplifts that produced the mid-shelf ridge and submarine canyons in stage 3 of Officer Basin development. The Levenger and Moorilyanna 'Grabens' on the eastern Musgrave Block are interpreted here as releasing bend basins formed as a result of dextral shear. The **Moorilyanna Formation** comprises 300m of conglomerate with well rounded basement clasts followed by 200m of coarse arkosic grit. The **Levenger Formation**, in a fault-bounded trough 150 km to the west, is shale, siltstone, arkose and arkosic pebble conglomerate 15500m thick (Major, 1973c). The thickness, if correct, implies a strongly progradational syntectonic origin. Thus, by the end of the Petermann Ranges Orogeny a new geometry was imposed on the northeast Officer Basin.

CAMBRIAN COVER SEQUENCES

Stratigraphy

Uplift and erosion resulting from the Petermann Ranges Orogeny spanned approximately 20 m.y. across the Neoproterozoic-Cambrian boundary. A section across the east Officer Basin (Fig. 2) illustrates the distribution of Neoproterozoic and Cambrian sedimentary and volcanic rocks and their bounding unconformities.

Renewed subsidence was greatest along the former Marinoan inner-outer shelf creating a depression, known as the **Manya Trough**, which accommodated the oldest Cambrian sediments of the Marla Group (Benbow, 1982). The Manya Trough was connected via the Wintinna-Boorthanna Troughs in the east and the Eringa Trough in the northeast, to the major Early Cambrian depositional systems of the Amadeus, Warburton and Arrowie Basins. These contained predominantly marine rocks on the Pacific seaboard of Gondwana, whereas deposition in the Manya Trough region was epeiric (Gravestock & Hibburt, 1991).

The oldest Cambrian formation, **Relief Sandstone** (Brewer *et al.*, 1987) is up to 168m thick (if correctly identified in Manya-5) and disconformably overlies either formations of the Ungoolya Group, Meramangye or Murnaroo Formation.

Figure 3 illustrates the likelihood that much of the Relief Sandstone could be recycled Punkerri Sandstone. No fossils have been found in the Relief which was deposited in aeolian, fluvial and tidal settings (Gaughan & Warren, 1990).

The lower part of the conformably overlying **Ouldburra Formation** (Brewer *et al.*, 1987) is a cyclic suite of halite-carbonate-siliciclastic units deposited in isolated salinas on a shallow marine to subaerially exposed sandy mudflat which extended southwest into the Tallaringa Trough (Dunster, 1987). The richest oil-prone source rocks in the Ouldburra Formation have been intersected in three wells in the Tallaringa Trough, namely Wilkinson-1, Duval KD-1 and KD-2A. The main part of the Ouldburra Formation comprises interbedded muddy limestone, dolostone, sandstone and anhydrite. These record 'sawtooth' epeiric sea transgressive-regressive parasequences in which trilobites and archaeocyaths are preserved, pointing to a middle Early Cambrian age (Botomian). The upper Ouldburra Formation is a regressive redbed-carbonate sabkha deposited as renewed rifting, and tectono-eustatic sea level fall, dramatically altered the geometry of the Arrowie and Stansbury Basins east of the Gawler Craton. The thickness of the formation ranged from 140m to at least 1100m and is the main contributor to the isopach shown on Figure 9.

As a result, non-marine conditions prevailed as the relatively widespread **Observatory Hill Formation** (Wopfner, 1969) was deposited conformably above the Ouldburra or Relief, and disconformably above the Ungoolya Group in the Manya and Munyarai Troughs. The lower unit, informally named the 'Cadney Park Formation' is up to 400m thick and is seismically mappable. It comprises red, sandy to calcareous siltstone with occasional conglomerates deposited in a distal fan to ephemeral lake environment. The remainder of the Observatory Hill Formation alternates between redbed, fluvial and alkaline playa lake environments in which three lacustrine complexes are recorded (White & Youngs, 1980; Southgate & Henry, 1984; Southgate *et al.*, 1989 Brewer *et al.*, 1987). The alkaline playa facies yielded the first oil shows from Byilkaoora-1 (Pitt *et al.*, 1980; McKirdy & Kantsler, 1980) and was Comalco's primary target for the evaporite mineral trona in the Marla Overthrust Zone.

In the Mount Johns Range and in Byilkaoora-1 the playa facies intertongues with alluvial fan conglomerate and sandstone of the **Wallatinna Formation** which attests to renewed tectonic activity on the Musgrave Block (Benbow, 1982). A cycle of fluvial to lacustrine sedimentation followed with deposition of the conformably overlying **Arcoeillinna Sandstone** (Benbow, 1982) which has numerous, thin mudstone interbeds (see Sandstone Reservoirs below) and the disconformably overlying but localised **Mount Johns Conglomerate** (Krieg, 1973).

The widespread, seismically mappable **Apamurra Formation** (Benbow, 1982) is composed of marine-tidal flat, calcareous to sandy mudstone with trilobite trace fossils. It is a potential seal above Arcoeillinna or older reservoirs. Total thickness of the 'Cadney Park'-Apamurra sediment package is estimated to have been up to 1000m (Fig 10).

The conformably overlying **Trainor Hill Sandstone** and **Wirrildar beds** (Krieg, 1973; Major, 1973a), are the upper units of the Marla Group; the latter unit overlying the Punkerri in the Birksgate sub-basin (Figs. 2,3). A separate isopach, illustrated in Figure 11, is restored to remove the effects of Delamerian (Late Cambrian) erosion and to show the former great thickness of these units: at least 420m (perhaps 1000m) in the Mount Johns range and ?2700m in the Birksgate sub-basin where it is gently folded (Major, 1973a).

The Trainor Hill Sandstone is composed of cross-bedded fine grained feldspathic sandstone with desiccation cracks and worm trails in lower units, while upper levels contain herringbone crossbeds in sandy dolostone. Wirrildar beds are of similar lithology. A tidal flat to marine-influenced deltaic environment is interpreted (Krieg, 1973). Age is presumed to be Middle Cambrian, comparable with the upper Lake Frome Group in the Arrowie Basin.

The Wirrildar beds underlie flat-lying **Kulyong Volcanics** with a slight angular unconformity (Major & Teluk, 1967; Major, 1968). Outcrop in the Birksgate sub-basin is only 3m thick but the equivalent **Table Hill Volcanics** in Western Australia exceed 100m in thickness and cover an area of 20 000 km^2 (outcrop, seismic and aeromagnetic data; Townson, 1985). The volcanics comprise a single tholeiitic basalt suite with a K-Ar minimum age of 485-475±20Ma and an Rb-Sr age of 570 Ma. The disconformably underlying Babbagoola beds in Western Australia may be Ediacaran or Early Cambrian. The volcanics are presumed here to be Late Cambrian in age and the slight folding of the underlying Wirrildar beds is ascribed to mild compression associated with terrane accretion and deformation in western New South Wales in Middle-Late Cambrian time.

Delamerian Orogeny

The tectonic shock of continental collision on the eastern side of the Gawler Craton at the end of the Cambrian was a consequence of global crustal plate movement. The collision caused the Delamerian Orogeny. Uplift, propagating northwest, affected the Peake and Denison Inliers and the northeast Officer Basin (Preiss, 1993). A contour map of suggested missing sediment removed (Fig. 12), illustrates a geometry that has begun to switch from the northeast Paterson orogenic trend to the northwest Delamerian orogenic trend. The amount of erosion is poorly constrained and dependent on the preservation of post-orogenic Ordovician rocks. At this stage it is a guesstimate. There is sufficient information, however, to calculate up to 800m of erosion in Manya-5 increasing eastward, and less than 400m of erosion in Munyarai-1, decreasing south and west. Cumulative subsidence at the end of the Delamerian Orogeny varies across the basin. Older potential source rocks such as the Alinya Formation and Dey-Dey Mudstone reached depths ranging from 1200m to 3000m and may thus have begun to generate oil. Younger potential source rocks such as the Ouldburra Formation and Observatory Hill Formation were at less than 1000m depth not yet mature.

Despite the abundance of metamorphic clasts in alluvial fan-fluvial conglomerate units such as the Wallatinna Formation and Mount Johns Conglomerate, the fact that these coarse clastics were localised indicates only minor uplifts of the Musgrave Block during the Cambrian. Thus although the Musgrave Block was elevated during the Petermann Ranges Orogeny, it was not elevated to any significant degree during the Delamerian Orogeny. This is evident from Ordovician isopach trends which thicken northward.

ORDOVICIAN AND DEVONIAN COVER SEQUENCES

Stratigraphy

Ordovician sediments deposited in the east Officer Basin were surprisingly thick, ranging from at least 400m in Ungoolya-1 to in excess of 1520m in outcrop at Cartu Hill (Packham & Webby, 1969). Seismic sections e.g. Amoco IP1-008 indicate northward thickening to 2000+m in the Munyarai Trough (Womer *et al.*, 1987). The Ordovician is interpreted to have reached 3000m or more over the eastern Musgrave Block (Fig. 13).

The Ordovician **'Munda Sequence'** (Krieg, 1973) comprises a number of siliciclastic units, the lowest of which is the **Byilkaoora Formation** (Benbow, 1982). This 15m thick unit, known only from the Mount Johns Range, disconformably overlies eroded Trainor Hill Sandstone and Mount Johns Conglomerate. Basal conglomerate with sandstone clasts (no igneous-metamorphic rocks) fines upward to clean, thinly bedded sandstone deposited in a tidal-marine setting.

The widespread **Mount Chandler Sandstone** (Krieg, 1973) disconformably overlies Trainor Hill Sandstone or older rocks (e.g. ?Relief Sandstone in Manya-5) and ranges from 167m in Munyarai-1 to more than 600m at Cartu Hill. It is composed of well-rounded and well-sorted, porous quartz sandstone with cross-bedding occasionally outlined by heavy minerals. A number of beds are disrupted by 'pipe-rock' bioturbation due to the abundance of vertical U-shaped burrows. The Mount Chandler Sandstone was deposited in a tide-dominated shoreface environment on the southern margin of the Ordovician Larapintine Sea (Webby, 1978).

The conformably overlying **Indulkana Shale** (Krieg, 1973) is a thin lenticular unit which has a maximum thickness of 60m in the Indulkana Range. It is composed of maroon and green shale with thin, flaggy sandstone beds bearing clay pellets near the base and top. Limestone lenses and micaceous silty sandstone occur locally. Packham & Webby (1969) recorded ripple marks, desiccation cracks and bioturbation in upper, sandy units. Rb-Sr whole rock ages of 460±15 Ma (Webb, 1978) and 438±10 Ma (Womer *et al.*, 1987) confirm a Late Ordovician age for the shale. Abrupt appearance of the Indulkana Shale, followed by interbedded sandstones in its upper levels, suggests a brief episode of marine flooding followed by regression.

The Indulkana Shale is overlain with apparent conformity by the **Blue Hills Sandstone** which reaches 800m in thickness (Krieg, 1973). It has a similar distribution to the Mount Chandler Sandstone in outcrops but is only 162m thick in Munyarai-1. Unlike the Mount Chandler, the Blue Hills Sandstone is kaolinitic; well sorted clean intervals alternate with pebbly beds. Cross-bedding (including trough crossbeds up to 3m thick), ripples, desiccation cracks, burrows and trilobite tracks, point to alternating marine, fluvial and aeolian environments of deposition. The **Cartu** and **Mintabie beds** are equivalents of the Blue Hills Sandstone and presumed to be Ordovician (Townsend, 1990). The Cartu beds are thinly bedded to laminated sandstone, siltstone and shale; Mintabie beds comprise upward coarsening parasequences of feldspathic, cross-bedded sandstone.

Total thickness of the Munda Sequence, when restored (Fig. 13), increased northward to an estimated 3 km on the eastern Musgrave Block. Silurian and Early Devonian sediments are unknown from the Officer Basin, suggesting a period of arrested subsidence or mild uplift known as the **Rodingan Movement**. Jackson *et al.*, (1984) estimate erosion of 1-3 km related to this movement in the northeast Amadeus Basin; Moussavi-Harami (1994) has assigned 500m of section loss in Munyarai-1, which is a best guess. However, overall, erosion is likely to have been of this order at the most. It is quite possible that the upper Blue Hills Sandstone may be Silurian in age since it strongly resembles the Mereenie Sandstone in the Amadeus Basin (R. Nicoll, AGSO, pers. comm. 1994).

Devonian sediments have been intersected only in Munyarai-1 which, at the time of drilling, was thought to have been in Devonian rocks to total depth (Continental Oil Co., 1969). However, Devonian rocks disconformably overlie Blue Hills Sandstone at 1018m in Munyarai-1. This well also intersected Ordovician to Neoproterozoic rocks from seismic and acritarch data (Womer *et al.*, 1987; Jenkins *et al.*, 1992; Zang in prep.). There are three facies present in the Devonian; 106m of planar to ripple laminated quartz sandstone of presumed Devonian age forms the basal unit. The middle unit is composed of 312m of olive green calcareous mudstone with fish fossils of Middle Devonian (Eifelian) age (Long *et al.*, 1988) although palynomorphs suggest a Late Devonian (Frasnian) age (Womer *et al.*, 1987). The uppermost unit is composed of red-brown gypsiferous mudrocks which may be equivalents of the Parke Siltstone in the Amadeus Basin. They are unfossiliferous; reports of Triassic spores (contaminants) are regarded as spurious.

The Devonian is faulted out west of Mintabie opal field and wedges out to the south between Munyarai-1 and Ungoolya-1. In this area, Devonian limits appear to be between -120 and -130 mgal on gravity maps (Tucker, in prep.), the north margin being terminated by thrust faults. From a cross-section provided by Milton & Parker (1973, fig 2; Fig 14) a depth of 2500m to base of Devonian is estimated in the northern Munyarai Trough on the footwall of the Everard Thrust.

Alice Springs Orogeny

Late Devonian deposition was halted by compression and uplift during the Alice Springs Orogeny. The present day north-deepening, north-thickening basin geometry is a result of northward basin tilt initiated by tectonically driven subsidence. The 3km of Ordovician rocks restored over the Musgrave Block suggest that subsidence increased during Ordovician time; which was also coincident with the onset of Canning Basin subsidence.

Estimates of crustal shortening in the Officer Basin range from 'at least 8 km' (Dunster, 1987), 18 km from restored seismic sections (J. Lindsay, pers. comm., 1994), to 55 km from gravity modelling (Milton & Parker, 1973).

Compressional structures, interpreted on the MESA OF93 seismic by Mackie (1994), indicate crustal shortening of the order of 20 km in the Marla Overthrust Zone.

The amount of uplift resulting from the Alice Springs Orogeny is difficult to gauge. There are no known syntectonic molasse deposits preserved on the Musgrave Block analogous to the Brewer Conglomerate of the Amadeus Basin (Jones, 1972), from which the height of advancing thrust fronts could be gauged. Vertical offsets on ramp anticlines are estimated to be around 2.5 km but whether this displacement is due entirely to the Alice Springs Orogeny is unknown. The major regional outcome of the Alice Springs Orogeny was northward basin tilt and burial, creating the northern sub-basins on the footwalls of the principal thrust sheets, the formation of compressional structures, and modification of structures formed during the Petermann Ranges Orogeny. Accelerated burial brought Cambrian source rocks to depths where oil could be generated.

PERMIAN AND YOUNGER COVER SEQUENCES

Stratigraphy

Recent mapping from seismic uphole and stratigraphic drillhole data by Shearer (1994) reveals three major features of the Permian:

- marine and non marine sediments are preserved in a northeast arc through the Tallaringa, Manya, Wintinna and Boorthanna Troughs;
- total Permian thickness, generally 100m to 400m, is greater in the troughs than over ridges; Permian is very thin to absent in the Marla Overthrust Zone;
- top of Permian below ground level is a structurally complex surface south and southeast of the Marla Overthrust Zone. Depth to top of Permian ranges from less than 20 to more than 200m and indicates fault reactivation at shallow depths.

Shearer's observations indicate that Devonian structures were still mildly active during the Permian or were subsequently reactivated. The complex top of Permian pattern suggests younger (?Tertiary) tectonism.

Discovery of organic-walled worm tubes in Officer-1 cuttings at 19.8m (65 ft) depth confirms a Permian age for sediments in this well. Identical tubes were found in upholes 14 and 19 drilled for the OF-93 seismic survey above the Stuart Range Formation (Boorthanna Formation of Gravestock, 1993). Their abundance in lithic sandstones in the upholes indicates the presence of a lower shoreface to shallow marine section which at maximum extent reached the Officer-1 location in the central Munyarai Trough. The underlying succession in that well consists of increasingly coarse sand, gravel and polymict conglomerate to the total depth drilled (183m). This is the reference section for the **Waitoona beds** (Krieg, 1973) hitherto thought to be Devonian. The lower, coarse clastic section is interpreted here as glaciofluvial outwash, suggesting an elevated land surface on the Musgrave Block (glacial upland) during the Early Permian.

Details of Permian and Mesozoic lithofacies in the general region are provided by Townsend (1976) and Moussavi-Harami (1994).

Vitrinite reflectance

Comalco undertook a coal exploration drilling programme of 8 holes in 1983 to evaluate the Permian Mount Toondina Formation (Bourke & Senapati, 1983). Coal and carbonaceous sandstone in cuttings in cuttings from Coalhole 3 (= Comalco hole 07201) and Coalhole 4 (= Comalco hole 07202), drilled 33 km east of Manya 4, were sampled for vitrinite reflectance and other data necessary for geohistory analysis. The results are presented in Appendix 2.

Mean maximum reflectance from 3 samples in the depth range 187 - 216 m is 0.33 to 0.37 per cent. These values differ markedly from MPI-derived, calculated vitrinite reflectance of at least 0.74 per cent from a sample at 196 m depth in Coalhole 3. This discrepancy is unresolved and warrants further study. Of interest is the presence of *Botryococcus*-related telaginite with possible *Tasmanites* (Appendix 2), leading to facies with oil shale potential.

SANDSTONE RESERVOIRS

Introduction

Seven sandstone formations with poor to excellent reservoir potential occur in the east Officer Basin. Five of these (Neoproterozoic Pindyin and Tarlina Sandstones and Murnaroo Formation; Cambrian Relief Sandstone and Arcoeillinna Sandstone) are sealed structurally and stratigraphically through most of their preserved subsurface extent; they only reach the surface on the southern Murnaroo Platform. The remaining units (Cambrian Trainor Hill Sandstone and Ordovician Mount Chandler Sandstone) outcrop in the Mount Johns Range-Cartu Hill area and both are locally eroded on elevated thrust slices. Thus they lack stratigraphic and structural seal locally. However, both formations occur at depth and there is some chance of both being sealed beneath overthrust hanging wallrocks.

To date not one of these reservoirs has been a primary target for petroleum.

Only four wells were sited such that sandstones may have been inside mapped closure when drilled: Giles-1 (Relief and Murnaroo), Karlaya-1 (Arcoeillinna), Ungoolya-1 (Arcoeillinna) and Munyarai-1 (Mount Chandler, Trainor Hill and Arcoeillinna). Structure contour maps are few and limited in area (near top Relief, Stainton *et al.*, 1988; near top Murnaroo, Thomas, 1990). The only detailed core study until now had been carried out by Gaughan (1989) and Gaughan & Warren (1990) on the Relief Sandstone.

Results of the present study of seven reservoirs are given below. A preliminary compaction curve is constructed from Relief Sandstone data. Appendix 1 contains routine core analysis and XRD data.

Carbonate and intraformational sandstone reservoirs of the Ouldburra Formation are being studied separately by M. Kamali at the National Centre for Petroleum Geology & Geophysics. Preliminary results (Kamali *et al.*, 1993) indicate locally excellent reservoir properties in both sandstones and dolomites.

Pindyin Sandstone

This oldest sandstone in the basin unconformably overlies basement and conformably underlies the Alinya Formation (a potential source rock). Outcrops in the Birksgate sub-basin are composed of quartzose-feldspathic, medium to coarse-grained sandstone with tabular and herringbone cross-beds and ripple marks. Environment is predominantly tidal (Major, 1973b). Pindyin Sandstone has only been intersected in Giles-1 where it consists of well sorted and well-rounded quartzose sandstone, with haematite rimmed grains. Illite-smectite clays occur in trace amounts; minor anhydrite and halite occur near the top of the unit. Environment is aeolian (Zang, in prep.).

Twelve samples from Giles-1 range from 3.8 to 22.5 per cent porosity, and permeability values reach 1538 md. The porosity-log permeability (phi log k) plot is linear (Fig. 15A). Calculated Vshale rarely exceeds 5 per cent and the Gamma Ray is generally between 20 and 40 api units (Fig. 16A). Wireline log porosity is readily calculated from the density log using a quartz matrix density of 2.65 gm cm^{-3}. The Pindyin Sandstone aeolian facies is the cleanest potential reservoir in the basin.

Tarlina Sandstone

Disconformably overlies the Alinya Formation and conformably underlies the Meramangye Formation, thus it is sandwiched between a potential source rock and an effective seal. Tarlina was cored in Giles-1 with an equivalent unit in SMD5002 (Lake Maurice East-1) on the southern Murnaroo Platform. Tarlina Sandstone is quartzose to feldspathic, massive fine to medium-grained and occasionally gritty. Clay content, chiefly mica-illite and smectite, is variable. Large mudclasts occur locally in slumped horizons which may be bank collapse features. Sukanta (1993) interprets a tidal flat environment becoming shallow marine near the top.

Twelve samples from Giles-1 range from 9 to 19.6 per cent porosity but with low permeabilities which average 1.0 md. The phi log k plot is clustered (Fig. 15B). Calculated Vshale is mainly 10 to 20 per cent with few values exceeding 30 per cent. Gamma Ray (Fig. 16B) is chiefly 60-90 api units reflecting the feldspar content. Scattered high values to 150 api are attributed to slumped mudclast horizons. Porosity from the wireline density log (quartz matrix) correlates reasonably well with measured values (Fig. 17E). The relatively low permeability values, despite good porosity, suggest that pore-bridging clays might be responsible.

Murnaroo Formation

This formation is widespread on the Murnaroo Platform (up to 580 m thick) and extends to the Marla area where it was fully cored in Manya-5 (620m thick). It underlies the Dey-Dey Mudstone (a potential source rock), on the northwestern Murnaroo Platform margin and overlies Meramangye Formation or Tarlina Sandstone on the platform. In Manya-5 it unconformably overlies the Cadlareena Volcanics and is unconformably overlain by the Cambrian Relief Sandstone (see below). In Marla-9, however, a thin condensed tongue is interposed between Giles Mudstone and Rodda beds. It is thus favourably placed in several areas with respect to potential source and sealing units. Migrated hydrocarbons have been detected in Murnaroo-1 and Manya-5.

The Murnaroo Formation is laterally and vertically heterogeneous. It comprises cross-bedded to flat laminated, poorly sorted, fine to coarse-grained, often gritty and conglomeratic, feldspathic to arkosic sandstone. Mudrock interbeds, laminations and intraclasts are frequent. Heavy minerals, muscovite and biotite occur; glauconite is locally abundant as pellets (Gatehouse *et al.*, 1986).

Sukanta (1993), who has distinguished two members of the Murnaroo Formation, recognises local aeolian facies in the hinterland to the southwest, alluvial, channelised fluvial and tidal deposits progressing northward. Manya-5 contains mainly distal fan, sheet outwash and fluvial deposits. Glauconite in Marla-9 indicates marine shelf conditions close to the Murnaroo/Meramangye Formation transition.

As can be expected, the reservoir quality is variable, ranging from 3 to 20 per cent in the three sampled wells (Giles-1, Munta-1, Manya-5; n = 37). The phi log k plot (Fig. 15C) shows that permeability can reach 100 md and is generally greater than 0.2 md. Slightly higher porosity but lower permeability values in Manya-5 near the Marla Overthrust Zone, may be related to early cementation by illitic clay prior to burial.

On average, however, there is no great difference in porosity distribution between Manya-5 (Marla area) and the other two wells (Munta area, Fig. 17A). The Gamma Ray varies from 20 to 200 api probably due to the feldspar, mica, heavy mineral and glauconite composition.

Vshale ranges up to 40 per cent, but is predominantly 20 per cent or less (Fig. 16C). Air-mercury capillary pressure curves for three samples from Manya-5 are provided in Appendix 1. Based on limited data, permeability of the Murnaroo Formation increases to the southwest while porosity is a fairly uniform 14 to 15 per cent.

Relief Sandstone

This basal Cambrian sandstone (thickness approx. 100m) occurs in the Manya Trough where it disconformably overlies Ungoolya Group or older sediments. It is overlain conformably by and intertongues with the Ouldburra Formation (transitional, with halite interbeds) and is overlain conformably to disconformably by the Observatory Hill Formation. In Manya-5, however, the Relief is overlain by Ordovician Mount Chandler Sandstone due to Delamerian erosion. The position of the Relief Sandstone with respect to both source and seal thus varies considerably with locale. Migrated hydrocarbons (oil staining) have been detected in this formation in Observatory Hill-1 (Gatehouse & Hibburt, 1987).

The Relief is well sorted fine to medium-grained or poorly sorted fine to coarse-grained, slightly feldspathic sandstone with clay-coated grains (illite, variably corroded), quartz overgrowths (mainly in the Marla area) and carbonate cement (also mainly in the Marla area). Gaughan & Warren's (1990) observations indicate the order of cementation is: syntaxial quartz overgrowth, authigenic clay, dolomite/calcite and, finally, halite.

Gaughan & Warren also recognised eight subunits representing aeolian, fluvial and tidal depositional environments related to marine lowstand-highstand cycles. These are thought to be synchronous with sequences in the adjacent marine Ouldburra Formation (Gravestock & Hibburt, 1991). Upper levels of the Relief Sandstone in Manya-6 are transitional with halite-carbonate-siliciclastic cycles deposited in lower Ouldburra salinas (Dunster, 1987).

Porosity is secondary; Gaughan & Warren (1990) cited one sample from Observatory Hill-1 with a permeability of 4839 md. Here we report a sample from Giles-1 with a permeability of 8033md. Five samples from a 40m interval in this well exceed 1400 md. Five samples from Meramangye-1 over a 17m interval range from 2607 to 6297 md. In contrast, the Relief Sandstone in Manya-6 rarely exceeds 0.08 md.

A porosity histogram shown in Figure 17B (3 wells in Marla area, n =19: 2 wells in Munta area, n =25), clearly illustrates the bimodal porosity distribution pointed out by Gaughan & Warren (1990). The phi log k crossplot (Fig. 15D) illustrates the marked difference between the two regions. Two trends are evident: one related to high secondary porosity/low compaction in the Munta area; the other related to low secondary porosity/high compaction in the Marla area and related to Carboniferous depth of burial (see below).

The Gamma Ray (Giles-1) ranges chiefly from 20 to 80 api with scattered higher readings to 200 api. Vshale remains generally between 10 and 30 per cent (Fig. 16D). Vshale from neutron logs run in Marla, Manya and Byilkaoora wells is unreliable because of uncalibrated substandard logs. Examples of log quality are shown in Enclosures 2 to 12. Core to log correlation (Fig. 17F) is poor.

Relief Sandstone reservoir quality is superb in the Munta area due to high dissolution and low compaction effects. Porosity in the Marla area should not be written off. It is only dismal in deeply buried footwall situations. In hanging wall structures porosity reaches 13 per cent and permeability reaches 124 md. In Manya-5 adjacent to, but not within the Marla Overthrust Zone, porosity reaches 10.9 per cent with a permeability of 0.44 md. Commercial reservoirs may be found in both the Munta and Marla areas.

Arcoeillinna Sandstone

The Arcoeillinna Sandstone is a southwest thickening unit (60-170m) which extends through the Manya and Munyarai Troughs. It occurs between the Observatory Hill Formation (source rock) and the dolomitic mudstone seal of the Apamurra Formation. It is a fine to medium-grained, immature micaceous arkose with numerous muddy laminae and mudstone interbeds. Benbow (1982) gives the following sandstone composition: quartz (50%), potash feldspar (35%), minor plagioclase, lithic grains (10%) and muscovite and biotite (5%). His interbedded siltstone and claystone composition is: quartz and feldspar (35%), muscovite and biotite (35%), chlorite (30%). This heterogeneous composition is confirmed by XRD data (Appendix 1). Benbow (1982) interprets a fluvio-lacustrine environment with minor aeolian input.

As with the older Relief Sandstone, the porosity distribution between the Marla and Munta areas is bimodal, the latter area having a very high average porosity value of 24 per cent. However, the Arcoeillinna in the Marla area has quite high porosity values averaging 13.4 per cent and ranging up to 19 per cent (Fig. 17C).

The phi log k plot (Fig. 15E) is remarkably linear, with Marla area permeability values ranging between 0.1 and 50 md, and Munta area permeabilities averaging 291 md with a maximum exceeding 1700 md.

Gamma Ray and Vshale values are very high (Fig. 16E) but two fields can be distinguished on the cross-plot. One, which comprises mostly sandstone (with muddy laminae), has a 'low' Gamma Ray and very high Vshale. Abundant mica may be responsible. The other, which comprises mostly mudstone, has a very high Gamma Ray and low to moderate Vshale. These observations must be taken with caution because of the poor quality logging in the Marla area.

Because of its abundant thin muddy interbeds, the Arcoeillinna Sandstone is not a high quality reservoir but could be considered a potential secondary target.

Trainor Hill Sandstone

The Trainor Hill was originally widespread, but due to Delamerian erosion, it has been thinned and locally removed in the east Marla area. Maximum thickness in Marla-10 is 316m but in the Munta area it exceeds 440m, reaching a maximum preserved thickness of 520m in Lairu-1. Where preservation is more complete it thus rivals the Murnaroo Formation in thickness.

In outcrop and core the sandstone is very fine to medium grained, well sorted and cross-bedded with minor mudstone interbeds. Upper levels in outcrop are calcareous and dolomitic, but the abundant kaolin reported from outcrops (Benbow, 1982) is not matched by the XRD data from cores (Appendix 1). The near surface kaolin results from a Tertiary weathering event which affected sandstones as young as Jurassic (Algebuckina Sst) and is evident in most of the upholes drilled for velocity data in the region. Feldspar content is usually low but in outcrop it ranges up to 35 per cent; biotite is lacking in contrast to the Arcoeillinna (Benbow, 1982). Benbow suggests a fluvio-deltaic environment of deposition with sand source areas mainly from the southwest.

Like the preceding Arcoeillinna and Relief Sandstones, porosity distribution of the Trainor Hill is bimodal (Fig. 17D). Mean porosity values are very good: 15 per cent in the Marla area and 22 percent in the Munta area. Permeability values on the phi log k cross-plot (Fig. 15F) are high, usually tens to hundreds of millidarcies in the Marla area and up to 5249 md in the Munta area (Ungoolya-1, depth 667m). Core-log porosity correlation (calcite matrix density) is good (Sansome & Gravestock, 1993; Fig. 17G).

The Trainor Hill Sandstone is disconformably overlain by the Ordovician Mount Chandler Sandstone and is not stratigraphically sealed. However, in Devonian thrust zones there is a good chance of fault seal and of juxtaposition against potential Cambrian source rocks.

Mount Chandler Sandstone

Few cores are available for this Ordovician sandstone which was widespread, thickening north over the Musgrave Block. Maximum drilled thickness ranges from 212m in the Marla area (Byilkaoora-2) to 472m in the Munta area (Karlaya-1). The formation is a clean, well sorted, well rounded, very fine to fine-grained quartzose sandstone (Krieg, 1973; Benbow, 1982; Womer *et al.*, 1987). Cross-beds, often recumbently folded, indicate north to northeasterly directed currents. Bioturbation (pipe rock) is prominent at several levels. A tidal-deltaic environment of deposition is interpreted by Packham & Webby (1969), perhaps with fluvial influence in the lower part (Benbow, 1982).

There are too few samples from the Munta area to compare porosity distribution but the phi log k plot indicates consistently high porosity and permeability (Fig. 15G). Log porosity data agree well with core data (Sansome & Gravestock, 1993) using a quartz matrix density of 2.65 gm cm^{-3} (not calcite - this was an error in the above abstract). Gamma Ray and Vshale values are correspondingly low.

The Mount Chandler Sandstone is locally sealed in the northern Munyarai Trough-Mount Johns region by the Indulkana Shale, but this unit is thin to absent elsewhere. It thus requires hanging wall fault structures for seal. The Mount Chandler and the stratigraphically younger Blue Hills Sandstone (not studied) also run the risk of being breached by Permian erosion. Despite its excellent reservoir qualities it is thus unlikely to be a major target for petroleum.

A preliminary compaction model for the Relief Sandstone

In their study of the Relief Sandstone Gaughan & Warren (1990) noted that compaction due to greater burial depth was more extensive in the Marla region (represented in our core analysis dataset by Marla-3 and Manya-6) than in the Munta region (represented by Giles-1 and Meramangye-1). They also noted that *present day depth* to top Relief was not that dissimilar between Marla-3 (607m) and Giles-1 and Meramangye-1 (304m and 359m respectively). Top Relief in Manya-6 is 1686m (these are KB depths). Gaughan & Warren (1990, p.188) suggested three possible causes of the compaction differences between the Marla and Munta areas:

1. an early framework-supporting cement in the west, not present in the east [west = Munta area, east = Marla area],

2. a difference in pore water conditions, with those in the east facilitating chemical compaction, or

3. a direct relationship with depth-of-burial.

We propose the third mechanism is dominant - but is not related to present-day depth of burial. We suggest that the porosity variations result from burial depth changes caused by the Alice Springs Orogeny *at the beginning of the Carboniferous.*

We have selected three wells: Giles-1 to represent the Munta area (average porosity 16.4%, n =14), Manya-6 to represent the Marla area structurally *beneath* the Marla Overthrust Zone (average porosity 2.9%, n =9), and Marla-3 *structurally within* the Marla Overthrust Zone (average porosity 6.7%, n =6).

We assume that 30 km of southeast-directed tectonic transport has brought Marla-3 to its present distance of 45 km from Manya-6. Thus before the Alice Springs Orogeny the two locations were 75 km apart. Tectonic transport is assumed not to have affected the distance between Manya-6 and Giles-1 which remain a constant 150 km apart.

By adding restored isopachs of Relief to Blue Hills Sandstone (and hypothetical Devonian), and by subtracting section lost by Delamerian erosion, we obtain the approximate Devonian burial depths for Relief Sandstone of 1.4 km for Giles-1, 3.8 km for Manya-6 and 5.2 km for Marla-3. These initial conditions are shown on Figure 18A.

We then introduce the major thrust that forms the southern boundary of the Marla Overthrust Zone and shorten the crust by 30 km to bring Marla-3 and Manya-6 to their present-day distance apart. We also assume 1 km erosion of the original land surface, such that by Carboniferous time the section resembled that shown on Figure 18B. Depth of burial of the Relief beneath this reconstructed Carboniferous land surface is 1.4 km for Giles-1 (unchanged), 5.8 km for Manya-6 (down 2.0 km) and 4.3 km for Marla-3 (up 0.9 km). The land elevation due to the Alice Springs Orogeny across central Australia has been suggested as a major cause of the Carboniferous glaciation (Veevers & Powell, 1989). Glaciofluvial outwash sands and gravels occur in Officer-1 (Waitoona beds). These and subsequent events clearly modified the landscape depicted in Figure 18B, but we suggest that the core porosity values seen today are very largely due to the post-Alice Springs, pre-Permian paleodepths.

A plot of mean porosity versus paleodepth (Fig. 19) yields a curve mid-way between curves for cemented quartz sandstone and compacted quartz sandstone published by Bond *et al.* (1983). Using the exponential compaction equation-

$$Ø = Øo \exp(-cz)$$

Ø = porosity of unit
Øo = initial porosity
C = compaction constant (m^{-1})
Z = depth (m),

we can describe the Relief Sandstone compaction curve with the values Øo = 25 per cent, and C = 0.000313 m^{-1}. In his preliminary burial history analysis Moussavi-Harami (1994) assumed (in the absence of data), compaction-dominated conditions for sandstones, with the values Øo = 45 per cent, and C = 0.000175 m^{-1}. The analysis above suggests a combination of both compaction and cementation. Quartz overgrowths are abundant in the Marla area as Gaughan & Warren (1990) have observed. Late stage carbonate cements were probably precipitated from bicarbonate released by the Ouldburra Formation during compaction.

Even though the Relief and other sandstones have deteriorated at depths approaching 6 km, they should not be written off in the Marla Overthrust Zone as shown by Marla-3. These burial depths are also good news for the compaction of carbonate and calc-siltstone source rocks such as the Ouldburra Formation and Ungoolya Group units. It is only at depths comparable with those proposed in this analysis that hydrocarbons can be expelled from such intractable rocks.

DISTRIBUTION OF POTENTIAL SOURCE ROCKS

Introduction

Oil bleeds from vugs and fractures in Byilkaoora-1 confirmed the existence of Cambrian petroleum in the Officer Basin (Pitt *et al.*, 1980). The oil was generated *in situ* in the alkaline playa facies of the Observatory Hill Formation (McKirdy & Kantsler, 1980; McKirdy *et al.*, 1984). Since then numerous oil shows have been reported from mineral drillhole intersections in the Marla Overthrust Zone (Weste, 1984) and two 'petroliferous shale' occurrences were reported from the KD-1 and KD-2A drillholes in the Tallaringa Trough (Gillan, 1983). The oil source potential of the Observatory Hill Formation has been well-documented (see review, McKirdy, 1993).

By the mid-1980s, however, it was realised that a shallow marine to coastal sabkha unit, the Ouldburra Formation, had been mistaken for the Observatory Hill Formation (as had some Proterozoic carbonates) and thus some source rock data were wrongly attributed to the Observatory Hill Formation. The first comparison between the Observatory Hill playa source rocks and the sabkha-marine Ouldburra source rocks was published by McKirdy *et al* (1984), the Ouldburra Formation was formally defined by Brewer *et al.* (1987) and its facies studied by Dunster (1987).

In the mid - 1980s Comalco focused attention on the Neoproterozoic Rodda beds in which minor oil stains and fluorescence were reported, but the hoped for fracture porosity sought in three wells, did not materialise (Stainton *et al.*, 1988). Sedimentary facies and sequence stratigraphic studies of the Neoproterozoic by Sukanta (1993) and the discovery of new source potential in the Alinya Formation (Zang & McKirdy, 1993), necessitate a review of existing data. This section describes the distribution of potential source rocks in the latest stratigraphic context. Total Organic Carbon (TOC) distribution is used to screen source potential by means of histograms (Fig. 20). Using Sukanta's stratigraphic scheme the 243 samples formerly assigned to the Rodda beds can be broken down into the constituent units. The Alinya Formation at the base of the sequence and the Early Cambrian Ouldburra Formation are similarly treated. The latter unit is being studied in detail for its source and reservoir potential by M. Kamali (National Centre for Petroleum Geology & Geophysics) from analyses funded by the SAEI.

Alinya Formation and Coominaree Dolomite

The Alinya Formation overlies the basal Neoproterozoic Pindyin Sandstone in Birksgate sub-basin outcrops and in Giles-1 on the Murnaroo Platform. Seismic evidence suggests that the Pindyin-Tarlina sequence is more than 1000m thick in the eastern Munyarai Trough (e.g. 930F-6, Mackie, 1994), but how much of this can be attributed entirely to the Alinya Formation is not known.

Zang (in prep, Appendix 3) and Zang & McKirdy (1993) divide the Alinga Formation in Giles-1 into two units. The lower unit of anhydritic siltstone and sandstone was deposited on a tidal flat. The upper unit comprises stacked cyclic sediments deposited in a coastal sabkha setting. Complete cycles comprise grey siltstone, black shale, grey-green silty shale, anhydrite and siltstone dolomite beds rich in microbial matter. Aeolian sands cap the cycles. TOC values range up to 0.62 per cent in the upper unit which is only 35m thick in Giles-1 and has yielded ten samples (Figs. 20I). Further drilling is required to more fully appraise the source potential of this unit but maturation levels corresponding to the oil generation window confirm that the Murnaroo Platform has not been buried to great depth.

The Coominaree Dolomite is correlated here with the Alinya Formation but is restricted to the eastern margin of the basin. Zang (in prep, Appendix 3), however, considers the Coominaree Dolomite to be older than the Alinya Formation which he regards as Torrensian in age. The Coominaree Dolomite was cored in Manya-5 where, despite its sub-graphitic overmature kerogen content (the dolomite underlies basalt), TOC values did exceed 0.4 per cent in one sample (McKirdy in Weste, 1984) (Fig. 20J).

Dey-Dey Mudstone

Five of the fifty-two samples from this interval have TOC values greater than 0.4 per cent, with a maximum value of 1.47 per cent (Fig. 20F).

The location of samples with elevated TOCs is significant. The richest source interval is in SMD5001 drillhole on the Murnaroo Platform. It occurs in massive to laminated mudstone 40-80 m above the base of the unit, which is interpreted by Sukanta (1993, p. 65) as 'likely to have been deposited during deepening, conditions associated with a continuing marine transgression.

On the other hand, the highest TOC value in Karlaya-1 (0.81%) is only 4m below the top of the Dey-Dey Mudstone. Sukanta (1993) has identified a sequence boundary a few centimetres beneath the overlying Karlaya Limestone and considers the upper part of the Dey-Dey Mudstone to represent a highstand systems tract.

Thus, on present evidence, the richest source potential in the Dey-Dey Mudstone is in sediments deposited in transgressive and late highstand systems tracts in intervals ranging in thickness from 1m (HST) to 40m (TST). Average sample spacing in this unit is 13m, thus the chance of sampling the late highstand facies is small without the aid of a sequence stratigraphic framework.

Karlaya Limestone

Six of the twenty-six samples from this limestone have TOC values greater than 0.4 per cent, with a maximum of 0.72 per cent in Murnaroo-1 (Fig. 20G). Sukanta (1993) describes the Karlaya Limestone as an upward-deepening suite of micrtic limestone with mudstone interbeds. The richest samples in Murnaroo-1 are 1 m from the top of the formation which is 27m thick in this well. However, very low TOC values (<0.2%) occur in Giles-1 (13m thick) and Karlaya-1 (66m thick) thus formation thickness is apparently not a factor. In Giles-1 the uppermost 4m of Karlaya Limestone were not sampled. Similarly in Karlaya-1 the uppermost 10m were not sampled. The richest source rocks, which may be at the top of the Karlaya Limestone, should be sampled in these two wells.

Leemurra Mudstone

Forty-one samples from the Leemurra Mudstone yielded TOC values less than 0.3 per cent (Fig. 20H). The samples were taken from Karlaya-1 (n = 21), Munyarai-1 (n = 9), Munta-1 (n = 7) and Giles-1 (n = 4). Sukanta (1993) describes the Leemurra as an upward-coarsening unit, culminating in tidal flat redbeds in Karlaya-1. Giles-1 in contrast, is rhythmically laminated subtidal mudstone.

Sampling to date indicates that the Leemurra Mudstone is not a source rock. However, in the most basinward well Munyarai-1, equivalents of the Karlaya Limestone, Leemurra Mudstone and the Munyarai unit are 873 m thick, of which only 16m have been cored. Sampling of cuttings is required to assess the source potential of the deeper marine facies of the Leemurra Mudstone in this well.

Canyon fill

Sukanta (1993) interprets a variety of canyon fill facies which range from below storm wave base turbidites to upward-coarsening tidal flat deposits. The canyon filling units are heterogeneous but there is a distinct predominance of silty and limy units with relatively little shale. As expected, canyon fill facies reflect transport of clastics from the shelf into a relatively shallow (≤200m) basinal setting. There is a lack of source potential in the four wells drilled into this unit (Fig. 20C).

Munta Limestone

The thin (20-45m) Munta Limestone is represented by six samples with a maximum TOC value of 0.32 per cent in Karlaya-1 (Fig. 20D). The Munta Limestone is massive and micritic in Karlaya-1 but is laminated and muddy in Lairu-1 and Ungoolya-1. The formation was deposited in a low energy environment possibly below storm wave base and passing up into highstand deposits of the Mena Mudstone (Sukanta, 1993).

Mena Mudstone

The Mena Mudstone is a potential source rock with 14 samples exceeding 0.4 per cent TOC and values up to 0.92 per cent in Marla-9 (Fig. 20E, Appendix 2). It is assumed that the middle-upper Rodda beds intersected in this well represent the Mena Mudstone although correlation is not yet firm. The formation comprises green-grey, parallel laminated mudstone with frequent thin sandstone interbeds and rare slumped horizons. Sandy rhythmites, scour surfaces, graded bedding and current ripples suggest progradational, highstand deposition on a mildly unstable slope. Preserved thickness of the Mena Mudstone is variable due to erosion during the Petermann Ranges Orogeny. As a result the source potential of this unit is poor to fair, but distribution is unpredictable. The Mena Mudstone is the youngest Proterozoic unit drilled with source potential.

Ouldburra Formation

There are 210 TOC measurements available for the Ouldburra Formation, the older of two Early Cambrian units with hydrocarbon source potential. Source rock richness in this carbonate - clastic - evaporite unit is stratigraphically and geographically variable but TOC exceeds 0.5 per cent in one sixth of the total samples measured (Fig. 20A).

Stratigraphic variation is governed by the low paleoslope, rapid sea-level oscillations and influxes of siliceous clastics associated with an epeiric sea setting (Gravestock & Hibburt, 1991). Organically rich beds are thin but widespread and appear to be concentrated in transgressive to early highstand systems tracts and in sabkha facies (Kamali *et al.*, 1993).

Geographic variation in TOC and organic maturity is governed by facies change and differing burial histories. Ouldburra source rocks in the once deeply buried Marla Overthrust Zone and Manya Trough are overmature and gas-prone. In contrast, the richest oil-prone source rocks occur in the Tallaringa Trough (wells Wilkinson-1, Duval KD-1, KD-2A) which has not been subjected to deep burial. Unusual molecular biomarkers in the Ouldburra from these wells point to a strongly reducing depositional environment (M. Kamali, NCPGG, pers. comm., 1994). Investigation of this unusual geochemistry are continuing at the University of Adelaide and NCPGG.

Observatory Hill Formation

The 71 samples from this stratigraphic unit are distributed between the Moyles Chert Marker bed, the Parakeelya Alkali Member and 'Cadney Park Formation' (Fig. 20B). By far the richest organic matter is found in alkaline playa facies of the Parakeelya Alkali Member, specifically in Byilkaoora-1 and -2 in the Marla Overthrust Zone (McKirdy & Kantsler, 1980; Weste, 1984). As Stainton *et al.* (1988) have indicated, the Parakeelya Alkali Member is 80-100 m thick in the Marla area and exhibits oil bleeds in nearly every drill intersection. Oil in the mud pit at Byilkaoora-2 is from the same source and the highest TOC value of 2.29 per cent is from core in this well. The Parakeelya Alkali Member is thinner (60-70 m) and leaner in the Munta area where TOC values range most commonly between 0.1 and 0.3 per cent; these comprise the majority of the low values shown on Figure 20B.

HYDROCARBON INDICATIONS

Oil shows

Only seven of the thirty deep (≥500m) wells in the eastern Officer Basin were drilled for petroleum. Three of these (Karlaya-1, Lairu-1, Munta-1) were drilled where hydrocarbon microseepage anomalies had been detected from the air and mapped on the ground. Table 2 lists all thirty wells, half of which were drilled for the sodium carbonate mineral trona. The remainder are stratigraphic, base metal or uranium drillholes. Despite the diversity of rationales for selecting well locations, which resulted in most being drilled off-structure, more than one third of them had hydrocarbon shows. Details of the more conventional shows (oil bleeds, fluorescence) are listed in Table 3, which also gives shows from wells less than 500m deep. Nearly all of the more significant oil bleeds are in cored intersections of the Observatory Hill Formation in the Marla Overthrust Zone. Two drillstem tests only have been conducted in wells Munta-1 and Lairu-1 (Table 4) but these were to test the tools rather than the formations encountered.

Oil extracts

In addition to conventional shows in drillcores, a number of unconventional hydrocarbon indications occur in the form of oil stains ($\pm$ fluorescence) in thin sections and oil extracts from potential source rocks and reservoirs (usually 100-200 ppm). Biomarker studies of extracts and oils reveal four oil families in the Officer Basin, two in the Neoproterozoic and two in the Cambrian (McKirdy, 1993). Of particular interest is the presence of biomarkers peculiar to the Alinya Formation (at the base of the Neoproterozoic sequence) in oils which have stained reservoir sands in the Murnaroo Formation (wells SMD5001, SMD5002: McKirdy & Watson, 1989) and in the Relief Sandstone (well Observatory Hill-1). This is clear evidence of hydrocarbon migration into stratigraphically overlying reservoirs.

The most intriguing shows is a hydrocarbon extract associated with the manganese mineral cryptomelane (KMn_4O_8) in the upper Trainor Hill Sandstone in Marla-10. This oil-cryptomelane association may be fortuitous and is currently under investigation. The significance of the show is that it occurs in the Late Cambrian, and thus represents the youngest occurrence to date in the Officer Basin.

REFERENCES

AMBROSE, G.J., FLINT, R.B. & WEBB, A.W., 1981- Precambrian and Palaeozoic geology of the Peake and Denison Ranges. South Australian geological survey bulletin, 50, 5-71.

BENBOW, M.C., 1982 - Stratigraphy of the Cambrian - ? Early Ordovician, Mount Johns Range NE Officer Basin, South Australia. Royal Society of South Australia, Transactions, 106, 191-211.

BOND, G.C., KOMINZ, M.A. & DEVLIN, W.J., 1983 - Thermal subsidence and 775 ecstasy in the Lower Paleozoic miogeocline of western North America. Nature, 306, 775-779.

BOURKE, D.J. & SENAPATI, N., 1983 - Technical report on the drilling for the 1983 coal exploration programme. Report for Comalco. Dept Mines & Energy open file envelope 6259, 1108-1154 (unpublished).

BREWER, A.M., DUNSTER, J.N., GATEHOUSE, C.G., HENRY, R.L. & WESTE, G., 1987 - A revision of the stratigraphy of the eastern Officer Basin. South Australian Geological Survey, Quarterly Notes, 102, 2-15.

CHRISTIE-BLICK, N., VON DER BORCH, C.C. & DIBONA, P.A., 1990 - Working hypotheses for the origin of the Wonoka canyons (Neoproterozoic), South Australia. American Journal of Science, 290A, 295-332.

CRUSE, T., HARRIS, L.B. & RASMUSSEN, B., 1993 - Geological Note: The discovery of Ediacaran trace and body fossils in the Stirling Range Formation, Western Australia: implications for sedimentation and deformation during the 'Pan-African' orogenic cycle. Australian Journal of Earth Sciences, 40(3), 293-296.

DEVINE, S.B., 1975 - An assessment of the onshore petroleum potential of Central and South Australia. APEA Journal, 15, 60-71.

DREXEL, J.F., PREISS, W.V. & PARKER, A.J. (eds), 1993 - The geology of South Australia. Volume 1 The Precambrian. South Australian Department of Mines and Energy Bulletin, 54.

DUNSTER, J.N., 1987 - Sedimentology of the Ouldburra Formation (Early Cambrian) northeastern Officer Basin. University of Adelaide, M.Sc. Thesis (unpublished).

GATEHOUSE, C.G., BENBOW, M.C. & MAJOR, R.B., 1986 - The Murnaroo Formation of the Officer Basin. South Australian Geological Survey, Quarterly Notes, 97, 17-20.

GATEHOUSE, C.G. & HIBBURT, J.E., 1987 - Observatory Hill 1 well completion report and geology of adjacent Observatory Hill Formation. South Australian Department of Mines & Energy Report Book 87/58 (unpublished).

GAUGHAN, C.J., 1989 - Early Cambrian Relief Sandstone, Officer Basin, South Australia: subdivision, diagenesis and porosity - permeability distribution. B.Sc. (Hons) thesis, University of Adelaide (unpublished).

GAUGHAN, C.J. & WARREN, J.K., 1990 - Lower Cambrian Relief Sandstone, eastern Officer Basin, South Australia: an example of secondary porosity development. APEA Journal, 30(1), 184-195.

GRAVESTOCK, D.I., 1993 - 930F (Wallatinna) Seismic Survey. Uphole drilling programme cuttings descriptions. South Australian Department of Mines & Energy Open file Envelope 8591 (unpublished).

GRAVESTOCK, D.I. & HIBBURT, J.E., 1991 - Sequence stratigraphy of the eastern Officer and Arrowie basins: a framework for Cambrian oil search. APEA Journal, 31(1), 177-190.

GRAVESTOCK, D.I. & LINDSAY, J.F., 1994 - Summary of 1993 seismic exploration in the Officer Basin, South Australia. PESA Journal, 22 (in press).

JACKSON, K.S., McKIRDY, D.M., & DECKELMAN, J.A., 1984 - Hydrocarbon generation in the Amadeus Basin, Central Australia. APEA Journal, 24, 42-65.

JENKINS, R.J.F., MCKIRDY, D.M., FOSTER, C.B., O'LEARY, T. & PELL, S.D., 1992 - The record and stratigraphic implications of organic - walled microfossils from the Ediacaran (terminal Proterozoic) of South Australia. Geological Magazine, 129, 401-410.

JONES, B.G., 1972. Upper Devonian to Lower Carboniferous stratigraphy of the Pertnjara Group, Amadeus Basin, Central Australia. Geological Society of Australia Journal, 19 (2), 229-249.

KAMALI, M., LEMON, N.M. & McKIRDY, D.M., 1993 - Ouldburra Formation as a potential source and reservoir for petroleum in the Manya Trough, eastern Officer Basin. Central Australian Basins Workshop, Alice Springs, Programme & Abstracts, 65-66.

KRIEG, G.W., 1973 - EVERARD, South Australia, sheet SH/53-13. South Australian Geological Survey, 1:250 000 Series, Explanatory Notes.

LEVEN, J.H. & LINDSAY, J.F., 1992 - Morphology of the Late Proterozoic to Early Palaeozoic Officer Basin, South Australia. Exploration Geophysics, 23, 191-196.

LINDSAY, J.F., LEVEN, J. & KRIEG, G., 1992 - Central Officer Basin South Australia. Seismic data acquisition 1993. AGSO Record 1992/89.

LOGAN, L.J., 1965. Active search under way in Australia's Amadeus Basin. World Oil, March 1965, 108-110.

LONG, J.A., TURNER, S. & YOUNG, G.C., 1988. A Devonian fish fauna from subsurface sediments in the eastern Officer Basin, South Australia. Alcheringa, 12, 61-78.

MACKIE, S.M., 1994 - Summary of seismic interpretation, Marla and Munta areas, Officer Basin. South Australian Department of Mines & Energy, open file Envelope, 8591 (unpublished).

MACKIE, S.M. & GRAVESTOCK, D.I., 1993 - Summary of seismic interpretation, Marla area Officer Basin. South Australian Department of Mines & Energy, open file Envelope, 8591 (unpublished).

MAJOR, R.B., 1968 - Preliminary notes on the geology of the BIRKSGATE 1:250 000 sheet area. South Australian Department of Mines Report Book 66/122 (unpublished).

MAJOR, R.B., 1973a - The Wirrildar Beds. South Australian Geological Survey, Quarterly Notes, 45, 8-11.

MAJOR, R.B., 1973b - The Pindyin Beds. South Australian Geological Survey, Quarterly Notes, 46, 1-5.

MAJOR, R.B., 1973c - The Wright Hill Beds. South Australian Geological Survey, Quarterly Notes, 46, 6-10.

MAJOR, R.B., 1974 - The Punkerri Beds. South Australian Geological Survey, Quarterly Notes, 51, 1-5.

MAJOR, R.B. & CONOR, C.H.H., 1993 - Musgrave Block. In: DREXEL, J.F., PREISS, W.V. & PARKER, A.J. (eds). The geology of South Australia. Volume 1, The Precambrian, 156 - 167.

MAJOR, R.B. & TELUK, J.A., 1967 - The Kulyong Volcanics. South Australian Geological Survey, Quarterly Notes, 22, 8-11.

McKIRDY, D.M., 1993 - Oil shows and source rocks in the eastern Officer Basin - a geochemical overview. Central Australian Basins Workshop, Alice Springs, Programme & Abstracts, 68-69.

McKIRDY, D.M., 1994 - Review of eastern Officer Basin source potential and maturity. Report for South Australian Department of Mines & Energy (in prep.).

McKIRDY, D.M. & KANTSLER, A.J., 1980 - Oil geochemistry and potential source rocks of the Officer Basin, South Australia. APEA Journal, 20(1), 68-86.

McKIRDY, D.M., KANTSLER, A.J., EMMETT, J.K. & ALDRIDGE, A.K., 1984 - Hydrocarbon genesis and organic facies in Cambrian carbonates of the eastern Officer Basin. In, PALACAS, J.G. (ed.). Petroleum geochemistry and source rock potential of carbonate rocks. AAPG Studies in Geology, 18, 13-31.

McKIRDY, D.M. & WATSON, B.L., 1989 - Biomarker geochemistry of oil shows in the Late Precambrian Murnaroo Formation, Lake Maurice West-1, Officer Basin, S.A. AMDEL Report F7224/89. South Australian Department of Mines & Energy, open file Envelope (unpublished).

MILTON, B.E. & PARKER, A.J., 1973 - An interpretation of geophysical observations on the northern margin of the eastern Officer Basin. South Australian Department of Mines & Energy, Quarterly Notes, 46, 10-14.

MOUSSAVI-HARAMI, R., 1994 - Burial history analysis of the east Officer Basin, South Australia. A preliminary study. South Australian Department of Mines & Energy, open file envelope, 8591 (unpublished).

MOUSSAVI-HARAMI, R., 1994 - Eastern Officer Basin, South Australia. Subsidence and thermal history analysis. South Australian Department of Mines & Energy open file envelope 8591 (unpublished).

NELSON, R.G., CRABB, T.N. & GERDES, R.A., 1986 - A review of geophysical exploration in the Polda Basin, South Australia. APEA Journal, 26, 319-333.

PACKHAM, G.H. & WEBBY, B.D., 1969 - The geology of the Officer Basin in the EVERARD 1:250 000 map area. Report for Marrumba Oil N.L. (unpublished).

PELL, S.D., McKIRDY, D.M., JANSYN, J. & JENKINS, R.J.F., 1993 - Ediacaran carbon isotope stratigraphy of South Australia - An initial study. Royal Society of South Australia, Transactions, 117(4), 153-161.

PITT, G.M., BENBOW, M.C. & YOUNGS, B.C., 1980 - A review of recent geological work in the Officer Basin, South Australia. APEA Journal, 20(1), 209-220.

POWELL, C.McA., GATEHOUSE, C.G., KRAPEZ, B., Li, Z.X. & PREISS, W.V., 1993 - South Australian record of a Rodinian epicontinental basin and its mid-Neoproterozoic breakup to form the Palaeo-Pacific Ocean. Central Australian Basins Workshop Abstracts, 32-36.

PREISS, W.V., 1987 - The Adelaide Geosyncline. Late Proterozoic stratigraphy, sedimentation, palaeontology and tectonics. South Australian Geological Survey, Bulletin 53, 1-438.

PREISS, W.V., 1993 - Neoproterozoic. In: DREXEL, J.F., PREISS, W.V. & PARKER, A.J. (eds). The geology of South Australia. Volume 1, The Precambrian. South Australian Department of Mines & Energy, Bulletin, 54, 171-203.

PREISS, W.V. & KRIEG, G.W., 1992 - Stratigraphic drilling in the northeastern Officer Basin: Rodda 2 well. Department of Mines & Energy. Mines & Energy Review, South Australia, 158, 48-51.

SANSOME, A & GRAVESTOCK, D., 1993 - Sandstone reservoirs in the eastern Officer Basin. Central Australian Basins Workshop, Abstracts, 60.

SHEARER, A., 1994 - Distribution of Permian sediments in the eastern Officer Basin, S.A. South Australian Department of Mines & Energy open file envelope 8591 (unpublished).

SOUTHGATE, P.N. & HENRY, R., 1984 - Lithofacies and cyclic sequences in an alkaline lake sequence of Lower to Middle Cambrian age from the Officer Basin. Geological Society of Australia, Abstracts, 15, 180.

SOUTHGATE, P.N. LAMBERT, I.P., DONNELLY, T.H., HENRY, R., ETMINAN, H. & WESTE, G., 1989 - Depositional environments and diagenesis in Lake Parakeelya: a Cambrian alkaline playa from the Officer Basin, South Australia. Sedimentology, 36, 1091-1112.

STAINTON, P.W., WESTE, G. & CUCUZZA, G., 1988 - Exploration of PEL 23 and PEL 30, eastern Officer Basin, S.A., 1983-1988. Report for Comalco Aluminium Ltd. South Australian Department of Mines & Energy, open file Envelope, 5073 (unpublished).

SUKANTA, U., 1993 - Sedimentology, sequence stratigraphy and palaeogeography of Marinoan sediments in the eastern Officer Basin, South Australia. Flinders University of South Australia, Ph.D. Thesis (unpublished).

SUKANTA, U., THOMAS, B., VON DER BORCH, C.C. & GATEHOUSE, C.G., 1991 - Sequence stratigraphic studies and canyon formation, South Australia. PESA Journal, 19, 68-73.

SUKANTA, U., VON DER BORCH, C.C. & GATEHOUSE, C.G., 1994a - Stratigraphy of early Marinoan sediments in the eastern Officer Basin, South Australia. South Australian Department of Mines & Energy, Quarterly Notes (in prep.).

SUKANTA, U., VON DER BORCH, C.C. & GATEHOUSE, C.G., 1994b- Late Marinoan Ungoolya Group in the eastern Officer Basin, South Australia. South Australian Department of Mines & Energy, Quarterly Notes (in prep.).

THOMAS, B., 1990 - Summary of seismic interpretation in the eastern Officer Basin. South Australian Department of Mines & Energy, Report Book 90/58 (unpublished).

TOWNSON, W.G., 1985 - The subsurface geology of the western Officer Basin - results of Shell's 1980-1984 petroleum exploration campaign. APEA Journal, 25(1), 34-51.

TOWNSEND, I.J., 1976 - Stratigraphic drilling in the Arckaringa Basin, 1969-1971. South Australian Geological Survey, Report of Investigations, 45, 1-30.

TOWNSEND, I.J., 1990 - Mintabie Opalfield mining and geology. South Australian Department of Mines & Energy, Report Book 90/73 (unpublished).

TUCKER, L.R., 1994 - Devonian geology of the Munyarai Trough. South Australian Department of Mines & Energy, Report Book 94/10 (unpublished).

VEEVERS, J.J., (ed.)., 1984 - Phanerozoic earth history of Australia. Oxford Geological Sciences Series, 2. Clarendon Press, Oxford.

VEEVERS, J.J. & POWELL, C.McA., 1989 - Phanerozoic tectonic regimes of Australia, Gondwanaland and the globe. Geological Society of Australia, Abstracts, 24, 159-160.

WALLACE, M.W., WILLIAMS, G.E., GOSTIN, V.A. & KEAYS, R.R., 1990 - The Late Proterozoic Acraman impact - Towards an understanding of impact events in the sedimentary record. Department of Mines & Energy, Mines & Energy Review, South Australia, 157, 29-35.

WALTER, M.R., VEEVERS, J.J., CALVER, C.R. & GREY, K., 1993 - The Neoproterozoic Centralian Superbasin. Central Australian Basins Workshop, Abstracts, 8.

WEBB, A.W., 1978 - Geochronology of the Officer Basin - Amdel Progress Report 1. South Australian Department of Mines & Energy, open file envelope 3325 (unpublished).

WEBB, E.A., 1965 - Will Officer and Amadeus Basins both be productive? World Oil, June 1965, 160-165.

WEBBY, B.D., 1978 - History of the Ordovician continental platform shelf margin of Australia. Geological Society of Australia, Journal 25, 41-63.

WESTE, G., 1984 - PEL 23 1983. Source rock geochemistry and porosity/permeability studies. South Australian Department of Mines & Energy, open file envelope 5073 (unpublished).

WHITE, A.H. & YOUNGS, B.C., 1980 - Cambrian alkali playa-lacustrine sequence in the northeastern Officer Basin, South Australia. Journal of Sedimentary Petrology, 50, 1279-1286.

WILSON, A.F., 1952 - Precambrian tillites east of the Everard Ranges, north-western South Australia. Royal Society of South Australia, Transactions, 75, 160-163.

WOMER, M.B., BAKER, R.N., NEWMAN, E.J. & VAN NIEUWENHUISE, R., 1987 - Amoco Australia Petroleum Company. Technical evaluation of PEL 29, east Officer Basin, South Australia. South Australian Department of Mines & Energy, open file envelope 6843 (unpublished).

WOPFNER, H., 1969 - Lithology and distribution of the Observatory Hill beds, eastern Officer Basin. Royal Society of South Australia, Transactions, 93, 169-185.

ZANG, W., 1993 - Review of Neoproterozoic and Early Palaeozoic acritarch biostratigraphy. Central Australian Basins Workshop, Alice Springs, Programme & Abstracts, 12-14.

ZANG, W., (in prep.). - Early Neoproterozoic sequence stratigraphy and acritarch biostratigraphy, eastern Officer Basin, South Australia. Precambrian Research.

ZANG, W. & McKIRDY, D.M., 1993 - Microfossils and molecular fossils from the Neoproterozoic Alinya Formation - a possible new source rock in the eastern Officer Basin. Central Australian Basins Workshop, Alice Springs, Programme & Abstracts, 62-63.

0306

EASTERN OFFICER BASIN

GEOLOGY AND HYDROCARBON POTENTIAL

D.I. Gravestock & A. Sansome

South Australian Department of Mines & Energy

VOLUME 2

FIGURES, TABLES AND ENCLOSURES

July 1994 Envelope 8591

NEOPROTE.ROZ

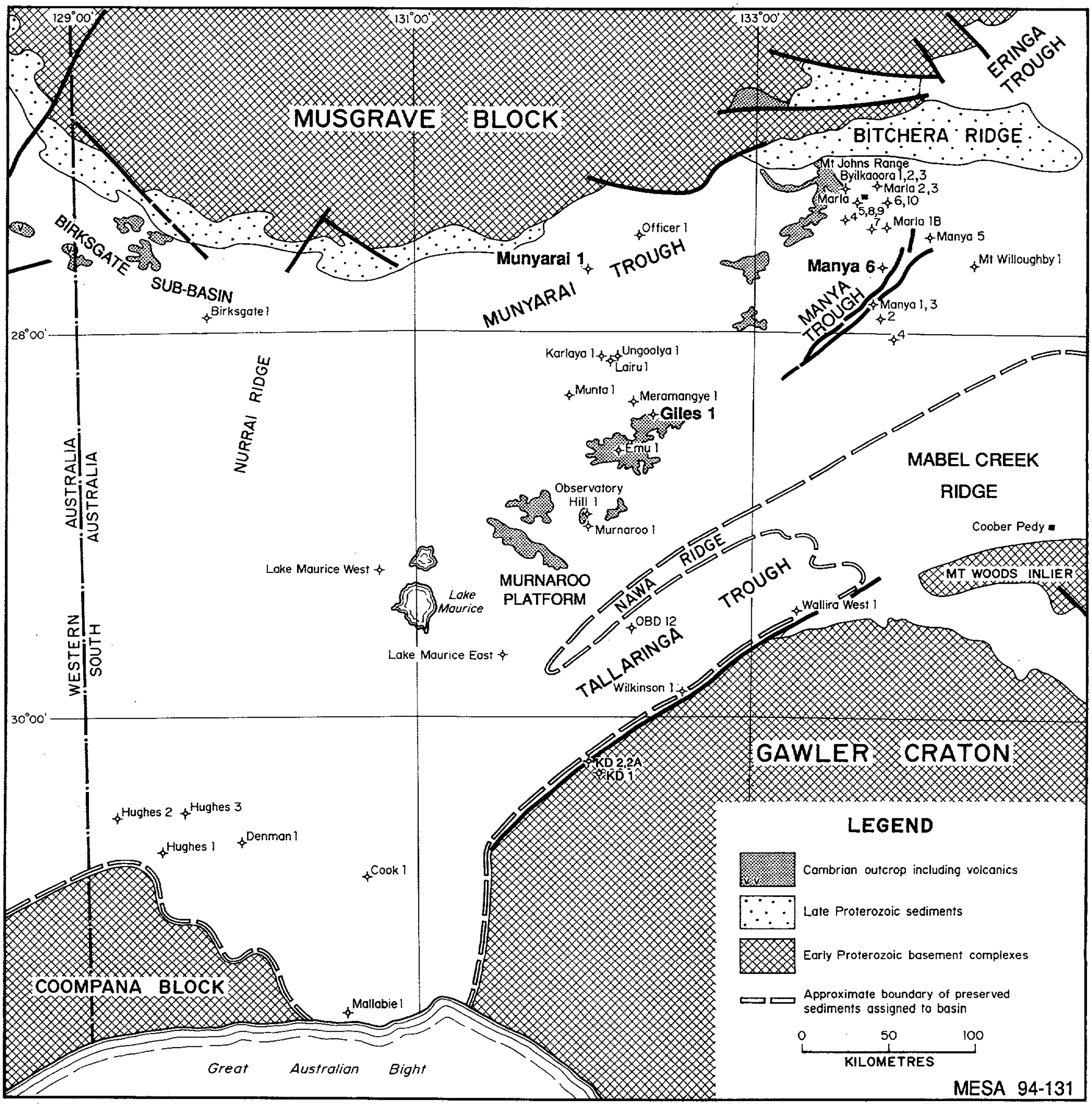

Figure 1. Principal geological features, Officer Basin SA

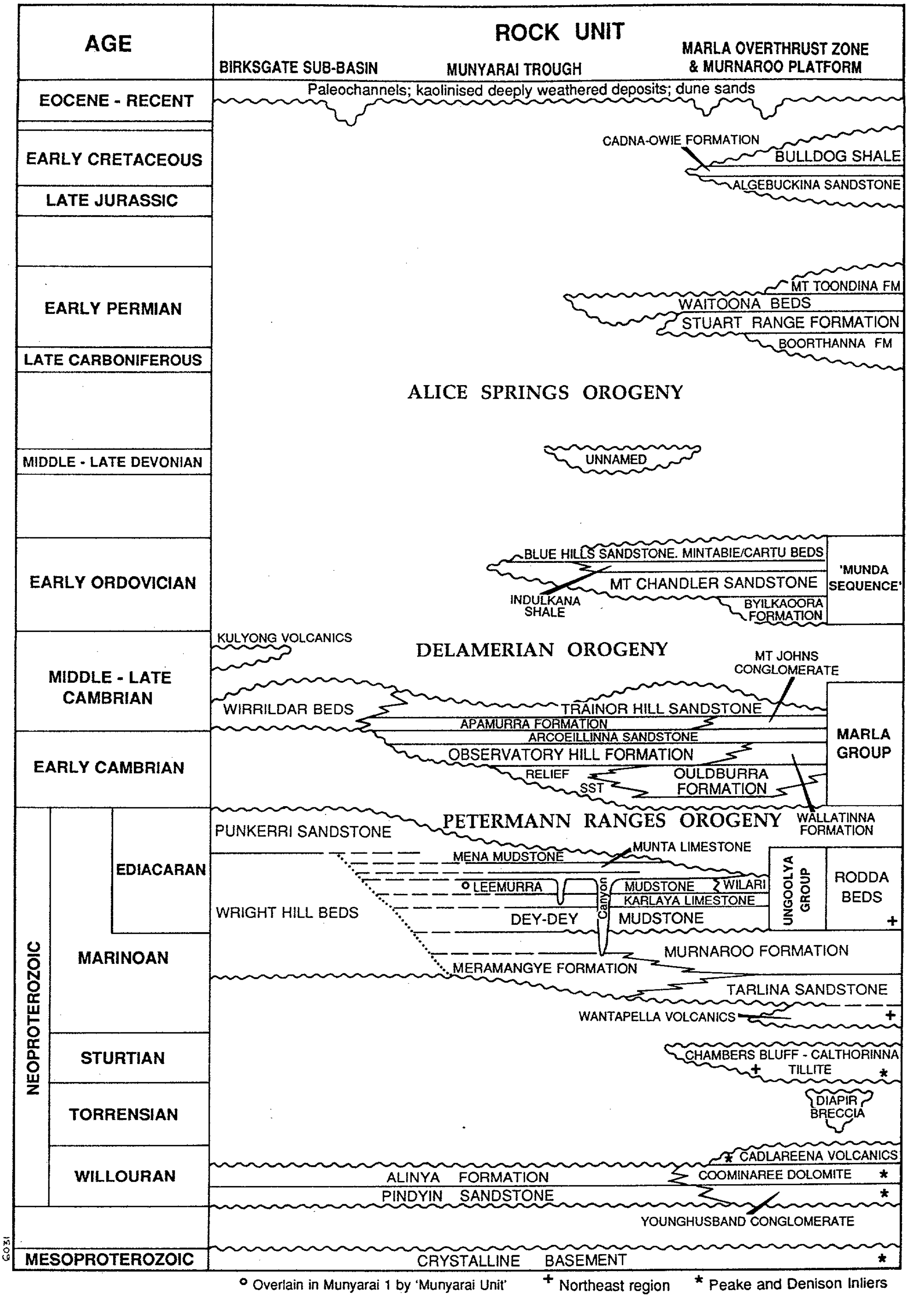

Figure 2 Stratigraphic column, central and east Officer Basin.

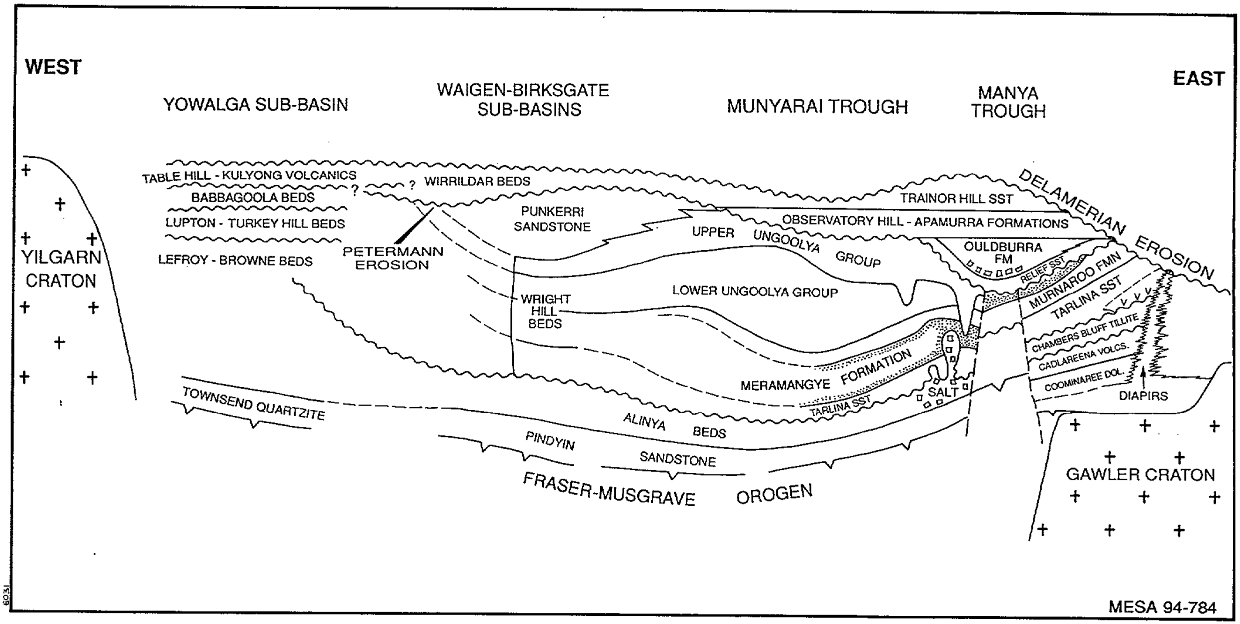

Figure 3 Geological section (not to scale) across the Officer Basin

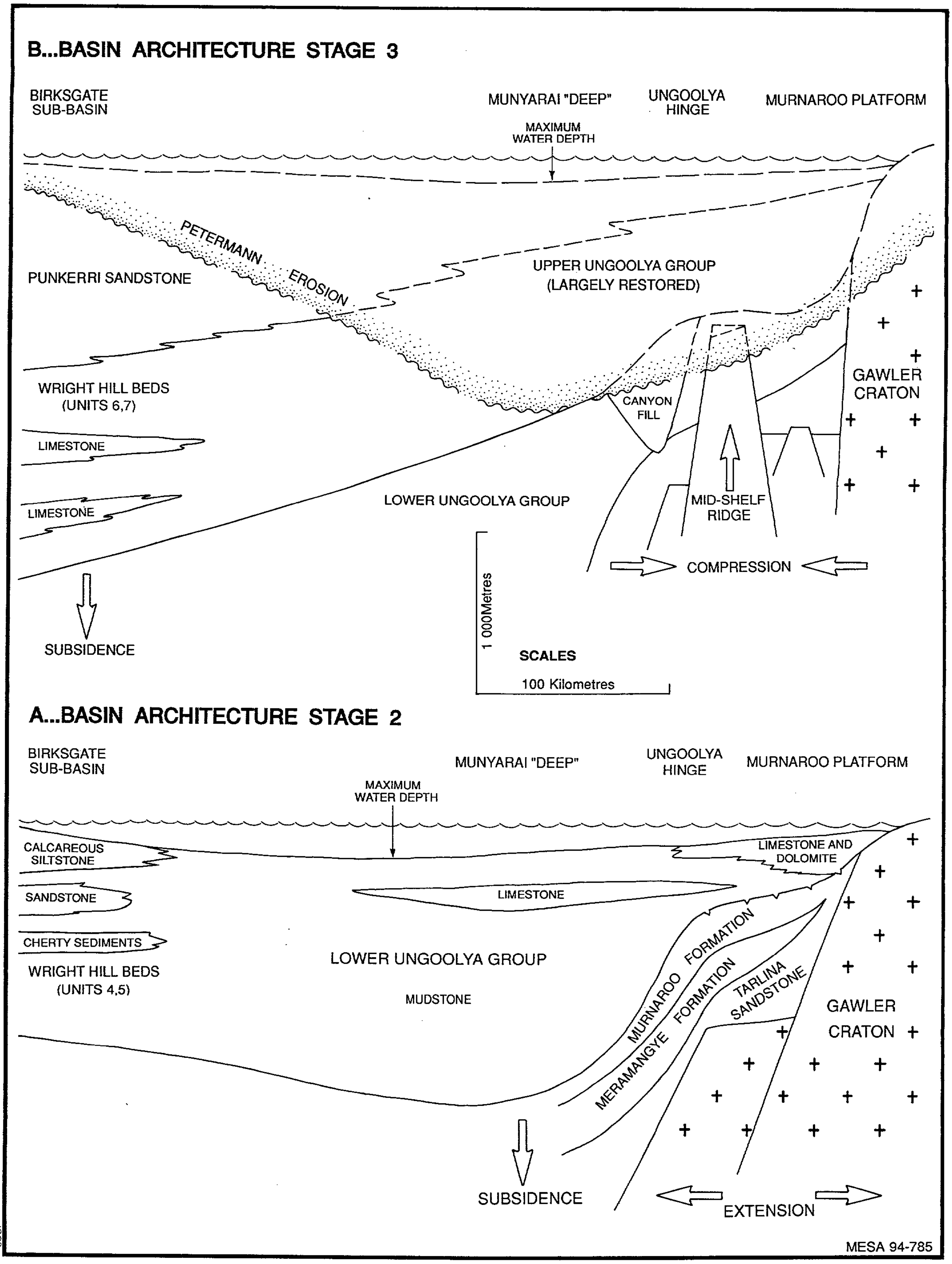

Figure 4 Stages 2 and 3 of basin development

0311

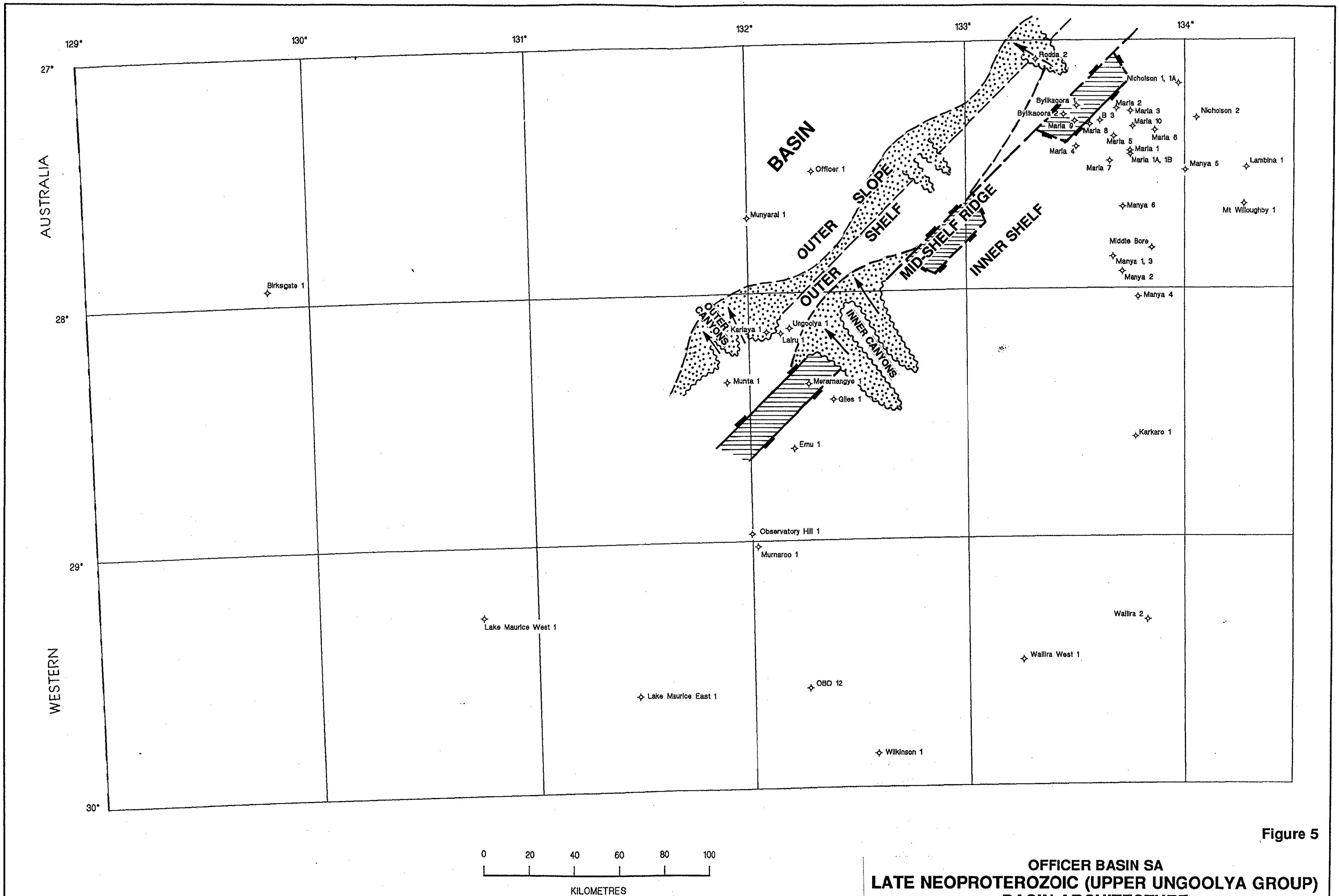

Figure 5

OFFICER BASIN SA
LATE NEOPROTEROZOIC (UPPER UNGOOLYA GROUP)
BASIN ARCHITECTURE

QD–DORA 5946AS.DTA

MINES AND ENERGY
SOUTH AUSTRALIA

94-793

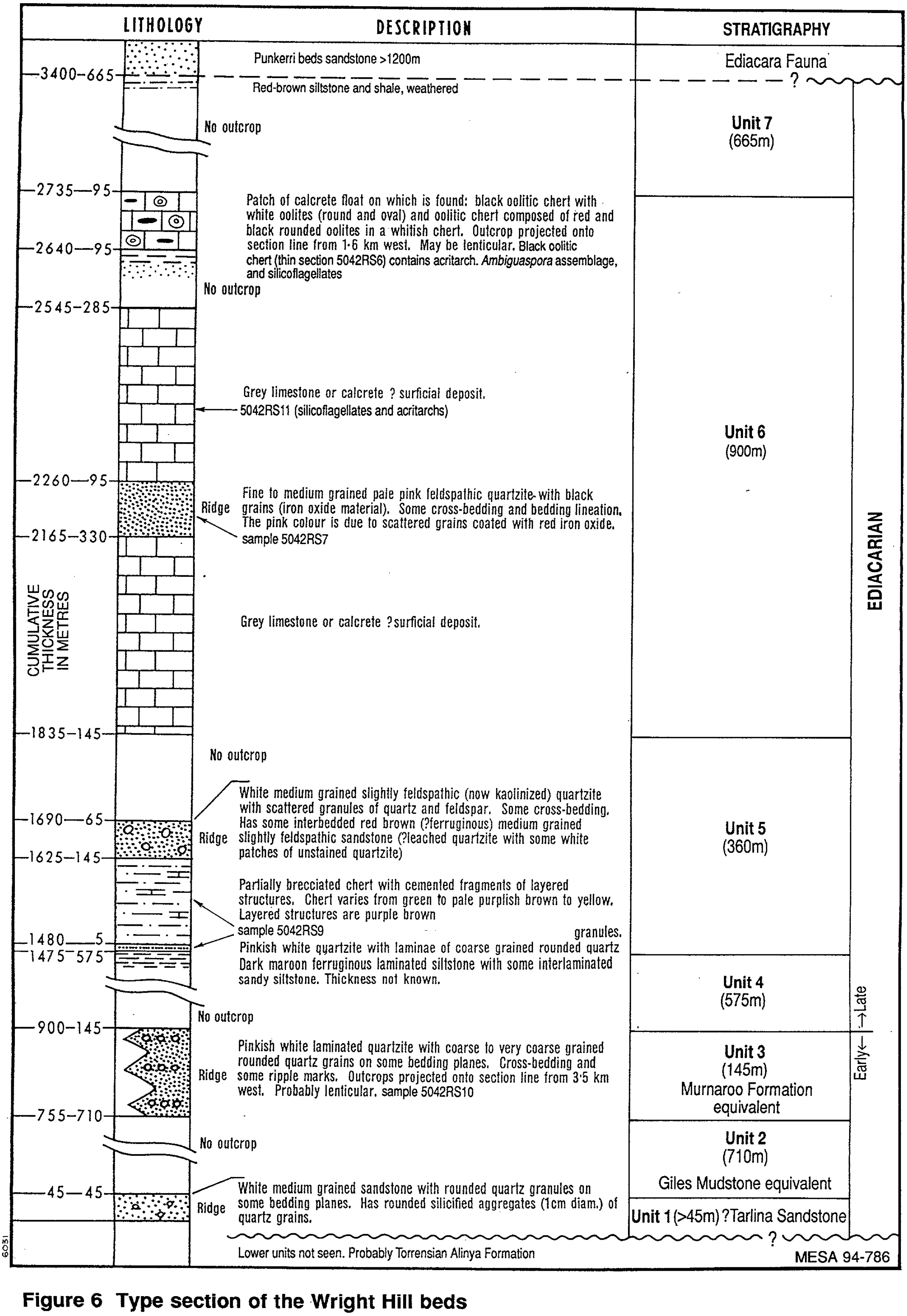

Figure 6 Type section of the Wright Hill beds

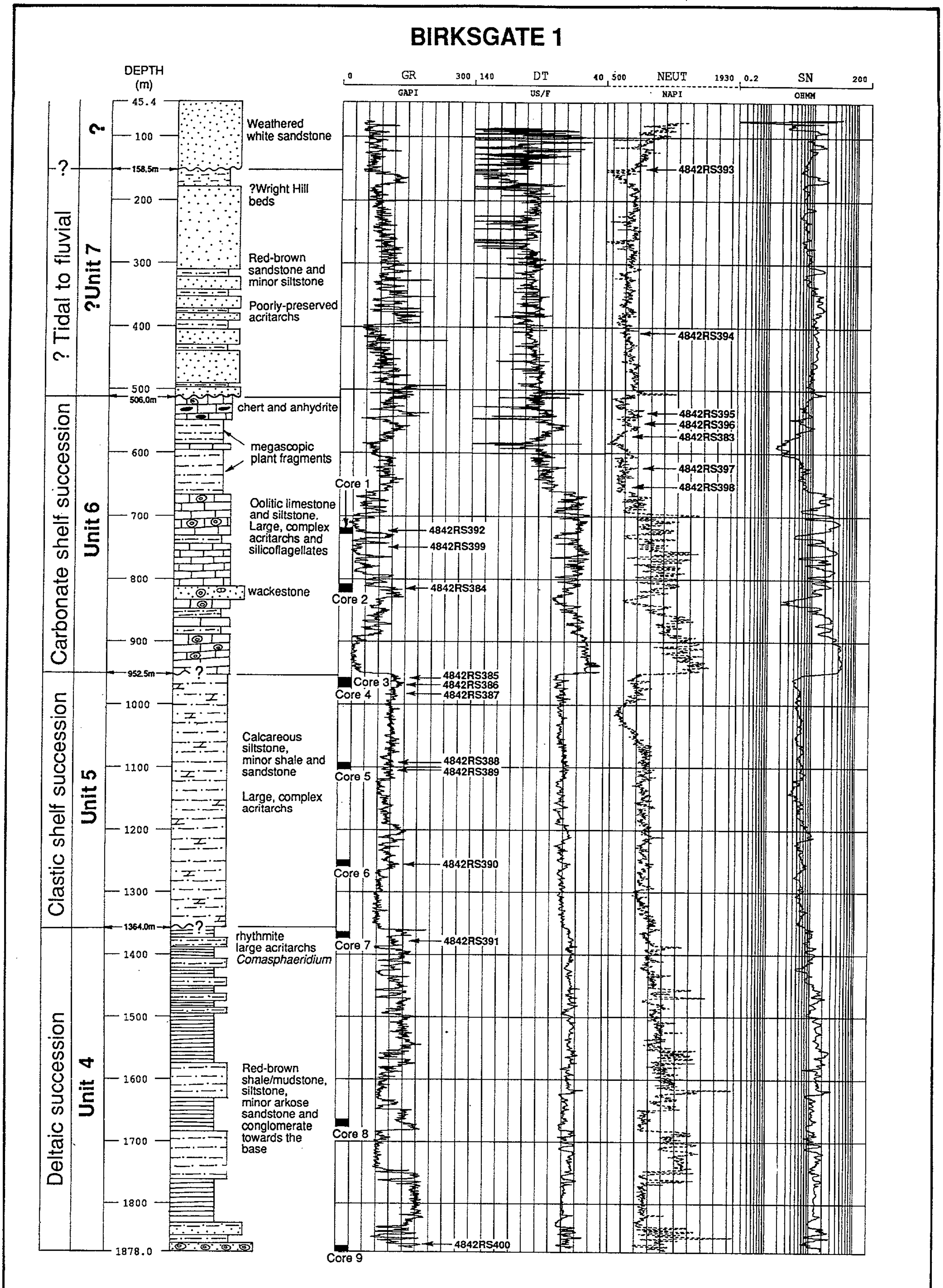

Figure 7 Birksgate 1 section

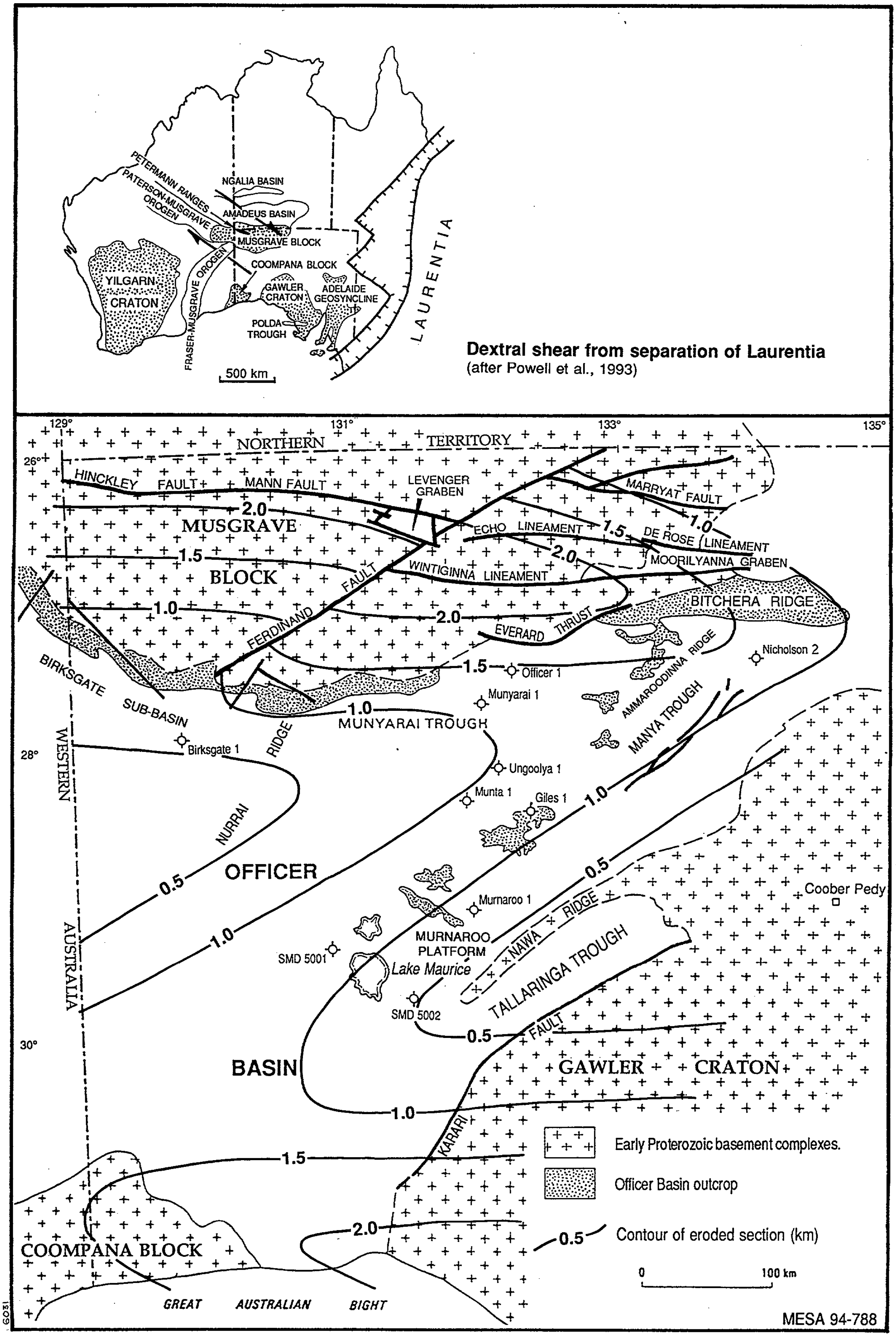

Figure 8 Sketch of geometry and amount of uplift in Petermann Ranges Orogeny

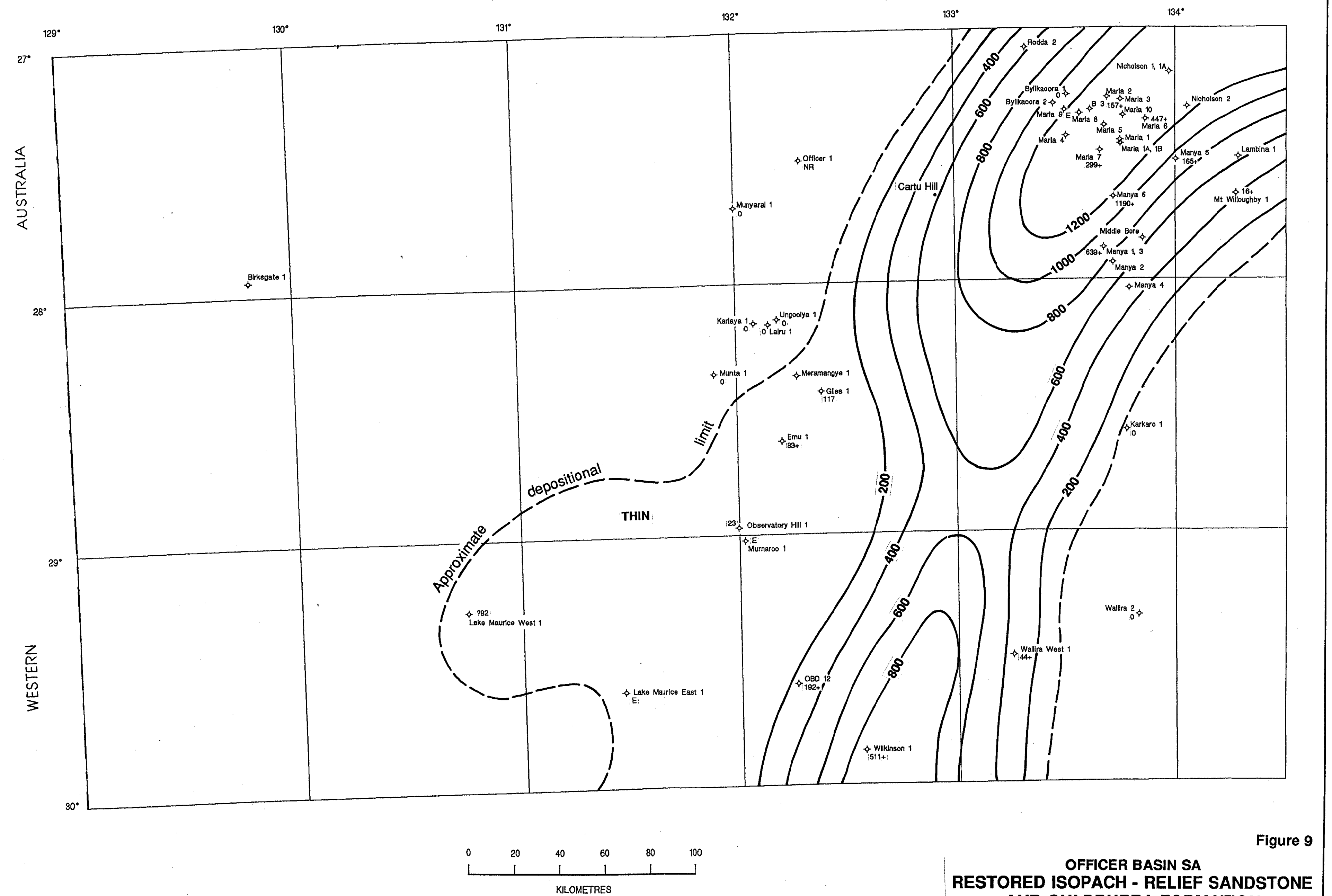

Note : Isopach values are metres

MINES AND ENERGY
SOUTH AUSTRALIA

QD-DORA 5946AS.DTA

Figure 9

OFFICER BASIN SA
RESTORED ISOPACH - RELIEF SANDSTONE AND OULDBURRA FORMATION

94-794

0316

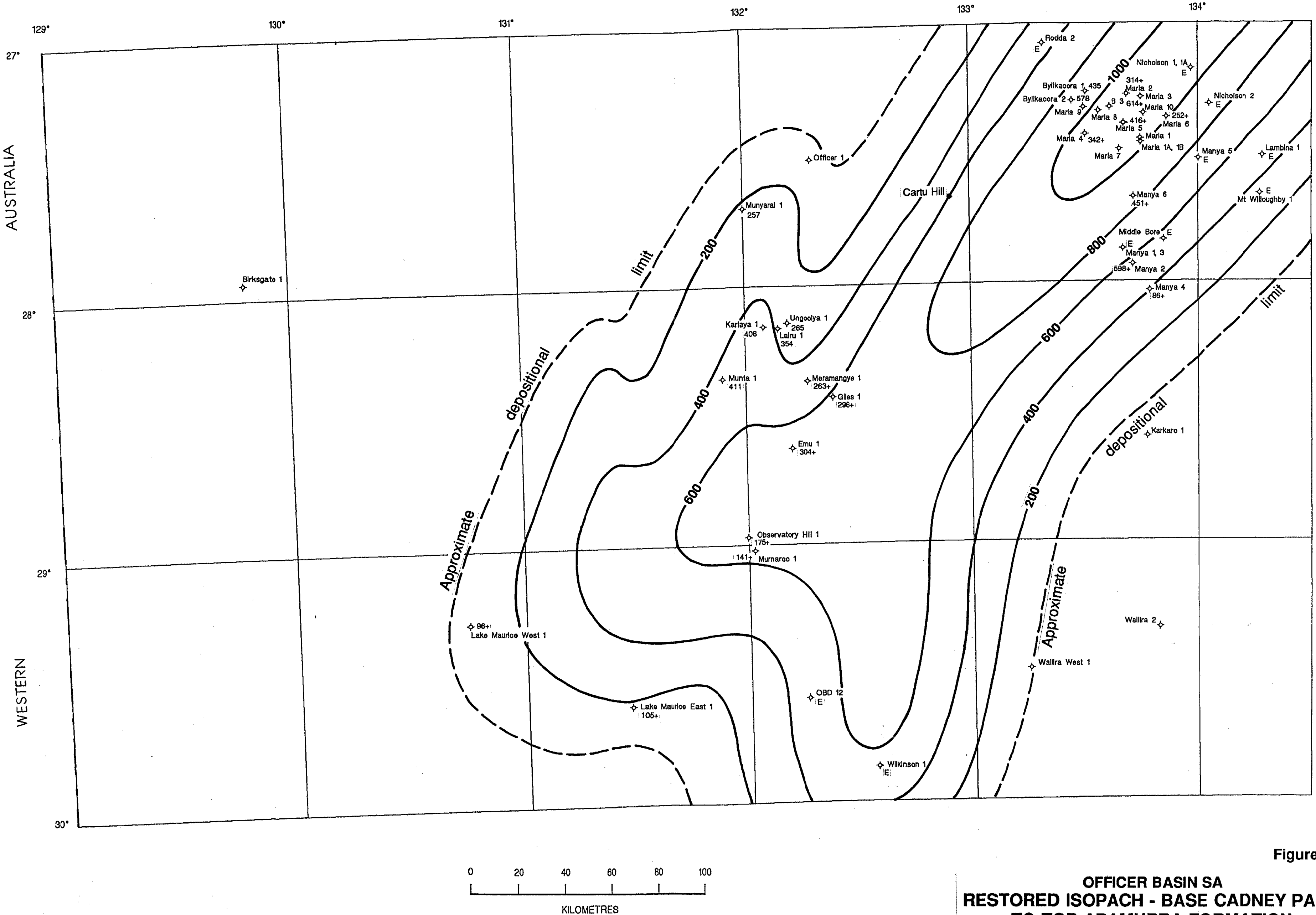

Note : Isopach values are metres

MINES AND ENERGY
SOUTH AUSTRALIA

QD-DORA 5946AS.DTA

Figure 10

OFFICER BASIN SA
RESTORED ISOPACH - BASE CADNEY PARK
TO TOP APAMURRA FORMATION

94-795

0317

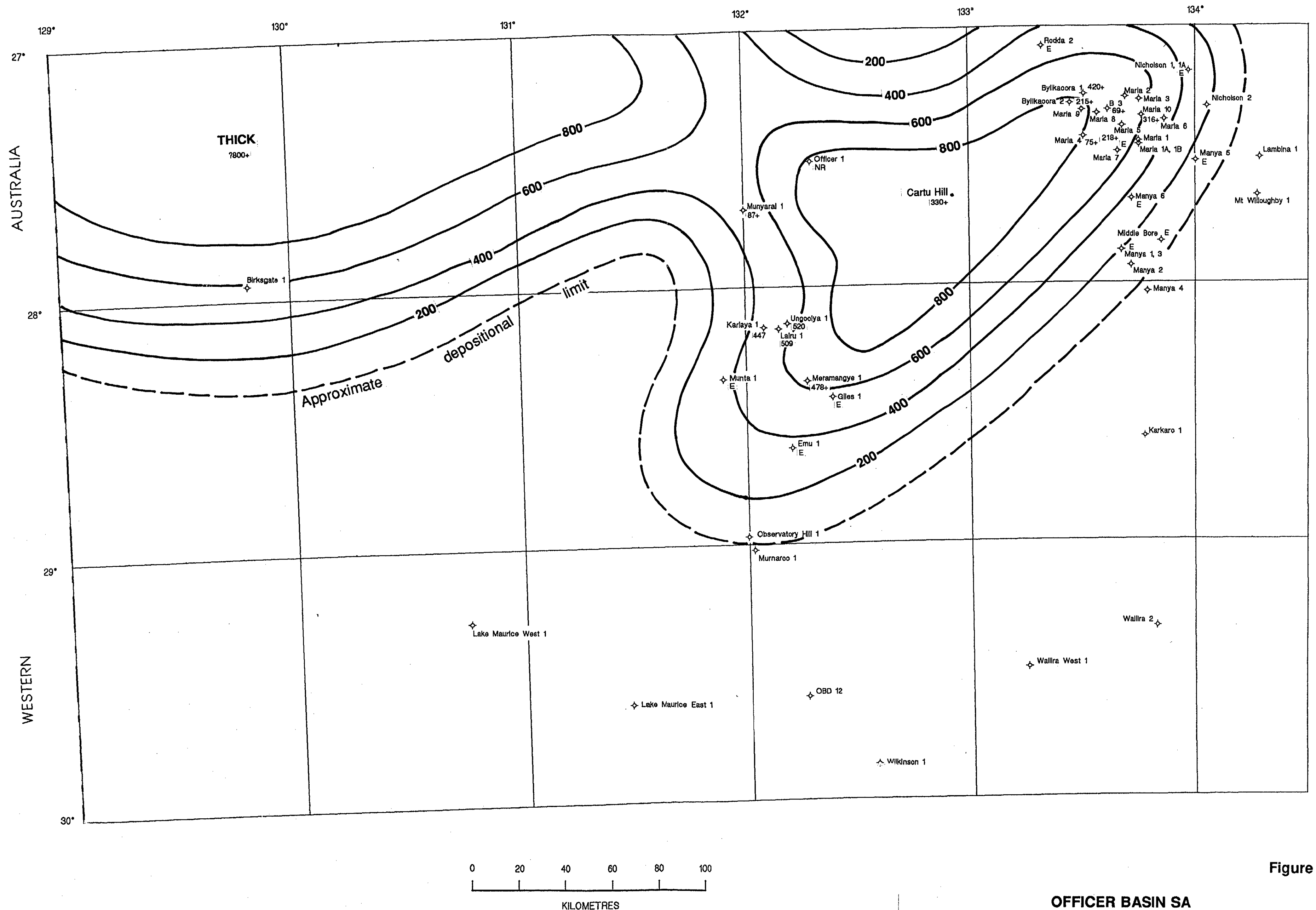

Note : Isopach values are metres

MINES AND ENERGY
SOUTH AUSTRALIA

Figure 11

OFFICER BASIN SA
RESTORED ISOPACH - TRAINOR HILL SANDSTONE

94-796

QD-DORA 5946AS.DTA

0318

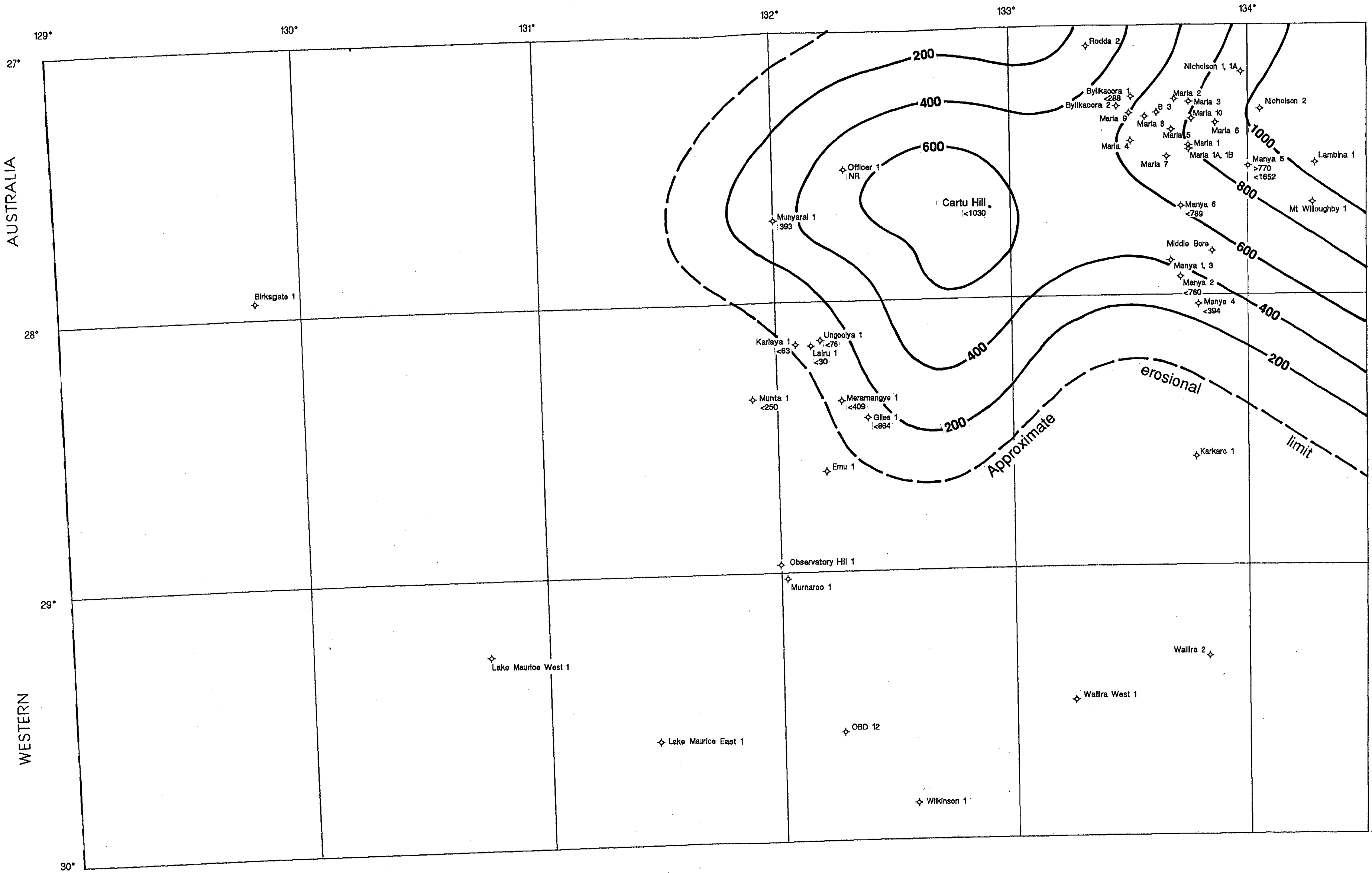

0 20 40 60 80 100

KILOMETRES

Note : Isopach values are metres

Figure 12

OFFICER BASIN SA
ESTIMATE OF DELAMERIAN SECTION LOSS

94-797

QD-DORA 5946AS.DTA

MINES AND ENERGY
SOUTH AUSTRALIA

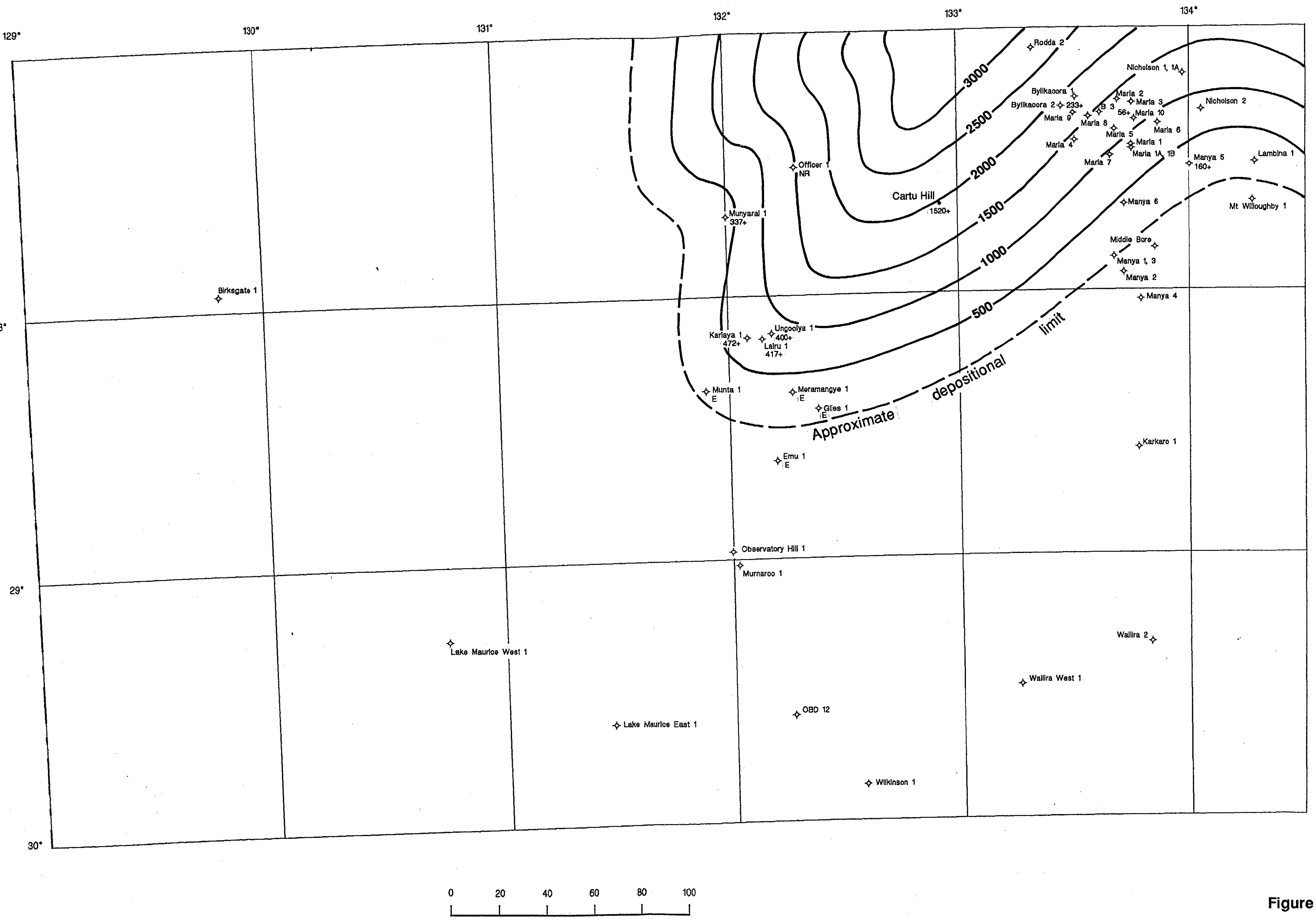

Note : Isopach values are metres

Figure 13

OFFICER BASIN SA
RESTORED ISOPACH - 'MUNDA SEQUENCE'

94-799

MINES AND ENERGY
SOUTH AUSTRALIA

QD-DORA 5946AS.DTA

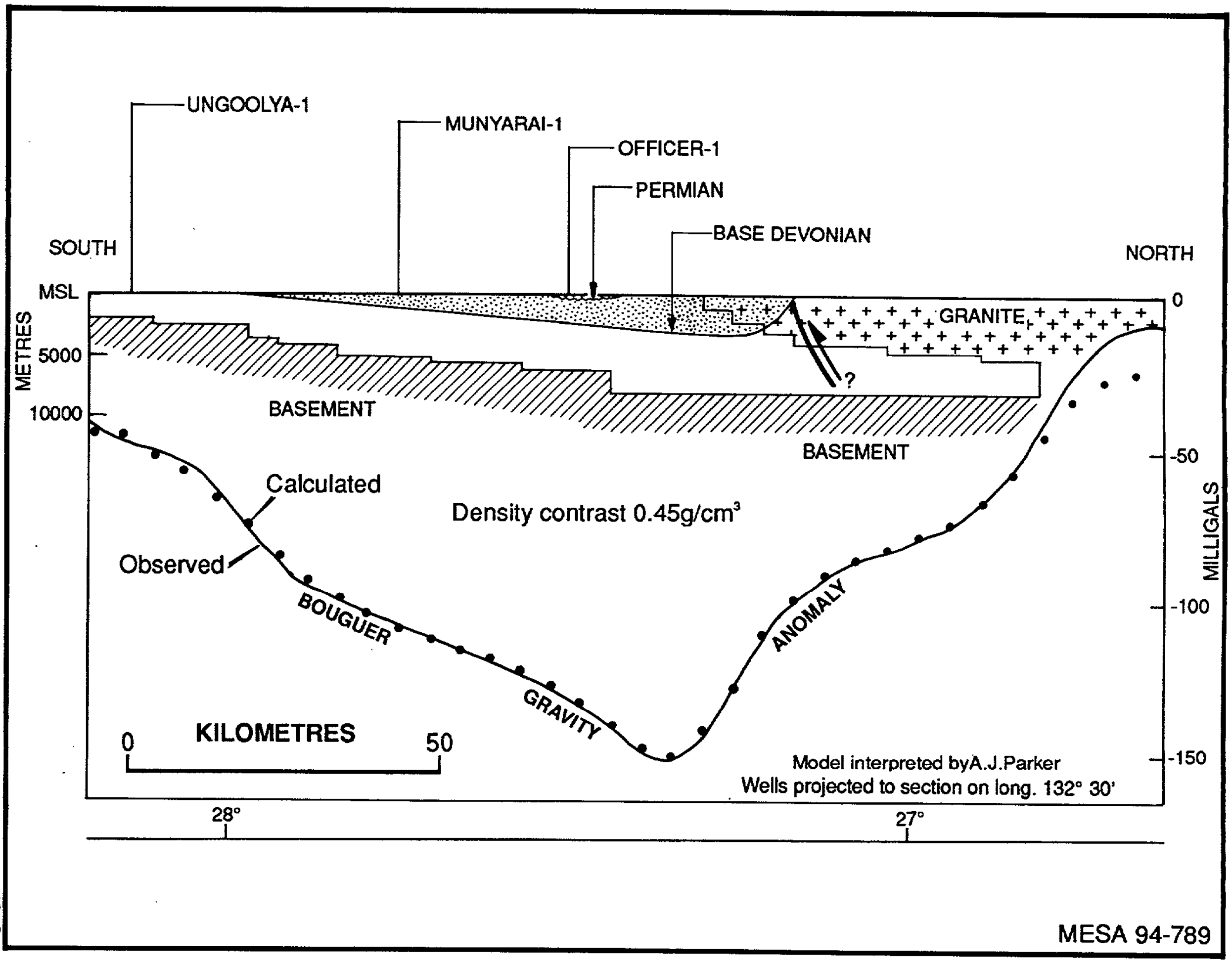

Figure 14 Calculated versus observed gravity profile and interpreted sediment thickness in the Munyarai Trough

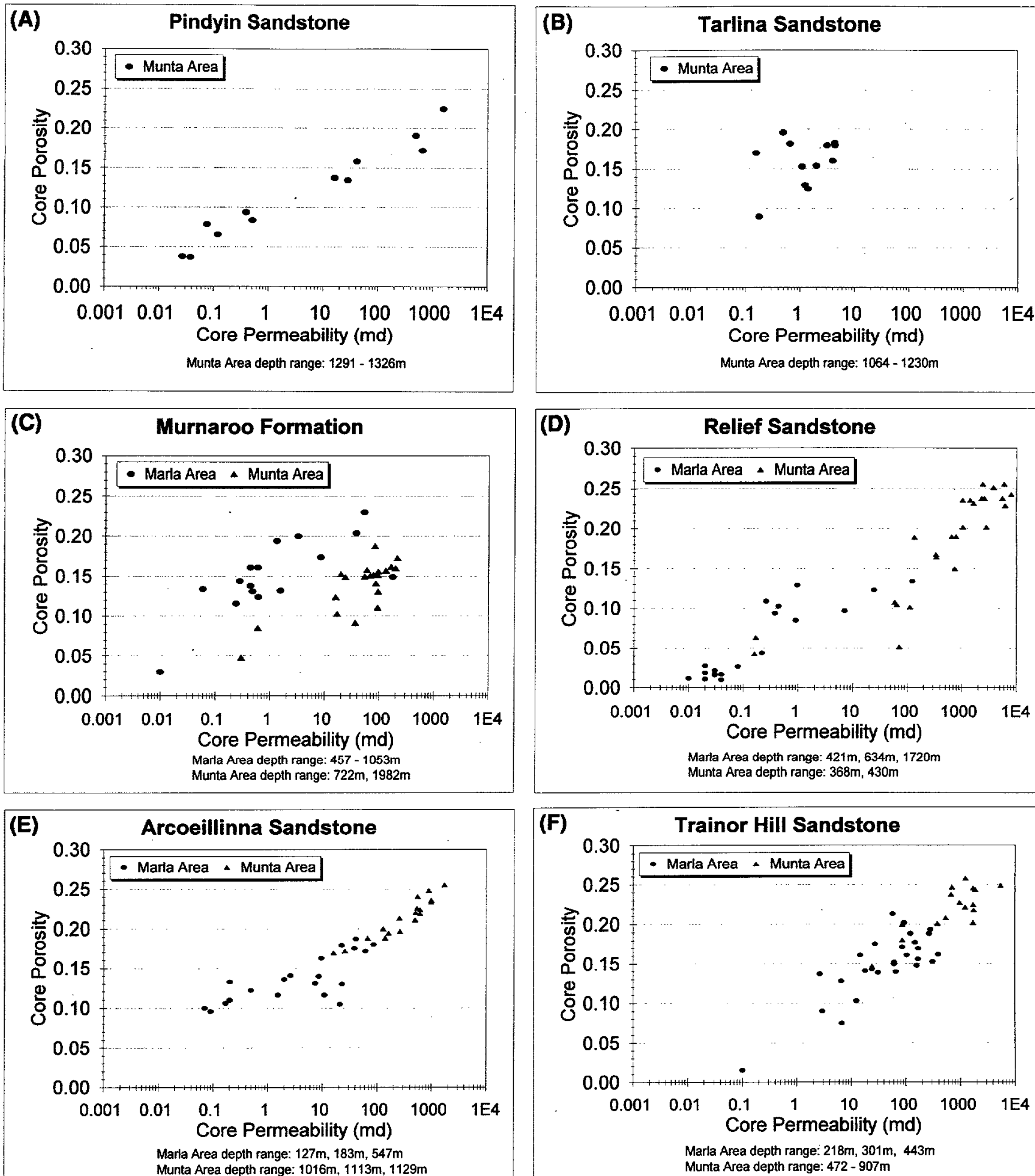

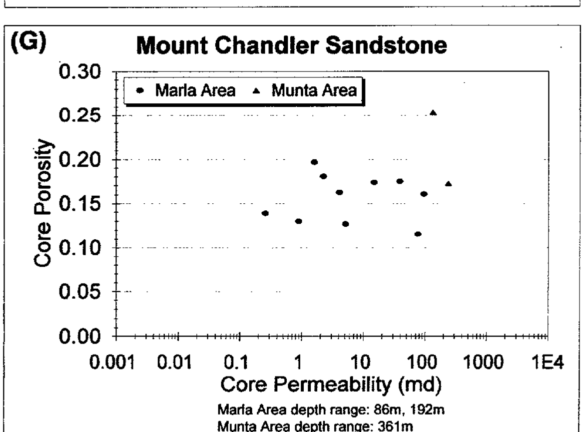

Figure 15

OFFICER BASIN SANDSTONES POROSITY PERMEABILITY CROSSPLOTS

MINES AND ENERGY SOUTH AUSTRALIA

94-271

6031

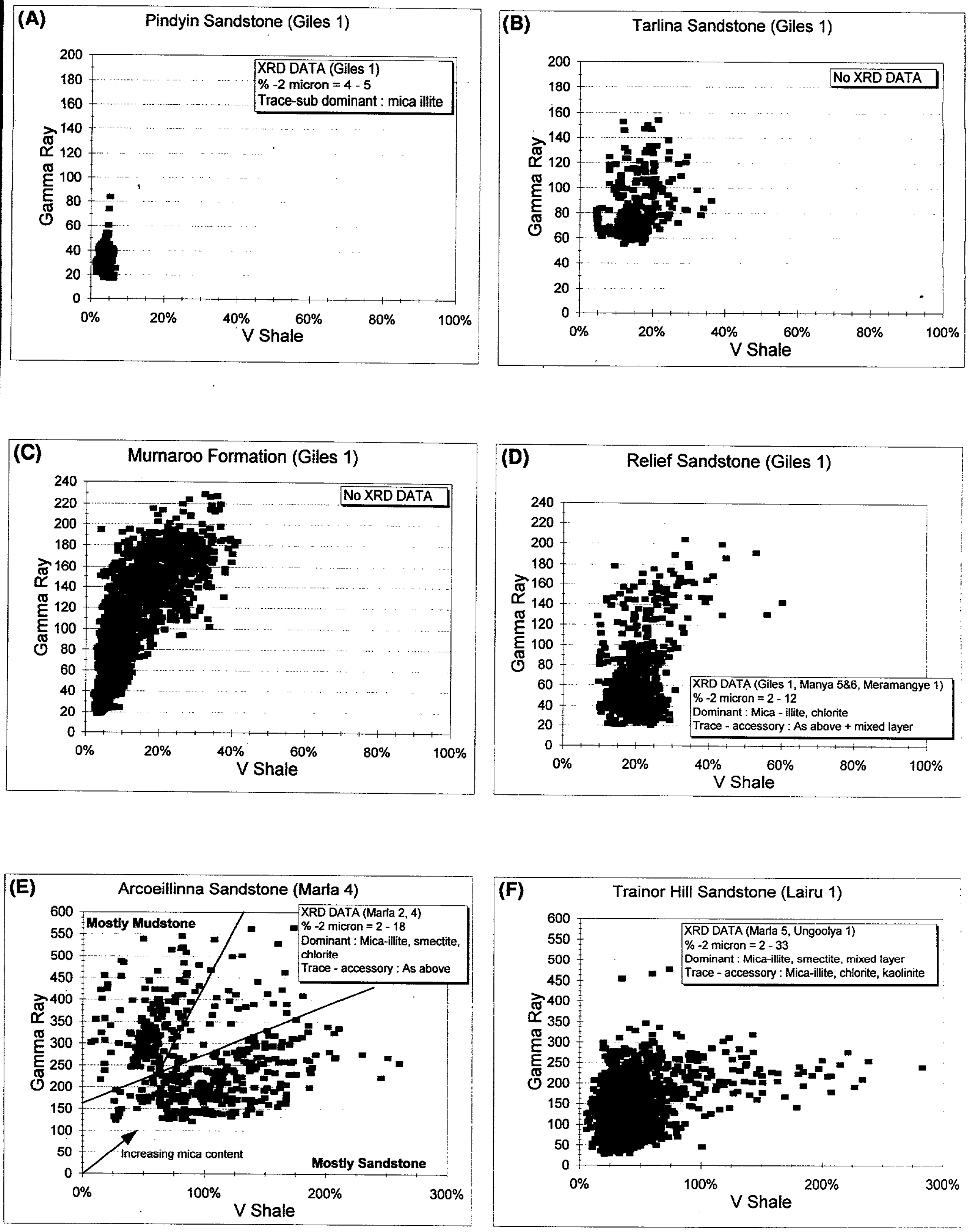

Figure 16

OFFICER BASIN SANDSTONES V SHALE GAMMA RAY CROSSPLOTS

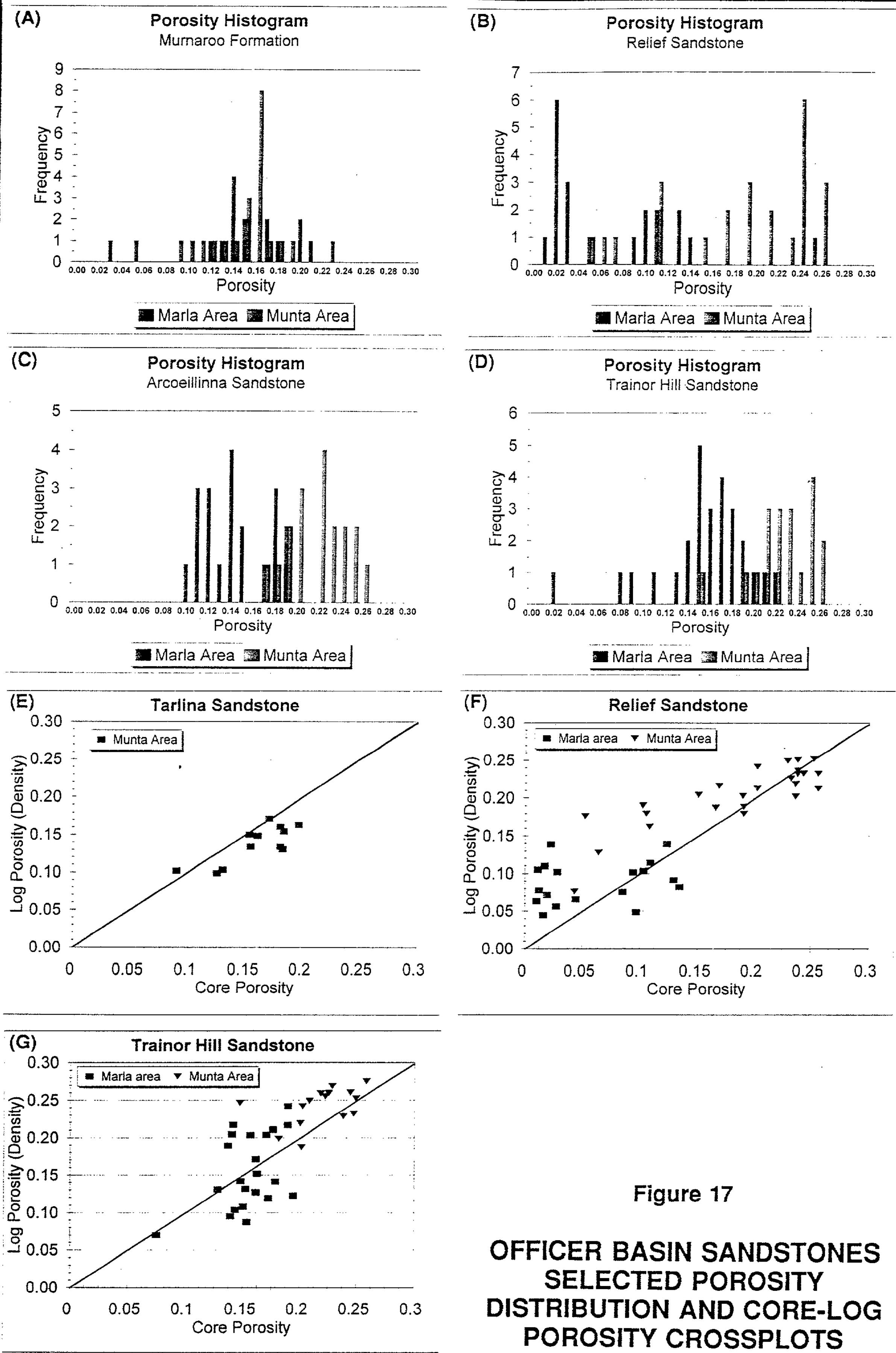

Figure 17

OFFICER BASIN SANDSTONES SELECTED POROSITY DISTRIBUTION AND CORE-LOG POROSITY CROSSPLOTS

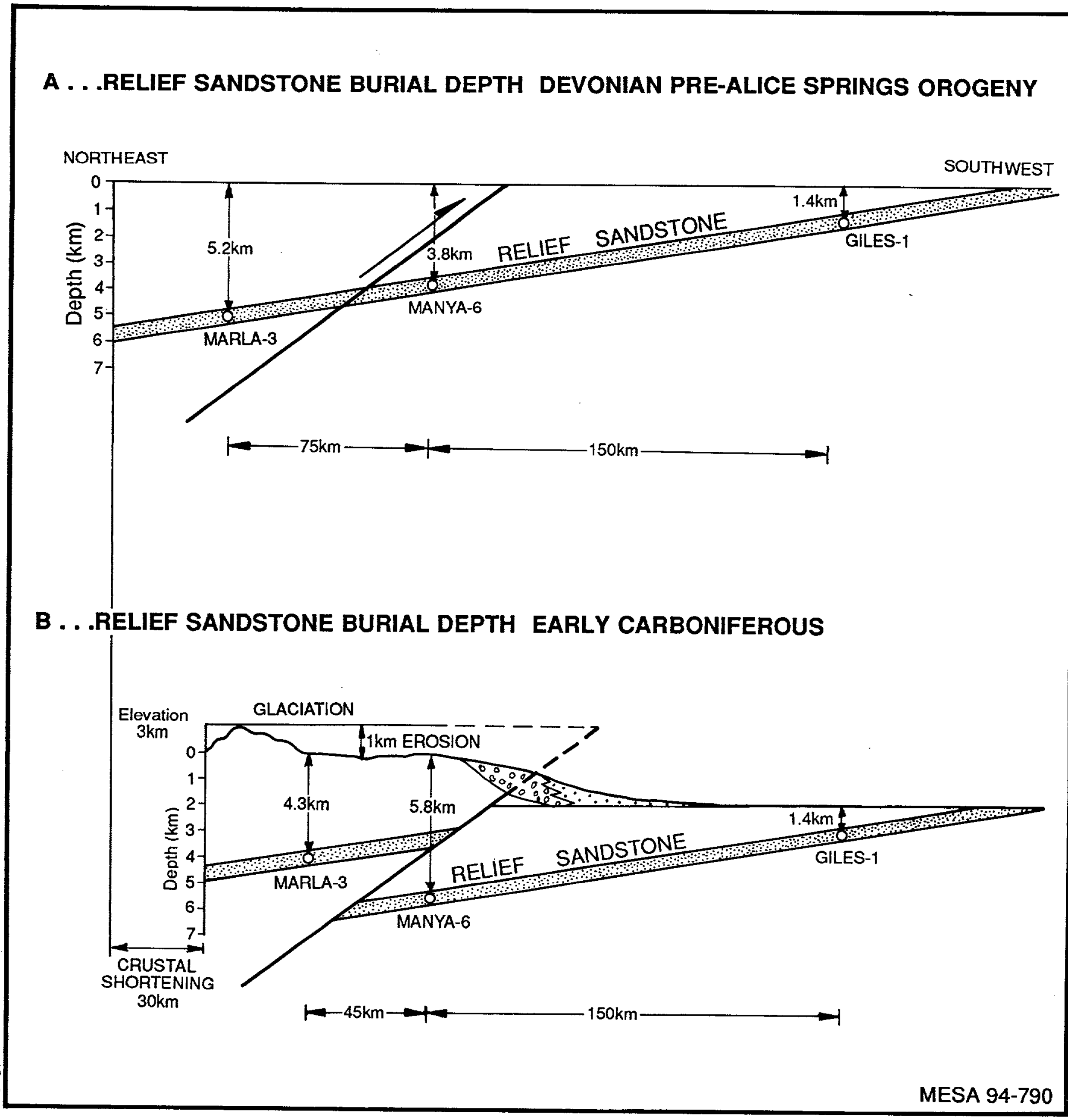

Figure 18 Suggested pre-orogenic (A) and post-orogenic (B) depths of burial for the Relief Sandstone

6031

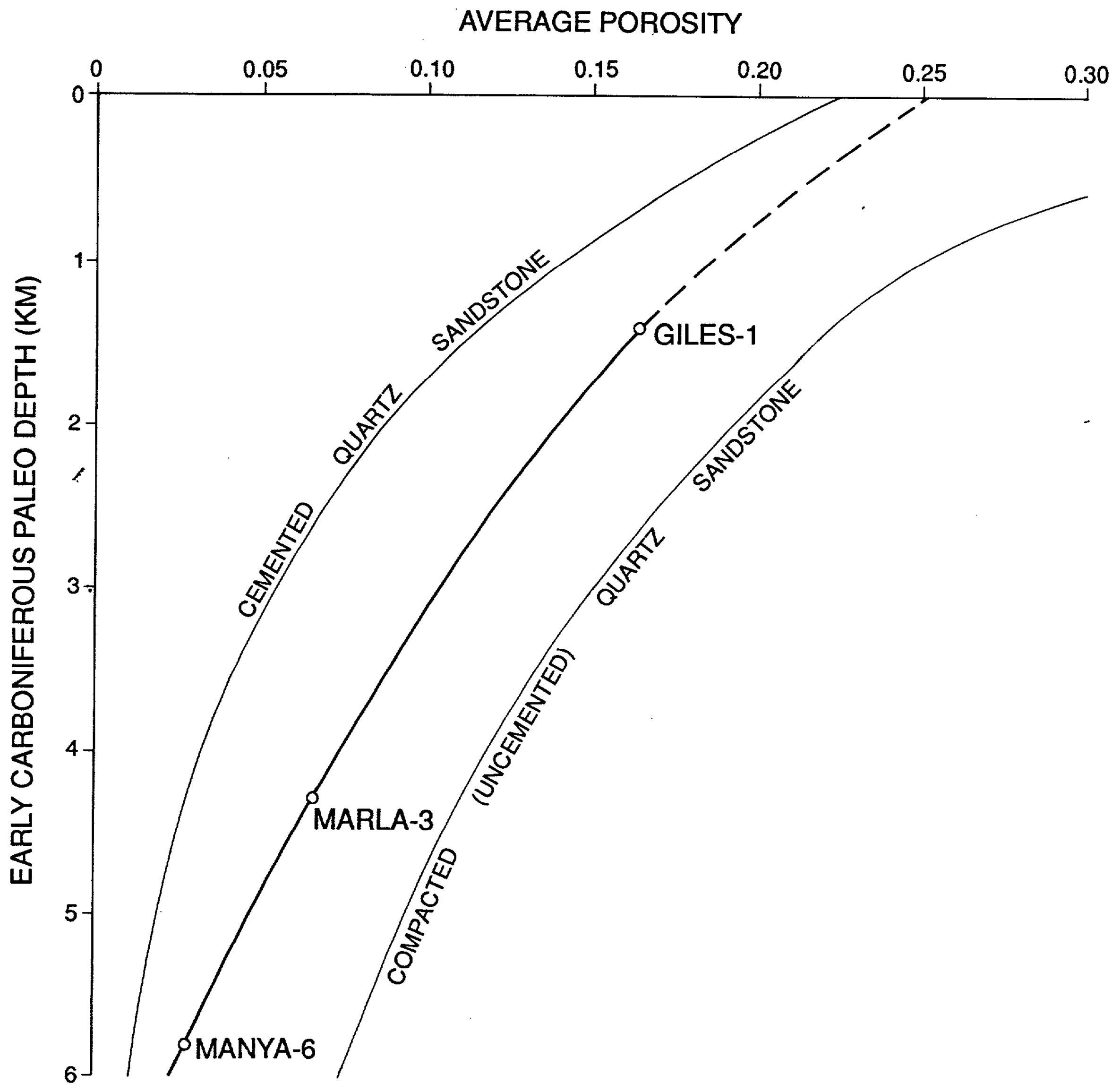

Compacted and cemented quartz sandstone curves from Bond *et al.*, (1993).

MESA 94-791

Figure 19 Relief Sandstone porosity/palaeodepth curve

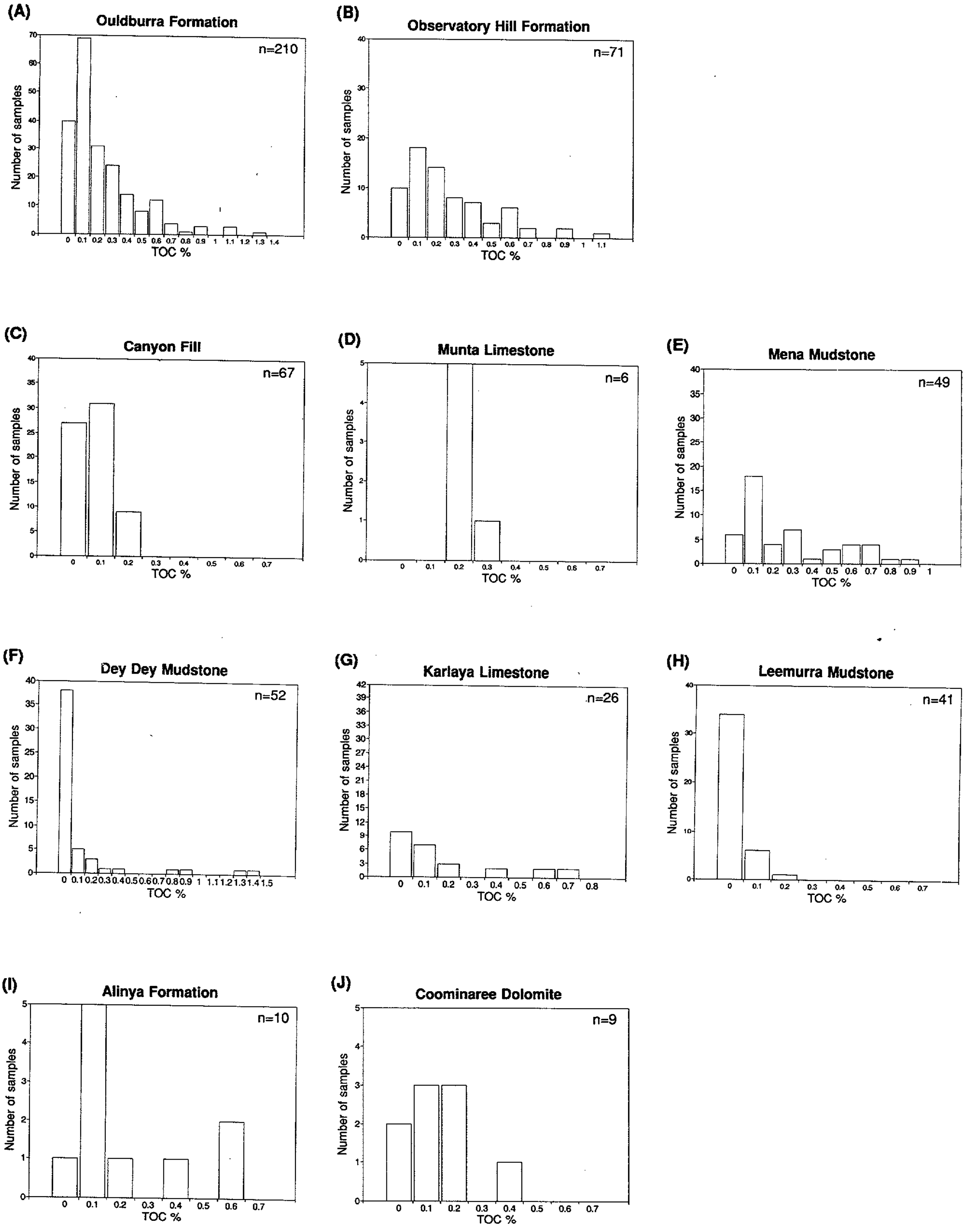

Figure 20

OFFICER BASIN TOTAL ORGANIC CARBON DISTRIBUTION BY FORMATION

Formation Tops (Metres KB)	Marla 3	Marla 4	Marla 5	Marla 6	Marla 7	Marla 8	Marla 9	Marla 10	Manya 1	Manya 2	Manya 3	Manya 4	Manya 5	Manya 6	Middle Bore 1	Byilkaoora 1	Byilkaoora 2	Byilkaoora 3
Tertiary - Recent	Surface	Surface	Surface	Surface	Surface		Surface		Surface	Surface	Surface	Surface	Surface	Surface			Surface	Surface
Jurassic - Cretaceous	9		12	4		Surface	3	Surface	32	23	3.2	14	10	8	Surface			10
Mt Toondina / Waitoona										216	54.5	98.5	? 83	? 128	? 40			
Stuart Range																		
Boorthanna									122	279	111	228		216				
Devonian																		
Blue Hills / Cartu / Mintabie																		
Indulkana Shale																	? 12	
Mount Chandler Sandstone								? 44					129				33	
Trainor Hill Sandstone		7	84					100								Surface	245	22
Apamurra Formation		82	302					416								49.6	460	91
Arcoeillinna Sandstone		150	366					476								98.5	506	148
Observatory Hill Formation	27	228	507			20		562		500						156	584	256
'Cadney Park' Formation	116	408	643	110	12	208		747		510 (3)		403		442		378 (3)	757 (3)	400 (3)
Ouldburra Formation	493			256	244				146	643	174			571	160			
Relief Sandstone	607												? 289	1686				
Upper Ungoolya Group							20 (1)											
Mena Mudstone																486 (1)		
Munta Limestone																		
Canyon Fill																		
Lower Ungoolya Group																		
Munyarai Unit																		
Leemurra Mudstone																		
Wilari Dolomite																		
Karlaya Limestone																		
Leemurra/Karlaya equivalent							170											
Dey-Dey Mudstone							288											
Murnaroo Formation							406						457					
Meramangye Formation							410											
Tarlina Sandstone + Equiv.																		
Cadlareena Volcanics													1076					
Alinya Formation													1155 (2)					
Pindyin Sandstone																		
Basement												796			371			
Total Depth	650	424	650	703	543	447	436	776	151.25	646	813	807	1333	1764.7	558	497	806.7	698
K.B.	307	311	306	311	290	329	318	300	242.5	236	244	234	294	267.1	262	335	354.5	328.1

Table 1. Officer Basin formation tops. Formations of unconfirmed identity prefixed by question mark; (1) refers to Middle-Upper Rodda Beds; (2) refers to Coominaree Dolomite; (3) refers to 'Cadney Park' + Wallatinna Formation

Formation Tops (Metres KB)	Wilkinson 1	KD-1	KD-2A	SMD 5001 L. Maurice West	SMD 5002 L. Maurice East	Murnaroo 1	Obs. Hill 1	Emu 1	Giles 1	Meramangye 1	Munta 1	Karlaya 1	Lairu 1	Ungoolya 1	Munyarai 1	Marla 1B	Marla 2
Tertiary - Recent	Surface	Surface	Surface	Surface	Surface	Surface			Surface	Surface	Surface	Surface	Surface	Surface	Surface	Surface	Surface
Jurassic - Cretaceous	? 16.5												? 9			3	2
Mt Toondina / Waitoona	? 41.5		?41												?		
Stuart Range	? 117																
Boorthanna																	
Devonian															242		
Blue Hills / Cartu / Mintabie													?95		1018		
Indulkana Shale													282		1180		
Mount Chandler Sandstone												40	293	8	1189		
Trainor Hill Sandstone											11	512	535	408	1355		
Apamurra Formation											489	959	1055	917	1442		32
Arcoeillinna Sandstone						? 27		Surface			530	1037	1091	956	1469		84
Observatory Hill Formation				60	12	45.6	Surface	30.5	8	96	702	1191	1251	1101	1562		155
'Cadney Park' Formation						? 139.1			236	254	816	1296	1355				327
Ouldburra Formation	199	26	54													83	
Relief Sandstone	685.5	402		? 156			155.2	335	304	359							
Upper Ungoolya Group																	
Mena Mudstone												1367	1409	1282			
Munta Limestone											900	1420	1650	1495			
Canyon Fill											945	1447	1670	1526	1699		
Lower Ungoolya Group																	
Munyarai Unit															1707		
Leemurra Mudstone									421			1695					
Wilari Dolomite						167.6	178.3										
Karlaya Limestone				237.6		181.9	239.6		484			2024					
Leemurra/Karlaya equivalent											1152				2155		
Dey-Dey Mudstone				316.3		208.9	259		497		1675	2090		2191	2645		
Murnaroo Formation				479.7	117.3	316.8	374.5		583		1973						
Meramangye Formation									869	451							
Tarlina Sandstone + Equiv.					508.3				1064								
Cadlareena Volcanics																	
Alinya Formation									1233								
Pindyin Sandstone									1289								
Basement					691.3												
Total Depth	710	455.9	342	603.5	738.74	627.5	400.1	417.6	1326.8	690.6	2075	2364	2039	2192.6	2898.6	379.4	352
K.B.	183.6			220	218	225.7	213	246	298	261.7	371.2	355	302	324.1	419.7	285.2	324

Table 1. Officer Basin formation tops. Formations of unconfirmed identity prefixed by question mark; (1) refers to Middle-Upper Rodda Beds; (2) refers to Coominaree Dolomite; (3) refers to 'Cadney Park' + Wallatinna Formation.

Well	Year Drilled	Objective	Total Depth (m)	Location Rationale or Trap Type	Hydrocarbon Shows
Birksgate-1	1967	Petroleum/Strat	1878	Low relief anticline	Nil
Munyarai-1	1968	Petroleum	2899	Anticline	Nil
Murnaroo-1	1976	Stratigraphic	628	Not applicable	Nil
Wilkinson-1	1978	Stratigraphic	710	Drilled in deepest part of trough	Nil
Manya-2	1980	Trona	646	Not known	Nil
Manya-3	1980	Trona	813	Not known	Non fluorescing bitumen
Manya-4	1981	Trona	807	Not known	Nil
Nicholson-1A	1981	Trona	1103	Gravity low	Nil
Nicholson-2	1981	Trona	815	Seismic/Magnetic low	Nil
WL-2	1981	Base metals	520	Magnetic anomaly	Nil
Byilkaoora-2	1982	Trona	807	LANDSAT Lineaments	*; Oil bleeds+fluorescence, Obs. Hill Fm.
Byilkaoora-3	1982	Trona	698	LANDSAT/Magnetic/Gravity	*; Oil bleeds+fluorescence, Obs. Hill Fm.
Lake Maurice East	1982	Uranium	739	LANDSAT/Radiometric/Mag.anomaly	Oil stain, Murnaroo Fm (thin section)
Lake Maurice West	1982	Uranium	604	LANDSAT/Radiometric/Mag.anomaly	Oil stain, Murnaroo Fm (thin section)
Manya-5	1982	Trona	1333	Flank of gravity high	OIl extract from core, Murnaroo Fm.
Manya-6	1982	Trona	1765	Graben indicated by Gravity/Magnetics.	Oil stain, Ouldburra Fm (thin section)
Mt Willoughby-2	1982	Trona/Coal	500	Not known	Nil
Marla-3	1984	Trona	650	Drilled to assist seismic interp.	Nil
Marla-5	1984	Trona	650	Drilled to assist seismic interp.	*; Oil bleeds+fluorescence, Obs. Hill Fm.
Marla-6	1984	Trona	703	Drilled to assist seismic interp.	Nil
Marla-7	1984	Trona	543	Drilled to assist seismic interp.	Nil
Meramangye-1	1984	Stratigraphic/Trona	691	Not known	Nil
Giles-1	1985	Petroleum	1327	Anticline	Nil
Marla-10	1985	Trona	776	Seismic pinchout	*; Oil bleeds+fluorescence, Obs. Hill Fm.
Middle Bore-1	1985	Base metals	558	Magnetic anomaly	Nil
Ungoolya-1	1985	Petroleum	2193	Anticline	Fluorescence, crush cut, Obs. Hill Fm & upper Ungoolya Group
Karlaya-1	1987	Petroleum	2363	Subunconformity/anticline	Poor-fair oil bleeds, Leemurra/Dey-Dey Mudstone. Very minor oil, Obs. Hill Fm
Lairu-1	1987	Petroleum	2040	Down flank fractures	V. minor oil shows, Observatory Hill Fm
Munta-1	1987	Petroleum	2075	Subunconformity	Nil
Rodda-2	1990	Stratigraphic	1083	Outcropping anticline	Nil

Table 2. Location rationale and hydrocarbon shows in drillholes 500m or deeper. ***: Refer to Table 3 for further details**

BYILKAOORA 2

Formation tops (m)

Post Observatory Hill Formation See Table 1.

584.0	**- 757.0**	**Observatory Hill Formation**
584.0	- 619.0	Oolarinna Member
619.0	- 655.0	Moyles Chert Marker bed
655.0	- 683.0	Unnamed
683.0	- 757.0	Parakeelya Alkali Member
757.0	- 769.0	'Cadney Park' Formation
769.0	- 806.7	Wallatinna Formation

Hydrocarbon shows (m)

Observatory Hill Formation

610.3 - 612.8	90-100% gold fluorescence occurs in intervals 6-24 cm thick. Shows are parallel to bedding. Oil staining is 70-100%. Minor oil bleeds.
639.0 - 645.9	Fractures filled with oily bituminous material. Gold fluorescence over 20-80% of fracture surface.
664.8 - 671.0	Minor (<5%) gold fluorescence from fractures and laminae. However to 30% fluorescence in intervals 670.0 - 670.4, 671.0 - 671.29 and 675.5 - 675.8.
671.0 - 673.7	60-100% gold fluorescence. Bituminous material bleeds from fractures and vugs.
673.7 - 685.7	Minor gold fluorescence from fractures and laminae.
685.7 - 744.6	Bleeding oil from fractures and vugs is common throughout. In the interval 710.4 - 719.9 solid buff fluorescence occurs in intervals to 10 cm thick. Gold fluorescence along laminae (5 mm maximum thickness) is apparent throughout.

'Cadney Park' Formation

764.0 - 772.0	Gold pin point fluorescence. Sample tested at 769.8 gave a slow cut and left a film residue. From 770.3 - 772.0 gold patchy to solid fluorescence. Bitumen filled fractures.

Wallatinna Formation

773.0 - 776.30	Trace gold pin point fluorescence in conglomerate matrix and siltstone. Bitumen filled fractures at 775.2 and 775.9.

Table 3 Oil shows in wells in the Marla Overthrust Zone.

BYILKAOORA 3

Formation tops (m)

Post Observatory Hill Formation See Table 1.

256.0 -	**400.0**	**Observatory Hill Formation**
256.0 -	296.5	Oolarinna Member
296.5 -	340.0	Moyles Chert Marker bed
340.0 -	400.0	Parakeelya Alkali Member
400.0 -	698.0	'Cadney Park' Formation

Hydrocarbon shows (m)

Observatory Hill Formation

263.0 -	270.3	Minor (<5%) gold fluorescence from vertical calcite filled fractures.
270.3 -	270.8	40% gold fluorescence along laminae.
270.8 -	282.3	Minor gold fluorescence associated with fractures and disturbed bedding. Small oil bleeds every metre.
298.3 -	298.4	Very small bleed from fracture.
306.9 -	307.0	Small bleed from fracture.
309.4 -	309.5	Patch of gold fluorescence, 10 x 50 mm
317.5 -	317.7	Minor fluorescence associated with fracture.
322.5 -	322.6	Bitumen bleed from 0.5 mm vug.
322.6 -	331.6	Minor light oil bleeds from fractures and laminae.
331.6 -	333.6	Trace (1%) oil bleeds from fractures.
335.1 -	343.2	Oil bleeds from predominantly vertical fractures. Fractures partly filled with calcite and vuggy. Significant bleeds at 338.3 - 338.7.
343.2 -	357.7	Minor to 10% fluorescence. Medium oil (and bitumen) bleeds from fractures (vertical, horizontal and cross-cutting). Minor bleeding from between intraclasts.
357.7 -	366.2	Trace gold fluorescence associated with fractures.
366.2 -	366.6	5% fluorescence. Oil bleeds from vuggy porosity associated with fractures.
369.0 -	374.9	Trace gold fluorescence associated with fractures. Oil bleed at 368.0 - 369.0.
378.2 -	382.3	Minor tarry oil to bitumen bleeds associated with fractures. Significant bleed at 378.4 - 378.6.

Table 3 Oil shows in wells in the Marla Overthrust Zone.

MARLA 2

Formation tops (m)

Post Observatory Hill Formation See Table 1.

154.5 -	**327.0**	**Observatory Hill Formation**
154.5 -	197.0	Oolarinna Member
197.0 -	212.0	Moyles Chert Marker bed
212.0 -	266.0	Unnamed
266.0 -	312.0	Parakeelya Alkali Member
312.0 -	327.0	Unnamed
327.0 -	352.0	'Cadney Park' Formation

Hydrocarbon shows (m)

Observatory Hill Formation

201.5 -	202.9	Minor (<5%) bitumen in calcite filled fractures. Fractures are mostly vertical along core axis.
202.9 -	205.5	Gold fluorescence along laminae to 30 mm thick and as occasional patches. Equals a mixture of mineral and petroleum fluorescence. The latter gives a slow crush cut. Minor bitumen in fractures as above.
259.7 -	272.5	Minor small tarry bleeds along calcite filled fractures. Diameter of the bleeds is mostly less than 3 mm, however to 10 mm at 262.9.
272.5 -	277.6	Bituminous to light oil bleeds associated with calcite filled fractures and small vugs (millimetre diameter). Extensive bleeds occur at 272.50 - 272.55, 274.8 - 274.9, 275.67 - 275.74, 275.86 - 275.94 and 277.47 - 277.54. At 273.5 10% light oil staining occurs associated with pin point vugs.
282.9 -	283.5	Minor bitumen associated with calcite filled fractures.
289.2 -	289.6	As above.
293.7 -	293.9	As above.
295.2 -	295.5	Minor bitumen in calcite filled fractures. Occasional oil bleeds to 5 mm diameter from fractures.
289.9 -	299.0	Minor bitumen in calcite filled fractures.
299.2 -	299.35	Gold fluorescence along laminae to 5 mm and patches to 10 mm diameter.
304.3 -	306.4	Dominantly bluish white mineral fluorescence with minor yellow oil fluorescence.
306.4 -	306.5	Fiery orange fluorescence along laminae to 10 mm. Medium crush cut, leaves ring residue.
307.4 -	307.6	Fiery orange fluorescence over 90% of core gives slow crush cut and leaves ring residue. Limestone with spotty evaporite pseudomorphs.
307.6 -	307.8	Minor bitumen in calcite filled fracture.

Table 3 Oil shows in wells in the Marla Overthrust Zone.

MARLA 4

Formation Tops (m)

Post Observatory Hill Formation See Table 1.

228.0 - 408.0	**Observatory Hill Formation**	
228.0 - 284.0	Oolarinna Member	
284.0 - 314.0	Moyles Chert Marker bed	
314.0 - 350.0	Unnamed	
350.0 - 408.0	Parakeelya Alkali Member	
408.0 - 424.0	'Cadney Park' Formation	

Hydrocarbon shows (m)

Observatory Hill Formation

288.5 - 290.0	Minor (<5%) light oil bleeds. Oil staining to 10 mm diameter, fluorescence to 50 mm. Shows associated with millimetre to pin point vuggy porosity.
343.1 - 346.9	5% gold fluorescence from light oil bleeds as above and along laminae to 5 mm.
346.9 - 361.6	Trace small oil bleeds. Approximately one per metre.
361.6 - 365.5	5-10% gold fluorescence. All from light oil bleeds associated with fractures, partially filled with calcite and having millimetre size vuggy porosity. Bleeds to 50 mm diameter.
365.5 - 373.9	To 5% oil bleeds as above.
376.2 - 397.9	Trace oil bleeds as above. One exception is a large bleed, 70 mm diameter from a rosette evaporite pseudomorph interval.

Table 3 Oil shows in wells in the Marla Overthrust Zone.

MARLA 5

Formation tops (m)

Post Observatory Hill Formation See Table 1.

507.0 - 643.0		**Observatory Hill Formation**
507.0 - 546.0		Oolarinna Member
546.0 - 549.0		Moyles Chert Marker bed
549.0 - 586.0		Unnamed
586.0 - 603.0		Parakeelya Alkali Member
603.0 - 643.0		Unnamed
643.0 - 650.0		'Cadney Park' Formation

Hydrocarbon shows (m)

Observatory Hill Formation

520.3 - 520.7	Light oil bleeds from vertical, calcite filled fracture. Bleeds to 10 mm diameter.
521.9 - 524.2	Minor (<5%) gold fluorescence along laminae to 5 mm thickness. Oil staining over half of this.
529.8 - 531.1	Fluorescence as above. Minimal oil staining. From 530.8 - 531.1 oil fluorescence associated with horizontal, calcite filled fractures.
531.8	Light oil bleed, 30 mm diameter.
533.0 - 533.1	Gold fluorescence associated with calcite filled fracture. Minimal oil staining.
545.0	Minor gold fluorescence along laminae. Laminae less than 5 mm.
574.2 - 577.3	Minor small oil bleeds from calcite filled fractures.
577.3 - 587.9	Large light oil bleeds over 5% of core surface. Trace (1%) gold fluorescence along laminae. Bleeds associated with vertical and horizontal fractures.
587.9 - 589.6	40% gold fluorescence along laminated to thinly bedded dolomite.
589.6 - 589.8	40% gold fluorescence. Lithology is silty limestone with rosette shaped evaporite pseudomorphs.
589.8 - 596.1	Minor gold fluorescence associated with fractures. No large oil bleeds.
596.7 - 600.1	5-10% gold fluorescence associated with fractures. Large bleed at 596.7.
600.1 - 605.9	Trace fluorescence associated with fractures. Large bleed at 605.9.
610.5	Large oil bleed.
614.2	Minor gold fluorescence along laminae.
618.4 - 619.0	Trace fluorescence associated with fractures which are partly filled with calcite.

Table 3 Oil shows in wells in the Marla Overthrust Zone.

MARLA 8

Formation tops (m)

Post Observatory Hill Formation See Table 1.

20.0 -	**209.0**	**Observatory Hill Formation**
20.0 -	97.0	Oolarinna Member
97.0 -	144.0	Moyles Chert Marker bed
144.0 -	209.0	Parakeelya Alkali Member
209.0 -	447.0	'Cadney Park' Formation

Hydrocarbon shows (m)

Observatory Hill Formation

74.9 -	77.8	Minor (<5%) oil bleeds associated with fractures and vuggy porosity.
82.9 -	84.7	As above.
133.3 -	134.6	Minor tarry to medium oil bleeds from vuggy porosity in a zone of disturbed bedding.
135.8 -	135.9	Very tarry oil bleed.
141.6		Small bleed.
148.1		Oil stained horizontal, calcite filled fracture.
150.8 -	171.5	Medium oil to tarry bleeds every 1 to 2 metres associated with fractures and vuggy porosity. Extensive medium oil bleed from 164.4-165.6m.
175.5 -	175.6	Medium oil bleed from 10 mm diameter vug.
190.4 -	191.9	Oil bleeds associated with vertical calcite filled fractures and vuggy porosity.
203.1 -	203.2	Bitumen filling vugs to 10 mm diameter.
204.7		Medium oil bleed, 30 mm diameter, from a vug.
204.9 -	205.5	Millimetre size flecks of bitumen in vugs.
207.3 -	207.4	Oil stained, calcite filled fracture.

Table 3 Oil shows in wells in the Marla Overthrust Zone.

MARLA 9

Formation tops (m)

Post Ungoolya Group See Table 1.

20.0	**406.0**	**Ungoolya Group**
20.0	170.0	Upper Ungoolya Group
170.0	288.0	Leemurra/Karlaya Equivalent
288.0	406.0	Dey-Dey Mudstone
406.0	410.0	Murnaroo Formation
410.0	436.0	Meramangye Formation

Hydrocarbon shows (m)

Ungoolya Group

232.6	288.3	Trace fluorescence associated with calcite filled fractures in siltstone. Rare flecks of bitumen. From 265.9 fractures occur every one to two metres. Fractures 2.5-30.0 mm thick. Oil bleeds reported in well completion report are not visible therefore may have evaporated. Samples tested gave a very slow crush cut and left a thin ring residue. Possible oil staining at 259.3 and 260.3.
327.9	328.0	Weak oil bleeds from vugs associated with calcite filled fractures in non-calcareous siltstone.

Table 3 Oil shows in wells in the Marla Overthrust Zone.

MARLA 10

Formation tops (m)

Post Observatory Hill Formation See Table 1.

561.5 - 747.0		**Observatory Hill Formation**
561.5	- 651.0	Oolarinna Member
651.0	- 692.0	Moyles Chert Marker bed
692.0	- 730.0	Parakeelya Alkali Member
730.0	- 747.0	Unnamed
747.0	- 776.0	'Cadney Park' Formation

Hydrocarbon shows (m)

Observatory Hill Formation

624.3 - 625.8	Minor (<5%) gold fluorescence from fractures and along laminae. Tarry oil bleeds to 10 mm diameter.
632.3 - 634.5	5% fluorescence from heavy oil bleeds from vugs and calcite filled fractures.
678.6 - 695.2	5% fluorescence from tarry to light oil bleeds, to 20 mm diameter, associated with fractures. Fractures are horizontal and vertical, are partly filled with calcite and have a vuggy porosity.
700.1 - 700.9	Minor fluorescence from medium oil bleeds from vertical fractures. Bleeds to 10 mm diameter.
709.2 - 709.7	Minor medium oil bleeds from vugs.
710.6 - 710.8	As above.
715.1 - 715.2	As above.

Table 3 Oil shows in wells in the Marla Overthrust Zone.

Table 4. Officer Basin DST's

Well	**Lairu 1**		
Formation	**Arcoeillinna Sandstone**	Water cushion	**0 m**
Depth	**1089.3 - 1097.5 metres**	Reservoir Pressure	**1495 psia**
DST	**1**	Reservoir Temperature	**565 R**
Flow	**No Flow To Surface**		
Recovery	**4 m Rat hole mud, 24 m Filtrate & muddy water, 793 m Cloudy water and fine sand.**		
Comments	**Calculated flow rate of 619 BWPD.**		

Well	**Munta 1**		
Formation	**Murnaroo Formation**	Water cushion	**0 m**
Depth	**1980.59 - 1985.5 metres**	Reservoir Pressure	**2787 psia**
DST	**1**	Reservoir Temperature	**624 R**
Flow	**163.9 BWPD**		
Recovery	**35 m Rat hole mud, 53 m Non H/C gas cut watery mud, 364 m Non H/C gas cut water.**		

0339

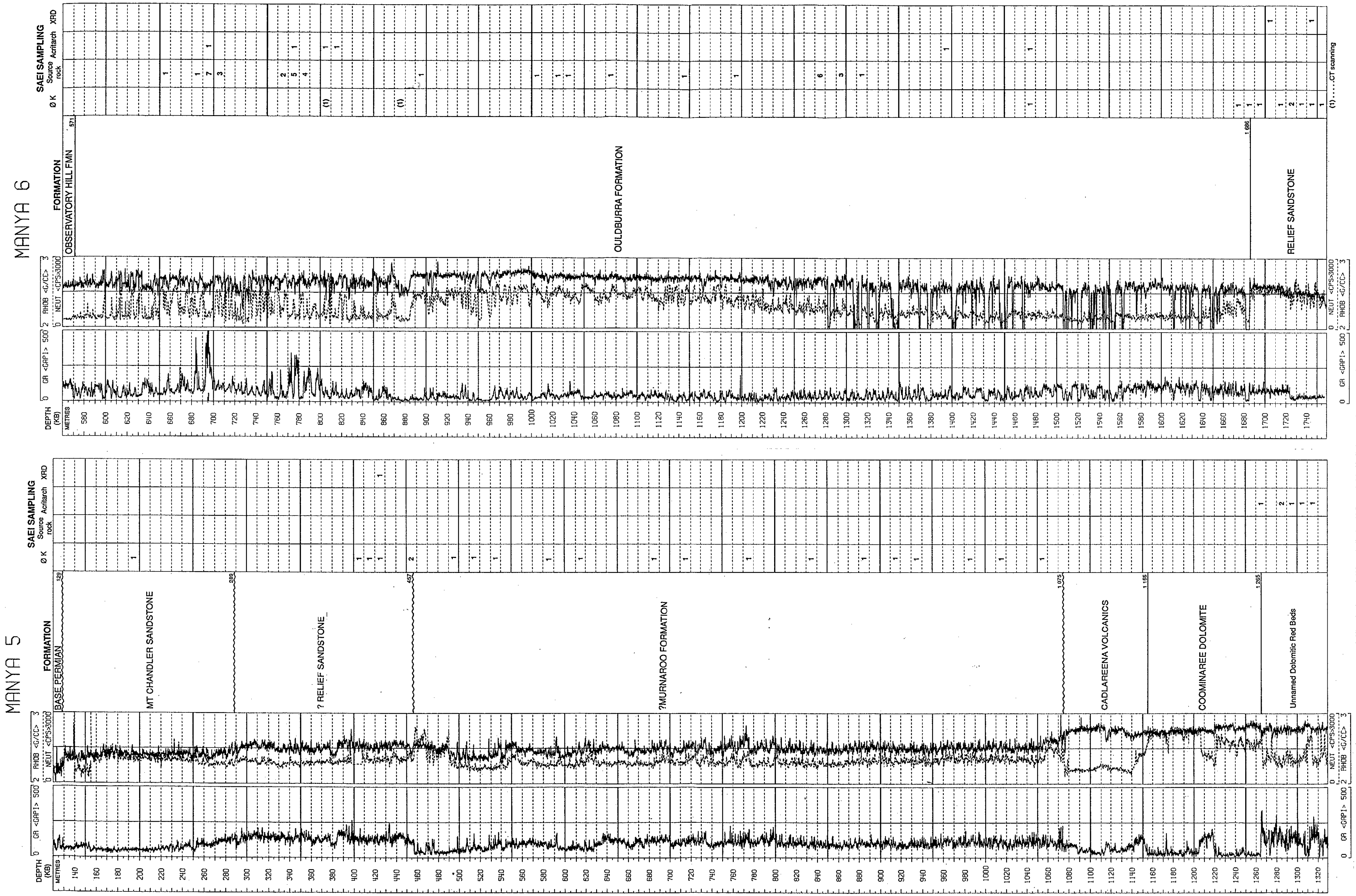

MINES AND ENERGY SOUTH AUSTRALIA

EASTERN OFFICER BASIN
SELECTED GEOLOGICAL SAMPLING
MANYA 5,6

94-148

Enclosure 2

MARLA 2

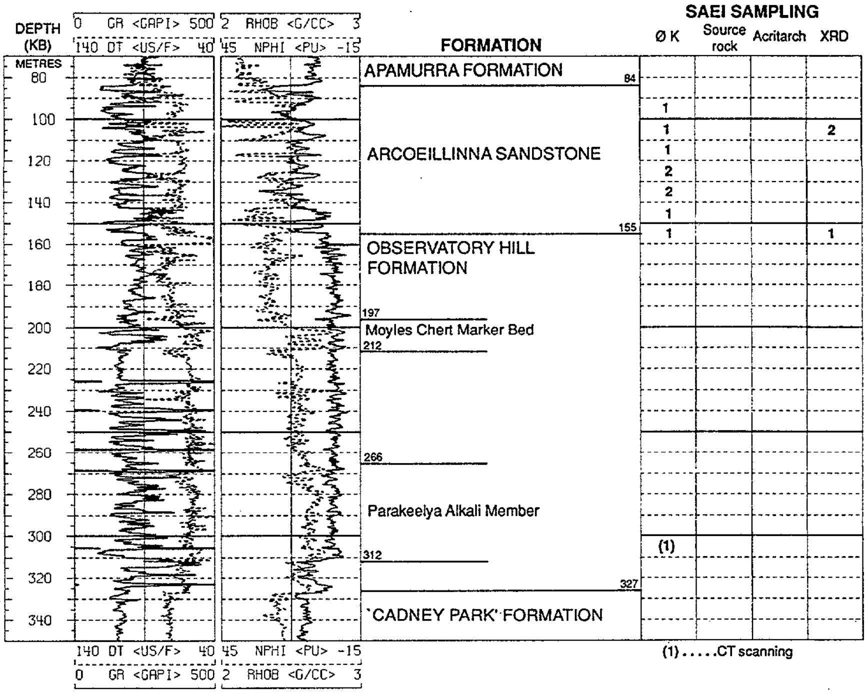

MARLA 3

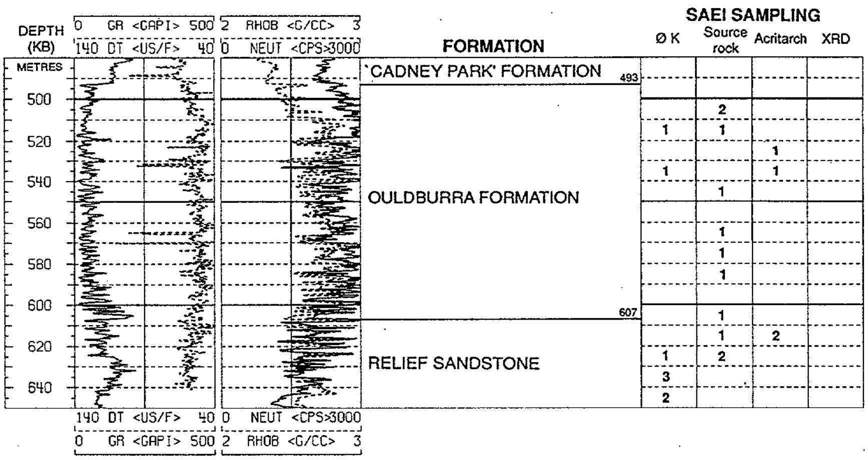

MARLA 4

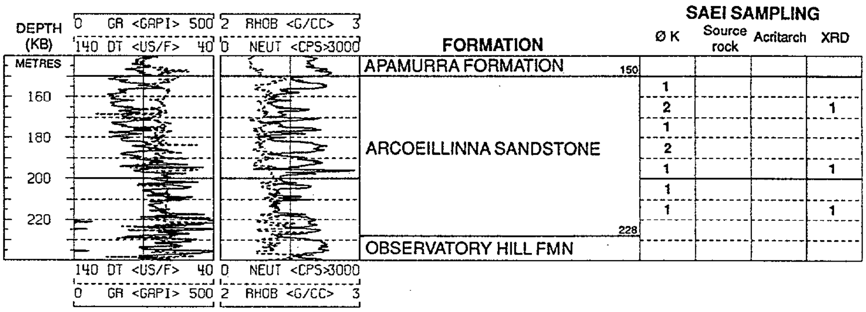

Enclosure 3

EASTERN OFFICER BASIN
SELECTED GEOLOGICAL SAMPLING
MARLA 2,3,4

MINES AND ENERGY
SOUTH AUSTRALIA

94-149

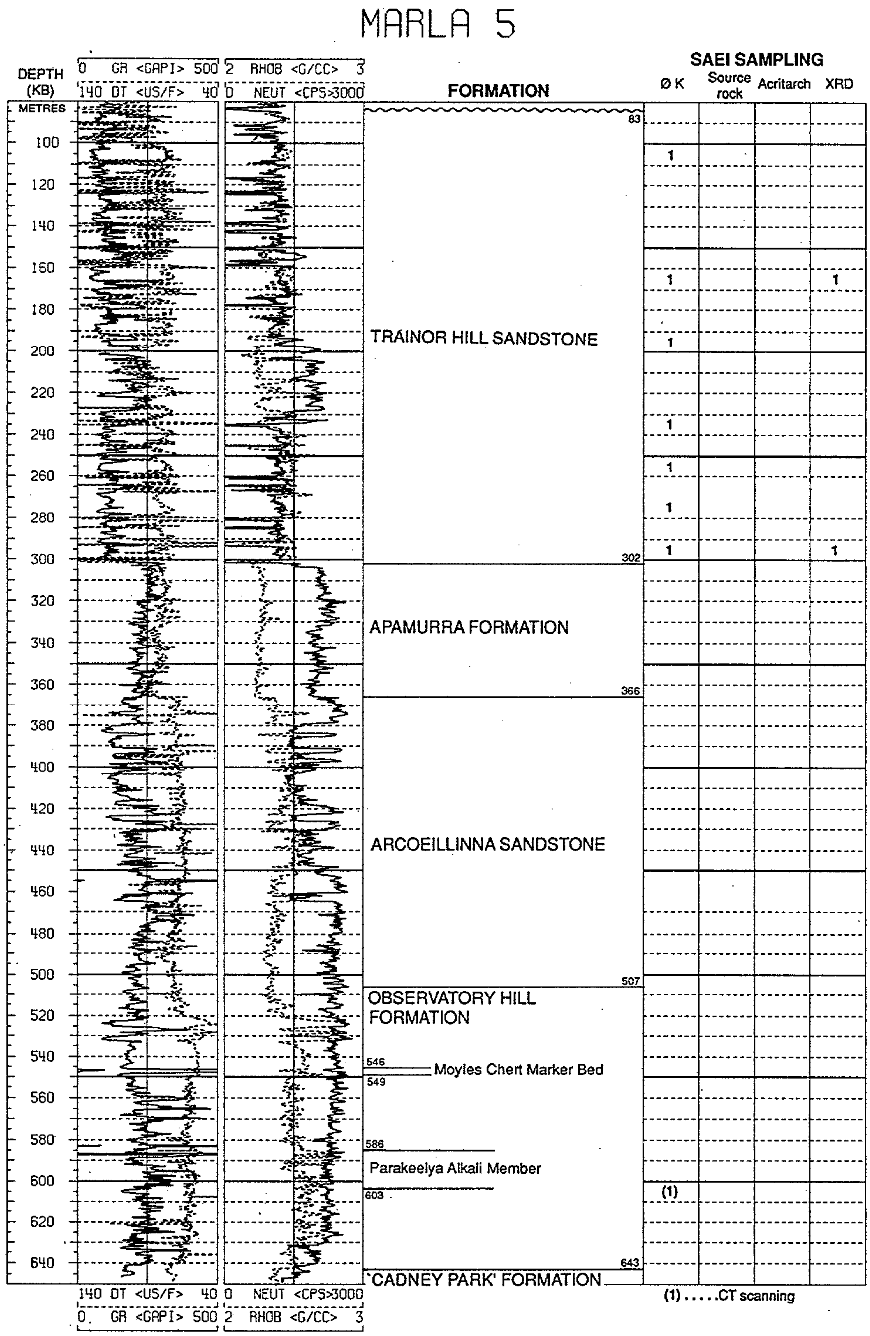

Enclosure 4

EASTERN OFFICER BASIN
SELECTED GEOLOGICAL SAMPLING
MARLA 5

MINES AND ENERGY
SOUTH AUSTRALIA

94-150

MARLA 6

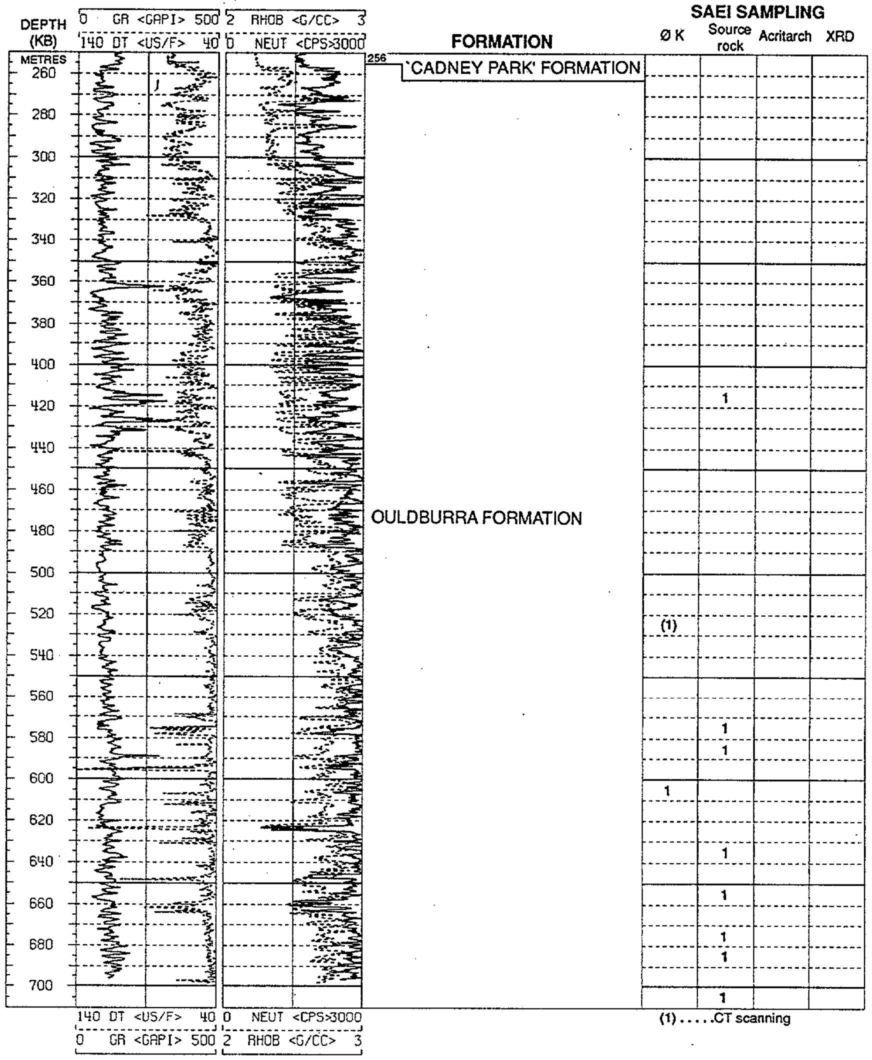

Enclosure 5

EASTERN OFFICER BASIN
SELECTED GEOLOGICAL SAMPLING
MARLA 6

MINES AND ENERGY
SOUTH AUSTRALIA

94-151

MARLA 7

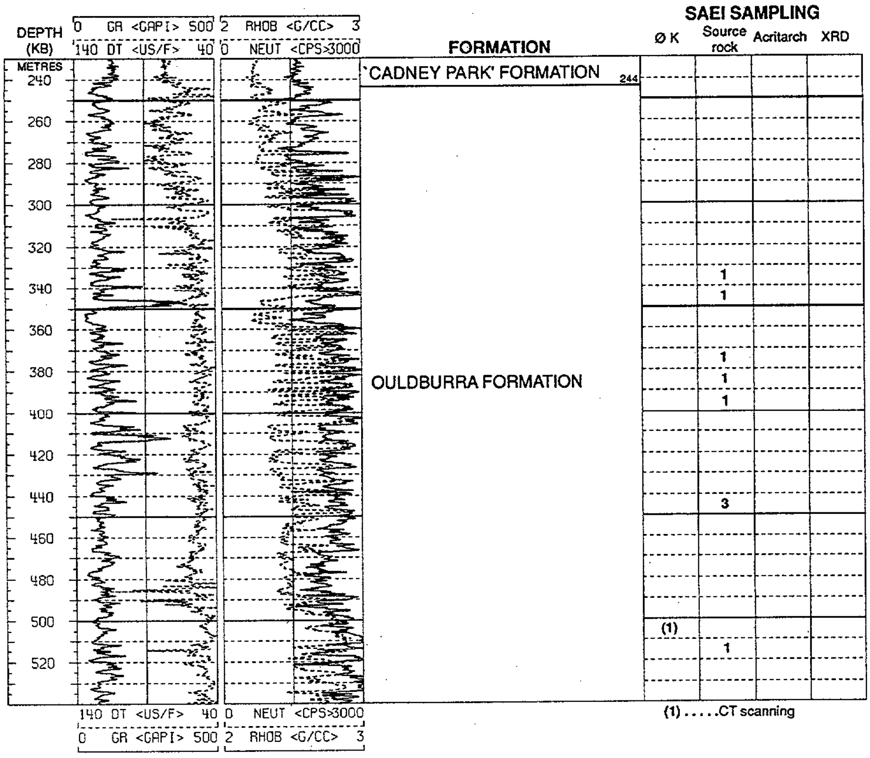

MARLA 9

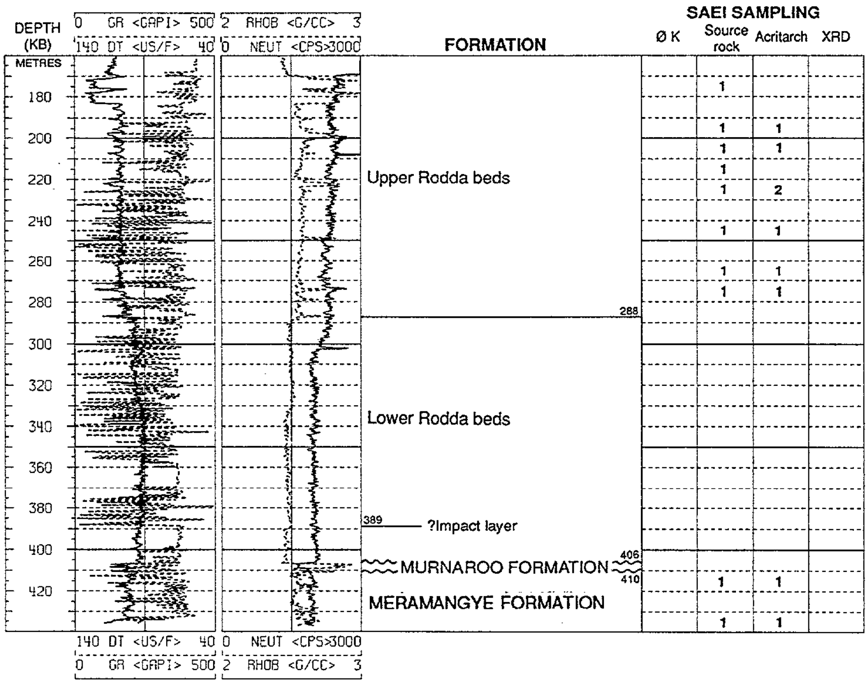

Enclosure 6

EASTERN OFFICER BASIN
SELECTED GEOLOGICAL SAMPLING
MARLA 7,9

MINES AND ENERGY
SOUTH AUSTRALIA

94-152

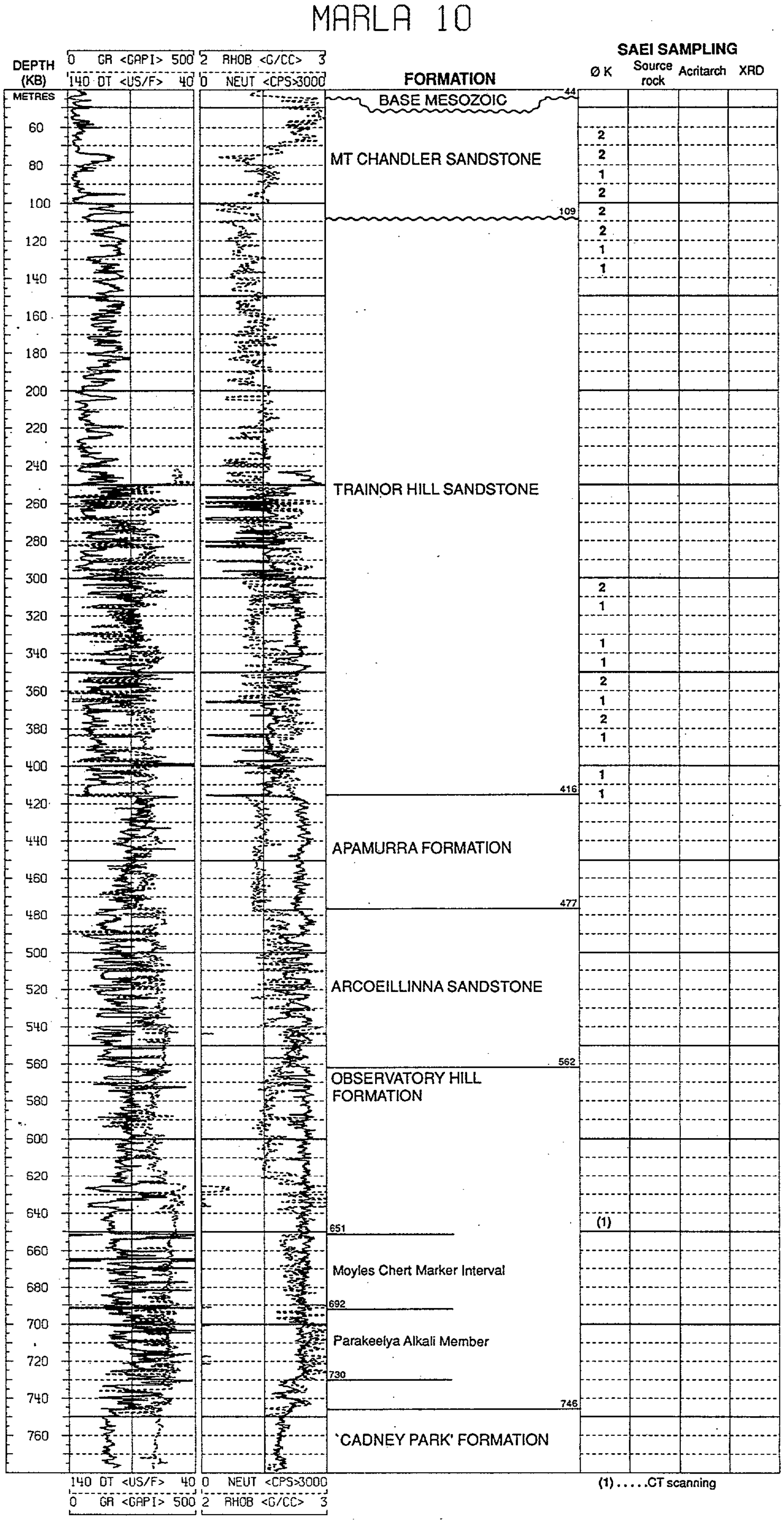

Enclosure 7

EASTERN OFFICER BASIN
SELECTED GEOLOGICAL SAMPLING
MARLA 10

MINES AND ENERGY
SOUTH AUSTRALIA

94-153

BIRKSGATE 1

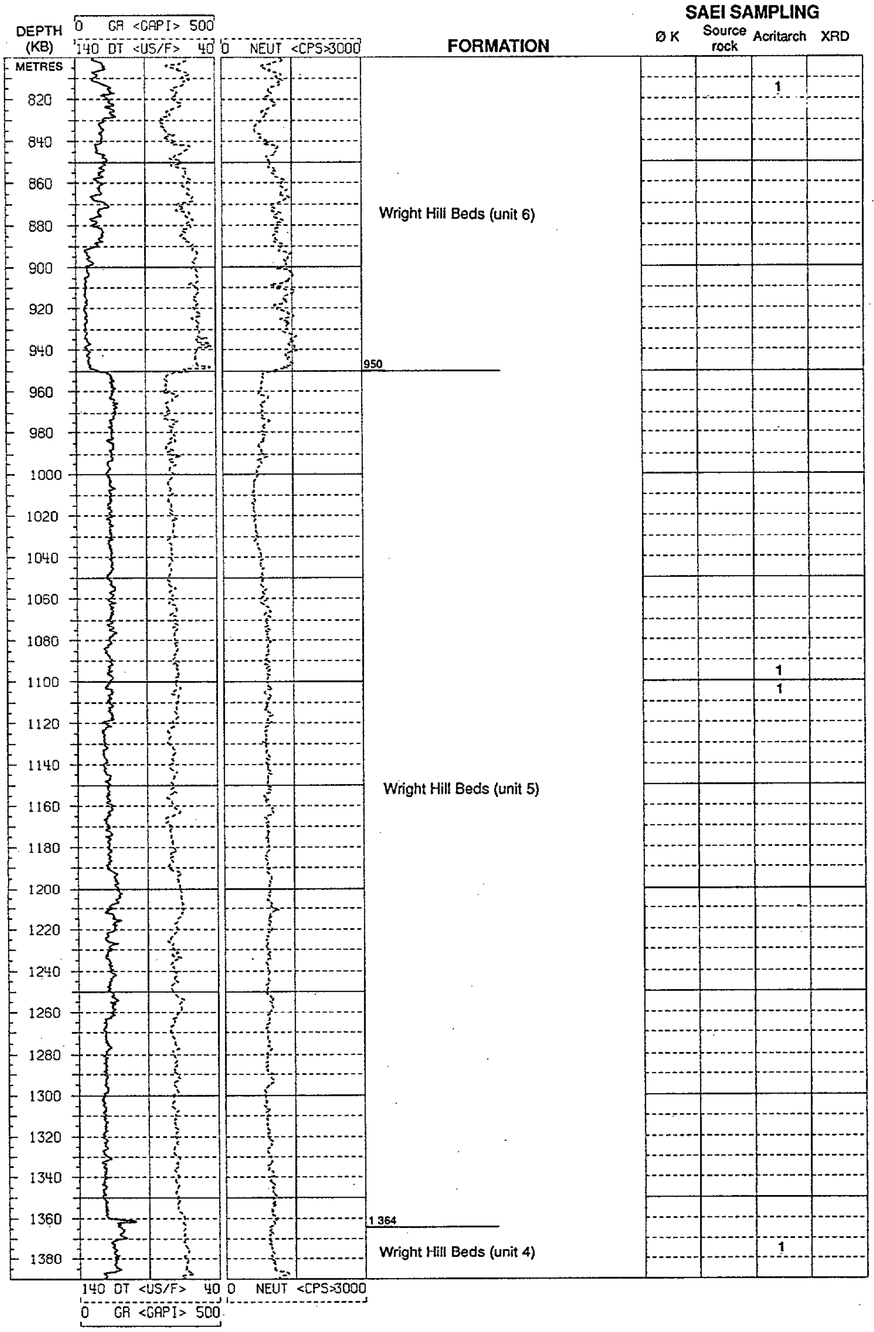

Enclosure 8

EASTERN OFFICER BASIN
SELECTED GEOLOGICAL SAMPLING
BIRKSGATE 1

MINES AND ENERGY
SOUTH AUSTRALIA

94-154

0346

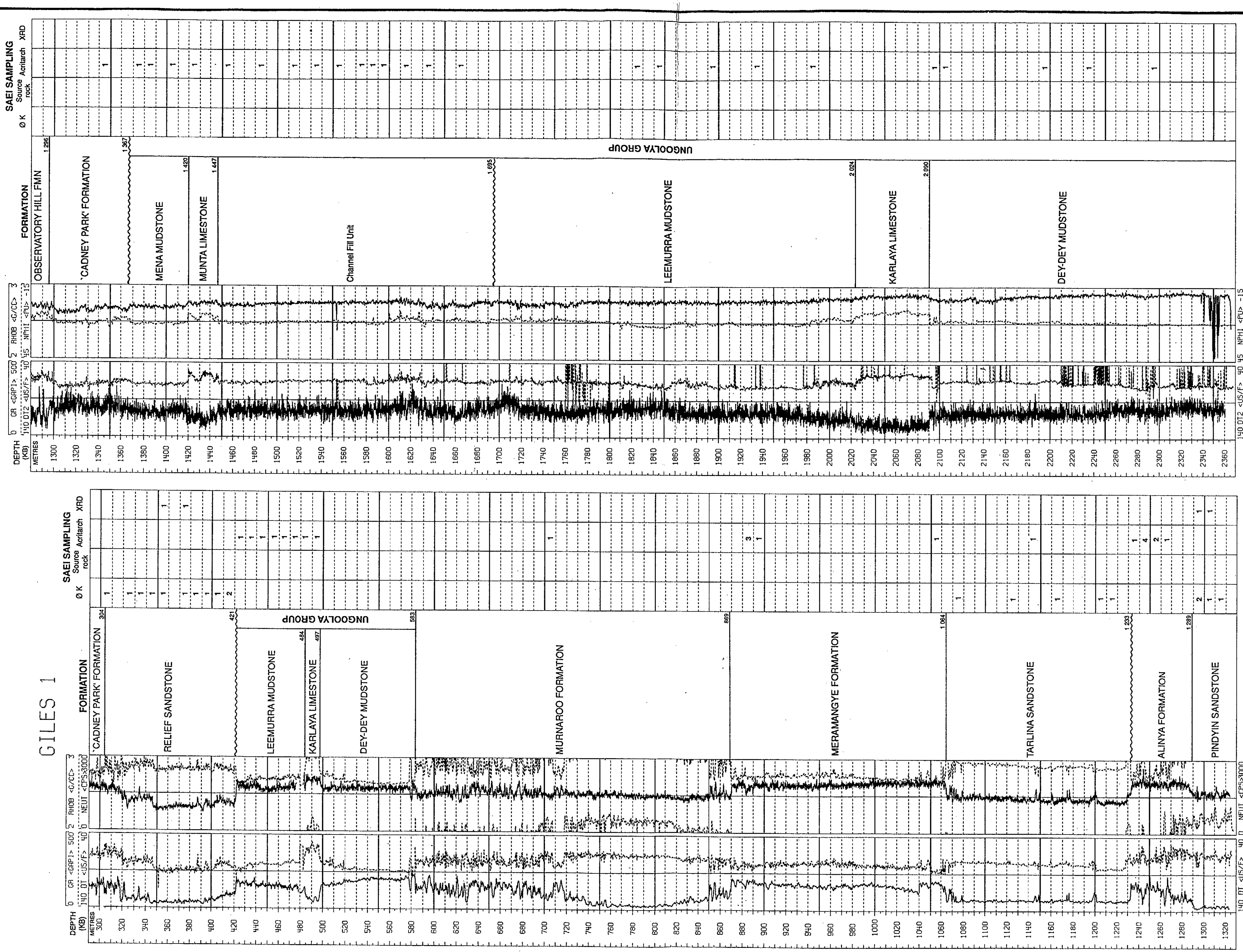

Enclosure 9

EASTERN OFFICER BASIN
SELECTED GEOLOGICAL SAMPLING
GILES 1, KARLAYA 1

MINES AND ENERGY SOUTH AUSTRALIA

94-155

0347

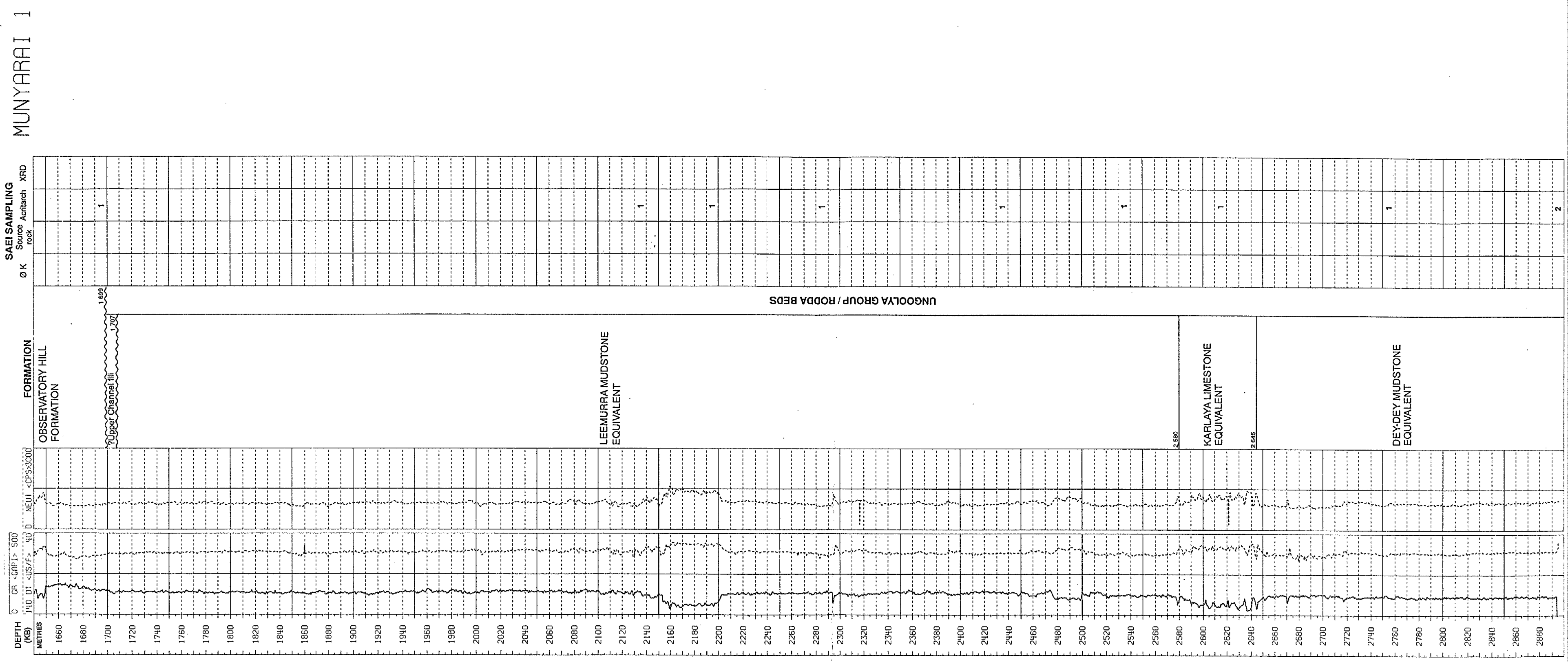

Enclosure 10

EASTERN OFFICER BASIN
SELECTED GEOLOGICAL SAMPLING
MUNYARAI 1

MINES AND ENERGY
SOUTH AUSTRALIA

94-156

0348

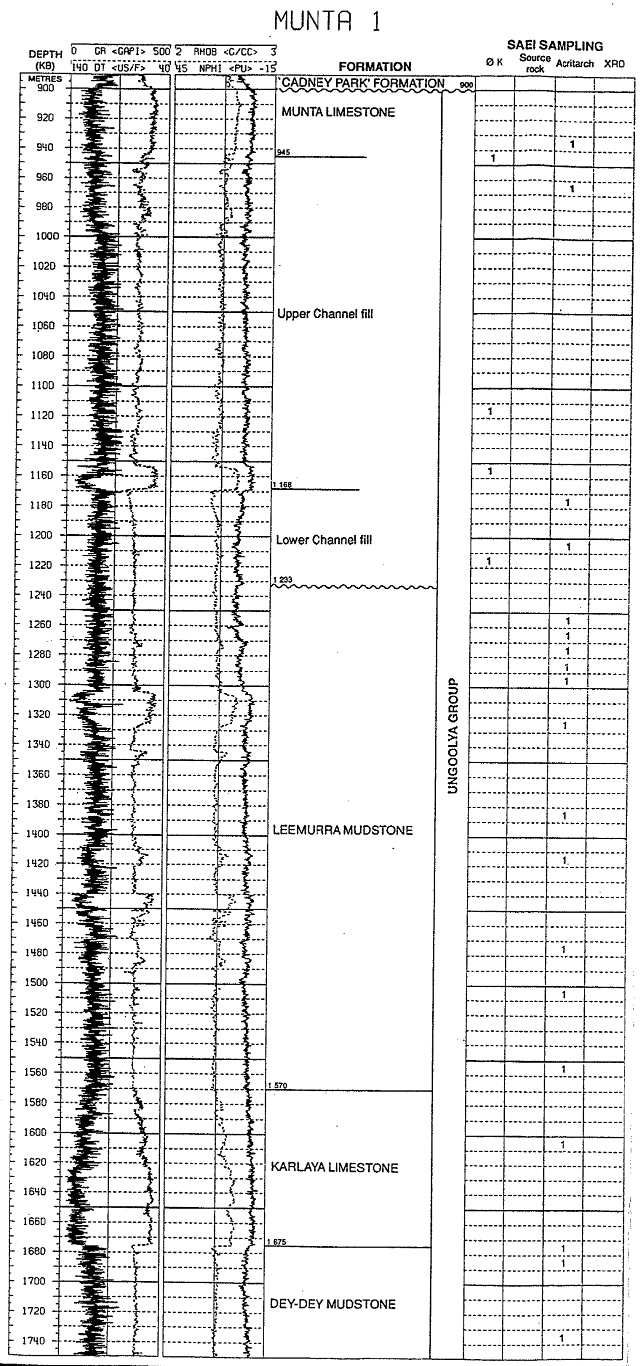

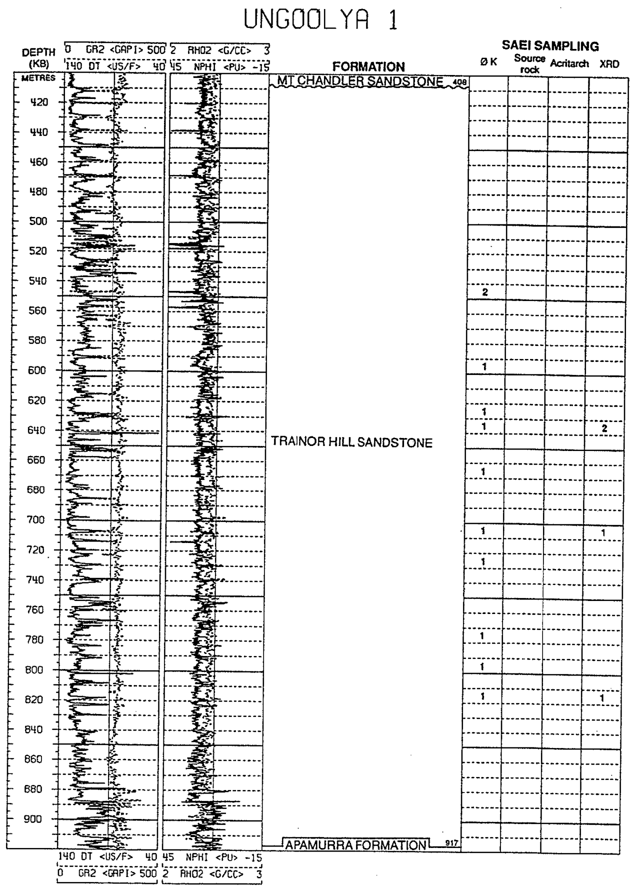

MINES AND ENERGY
SOUTH AUSTRALIA

94-158

Enclosure 11

EASTERN OFFICER BASIN
SELECTED GEOLOGICAL SAMPLING
MUNTA 1, UNGOOLYA 1

BYILKAOORA 1

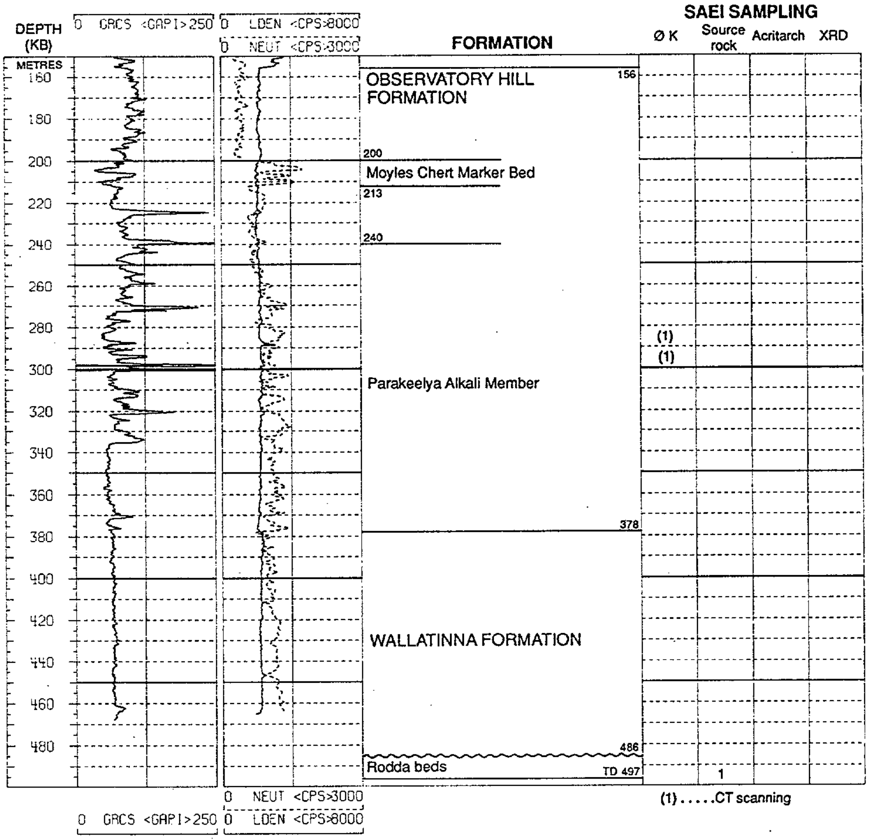

BYILKAOORA 2

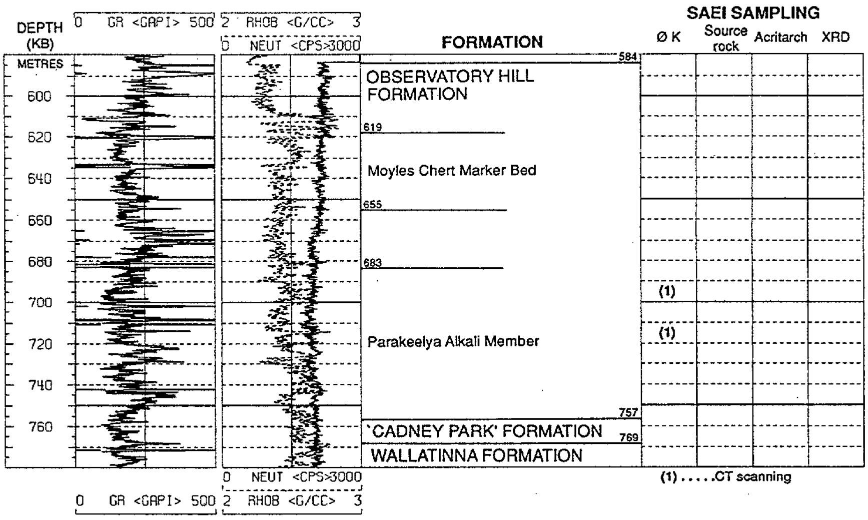

Enclosure 12

EASTERN OFFICER BASIN
SELECTED GEOLOGICAL SAMPLING
BYILKAOORA 1,2

MINES AND ENERGY
SOUTH AUSTRALIA

94-147

0350

EASTERN OFFICER BASIN

GEOLOGY AND HYDROCARBON POTENTIAL

D.I. Gravestock & A. Sansome

South Australian Department of Mines & Energy

VOLUME 3

APPENDICES

July 1994 Envelope 8591

NEOPROTE.ROZ

APPENDIX 1

Core analysis and XRD raw data reports

REPORT 008-244
OFFICER BASIN
CORE ANALYSIS

ACS
LABORATORIES
AUSTRALIA

25 November 1993

South Australian Department of Mines & Energy
191 Greenhill Road
PARKSIDE SA 5063

Attention: Information Officer

REPORT: 008-244

CLIENT REFERENCE:	58GR2/A06/956
MATERIAL:	Core
LOCALITY:	Officer Basin
WORK REQUIRED:	Core Analysis

Please direct technical enquiries regarding this work to the signatory below under whose supervision the work was carried out.

ROBERT D EAST
Technical Services Manager

ANTHONY M DRAKE
Laboratory Supervisor
Special Core Analysis

Adelaide Office: PO Box 109, Eastwood, SA 5063 Australia
Phone: 61 8 379 9888 Facsimile: 61 8 379 9288

ACS Laboratories Pty. Ltd.
ACN: 008 273 005

CONTENTS

LIST OF TABLES

1. INTRODUCTION

A order dated 21 October 1993 was received from Alan Sansome of SADME requesting Routine Core Analysis services on selected samples from the Officer Basin.

2. SAMPLE PREPARATION

2.1 Plug Drilling

One inch diameter plug samples were drilled and trimmed from the whole core using tap water to cool the bit and remove drilled solids.

2.2 Sample Drying

Samples were dried in a conventional oven at 80°C to constant weight and placed in a desiccator.

3. PERMEABILITY TO AIR - Ambient

Air permeability was determined on the plug samples. The samples were firstly placed in a Hassler cell with a confining pressure of 250 psi. The confining pressure was used to prevent bypassing of air around the samples when the measurement was made. To determine permeability a known air pressure was applied to the upstream face of the sample, creating a flow of air through the core plug. Permeability for the samples was calculated using Darcy's Law through knowledge of the upstream pressure, flow rate, viscosity of air and the samples' dimensions.

4. HELIUM INJECTION POROSITY - Ambient

The porosity of the clean dry core plugs was determined as follows. The plugs were first placed in a sealed matrix cup. Helium held at 100 psi reference pressure was then introduced to the cup. From the resultant pressure change the unknown grain volume was calculated using Boyle's Law (ie, $P_1V_1 = P_2V_2$).

The bulk volume was determined by mercury immersion. The difference between the grain volume and the bulk volume is the pore volume and from this the 'effective' porosity was calculated as the volume percentage of pores with respect to the bulk volume.

5. ABSOLUTE GRAIN DENSITY

A dried plug offcut was used for this measurement. The sample was crushed to grain size and weighed. The volume of the grains was determined by pycnometry and density calculated through knowledge of the sample weights and volumes.

30 November 1993

POROSITY AND AIR PERMEABILITY

Company South Australian Department of Mines & Energy
Well Officer Basin

Ambient

Sample Number	Well	Depth	Ambient Permeability to Air, millidarcys	Ambient Porosity, fraction	Grain Density (gms/cm^3)
RS516	Marla 2	98.3	2.58	14.1	2.62
RS519	Marla 2	106.5	0.49	12.2	2.66
RS520	Marla 2	113.1	0.20	11.0	2.66
RS521	Marla 2	121.6	8.58	14.0	2.65
RS522	Marla 2	126.3	1.53	11.6	2.64
RS523	Marla 2	136.4	1.99	13.6	2.67
RS524	Marla 2	139.0	0.17	10.6	2.64
RS525	Marla 2	140.5	0.09	9.6	2.66
RS526	Marla 2	150.1	22.8	13.0	2.63
RS527	Marla 3	627.3	0.22	4.4	2.64
RS528	Marla 3	630.35	7.04	9.7	2.61
RS529	Marla 3	632.0	0.02	2.8	2.66
RS530	Marla 3	635.45	0.03	1.6	2.66
RS531	Marla 4	156.0	7.39	13.1	2.63
RS532	Marla 4	162.0	61.2	17.2	2.63
RS533	Marla 4	169.1	85.8	18.1	2.63
RS534	Marla 4	173.15	0.20	13.3	2.65
RS535	Marla 4	180.3	41.0	18.8	2.65
RS536	Marla 4	187.45	22.5	18.0	2.63
RS538	Marla 4	196.5	38.4	17.6	2.66
RS539	Marla 4	208.1	0.07	10.0	2.84
RS540	Marla 4	214.8	9.53	16.3	2.66
RS541	Marla 5	105.7	18.0	14.1	2.63
RS543	Marla 5	167.2	27.2	17.6	2.63
RS544	Marla 5	192.6	269	18.9	2.63
RS545	Marla 5	238.9	169	17.0	2.62
RS546	Marla 5	256.6	167	15.6	2.68
RS547	Marla 5	273.0	121	18.9	2.64
RS548	Marla 5	294.2	65.9	14.0	2.65
RS90	Manya 5	410.2	0.44	10.3	2.65
RS91	Manya 5	420.0	0.26	10.9	2.66
RS92	Manya 5	450.0	0.38	9.4	2.67
RS203	Manya 6	1698.3	0.08	2.7	2.66
RS204	Manya 6	1706.4	0.02	1.9	2.64
RS206	Manya 6	1713.8	0.04	1.0	2.66

Sample Number	Well	Depth	Ambient Permeability to Air, millidarcys	Ambient Porosity, fraction	Grain Density (gms/cm^3)
RS207	Manya 6	1720.9	0.03	1.7	2.64
RS208	Manya 6	1725.8	0.03	2.2	2.63
RS209	Manya 6	1732.75	0.02	1.1	2.66
RS210	Manya 6	1741.8	0.04	1.7	2.64
RS211	Manya 6	1755.0	24.6	12.3	2.63
RS386	Giles 1	304.1	0.16	4.3	2.65
RS387	Giles 1	327.5	58.9	10.8	2.68
RS388	Giles 1	337.1	651	19.0	2.65
RS389	Giles 1	346.8	8033	24.3	2.63
RS390	Giles 1	356.0	3788	25.2	2.63
RS392	Giles 1	374.0	2319	23.8	2.63
RS394	Giles 1	386.1	1424	23.6	2.64
RS395	Giles 1	396.0	733	15.0	2.66
RS396	Giles 1	406.6	71.6	5.2	2.63
RS397	Giles 1	410.7	113	10.2	2.62
RS398	Giles 1	418.9	1053	20.2	2.63
RS399	Giles 1	1079.3	1.24	13.0	2.69
RS400	Giles 1	1125.4	1.09	15.3	2.69
RS401	Giles 1	1164.35	3.18	18.0	2.69
RS402	Giles 1	1201.6	0.67	18.2	2.72
RS403	Giles 1	1211.35	0.50	19.6	2.71
RS404	Giles 1	1296.6	0.12	6.5	2.68
RS406	Giles 1	1298.8	0.51	8.4	2.67
RS407	Giles 1	1302.1	16.2	13.8	2.68
RS409	Giles 1	1311.6	0.39	9.4	2.67
RS410	Meramangye 1	410.0	5526	23.8	2.64
RS411	Meramangye 1	417.9	2607	23.8	2.64
RS413	Meramangye 1	421.1	2842	20.2	2.68
RS414	Meramangye 1	422.9	5947	25.6	2.63
RS415	Meramangye 1	426.9	6297	22.9	2.65
RS417	Meramangye 1	430.15	334	16.8	2.64
RS418	Meramangye 1	433.1	782	19.0	2.64
RS419	Meramangye 1	437.5	1667	23.2	2.63
RS420	Meramangye 1	440.7	64.7	10.5	2.67
RS421	Meramangye 1	443.7	135	18.9	2.62
RS423	Meramangye 1	447.1	1036	23.6	2.62
RS373	Ungoolya 1	546.8	1713	24.6	2.63
RS374	Ungoolya 1	547.9	24.0	14.7	2.63
RS375	Ungoolya 1	599.7	377	20.1	2.63
RS376	Ungoolya 1	621.1	1712	22.5	2.64
RS378	Ungoolya 1	639.0	1711	20.2	2.64
RS379	Ungoolya 1	667.2	5429	24.9	2.64
RS381	Ungoolya 1	702.3	1746	21.8	2.64
RS382	Ungoolya 1	724.35	666	23.8	2.64
RS383	Ungoolya 1	775.4	1872	24.4	2.64
RS384	Ungoolya 1	795.1	536	20.8	2.65
RS385	Ungoolya 1	812.25	1212	22.2	2.64
RS27	Munta 1	1975.0			2.68
RS28	Munta 1	1976.2			2.66
RS29	Munta 1	1976.9			2.65

Sample Number	Well	Depth	Ambient Permeability to Air, millidarcys	Ambient Porosity, fraction	Grain Density (gms/cm^3)
RS30	Munta 1	1977.9			2.64
RS31	Munta 1	1978.65			2.85
RS32	Munta 1	1979.25			2.65
RS33	Munta 1	1980.0			2.64
RS34	Munta 1	1981.1			2.63
RS35	Munta 1	1982.0			2.63
RS36	Munta 1	1982.9			2.63

0360

AMDEL CORE SERVICES

7 May 1993

Department of Mines and Energy
PO Box 151
EASTWOOD SA 5063

Attention: The Information Officer

REPORT: HF/212

CLIENT REFERENCE: 11/06/0800

MATERIAL: Core Plugs

LOCALITY: Officer Basin

WORK REQUIRED: Special Core Analysis

Please direct technical enquiries regarding this work to the signatory below under whose supervision the work was carried out.

ROBERT D EAST
Technical Services Manager

ANTHONY M DRAKE
Laboratory Supervisor
Special Core Analysis

Adelaide Office: P.O. Box 109, Eastwood, SA 5063 Australia.
Telephone: 61 8 379 9888 Facsimile: 61 8 379 9288
Amdel Core Services Pty Limited
(Incorporated in South Australia)
ACN: 008 273 005

CONTENTS

LIST OF FIGURES

PAGE

LIST OF TABLES

PAGE

1. INTRODUCTION

Correspondence between Amdel Core Services (ACS) and SA Dept Mines & Energy resulted in a special core analysis study being ordered on selected samples from the Officer Basin.

The principal aims of the analysis were to provide the following information:

- **Porosity and Air Permeability at Ambient**

  These data were requested at ambient conditions. The procedure is outlined in sections 3 and 4.

- **High Pressure Mercury Injection**

  High pressure mercury injection capillary pressure data was also requested. This data is useful for rock typing as the shape of the capillary pressure curve, and the resultant pore throat size distribution data can be useful in identifying lithological units. Common shape characteristics and distribution data often signify a common depositional environment and diagenetic sequence assisting subdivision of the reservoir section into units with similar geological and petrophysical characteristics.

2. SAMPLE PREPARATION

One inch diameter samples were taken at the selected points through the core. Tap water was used as the bit lubricant and coolant to drill the plugs.

The samples were trimmed to suitable length and faced square.

3. PERMEABILITY TO AIR

Air permeability was determined on the plug samples. The samples were firstly placed in a Hassler cell with a confining pressure of 250 psi (1720 kPa). The confining pressure was used to prevent bypassing of air around the samples when the measurement was made. To determine permeability a known air pressure was applied to the upstream face of the sample, creating a flow of air through the core plug. Permeability for the samples was calculated using Darcy's Law through knowledge of the upstream pressure, flow rate, viscosity of air and the samples' dimensions.

4. HELIUM INJECTION POROSITY

The porosity of the clean dry core plugs was determined as follows. The plugs were first placed in a sealed matrix cup. Helium held at 100 psi reference pressure was then introduced to the cup. From the resultant pressure change the unknown grain volume was calculated using Boyle's Law (ie, $P_1V_1 = P_2V_2$).

The bulk volume was determined by mercury immersion. The difference between the grain volume and the bulk volume is the pore volume and from this the 'effective' porosity was calculated as the volume percentage of pores with respect to the bulk volume.

5. CAPILLARY PRESSURE - Mercury Injection (Air-Mercury)

Offcuts from selected samples were utilised for capillary pressure determinations by the mercury injection technique. The mercury injection apparatus used is a semi-automatic Micromeritics Autopore 9200 which operates up to a pressure of 60,000 psia, and can measure intrusions as small as 0.0001 cm^3 per gram of sample. This instrument was chosen for these analyses as opposed to the standard mercury pump because of its greater accuracy and ability to reach very high pressures. This was thought to be important as mineralogical studies had indicated that microporosity could be present in these samples in association with clay platelets.

The Micromeritics Autopore records mercury intrusion by measuring the capacitance change between the capillary of mercury contained in the penetrometer and an outer metal sheath as mercury invades the samples. For pressures up to 24 psia, air pressure is used. Hydraulic oil is used to achieve the higher pressures. No volume corrections for pressure effects were made, since below 24 psia they are negligible, whilst for higher pressures, the penetrometer experiences equal external and internal pressures and mercury compression is offset by penetrometer compression.

All samples were dried in a vacuum oven at temperatures not exceeding 90°C and placed into calibrated glass penetrometers. These consist of a sample chamber and attached precision bore capillary. The sample sizes are selected so that the estimated pore volume is less than the capillary volume. Once the samples are placed into the penetrometer a vacuum is applied until less than 50 micro-metres of mercury has been achieved. Mercury is then introduced into the penetrometer and the run commences along pre-defined pressure points on a logarithmic scale. After equilibration at each pressure point a capacitance reading was taken which was then converted into an equivalent intrusion volume.

Porosity of the actual samples used is calculated from the following equation:-

$$\text{Grain Volume} = \frac{\text{Bulk Volume x Bulk Density}}{\text{Grain Density}}$$

$$\text{Porosity} = \frac{\text{Bulk Volume - Grain Volume}}{\text{Bulk Volume}}$$

Pore diameter has been calculated from the following equation:-

$$d = \frac{4 \gamma \cos \theta}{P_c \times 6.89476}$$

where:
d = pore diameter (microns)
γ = air/mercury surface tension (dynes/cm)
θ = air/mercury contact angel (degree)
P_c = capillary pressure (psia)

CONVENTIONAL CORE ANALYSIS

Company South Australian Department of Mines and Energy

Table I

Sample Number	Depth (m)	Porosity (%) Ambient	Grain Density Absolute	Permeability (md) Ambient	Remarks
Well: Manya No 4					
26	620.4	14.2	2.64	0.99	SP
27	716.5	16.3	2.67	4.68	SP
28	747.6	20.4	2.64	8.07	SP
Well: Manya No 5					
64	193.0	11.6	2.65	76.1	
66	404.6	12.9	2.64	0.96	SP
67	457.9	3.0	2.65	0.01	SP
68	499.0	23.0	2.64	53	SP
69	511.1	19.4	2.64	1.32	SP
70	531.8	20.0	2.65	3.25	SP
71	583.1	17.4	2.66	8.45	SP
72	619.4	20.4	2.64	37.9	SP
73	686.4	14.9	2.62	177	SP
74	714.7	12.4	2.67	0.61	SP
75	778.0	16.1	2.65	0.44	SP
76	833.8	14.4	2.67	0.28	SP
77	888.0	13.1	2.65	0.48	SP
79	919.2	13.8	2.64	0.44	SP
80	932.1	16.1	2.67	0.60	SP
81	982.5	13.2	2.66	1.56	SP
82	1018.1	11.6	2.66	0.24	SP
83	1053.4	13.4	2.66	0.06	SP
Well: Manya No 6					
193	906.6	10.2	2.67	8.80	SP
194	1471.0	6.1	2.75	0.08	SP
195	1676.6	2.6	2.67	0.46	SP
196	1687.2	1.2	2.63	0.01	SP
Well: Marla No 3					
468	519.8	9.3	2.84	305	SP
469	532.2	21.0	2.82	23.1	SP
470	640.2	8.5	2.64	0.90	SP
471	642.8	13.4	2.64	124	SP
Well: Marla No 6					
467	602.8	6.2	2.83	338	SP

SP = short plug

Figure 1

Porosity vs Permeability

Company: SADME
Wells: Manya 4,5,6 Marla 3 6

Ambient

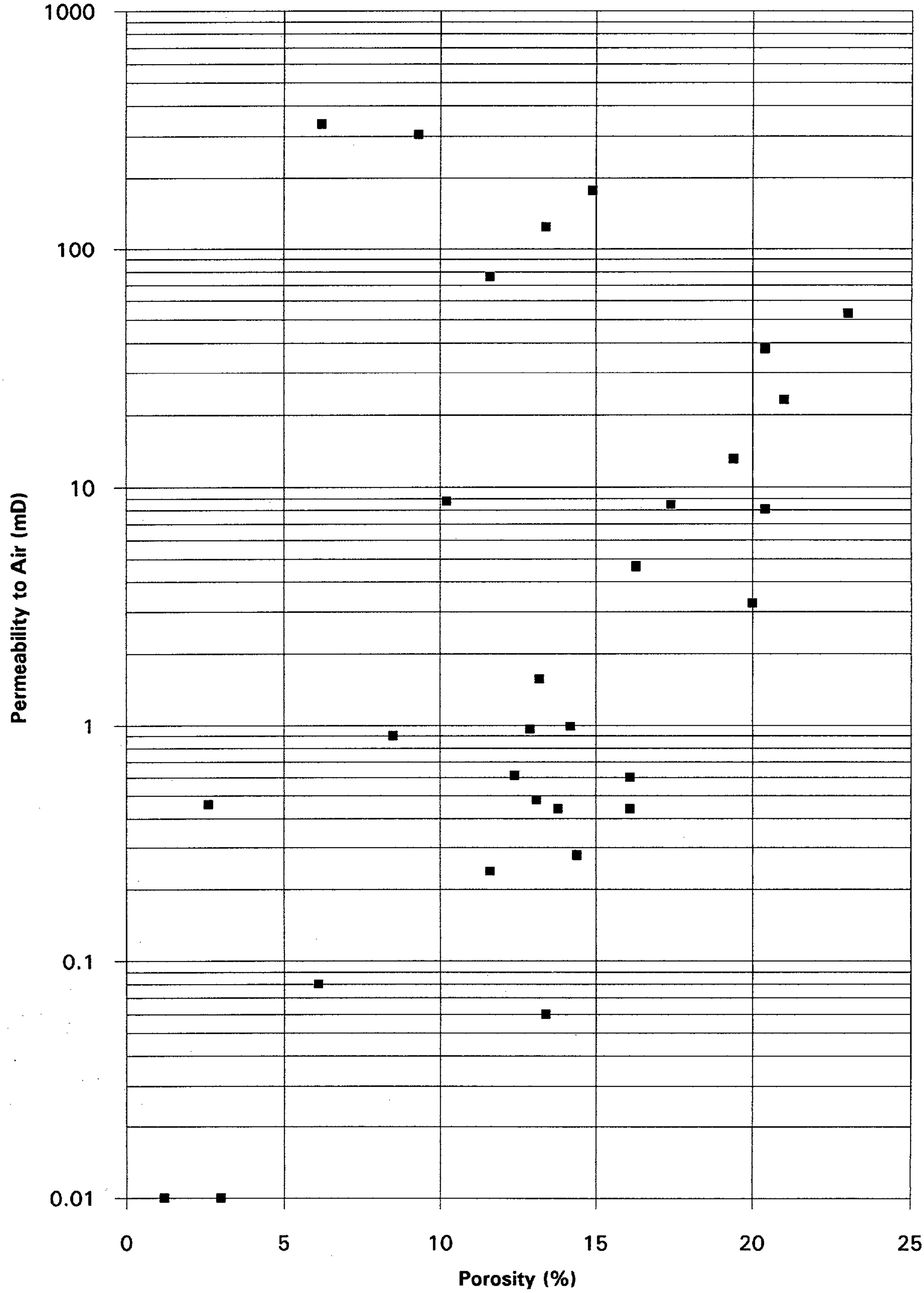

25 May 1993

CAPILLARY PRESSURE

Company	SADME		
Well	MANYA -5		
Test Method	Air/Mercury Capillary Pressure Micromeritics Autopore 9200		
Sample Number	69		
Depth	511.1	metres	
Porosity	0.180	fraction	(determined from Hg Intrusion data)
Grain Density	2.69	gms/cm^3	(determined from Hg Intrusion data)
Bulk Density	2.21	gms/cm^3	(determined from Hg Intrusion data)

Table II

Pressure (psia)	Cumulative Intrusion (ml)	Saturation, fraction	Pore Diameter (μm)
2.47	0.000	0.000	87.080
2.89	0.001	0.003	74.425
3.42	0.001	0.003	62.891
4.06	0.001	0.003	52.977
4.81	0.001	0.003	44.717
5.71	0.001	0.003	37.669
6.77	0.001	0.003	31.771
8.05	0.001	0.003	26.719
9.52	0.001	0.003	22.593
11.32	0.001	0.003	19.001
13.44	0.001	0.003	16.004
15.98	0.001	0.003	13.460
18.94	0.001	0.003	11.356
21.94	0.001	0.003	9.803
24.93	0.004	0.012	8.628
29.45	0.004	0.012	7.303
32.97	0.005	0.016	6.524
39.31	0.005	0.016	5.472
46.69	0.005	0.016	4.607
54.33	0.007	0.022	3.959
65.35	0.010	0.031	3.291
77.91	0.015	0.047	2.761
91.08	0.030	0.093	2.362
106.17	0.065	0.202	2.026
127.76	0.121	0.376	1.684
148.36	0.162	0.503	1.450
176.88	0.194	0.602	1.216
212.59	0.217	0.674	1.012
254.29	0.234	0.727	0.846
291.26	0.245	0.761	0.738
358.44	0.262	0.814	0.600
422.41	0.272	0.845	0.509

Pressure (psia)	Cumulative Intrusion (ml)	Saturation, fraction	Pore Diameter (μm)
506.78	0.281	0.873	0.424
601.13	0.287	0.891	0.358
712.50	0.292	0.907	0.302
849.28	0.296	0.919	0.253
1010.32	0.299	0.929	0.213
1200.61	0.302	0.938	0.179
1427.22	0.304	0.944	0.151
1698.84	0.306	0.950	0.127
2020.11	0.307	0.953	0.106
2385.43	0.309	0.960	0.090
2847.49	0.310	0.963	0.076
3401.65	0.312	0.969	0.063
4012.48	0.313	0.972	0.054
4799.75	0.314	0.975	0.045
5715.84	0.316	0.981	0.038
6810.86	0.317	0.984	0.032
8106.28	0.318	0.988	0.027
9633.11	0.319	0.991	0.022
11501.08	0.320	0.994	0.019
13607.63	0.320	0.994	0.016
16262.87	0.321	0.997	0.013
19349.93	0.321	0.997	0.011
23019.08	0.321	0.997	0.009
27349.07	0.321	0.997	0.008
32516.42	0.321	0.997	0.007
38513.98	0.322	1.000	0.006
45518.30	0.322	1.000	0.005

Figure 2

Capillary Pressure

Company: SADME
Well: Manya 5
Sample No. 69

Test Method: Mercury Injection

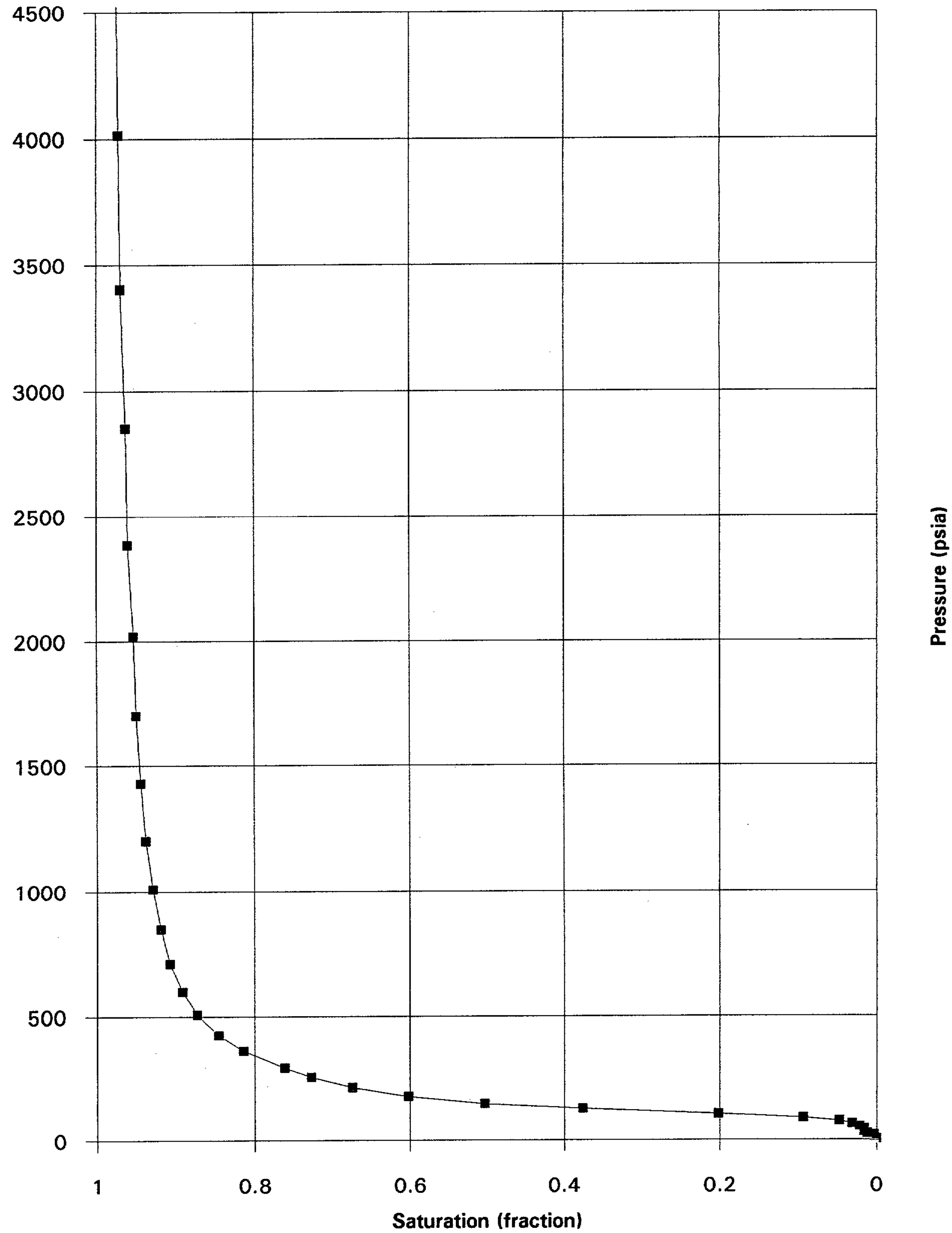

Amdel Core Services Pty Limited
(Incorporated in South Australia)

25 May 1993

CAPILLARY PRESSURE

Company SADME
Well MANYA -5

Test Method Air/Mercury Capillary Pressure
Micromeritics Autopore 9200
Sample Number 73
Depth 686.4 metres
Porosity 0.149 fraction (determined from Hg Intrusion data)
Grain Density 2.62 gms/cm^3 (determined from Hg Intrusion data)
Bulk Density 2.23 gms/cm^3 (determined from Hg Intrusion data)

Table III

Pressure (psia)	Cumulative Intrusion (ml)	Saturation, fraction	Pore Diameter (μm)
2.46	0.026	0.234	87.434
2.89	0.026	0.234	74.425
3.45	0.028	0.252	62.344
4.09	0.030	0.270	52.589
4.83	0.032	0.287	44.532
5.70	0.033	0.296	37.735
6.78	0.034	0.305	31.724
8.02	0.035	0.314	26.819
9.52	0.035	0.314	22.593
11.31	0.037	0.332	19.017
13.44	0.038	0.341	16.004
15.98	0.039	0.350	13.460
18.96	0.040	0.359	11.344
21.95	0.041	0.368	9.799
24.92	0.042	0.377	8.631
29.31	0.042	0.377	7.338
32.82	0.042	0.377	6.554
38.94	0.044	0.394	5.524
46.54	0.047	0.421	4.622
55.03	0.051	0.457	3.909
65.39	0.054	0.483	3.289
76.99	0.058	0.519	2.794
91.54	0.061	0.546	2.350
107.75	0.064	0.572	1.996
128.71	0.067	0.599	1.671
152.76	0.070	0.626	1.408
180.81	0.072	0.644	1.190
214.20	0.075	0.670	1.004
255.48	0.077	0.688	0.842
292.64	0.079	0.706	0.735
358.22	0.082	0.733	0.600

Pressure (psia)	Cumulative Intrusion (ml)	Saturation, fraction	Pore Diameter (μm)
427.97	0.084	0.751	0.503
510.10	0.087	0.777	0.422
603.63	0.089	0.795	0.356
719.19	0.092	0.822	0.299
853.39	0.094	0.840	0.252
1014.11	0.096	0.857	0.212
1202.47	0.098	0.875	0.179
1433.27	0.100	0.893	0.150
1704.08	0.101	0.902	0.126
2024.71	0.102	0.911	0.106
2399.03	0.103	0.920	0.090
2862.70	0.104	0.929	0.075
3420.88	0.105	0.938	0.063
4045.38	0.106	0.947	0.053
4870.82	0.106	0.947	0.044
5765.45	0.107	0.955	0.037
6841.38	0.107	0.955	0.031
8139.18	0.108	0.964	0.026
9651.70	0.108	0.964	0.022
11488.66	0.108	0.964	0.019
13685.86	0.109	0.973	0.016
16250.45	0.109	0.973	0.013
19325.58	0.109	0.973	0.011
22989.96	0.110	0.982	0.009
27305.63	0.110	0.982	0.008
32115.13	0.111	0.991	0.007
38041.13	0.112	1.000	0.006
45379.44	0.112	1.000	0.006

Figure 3

Capillary Pressure

Company: SADME
Well: Manya 5
Sample No. 73

Test Method: Mercury Injection

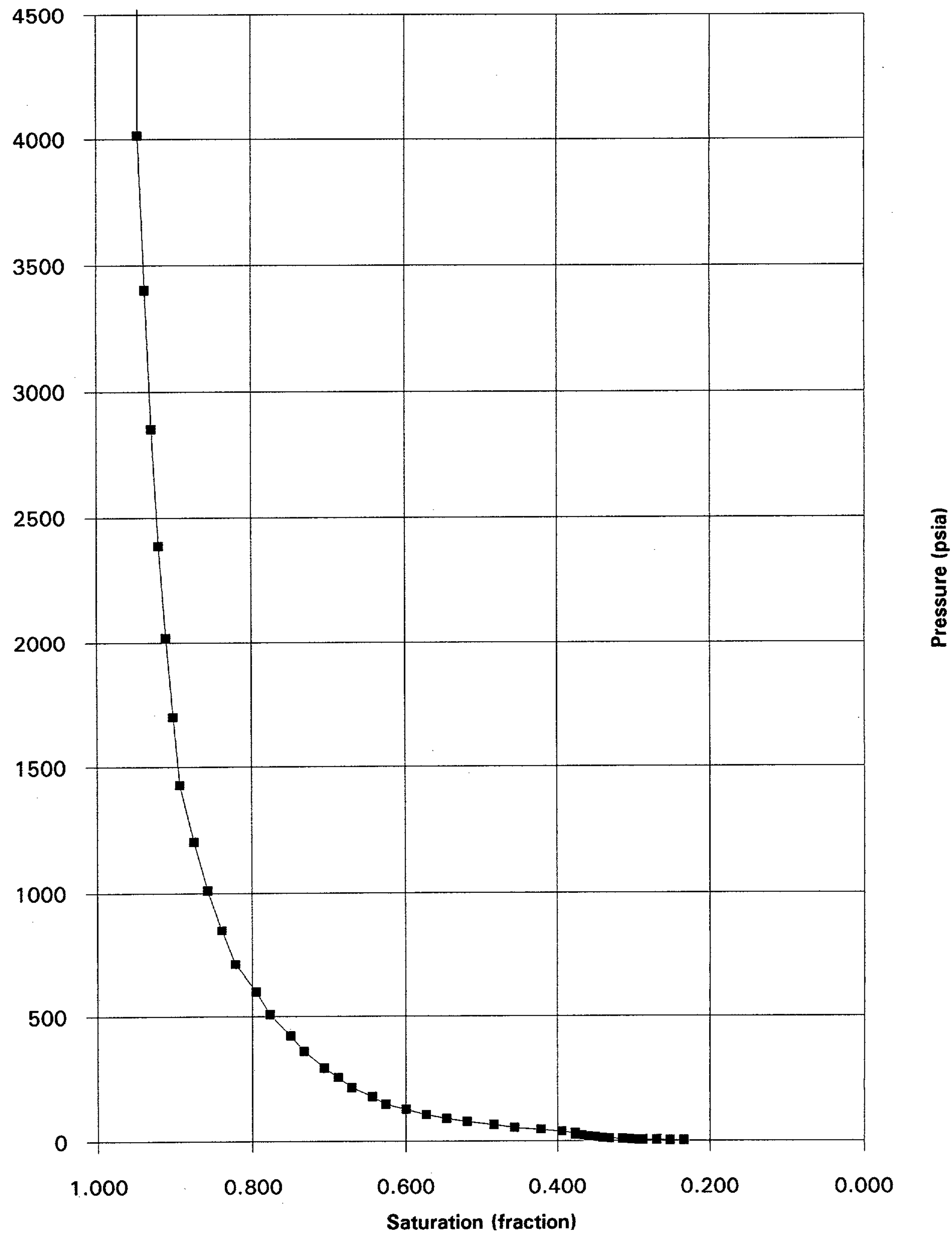

Amdel Core Services Pty Limited
(Incorporated in South Australia)

1 June 1993

CAPILLARY PRESSURE

Company	SADME	
Well	MANYA -5	
Test Method	Air/Mercury Capillary Pressure Micromeritics Autopore 9200	
Sample Number	81	
Depth	982.5	metres
Porosity	0.152	fraction (determined from Hg Intrusion data)
Grain Density	2.66	gms/cm^3 (determined from Hg Intrusion data)
Bulk Density	2.25	gms/cm^3 (determined from Hg Intrusion data)

Table IV

Pressure (psia)	Cumulative Intrusion (ml)	Saturation, fraction	Pore Diameter (μm)
2.46	0.002	0.007	87.434
2.89	0.005	0.018	74.425
3.45	0.010	0.036	62.344
4.09	0.034	0.122	52.589
4.83	0.038	0.137	44.532
5.70	0.040	0.144	37.735
6.78	0.042	0.151	31.724
8.02	0.045	0.162	26.819
9.52	0.048	0.173	22.593
11.31	0.057	0.205	19.017
13.44	0.062	0.223	16.004
15.98	0.065	0.234	13.460
18.96	0.068	0.245	11.344
21.95	0.070	0.252	9.799
24.92	0.072	0.259	8.631
29.41	0.075	0.270	7.313
32.85	0.078	0.281	6.548
39.21	0.080	0.288	5.486
46.72	0.082	0.295	4.604
55.07	0.085	0.306	3.906
65.98	0.087	0.313	3.260
77.78	0.090	0.324	2.765
91.64	0.093	0.335	2.347
108.75	0.096	0.345	1.978
128.04	0.100	0.360	1.680
151.57	0.112	0.376	1.419
180.54	0.119	0.399	1.191
215.36	0.128	0.430	0.999
254.25	0.135	0.453	0.846
293.03	0.142	0.477	0.734
360.70	0.153	0.513	0.596

Pressure (psia)	Cumulative Intrusion (ml)	Saturation, fraction	Pore Diameter (μm)
428.84	0.163	0.547	0.502
508.56	0.174	0.584	0.423
604.02	0.184	0.617	0.356
720.06	0.196	0.658	0.299
852.50	0.208	0.698	0.252
1014.34	0.218	0.732	0.212
1205.76	0.229	0.768	0.178
1431.89	0.238	0.799	0.150
1705.27	0.247	0.829	0.126
2027.99	0.256	0.859	0.106
2401.02	0.263	0.883	0.090
2863.73	0.269	0.903	0.075
3431.88	0.274	0.919	0.063
4060.17	0.277	0.930	0.053
4859.37	0.280	0.940	0.044
5765.92	0.283	0.950	0.037
6865.71	0.285	0.956	0.031
8142.05	0.288	0.966	0.026
9685.57	0.290	0.973	0.022
11505.84	0.293	0.983	0.019
13674.41	0.294	0.987	0.016
16260.47	0.296	0.993	0.013
19349.91	0.297	0.997	0.011
23042.92	0.298	1.000	0.009
27341.89	0.295	1.000	0.008
32487.78	0.292	1.000	0.007
38416.15	0.288	1.000	0.006
45508.74	0.278	1.000	0.005

Figure 4

Capillary Pressure

Company: SADME
Well: Manya 5
Sample No. 81

Test Method: Mercury Injection

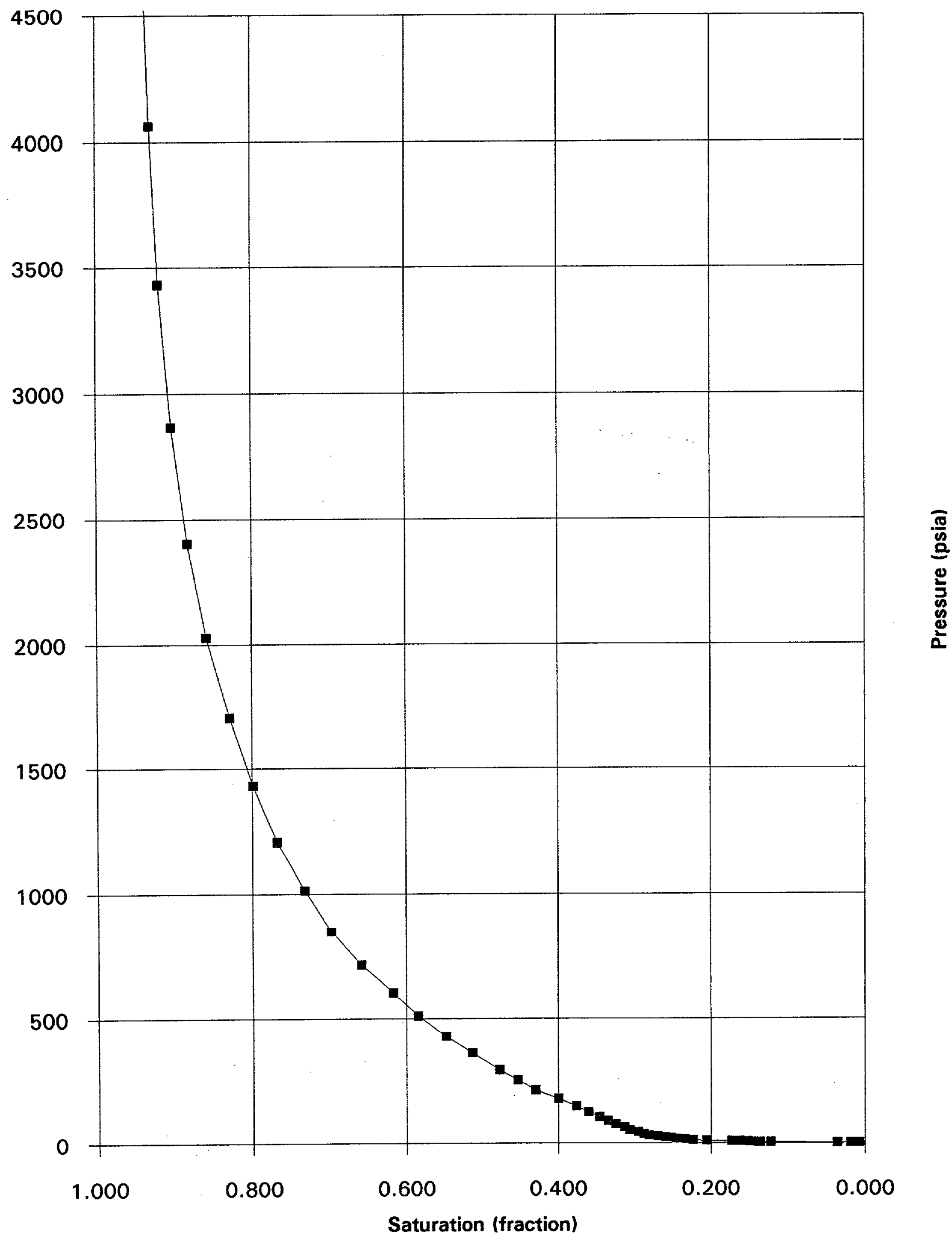

AMDEL
CORE
SERVICES

2 July 1993

Department of Mines & Energy
PO Box 151
EASTWOOD SA 5063

Attention: Information Officer

REPORT: FF/219

CLIENT REFERENCE: 11/06/0800

MATERIAL: Core

LOCALITY: Marla -10

WORK REQUIRED: Core Analysis

Please direct technical enquiries regarding this work to the signatory below under whose supervision the work was carried out.

ROBERT D EAST
Technical Services Manager

ANTHONY M DRAKE
Laboratory Supervisor
Special Core Analysis

CONTENTS

1. INTRODUCTION

A purchase order No EX/339 was received from the Department of Mines and Energy requesting core analysis on 27 samples from Marla-10. Sample RS 482 was listed on the purchase order but not included in the shipment.

2. SAMPLE PREPARATION

One inch diameter samples were drilled at selected points using tap water to cool and lubricate the bit. Samples were trimmed, faced square and dried in a conventional oven at 80°C.

3. PERMEABILITY TO AIR - Ambient

Air permeability was determined on the plug samples. The samples were firstly placed in a Hassler cell with a confining pressure of 250 psi. The confining pressure was used to prevent bypassing of air around the samples when the measurement was made. To determine permeability a known air pressure was applied to the upstream face of the sample, creating a flow of air through the core plug. Permeability for the samples was calculated using Darcy's Law through knowledge of the upstream pressure, flow rate, viscosity of air and the samples' dimensions.

4. HELIUM INJECTION POROSITY

The porosity of the clean dry core plugs was determined as follows. The plugs were first placed in a sealed matrix cup. Helium held at 100 psi reference pressure was then introduced to the cup. From the resultant pressure change the unknown grain volume was calculated using Boyle's Law (ie, $P_1V_1 = P_2V_2$).

The bulk volume was determined by mercury immersion. The difference between the grain volume and the bulk volume is the pore volume and from this the 'effective' porosity was calculated as the volume percentage of pores with respect to the bulk volume.

5. MEASURED GRAIN DENSITY

Plug offcuts were used for these analyses. After drying the offcuts were crushed to grain-size and weighed. The volume of grains was determined by pycnometry (Archimedes principal) using methanol as the wetting liquid.

2 July 1993

POROSITY AND AIR PERMEABILITY

Company SADME
Well Marla No 10

Ambient

Table I

Sample Number	Depth, metres	Permeability to Air, millidarcys	Porosity, percent	Measured Grain Density (gms/cm^3)
473	63.6	1.59	19.7	2.68
474	67.0	0.26	13.9	2.63
475	73.6	4.10	16.3	2.61
476	78.6	2.25	18.1	2.60
477	84.1	14.9	17.4	2.60
478	91.4	39.0	17.5	2.60
479	98.4	96	16.1	2.62
480	106.0	5.1	12.7	2.58
481	108.9	0.89	13.0	2.60
483	114.1	93	20.2	2.58
484	116.8	57	21.3	2.63
485	129.8	12.3	10.3	2.65
486	131.4	2.89	9.0	2.63
487	300.0	158	14.8	2.60
488	307.5	6.6	7.5	2.60
489	314.8	24.0	14.3	2.61
490	339.3	0.10	1.5	2.64
491	344.0	31.1	13.9	2.61
492	352.3	61	15.0	2.61
493	359.5	308	15.3	2.60
494	368.0	392	16.2	2.62
495	372.2	61	15.2	2.63
496	378.8	14.5	16.1	2.62
497	387.8	86	17.2	2.61
498	401.1	147	17.8	2.59
499	410.8	284	19.4	2.60

Figure 1

Porosity vs Permeability

Company: SADME
Well: Marla 10

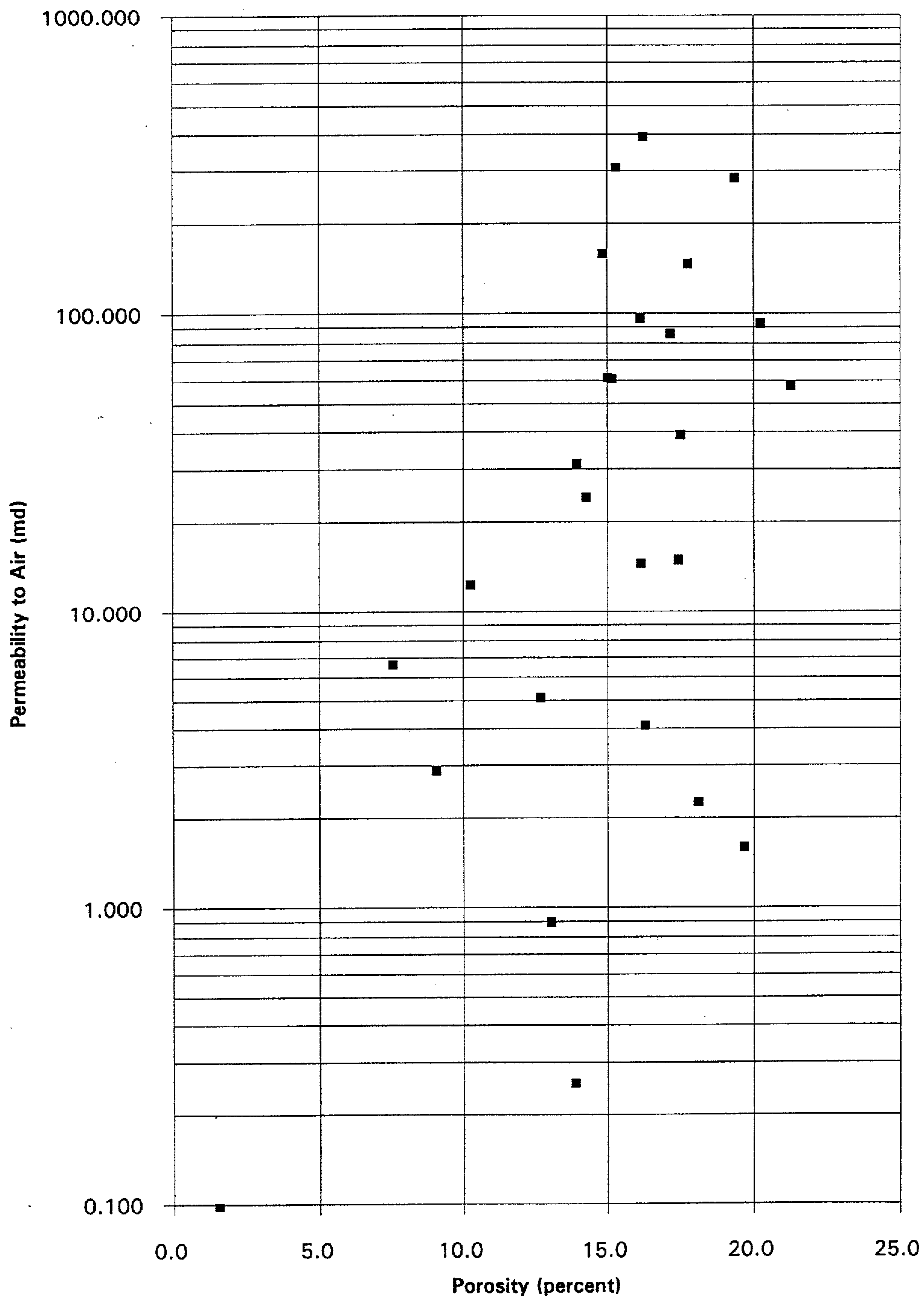

amdel
Amdel Limited
A.C.N. 008 127 802

Mineral Services Laboratory
31 Flemington Street
Frewville SA 5063
AUSTRALIA

PO Box 338
Torrensville SA 5031
AUSTRALIA

Telephone: (08) 372 2700
Facsimile: (08) 379 6623
Telex: AA 82520

30 July 1993

Dr D Gravestock
SA Department of Mines & Energy
PO Box 151
EASTWOOD SA 5063

REPORT G10/94
BULK AND CLAY MINERALOGY OF TEN SAMPLES

YOUR REFERENCE:	EX 1356, 11/06/0800
SAMPLE IDENTIFICATION:	5342RS109-152; 5643RS506
MATERIAL:	10 core chip cuttings
LOCATION:	Munyarai, Marla
DATE RECEIVED:	2 July 1993
WORK REQUIRED:	Determination of bulk and -2 μm mineralogy

Investigation and Report by: Michael Till

Keith Henley

Dr Keith J Henley
Manager, Mineral Services Laboratory

The results contained in this report relate only to the sample(s) submitted for testing. Amdel Ltd accepts no responsibilities for the representivity of the sample(s) submitted.

hk

BULK AND CLAY MINERALOGY OF TWO SAMPLES

1. INTRODUCTION

Samples were received from Dr D Gravestock of SA Department of Mines & Energy with a request for determination of the bulk and clay mineralogy.

2. PROCEDURE

Portion of each sample was powdered finely and used to prepare an X-ray diffractometer trace which was interpreted by standard procedures.

Further, weighed, lightly pre-ground subsamples were taken and dispersed in water with the aid of deflocculants and a mechanical shaker, and allowed to sediment to produce -2 μm e.s.d. size fractions by the pipette method. The resulting dispersions were examined by plummet balance to determine their solids contents, and were then used to produce oriented clay preparations on ceramic plates. Two plates were prepared per sample, both being saturated with Mg^{++} ions, and one in addition being treated with glycerol. When air-dry, these were examined in the X-ray diffractometer. An additional diagnostic examination carried out consisted of examination of the glycerol-free plate after heating for one hour at 550°C.

3. RESULTS

The results are given in Table 1, which lists the following :

(a) The mineralogy of the bulk sample, as derived from examination of the bulk material, with supporting evidence as available. The minerals found are listed in approximate order of decreasing abundance, using the semiquantitative abbreviations given. Minerals bracketed were not detectible in this examination but were found in the clay fraction examination.

(b) The mineralogy of the -2 μm fraction, given as in Section (a).

Given below is the proportion of the sample found to separate into the -2 μm size fraction, as determined by the plummet balance. The figure obtained applies only to the pre-treatment and dispersion conditions used.

WELL	DRILLER'S DEPTH (m)	FORMATION	Sample	-2 µm, %
MUNYARAI-1	255.6	DEVONIAN	5342RS109	24
MUNYARAI-1	546.5	DEVONIAN	5342RS120	34
MUNYARAI-1	597.4	DEVONIAN	5342RS124	22
MUNYARAI-1	633.7	DEVONIAN	5342RS130	37
MUNYARAI-1	869.3	DEVONIAN	5342RS142	20
MUNYARAI-1	921.1	DEVONIAN	5342RS143	10
MUNYARAI-1	1018.0	ORD/DEV	5342RS146	10
MUNYARAI-1	1197.3	INDULKANA	5342RS150	9
MUNYARAI-1	1199.7	INDULKANA	5342RS152	15
MARLA-9	226.0	U. RODDA	5643RS506	8

MUNYARRA-1
DEVONIAN

TABLE 1: BULK AND -2 µm MINERALOGY OF TEN SAMPLES

	5342RS109		5342RS120		5342RS124		5342RS130		R5342RS142	
	Bulk	-2 µm	Bulk	-2 µm	Bulk	-2 µm	Bulk	-2 µm	Bulk	-2 µm
Quartz	CD	Tr-A	SD	A	D	A	SD	A	D	A
Mica/illite	CD	D	D	CD	A-SD	D	D	D	A	D
Smectite					(Tr-A)	A-SD	(Tr)	A		
Mixed-layer*	(Tr)	A	(A)	CD	(Tr)	A	(Tr)	A	(Tr-A)	SD
Chlorite	Tr-A	SD	A	A	Tr-A	A	(Tr)	A	Tr	Tr-A
Kaolinite									(Tr)	Tr
K-feldspar	A	Tr	A	Tr	A	Tr-A	A-SD	Tr	A	
Plagioclase	A	Tr	A	Tr-A	A	Tr-A	Tr-A	Tr	A	
Calcite	Tr-A	Tr	Tr-A		A	Tr-A	Tr-A		Tr	
Dolomite							?Tr		?Tr	
Hematite			Tr-A		?Tr		Tr			

* Mixed-layer clay: interstratified smectite/illite (in sample 5342RS152, illite with an appreciable proportion of interlayered smectite)

Semi-quantitative Abbreviations

D = Dominant. Used for the component apparently most abundant, regardless of its probable percentage level.

CD = Co-dominant. Used for two (or more) predominating components, both or all of which are judged to be present in roughly equal amounts.

SD = Sub-dominant. The next most abundant component(s) providing its percentage level is judged above about 20.

A = Accessory. Components judged to be present between the levels of roughly 5 and 20%.

Tr = Trace. Components judged to be below about 5%.

0386

MUNYARAI-1 DEVONIAN

TABLE 1: BULK AND -2 µm MINERALOGY OF TEN SAMPLES (Contd..)

MARLA 9

BASE DEVONIAN INDULKANA SHALE INDULKANA SHALE UPPER RODDA

	5342RS143		5342RS146		5342RS150		5342RS152		5643RS506	
	Bulk	-2 µm	Bulk	-2 µm	Bulk	-2 µm	Bulk	-2 µm	Bulk	-2 µm
Quartz	D	CD	D	D	D	D	SD	A	CD	SD
Mica/illite					(?M)	?M	A	D	CD	D
Smectite	(?Tr)	?Tr	(Tr)	Tr						
Mixed-layer*	(?Tr)	?Tr					(Tr)	A-SD		
Chlorite									A	A-SD
Kaolinite			Tr	Tr						
K-feldspar	Tr				Tr	Tr	A	Tr-A	Tr-A	Tr
Plagioclase							Tr		A	Tr-A
Calcite	A	CD					Tr		?Tr	
Dolomite					?Tr	?Tr	D	SD	Tr-A	
Pyrite									Tr-A	

* Mixed-layer clay: interstratified smectite/illite (in sample 5342RS152, illite with an appreciable proportion of interlayered smectite)

INDULKANA

Semi-quantitative Abbreviations

D = Dominant. Used for the component apparently most abundant, regardless of its probable percentage level.

CD = Co-dominant. Used for two (or more) predominating components, both or all of which are judged to be present in roughly equal amounts.

SD = Sub-dominant. The next most abundant component(s) providing its percentage level is judged above about 20.

A = Accessory. Components judged to be present between the levels of roughly 5 and 20%.

Tr = Trace. Components judged to be below about 5%.

amdel
Amdel Limited
A.C.N. 008 127 802
Mineral Services Laboratory
31 Flemington Street
Frewville SA 5063
AUSTRALIA
PO Box 338
Torrensville SA 5031
AUSTRALIA
Telephone: (08) 372 2700
Facsimile: (08) 379 6623
Telex: AA 82520

30 November 1993

Mr Alan Sansome
SA Department of Mines & Energy
PO Box 151
EASTWOOD SA 5063

REPORT G162/94
BULK AND CLAY MINERALOGY OF 22 SAMPLES

YOUR REFERENCE:	EX 1404, 58GR2/A06/956
SAMPLE IDENTIFICATION:	5341, 5642, 5643, 5742 (various RS numbers)
MATERIAL:	22 sandstone samples
DATE RECEIVED:	16 November 1993
WORK REQUIRED:	Determination of bulk and -2 μm mineralogy

Investigation and Report by: Michael Till

Keith Henley

Dr Keith J Henley
Manager, Mineral Services Laboratory

The results contained in this report relate only to the sample(s) submitted for testing. Amdel Ltd accepts no responsibilities for the representivity of the sample(s) submitted.

hk

BULK AND CLAY MINERALOGY OF 22 SAMPLES

1. INTRODUCTION

Samples were received from Mr A Sansome of SA Department of Mines & Energy with a request for determination of the bulk and clay mineralogy.

2. PROCEDURE

Portion of each sample was powdered finely and used to prepare an X-ray diffractometer trace which was interpreted by standard procedures.

Further, weighed, lightly pre-ground subsamples were taken and dispersed in water with the aid of deflocculants and a mechanical shaker, and allowed to sediment to produce -2 μm e.s.d. size fractions by the pipette method. The resulting dispersions were examined by plummet balance to determine their solids contents, and were then used to produce oriented clay preparations on ceramic plates. Two plates were prepared per sample, both being saturated with Mg^{++} ions, and one in addition being treated with glycerol. When air-dry, these were examined in the X-ray diffractometer. An additional diagnostic examination carried out consisted of examination of the glycerol-free plate after heating for one hour at 550°C.

3. RESULTS

The results are given in Table 1, which lists the following :

(a) The mineralogy of the bulk sample, as derived from examination of the bulk material, with supporting evidence as available. The minerals found are listed in approximate order of decreasing abundance, using the semiquantitative abbreviations given. Minerals bracketed were not detectible in this examination but were found in the clay fraction examination.

(b) The mineralogy of the -2 μm fraction, given as in Section (a).

Given below is the proportion of the sample found to separate into the -2 μm size fraction, as determined by the plummet balance. The figure obtained applies only to the pre-treatment and dispersion conditions used.

WELL	DRILLER'S DEPTH (m)	FORMATION	Sample	-2 µm, %
MANYA 5	420	RELIEF	5742RS91	12
MANYA 6	1706.5	RELIEF	5642RS205	2
MANYA 6	1741.8	RELIEF	5642RS210	3
UNGOOLYA 1	631.1	TRAINOR HILL	5341RS377	33
UNGOOLYA 1	639	TRAINOR HILL	5341RS378	2
UNGOOLYA 1	702.2	TRAINOR HILL	5341RS380	2
GILES-1	358.3	RELIEF	5341RS391	4
GILES-1	379.2	RELIEF	5341RS393	2
GILES-1	1296.8	PINDYIN	5341RS405	5
GILES-1	1305	PINDYIN	5341RS408	4
MERAMANGYE-1	419	RELIEF	5341RS412	6
MERAMANGYE-1	427.7	RELIEF	5341RS416	6
MERAMANGYE-1	444.1	RELIEF	5341RS422	9
UNGOOLYA-1	812.2	TRAINOR HILL	5341RS424	14
MARLA-2	104.5	ARCOEILLINNA	5643RS517	18
MARLA-2	105.1	ARCOEILLINNA	5643RS518	7
MARLA-2	150.1	ARCOEILLINNA	5643RS526	2
MARLA-4	169.1	ARCOEILLINNA	5643RS533	10
MARLA-4	195.5	ARCOEILLINNA	5643RS537	4
MARLA-4	214.8	ARCOEILLINNA	5643RS540	9
MARLA-5	165.4	TRAINOR HILL	5643RS542	12
MARLA-5	294.2	TRAINOR HILL	5643RS548	2

TABLE 1: BULK AND -2 µ m MINERALOGY OF 22 SAMPLES

	MARLA-2 ARCOEILLINNA		MARLA-2 ARCOEILLINNA		MARLA-2 ARCOEILLINNA		MARLA-4 ARCOEILLINNA		MARLA-4 ARCOEILLINNA		MARLA-4 ARCOEILLINNA		MARLA-5 TRAINOR HILL		MARLA-5 TRAINOR HILL	
	5643RS517		5643RS518		5643RS526		5643RS533		5643RS537		5643RS540		5643RS542		5643RS548	
	Bulk	-2µm	Bulk	-2µm	Bulk	-2µm	Bulk	-2µm	Bulk	-2µm	Bulk	-2µm	Bulk	-2µm	Bulk	-2µm
Quartz	D		D	A	D	CD	D	D	D	A-SD	D	A	D	A-SD	D	D
K-feldspar	A		Tr-A	Tr	Tr-A	Tr	A	A	A	A	Tr-A	Tr-A	Tr-A	Tr-A	Tr-A	Tr-A
Plagioclase	Tr				A	Tr									Tr-A	
Mica/illite	Tr-A	SD	Tr-A	CD	Tr-A	CD	Tr-A	A	Tr-A	D	Tr-A	D	Tr	D	(Tr)	Tr-A
Chlorite	Tr	Tr			(Tr)	Tr-A	(Tr)	Tr	Tr	A-SD	Tr	A				
Kaolinite													(Tr-A)	SD	(Tr)	Tr-A
Smectite	(A)	D	(Tr)	CD					(Tr)	A	Tr	A				
Mixed-layer*											(Tr)	Tr-A				
Hematite	Tr										Tr	Tr				
Dolomite	A-SD	Tr-A	Tr-A	Tr-A												
Calcite			Tr-A	A												

* Interstratified illite/smectite in 5341RS377 and 5341RS424
Interstratified chlorite/smectite in 5643RS540

Semi-quantitative Abbreviations

D = Dominant. Used for the component apparently most abundant, regardless of its probable percentage level.

CD = Co-dominant. Used for two (or more) predominating components, both or all of which are judged to be present in roughly equal amounts.

SD = Sub-dominant. The next most abundant component(s) providing its percentage level is judged above about 20.

A = Accessory. Components judged to be present between the levels of roughly 5 and 20%.

Tr = Trace. Components judged to be below about 5%.

TABLE 1: BULK AND -2 μ m MINERALOGY OF 22 SAMPLES

	GILES-1 RELIEF		GILES-1 PINDYIN		GILES-1 PINDYIN		MERAMANGYE-1 RELIEF		MERAMANGYE-1 RELIEF		MERAMANGYE-1 RELIEF		UNGOOLYA-1 TRAINOR HILL	
	5341RS393		5341RS405		5341RS408		5341RS412		5341RS416		5341RS422		5341RS424	
	Bulk	-2μm	Bulk	-2μm	Bulk	-2μm	Bulk	-2μm	Bulk	-2μm	Bulk	-2μm	Bulk	-2μm
Quartz	D	D	D	D	D	SD	D	D	D	D	D	D	D	
K-feldspar	Tr						Tr	Tr	Tr	Tr	A	Tr-A	Tr-A	
Plagioclase											Tr			
Mica/illite	(Tr)	Tr-A	Tr	SD	Tr	D	(Tr)	SD	(Tr)	Tr	(Tr)	Tr-A	Tr-A	A
Chlorite	(Tr)	Tr					(Tr)	Tr-A			(Tr)	Tr	Tr-A	Tr
Kaolinite					(Tr)	Tr			(Tr)	Tr				
Smectite	(?Tr)	?Tr			(Tr)	SD								
Mixed-layer*													(A)	D
Hematite					Tr	Tr	Tr						Tr	

* Interstratified illite/smectite in 5341RS377 and 5341RS424
Interstratified chlorite/smectite in 5643RS540

Semi-quantitative Abbreviations

D = Dominant. Used for the component apparently most abundant, regardless of its probable percentage level.

CD = Co-dominant. Used for two (or more) predominating components, both or all of which are judged to be present in roughly equal amounts.

SD = Sub-dominant. The next most abundant component(s) providing its percentage level is judged above about 20.

A = Accessory. Components judged to be present between the levels of roughly 5 and 20%.

Tr = Trace. Components judged to be below about 5%.

TABLE 1: BULK AND -2 μ m MINERALOGY OF 22 SAMPLES

	MANYA-5 RELIEF		MANYA-6 RELIEF		MANYA-6 RELIEF		UNGOOLYA-1 TRAINOR HILL		UNGOOLYA-1 TRAINOR HILL		UNGOOLYA-1 TRAINOR HILL		GILES-1 RELIEF	
	5742RS91		5642RS205		5642RS210		5341RS377		5341RS378		5431RS380		5341RS391	
	Bulk	-2μm	Bulk	-2μm	Bulk	-2μm	Bulk	-2μm	Bulk	-2μm	Bulk	-2μm	Bulk	-2μm
Quartz	D	A	D	A	D	D	D		D	D	D	D	D	D
K-feldspar	A	Tr	A	Tr	Tr	Tr	Tr-A		Tr	Tr	Tr	Tr	A	Tr
Mica/illite	Tr-A	D	Tr-A	SD			Tr-A	A	(Tr)	Tr-A	(Tr)	Tr-A	(Tr)	A
Chlorite	Tr	Tr-A	(Tr)	D			Tr	Tr	(Tr)	Tr-A	(Tr)	Tr	(Tr)	A
Mixed-layer*							(SD)	D						
Hematite							Tr-A	Tr						

* Interstratified illite/smectite in 5341RS377 and 5341RS424
Interstratified chlorite/smectite in 5643RS540

Semi-quantitative Abbreviations

D = Dominant. Used for the component apparently most abundant, regardless of its probable percentage level.

CD = Co-dominant. Used for two (or more) predominating components, both or all of which are judged to be present in roughly equal amounts.

SD = Sub-dominant. The next most abundant component(s) providing its percentage level is judged above about 20.

A = Accessory. Components judged to be present between the levels of roughly 5 and 20%.

Tr = Trace. Components judged to be below about 5%.

APPENDIX 2

Source rock and vitrinite reflectance
raw data reports

GEOTECH GEOTECHNICAL SERVICES PTY LTD
125 Burswood Road, Victoria Park, Western Australia 6100

0395

Telephone (09) 362 5222
Facsimile (09) 362 5908

28 July, 1993

Dave Gravestock
Department of Mines & Energy
191 Greenhill Road
Parkside
SA 5063

Dear Dave,

Please find enclosed TOC and Rock-Eval results for samples from Munyarai-1, Byilkaoora-1 and Marla-9, as well as an invoice for this work.

As requested, sample leftovers from this job as well as from Marla-3, which you sent to us on behalf of BHPP, are included.

If you have further queries or if we can be of any assistance to you, please do not hesitate to contact us.

Yours sincerely,

Dr. Birgitta Hartung-Kagi
Managing Director

TABLE 1

ROCK-EVAL PYROLYSIS DATA (one run)

MUNYARAI 1 Jul-93

DEPTH (ft)	TMAX	S1	S2	S3	S1+S2	S2/S3	PI	PC	TOC	HI	OI
2078-2080	nd	nd	nd	nd	nd	nd	nd	nd	0.06	nd	nd

TMAX = Max. temperature S2
S1+S2 = Potential yield
PC = Pyrolysable carbon
OI = Oxygen Index

S1 = Volatile hydrocarbons (HC)
S3 = Organic carbon dioxide
TOC = Total organic carbon
nd = no data

S2 = HC generating potential
PI = Production index
HI = Hydrogen index

GEOTECHNICAL SERVICES PTY LTD

TABLE 1

ROCK-EVAL PYROLYSIS DATA (one run)

BYILKAOORA 1 Jul-93

DEPTH (m)	TMAX	S1	S2	S3	S1+S2	S2/S3	PI	PC	TOC	HI	OI
495.4	nd	nd	nd	nd	nd	nd	nd	nd	0.07	nd	nd

TMAX = Max. temperature S2
S1+S2 = Potential yield
PC = Pyrolysable carbon
OI = Oxygen Index
S1 = Volatile hydrocarbons (HC)
S3 = Organic carbon dioxide
TOC = Total organic carbon
nd = no data
S2 = HC generating potential
PI = Production index
HI = Hydrogen index

GEOTECHNICAL SERVICES PTY LTD

TABLE 1

ROCK-EVAL PYROLYSIS DATA (one run)

MARLA 9

Jul-93

DEPTH (m)	TMAX	S1	S2	S3	S1+S2	S2/S3	PI	PC	TOC	HI	OI
176.3	nd	nd	nd	nd	nd	nd	nd	nd	0.18	nd	nd
190.6	nd	nd	nd	nd	nd	nd	nd	nd	0.07	nd	nd
207.6	nd	nd	nd	nd	nd	nd	nd	nd	0.21	nd	nd
218.9	nd	0.02	0.03	0.10	0.05	0.30	0.40	0.00	0.92	3	11
229.2	nd	nd	nd	nd	nd	nd	nd	nd	0.36	nd	nd
244.3	nd	nd	nd	nd	nd	nd	nd	nd	0.36	nd	nd
269.3	438	0.14	0.53	0.15	0.67	3.53	0.21	0.06	0.53	100	28
277.2	nd	nd	nd	nd	nd	nd	nd	nd	0.18	nd	nd
410.9	nd	nd	nd	nd	nd	nd	nd	nd	0.07	nd	nd
430.5	nd	nd	nd	nd	nd	nd	nd	nd	0.09	nd	nd

TMAX = Max. temperature S2
S1+S2 = Potential yield
PC = Pyrolysable carbon
OI = Oxygen Index

S1 = Volatile hydrocarbons (HC)
S3 = Organic carbon dioxide
TOC = Total organic carbon
nd = no data

S2 = HC generating potential
PI = Production index
HI = Hydrogen index

GEOTECHNICAL SERVICES PTY LTD

THE UNIVERSITY OF ADELAIDE

Department of Geology and Geophysics
Dr David M. McKirdy

29 September 1993

Dr D. I. Gravestock
Oil, Gas and Coal Division
South Australian Department of Mines and Energy
191 Greenhill Road
PARKSIDE, SA 5063

Dear David

Source rock evaluation of Alinya Formation, Giles-1

Please find enclosed an invoice for our work on the above project. As you can see the analytical work is complete; and the collation and interpretation of the data has progressed to the stage where I was able to present a preliminary account of our findings at the recent Central Australian Basins Workshop in Alice Springs. The abstract, tables, figures and summary prepared for my talk are submitted as a progress report.

Wenlong and I plan to write a joint paper for *Precambrian Research.* The manuscript of this paper will accompany my invoice for the balance of the amount owing.

Thank you again for the opportunity to participate in your ongoing Officer Basin program.

Yours sincerely

David McKirdy

DAVID M. McKIRDY
Senior Lecturer and Consultant
in Petroleum Geology / Organic Geochemistry

Adelaide, South Australia 5005
Tel: (08) 303 5378 Fax: (08) 303 4347 Telex: UNIVAD AA89141
dmckirdy@geology.adelaide.edu.au

SOURCE ROCK EVALUATION OF ALINYA FORMATION, GILES-1

1. DATA SUMMARY AND PRELIMINARY INTERPRETATION

Report for South Australian Department of Mines and Energy

by

DAVID M. McKIRDY

Organic Geochemistry Laboratory

Department of Geology and Geophysics

University of Adelaide

September 1993

Microfossils and molecular fossils from the Neoproterozoic Alinya Formation – a possible new source rock in the eastern Officer Basin

Wenlong Zang[1] and David M. McKirdy[2]

[1] South Australian Department of Mines and Energy, P.O. Box 151, Eastwood, SA 5063

[2] Department of Geology and Geophysics, The University of Adelaide, SA 5005

The Alinya Formation, a subtidal shelf to coastal sabkha deposit comprising anhydritic shale and siltstone with minor sandstone, dolomite, limestone and chert, conformably overlies the aeolian Pindyin Sandstone in the northeastern Officer Basin. Prior to the drilling of Giles-1, this Neoproterozoic sequence was recognised only in sporadic, deeply weathered outcrop along the southern margin of the Musgrave Block. Seismic interpretation indicates that the Alinya Formation extends across the Munyarai Trough and onto the Murnaroo Platform where its evaporites have been remobilised into diapirs and other salt-related stuctures. The unit is 230 m thick at its North Pindyin Hills type section and 57.3 m thick in Giles-1. A north-trending basement high, the Nurrai Ridge, appears to have acted as a sill that isolated a saline embayment in the east from the open ocean to the west (Zang and Major, 1993).

Grey-green shales and red-brown siltstones of the upper Alinya Formation in Giles-1 contain a diverse array of microfossils, including benthic cyanobacteria (notably *Eoentophysalis* mats) and abundant phytoplankton (spheroidal and spinose acritarchs). The acritarch assemblage is dominated by spheroids such as *Leiosphaeridia*, *Lophosphaeridium*, *Paracrassosphaera*, *Synsphaeridium*, *Strictosphaeridium*, *Satka*, *Tasmanites*, *Simia*, *Sinianella*, *Sphaerocongregus*, *Valeria* and *Caudosphaera*. Distinctive spinose elements include *Trachyhystricosphaera vidalii*, *T. aimica*, *Trachyhystricosphaera* sp., *Cymatiosphaeroides kullingii*, *Vandalosphaeridium* sp. and *Micrhystridium* sp. which together indicate an early Neoproterozoic age. The vase-shaped *Melanocyrillium* and the octahedral species *Octoedryxium intrarium* are also present. Many (but not all) of these microfossils have previously been described from the Gillen Member (Bitter Springs Formation) in the Amadeus Basin (Zang and Walter, 1992). Biostratigraphic correlation of the lower Bitter Springs and Alinya Formations accords with the fact that both overlie the basal sandstone blanket (Heavitree Quartzite equivalent to Pindyin Sandstone) of the Centralian Superbasin and each is part of a transgressive systems tract.

The Alinya Formation intersected by Giles-1 can be divided into two units. The lower unit, anhydritic red-brown siltstone thinly interbedded with sandstone, was probably deposited on an intertidal flat. The upper unit consists of several upward-shallowing evaporite cycles deposited in a marine sabkha setting. A typical cycle comprises in turn grey siltstone; black shale; grey-green shale or siltstone; red-brown anhydrite, siltstone and dolomite rich in *Eoentophysalis* mats; and aeolian sandstone with minor anhydrite and halite. The enhanced preservation of microbial organic matter in the 35 m-thick upper unit makes it of interest as a possible source rock for petroleum. Preliminary analysis of six core samples from 1237–1266 m depth in Giles-1 revealed poor to fair organic richness (TOC = 0.10–0.62%), low concentrations of extractable organic matter (EOM = 6–15 ppm) and low hydrocarbon yields (4–15 mg/g TOC). Rock-Eval pyrolysis confirmed the presence of mature gas-prone kerogen (T_{max} = 439–445°C; hydrogen index = 58–106). Similar organic geochemical characteristics have been reported for the Gillen Member (McKirdy, 1977; Jackson et al., 1984; Summons and Powell, 1991). For the upper Alinya Formation at Giles-1, maturation levels corresponding to the oil-generation window are indicated by sterane epimer ratios (C_{29} $\alpha\alpha\alpha$ 20S/20S+20R = 0.48–0.54) and the isomer distributions of diaromatic and triaromatic hydrocarbons (e.g. dimethylnaphthalene ratio, DNR-1 = 1.5; methylphenanthrene ratio, MPR = 1.0–1.3).

GC and GC-MS analysis of saturated hydrocarbons in the evaporitic sediments of the upper Alinya Formation identified a diverse suite of steranes, triterpanes and acyclic isoprenoid alkanes. Features of these molecular fossil distributions are: pristane/*n*-heptadecane = 0.32–0.40; phytane/*n*-octadecane =

0.16–0.19; pristane/phytane = 1.6–2.0; 17α(H)-30-norhopane > 17α(H)-hopane; 29,30-bisnorhopane > 28,30-bisnorhopane; 2α-methyl hopanes; C_{27}–C_{30} desmethyl steranes in which cholestane (C_{27}) and 24-ethylcholestane (C_{29}) are co-dominant; and C_{30} 4-methyl steranes including dinosterane. The concentration of diasteranes is low relative to the regular steranes (diasterane/sterane = 0.2–0.6) and steranes are more abundant than hopanes (C_{30} hopane/C_{29} sterane = 0.4–0.5). An almost identical biomarker assemblage has been described from gypsiferous dolomite of the Gillen Member in Alice Springs-3 (Summons and Walter, 1990; Summons and Powell, 1991). Many of these biomarkers are commonly found in Phanerozoic marine carbonates and evaporites where they are consistent with inputs from eukaryotic algae and eubacteria. The occurrence of dinosterane, a marine dinoflagellate marker, in Proterozoic sediments remains problematical.

Reservoir facies of the underlying Pindyin Sandstone (5–20% porosity) and overlying Tarlina Sandstone (5–15% porosity) are well placed to receive any hydrocarbons expelled from source beds within the Alinya Formation. The upper reservoir unit is sealed by the Giles Mudstone, making this early Neoproterozoic sequence a target for petroleum exploration, particularly along the northern margin of the Murnaroo Platform where halokinesis has produced a great variety of potential traps. Organic-rich Neoproterozoic siliciclastics and carbonates are source rocks for commercial oil and gas accumulations in eastern Siberia, Oman and southern China (McKirdy and Imbus, 1992).

References

Jackson, K.S., McKirdy, D.M. and Deckelman, J.A., 1984. Hydrocarbon generation in the Amadeus Basin, central Australia. *APEA Journal,* **24(1),** 42–65.

McKirdy, D.M., 1977. The diagenesis of microbial organic matter: a geochemical classification and its use in evaluating the hydrocarbon-generating potential of Proterozoic and Lower Palaeozoic sediments, Amadeus Basin, central Australia. *Ph.D. Thesis, Australian National University* (unpublished).

McKirdy, D.M. and Imbus, S.W., 1992. Precambrian petroleum: a decade of changing perceptions. In: Schidlowski, M., Kimberley, M.M., Golubic, S., McKirdy, D.M. and Trudinger, P.A. (eds), *Early Organic Evolution: Implications for Mineral and Energy Resources*. Springer-Verlag, Berlin, pp. 176–192.

Summons, R.E. and Powell, T.G., 1991. Petroleum source rocks of the Amadeus Basin. In: Korsch, R.J. and Kennard, J.M. (eds), Geological and geophysical studies in the Amadeus Basin, central Australia. *Bureau of Mineral Resources, Australia, Bulletin,* **236,** 511–524.

Summons, R.E. and Walter, M.R., 1990. Molecular fossils and microfossils of prokaryotes and protists from Proterozoic sediments. *American Journal of Science,* **290-A,** 212–244.

Zang, Wenlong and Major, R.B., 1993. Early Neoproterozoic succession in the central and northeastern Officer Basin, South Australia: lithology and acritarch biostratigraphy. *South Australian Department of Mines and Energy Report Book* (in preparation).

Zang, Wenlong and Walter, M.R., 1992. Late Proterozoic and Cambrian microfossils and biostratigraphy, Amadeus Basin, central Australia. *Association of Australasian Palaeontologists Memoir* **12,** 132 p.

ALINYA FORMATION SOURCE ROCK DATA*

	TOC	EOM		Kerogen	
	%	ppm	Hydrogen Index	H/C	Type
Range	0.10 - 0.62	6 - 15	58 - 106	n.d.	III
Mean	0.36	10	75		
n	6	5	3		

* Data from Giles - 1

0403

ALINYA FORMATION MATURITY

Well	T max °C	PI	MPR	VR calc %
Giles - 1	439 - 445	0.21 - 0.29	1.04 - 1.27	1.04 - 1.12

MATURE

Murnaroo Platform

0404

HYDROGEN INDEX vs T max

ALINYA FORMATION

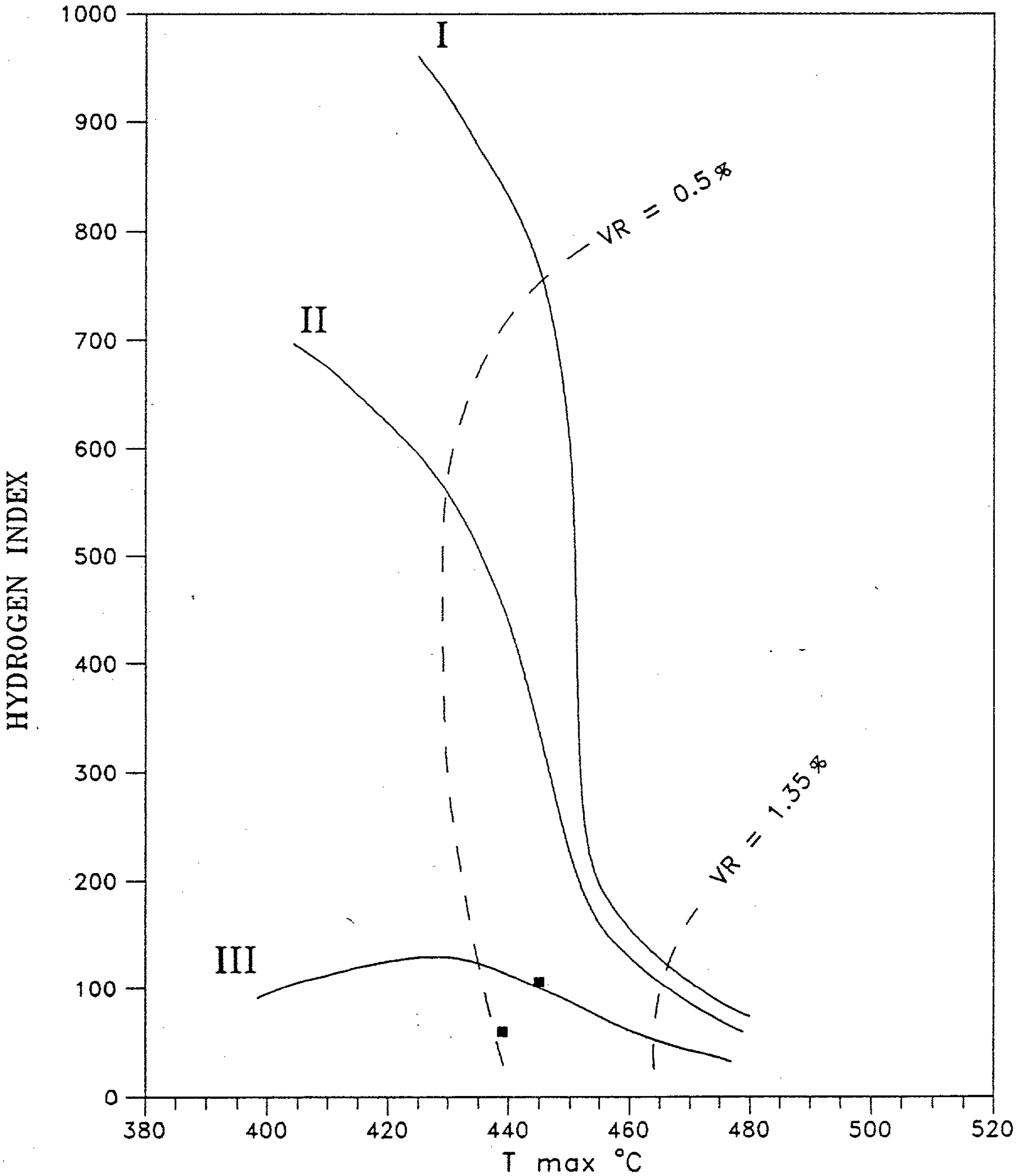

ALINYA FORMATION
Giles-1   1237.9 m
VR$_{calc}$ = 1.12%

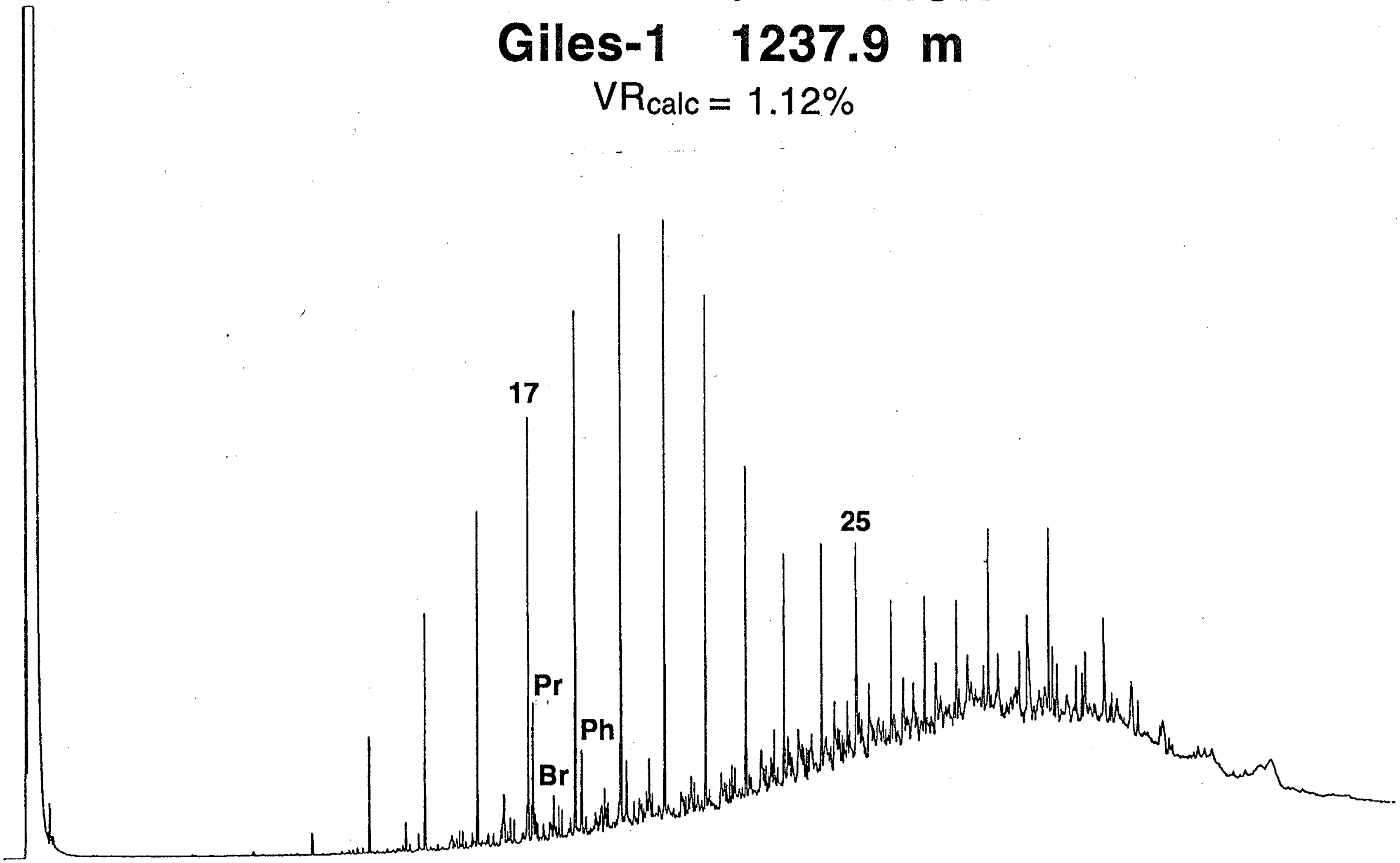

ALINYA FORMATION
Giles-1   1265.5 m
$VR_{calc} = 1.04\%$

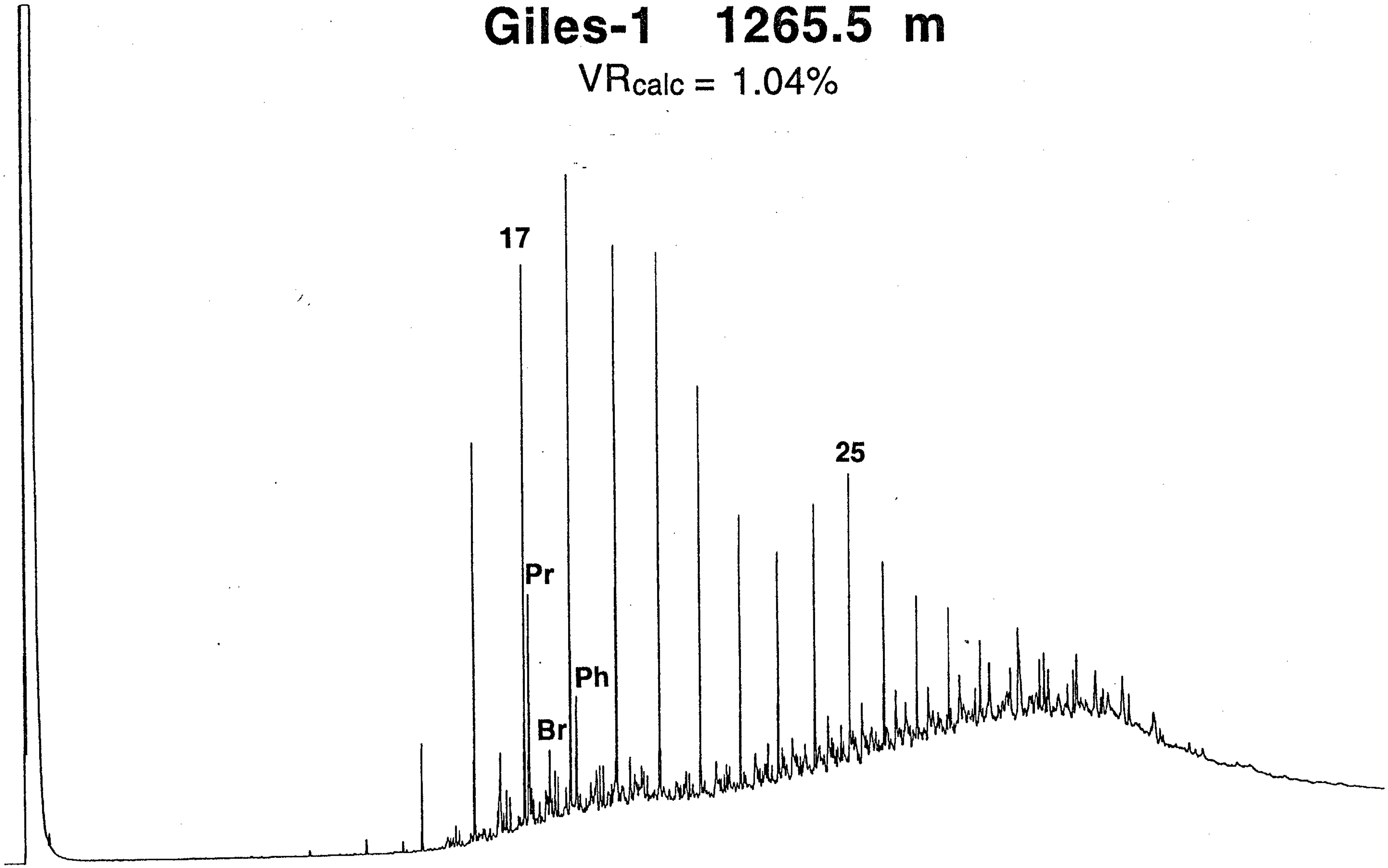

0407

GILLEN MEMBER
BITTER SPRINGS FORMATION

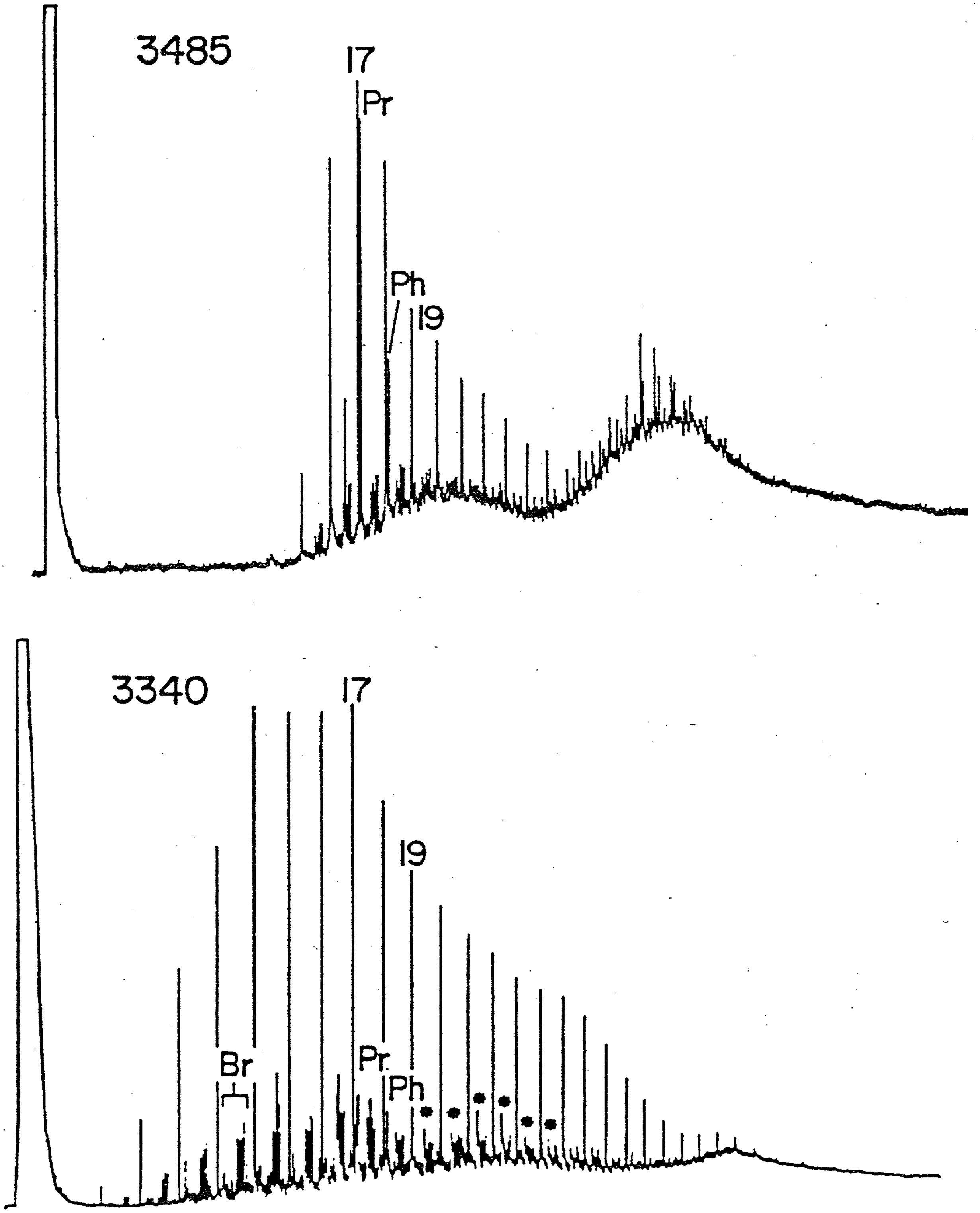

Summons & Walter (1990)

ALINYA FORMATION TRITERPANES

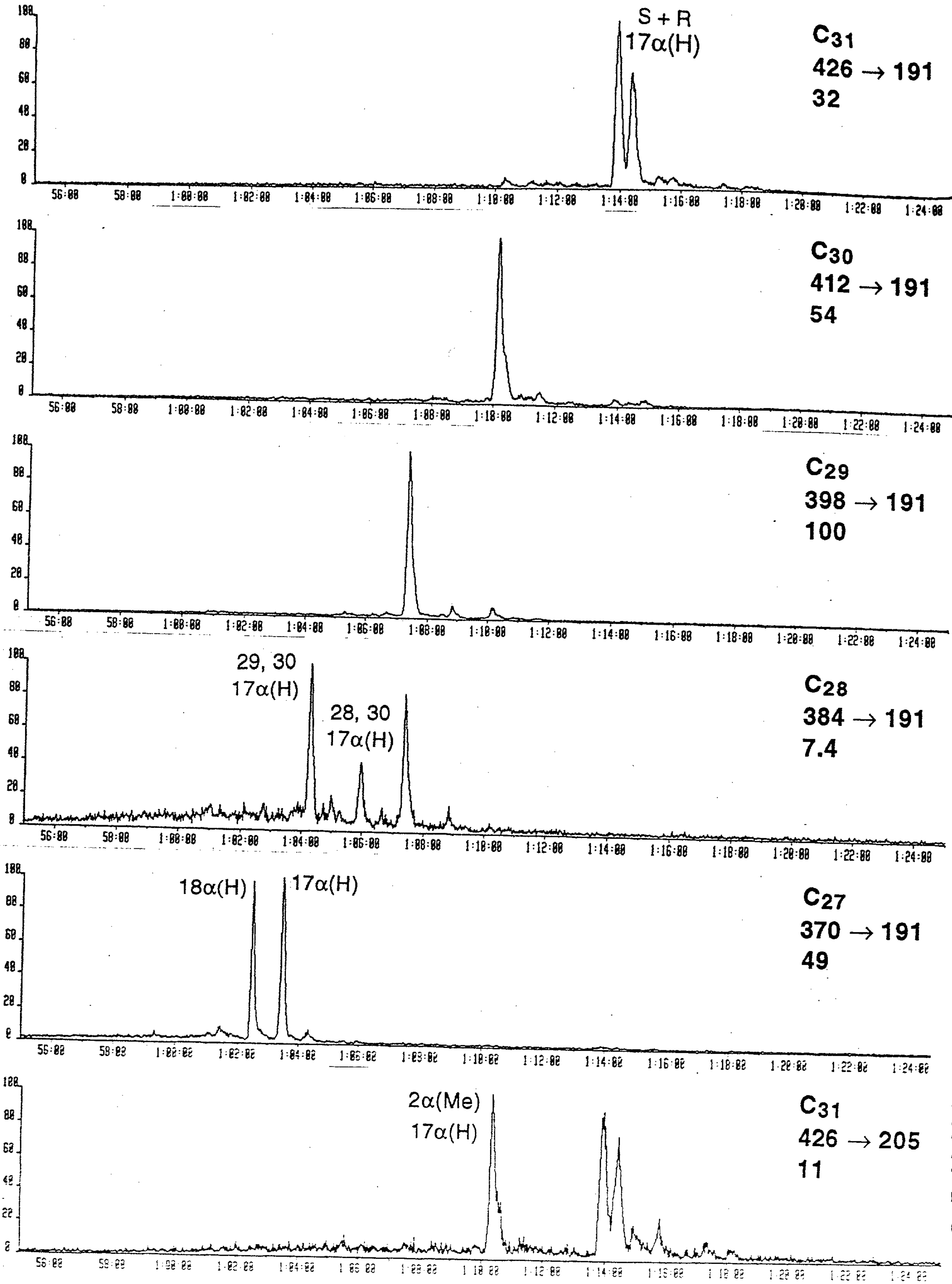

ALINYA FORMATION STERANES

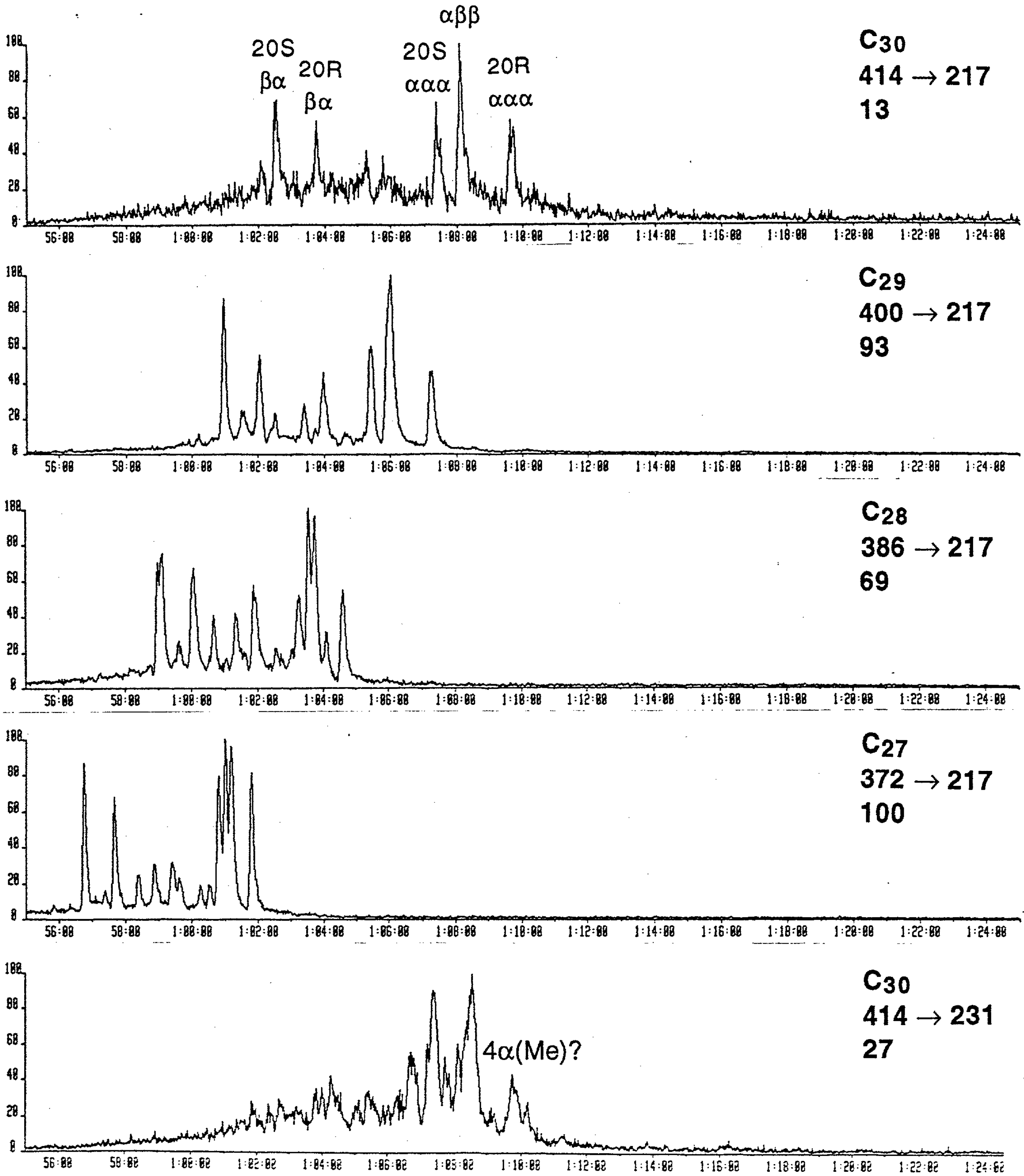

GILLEN MEMBER TRITERPANES

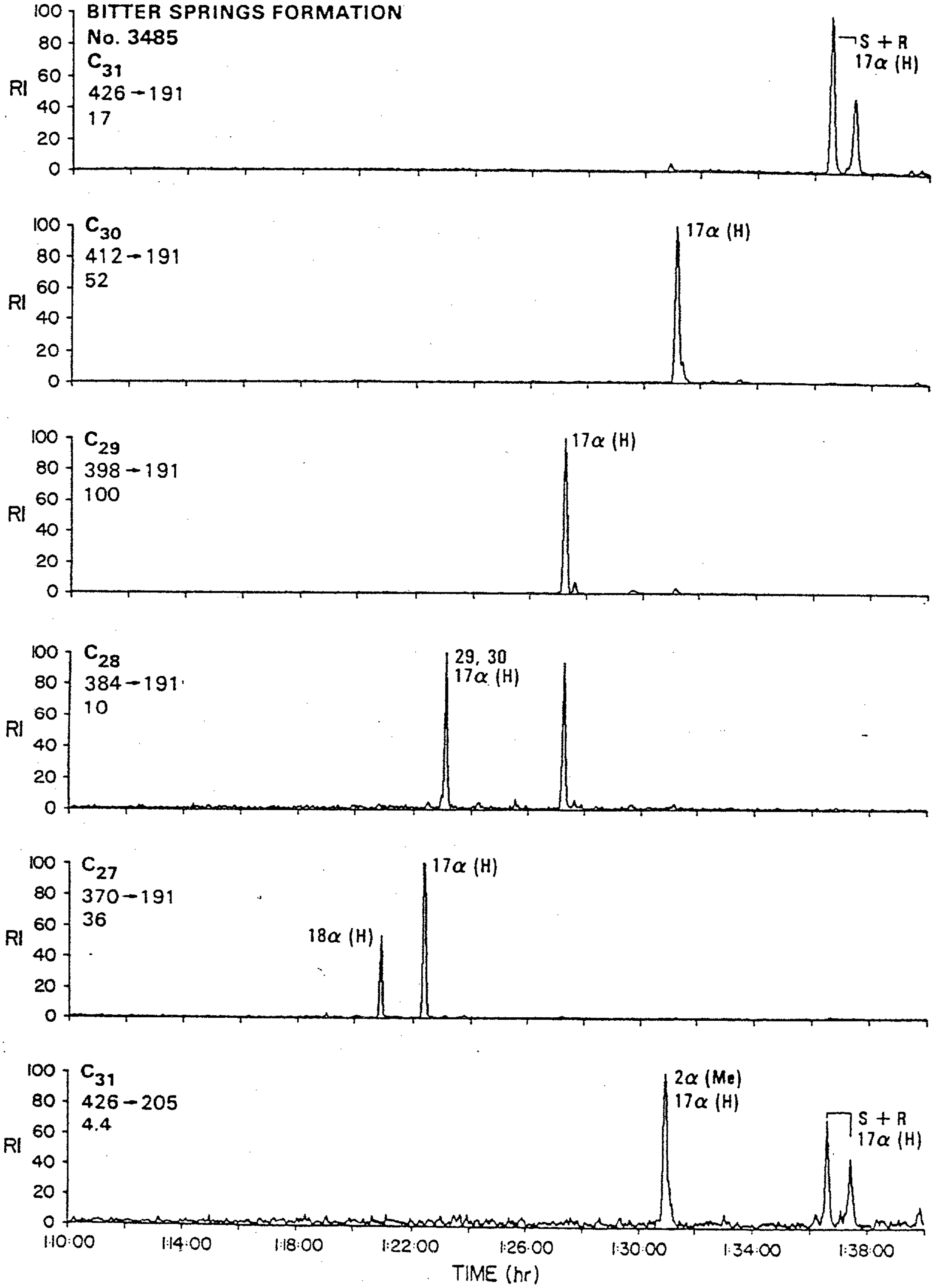

Summons & Walter (1990)

GILLEN MEMBER STERANES

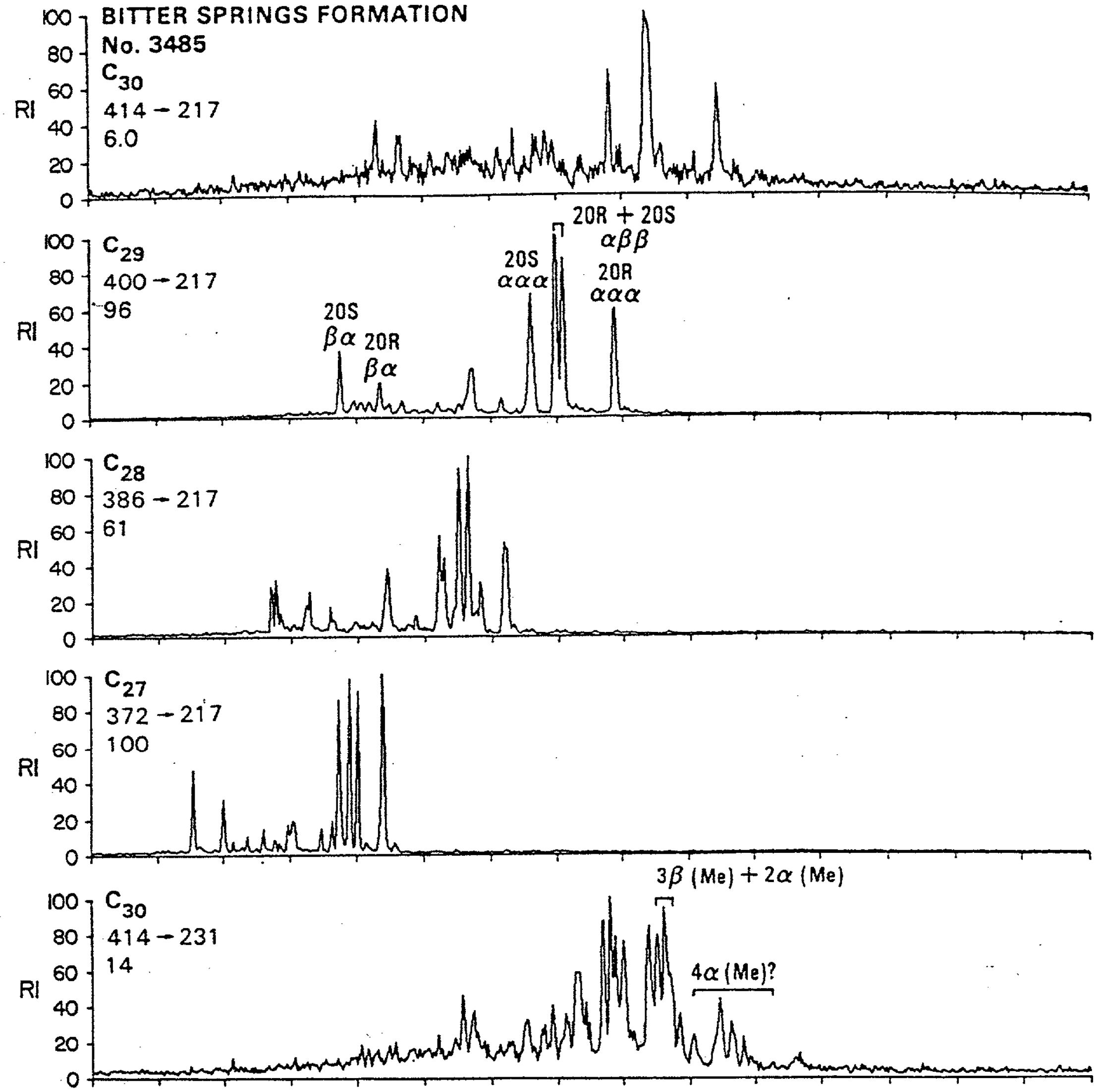

Summons & Walter (1990)

CONCLUSIONS

1. Anhydritic shales from the 35 metre-thick upper Alinya Formation in Giles-1 are organically lean (TOC = 0.1–0.6%).

2. The dispersed organic matter is gas-prone Type III kerogen.

3. Its maturation level corresponds to the oil generation window (VR_{calc} = 1.0–1.1%).

4. Reservoir facies of the underlying Pindyin Sandstone (5–20% porosity) and overlying Tarlina Sandstone (5–15% porosity) are well placed to receive any hydrocarbons expelled from source beds within the Alinya Formation.

5. Alinya shale extracts contain a diverse suite of molecular fossils derived from eukaryotic algae, cyanobacteria and eubacteria, including

   – methyl-branched alkanes
   – C_{27}–C_{35} hopanes
   – 2α-methylhopanes
   – C_{27}–C_{30} steranes
   – C_{30} 4-methylsterane (dinosterane ?)

CONCLUSIONS

6. Specific features of the Alinya biomarker distribution are identical to those reported in anhydritic dolomite of the Gillen Member, Bitter Springs Formation:

   - pristane/phytane = 1.6–2.0
   - 30-norhopane > hopane
   - 2α-methylhopanes present
   - C_{27} and C_{29} steranes co-dominant
   - dinosterane (?) present
   - diasterane/sterane = 0.2–0.6 .

7. Microfossils and molecular fossils provide a consistent basis for the biostratigraphic correlation of the Alinya Formation (Officer Basin) with the lower Bitter Springs Formation (Amadeus Basin).

8. The likely occurrence of dinosterane, a marine dinoflagellate marker, in Proterozoic sediments remains problematical.

AMDEL CORE SERVICES

30 April 1993

Department of Mines and Energy
PO Box 151
EASTWOOD SA 5063

Attention: David Gravestock

REPORT: HH/2259

CLIENT REFERENCE: 11/06/0800

MATERIAL: Rock Samples

LOCALITY: Manya-6

WORK REQUIRED: Source Rock Analysis

Please direct technical enquiries regarding this work to the signatory below under whose supervision the work was carried out.

Brian Watson

BRIAN L WATSON
Laboratory Supervisor
on behalf of Amdel Core Services Pty Ltd

Adelaide Office: P.O. Box 109, Eastwood, SA 5063 Australia.
Telephone: 61 8 379 9888 Facsimile: 61 8 379 9288
Amdel Core Services Pty Limited
(Incorporated in South Australia)
ACN: 008 273 005

1. INTRODUCTION

Thirty (30) samples from Manya-6 were received for TOC analysis and Rock-Eval pyrolysis. This report is a formal presentation of results which were forwarded by facsimile on 21 April 1993.

2. ANALYTICAL PROCEDURES

2.1 Sample Preparation

Samples (as received) were ground in a Siebtechnik mill for 20-30 seconds.

2.2 Total Organic Carbon (TOC)

Total organic carbon was determined by digestion of a known weight (approximately 0.2 g) of powdered rock in HCl to remove carbonates, followed by combustion in oxygen in the induction furnace of a Leco WR-12 Carbon Determinator and measurement of the resultant CO_2 by infra-red detection.

2.3 Rock-Eval Pyrolysis

A 100 mg portion of powdered rock was analysed by the Rock-Eval pyrolysis technique (Girdel IFP-Fina Mark 2 instrument; operating mode, Cycle 1).

3. RESULTS

TOC and Rock-Eval data are listed in Table 1. Figure 1 is a plot of T_{max} versus Hydrogen Index illustrating kerogen Type and maturity.

TABLE 1

AMDEL CORE SERVICES

Rock-Eval Pyrolysis 29/04/93

Client: South Australian Department of Mines and Energy

Well: Manya-6

Depth (m)	T Max	S1	S2	S3	S1+S2	PI	S2/S3	PC	TOC	HI	OI
689.90									0.06		
690.70									0.12		
691.15									0.19		
691.95									0.13		
695.25									0.12		
698.00	436	0.31	0.26	0.38	0.57	0.54	0.68	0.05	0.68	38	56
698.60	476	0.31	0.50	0.43	0.81	0.38	1.16	0.07	0.82	61	52
703.65									0.07		
704.50									0.09		
704.95									0.04		
767.00									0.09		
769.05									0.12		
771.30									0.19		
771.90									0.09		
777.10									0.06		
777.95									0.10		
779.60									0.26		
784.00									0.13		
785.10									0.15		
785.85									0.17		
1275.00									0.15		
1277.15	466	0.06	0.15	0.90	0.21	0.29	0.17	0.02	0.42	36	214
1277.30									0.31		
1277.85									0.19		
1278.25									0.35		
1279.15	304	0.09	0.06	0.69	0.15	0.60	0.09	0.01	0.52	12	133
1291.60									0.32		
1292.60									0.16		
1294.75									0.32		
1295.07									0.23		

FIGURE 1

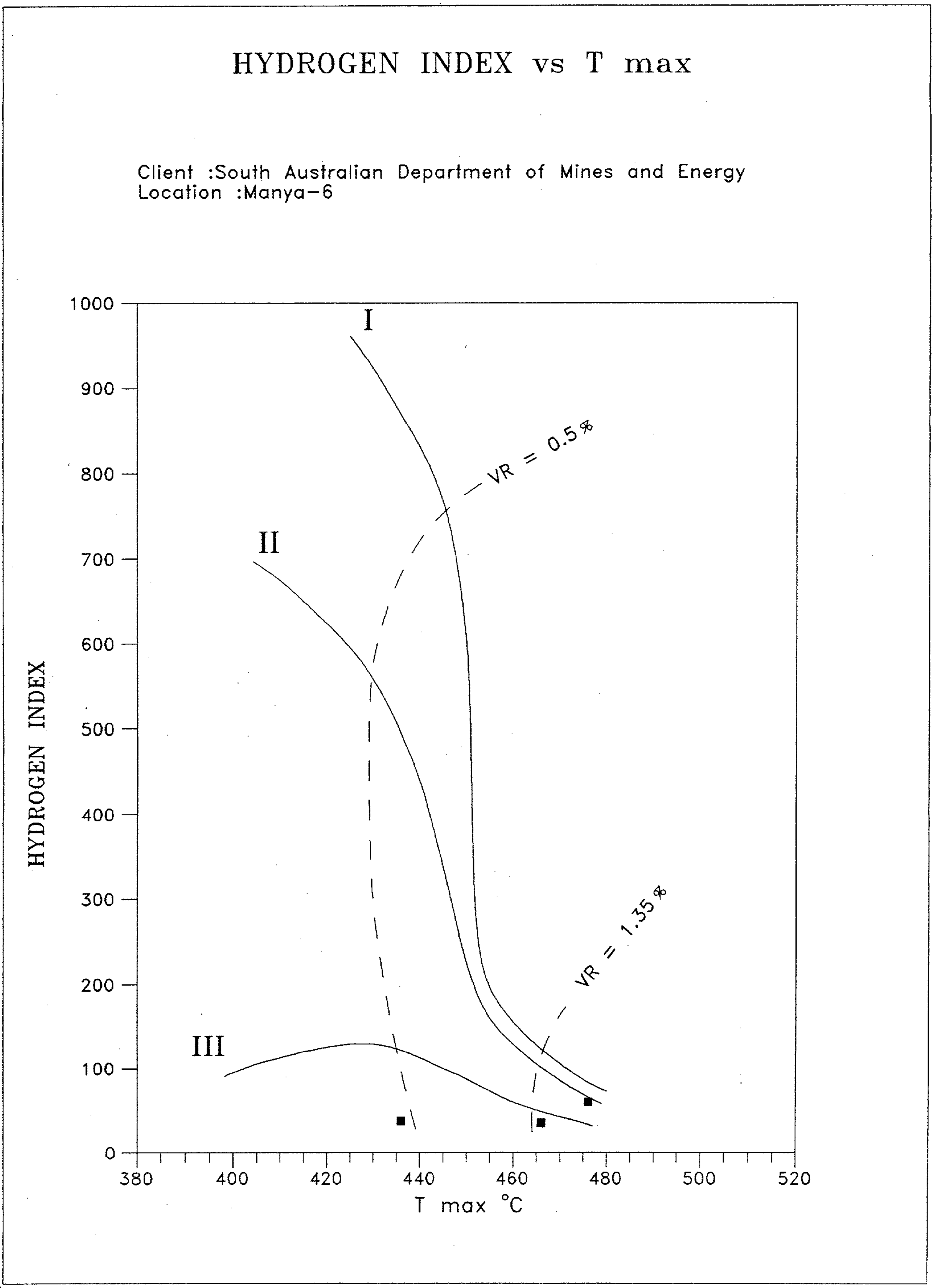
HYDROGEN INDEX vs T max
Client :South Australian Department of Mines and Energy
Location :Manya-6
I
II
III
VR = 0.5%
VR = 1.35%
HYDROGEN INDEX
T max °C
0
100
200
300
400
500
600
700
800
900
1000
380
400
420
440
460
480
500
520

SOURCE ROCK ASSESSMENT

WELL : MANYA #6

OFFICER BASIN

MOHAMMAD R. KAMALI
NATIONAL CENTRE FOR PETROLEUM GEOLOGY AND GEOPHYSICS ,FEB. 1993

SOURCE ROCK ASSESSMENT

WELL: MANYA #6

Sixty-four fine grained carbonate rocks in core samples were subjected to routine Rock-Eval pyrolysis to determine the source rock potential. Fifty-three samples were submitted previously by Comalco and a further 11 samples were added in this study.

Results:

Total Organic Carbon (TOC) values for majority of the samples are below 0.5%.
Average TOC = 0.2789%
TOC minimum = 0.04%

" maximum = 0.97%

A number of parameters are measured in this type of study which can be used to assess source richness and maturation. These include TOC, hydrocarbons released from the samples during pyrolysis (S1 and S2) and the temperature of peak generation (Tmax). Tables from Peters (1986) characterise the range of values for these parameters.

Geochemical Parameters Describing Source Rock Generative Potential

Quatity	TOC (wt%)	S1*	S2*
Poor	0-0.5	0-0.5	0-2.5
Fair	0.5-1	0.5-1	2.5-5
Good	1-2	1-2	5-10
Very good	2+	2+	10+

*Nomenclature: Table:1

S1= mg HC/g rock released at 250°C

S2= mg HC/g rock released between 250-550°C

S1 and S2 are considered to be poor, because their range is in between 0-0.5 and 0-2.5 respectively (see Table 1 and Geochemical log).

There were no vascular plants in the Cambrian so the organic matter in the sediment must have been derived from algae and bacteria. The traditional methods of determining source rock maturity (e.g. vitrinite reflectance) are of little use in rocks of this age. It is possible to measure reflectivity of inertinite instead and apply a correction factor to find the inertinite reflectance equivalence.

There is still uncertainty with the origin of inertinite maceral taken at depths 876.75 and 876.35m. The measured reflectance of this inertinite was reported to be Ro=2.2% and 2.5% respectively (D.McKirdy etal., 1983). In clastic sediments and coal containing inertinite and coexisting vitrinite, the reflectance of the latter maceral would fall in the range Ro=1.15-1.6% (Smith and Cook, 1980) but even these values are suspect.

However, all the samples from Manya #6 show low Tmax indicating that they are immature (see Table 2 and Geochemical log). Tmax values from Manya #6 vary from- 359°C suggesting suppression appears to have occurred as a result of "contamination"of organic matter by derived bitumens which have been unable to escape from the immediate environment because of the impermeable nature of the rock. Consequently, Tmax values are unreliable maturity indicators in this case.

Geochemical Parameters Describing Level of Thermal Maturation

Maturation	**PI** [S1/(S1+S2)]	**Tmax** (C°)	**Ro** (%)
Top Oil Window (birthline)	~0.1	~435-445*	~0.6
Bottom Oil Window (deadline)	~0.4	~470	~1.4

*Many maturity parameters (particularly Tmax) depend on type of organi matter (Peters, 1986). Table: 2

Hydrogen Index (HI) and Oxygen Index (OI) are other parameters derived from Rock-Eval pyrolysis. A cross plot of HI versus OI can be used as a pseudo van Krevelen Diagram and in this case suggests all the samples fall in the Type III kerogen region (see fig. 1 also Table 3).

This is unlikely to be the case as woody material for vitrinite generation was not available in the Cambrian.

The plot is a "bulk analysis" and probably represents a mixture of alginite and inertinite or oxidised organic matter. The low HI values for original algal material might be indicative of elevated maturation, supportive of the reflectance readings. The highest recorded Tmax value is 359 which suggests an immature O.M. but with the reservations expressed above.

Geochemical Parameters Describing Type of Hydrocarbon Generated

TYPE	**HI** [mg HC/gCorg]*	**S2/S3***
GAS	0-150	0-3
GAS and OIL	150-300	3-5
OIL	300+	5+

* Assumes a level of thermal maturation equivalent Ro= 0.6% Table:3

Conclusion:

Neither Tmax nor Ro are reliable here due to contamination and lack of vitrinite macerals.
Rock-Eval pyrolysis of 64 samples suggests that only 11 samples have TOC values above the minimum required (0.5%) and the remaining are immature having very low hydrocarbon potential.

Recommendation:

Analysis of 64 samples reveals that there are thin organic rich and organic poor layers. Organic rich intervals would be referred as transgressive phases where organic input was high. To determine organic facies the following is recommended.

-Sampling would be preferably done from organic rich layers for two meter intervals just below and above the highest TOC value (organic richness holds good for approximately two meters.

-The Methyl Phenanthrene Index (MPI) method of maturity assessment should be tried on the organic rich layers to provide perhaps a more reliable indication of the level of maturity in view of the problem with other indicators.

0423

amdel
A.C.N. 008 127 802

FACSIMILE TRANSMISSION FROM:

AMDEL LIMITED PETROLEUM SERVICES
35-37 STIRLING STREET, THEBARTON SA 5031
FACSIMILE NO: (08) 234 0355 or (08) 234 2760
TELEPHONE NO: (08) 416 5240

TO:	David Gravestock		
COMPANY:	MESA		
FAX NO:	373 3269	DATE:	6 June 1994
COPY TO:			
FROM:	Scott Wythe	TOTAL PAGES:	3

David,

TOC/Rock-Eval data follows for the five samples from KD-1 and KD-2A.

We apologise for the delay in getting these results to you which, as you know, has been due to equipment problems. Problems with our Rock-Eval have now been rectified and a much quicker turnaround for future work is anticipated.

Best Regards,

Scott Wythe
Petroleum Geochemist
Petroleum Services

AMDEL PETROLEUM SERVICES

Rock-Eval Pyrolysis

06/06/94

Client: *MESA*

Well: *As listed below*

Depth (m)	T Max	S1	S2	S3	S1+S2	PI	S2/S3	PC	TOC	HI	OI
KD-1											
263.35	427	0.59	4.59	5.37	5.18	0.11	0.85	0.43	1.18	388	455
275.43									0.20		
KD-2A											
211.80									0.34		
285.50	427	0.49	3.20	4.76	3.69	0.13	0.67	0.30	0.73	438	652
297.95	425	0.70	2.20	3.35	2.90	0.24	0.66	0.24	0.59	372	567

HYDROGEN INDEX vs T max

Client: MESA
Location: KD-1 & KD-2A

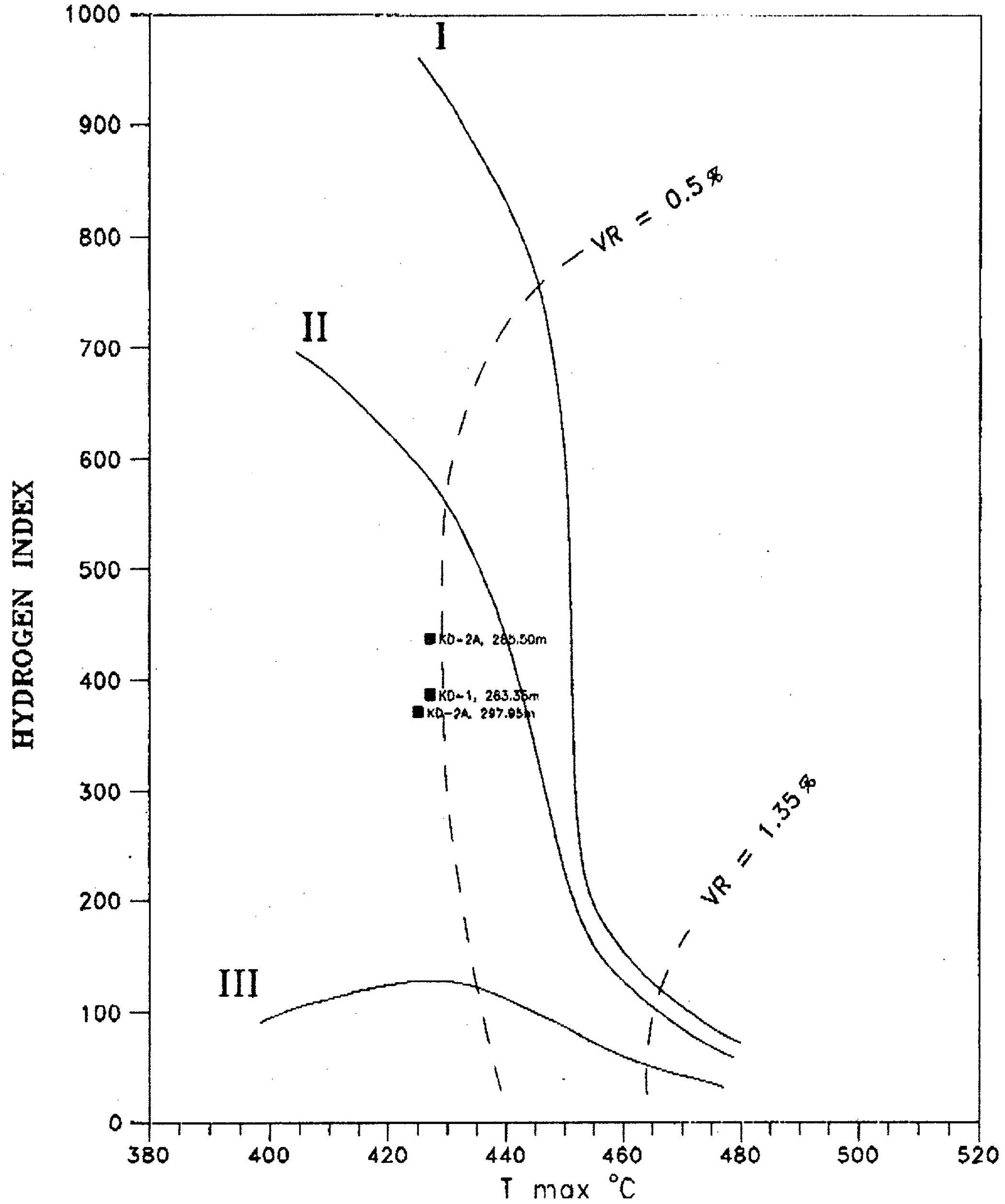

0426

AMDEL CORE SERVICES

FACSIMILE TRANSMISSION FROM:

AMDEL CORE SERVICES PTY LIMITED
31 FLEMINGTON STREET FREWVILLE SA 5063
FACSIMILE NO: (08) 379 9288
TELEPHONE NO: (08) 379 9888
ACN: 008 273 005

TO:	D. GRAVESTOCK		
COMPANY:	SADME		
FAX NO:	373 3269	DATE:	12/1/93
COPY TO:			
FROM:	SCOTT WYTHE	TOTAL PAGES:	2.

Dave,

TOC/Rock-Eval results follow for your Officer and Stansbury Basin samples. We are rechecking Rock-Eval data from the Marla-3 samples at 619.60 and 626.25 m. and I will get this to you this week.

Regards

Scott Wythe

AMDEL CORE SERVICES

Rock-Eval Pyrolysis 01/09/93

Client: South Australian Department of Mines and Energy

Well: Various

Depth (m)	T Max	S1	S2	S3	S1+S2	PI	S2/S3	PC	TOC	HI	OI
Investigator-2											
222.2									0.08		
Manya-6											
652.30									0.07		
691.75	308	0.35	0.40	0.67	0.75	0.47	0.59	0.06	0.97	41	69
780.90									0.14		
896.95									0.19		
1009.50									0.09		
1020.05									0.11		
1038.10									0.13		
1072.10									0.15		
1145.70									0.26		
1193.50									0.19		
1312.70	221	0.00	0.00	0.49	0.00	0.00	0.00	0.00	0.61	0	80
Marla-3											
508.30									0.02		
509.45									0.03		
513.05									0.01		
546.45									0.05		
568.45									0.09		
576.90									0.18		
586.20									0.14		
601.25									0.13		
619.60									0.79		
624.85									0.08		
626.25									0.66		
Marla-6											
416.00	422	0.22	1.22	0.41	1.44	0.15	2.97	0.12	1.34	91	30
573.10									0.19		
585.00									0.05		
637.05									0.27		
655.50									0.09		
671.25	341	0.14	0.13	0.18	0.27	0.54	0.72	0.02	1.13	11	15
684.70									0.28		
700.25	237	0.08	0.00	0.41	0.08	1.00	0.00	0.00	0.47	0	87
Marla-7											
333.75									0.09		
347.30									0.05		
378.50									0.13		
383.05									0.10		
392.85	403	0.11	0.32	0.25	0.43	0.26	1.28	0.03	0.53	60	47
443.15									0.12		
445.00									0.10		
448.45									0.21		
517.76									0.21		

0428

amdel
A.C.N. 008 127 802

FACSIMILE TRANSMISSION FROM:

AMDEL LIMITED PETROLEUM SERVICES
35-37 STIRLING STREET, THEBARTON SA 5031
FACSIMILE NO: (08) 234 0355 or (08) 234 2760
TELEPHONE NO: (08) 416 5240

TO:	David Gravestock		
COMPANY:	SADME		
FAX NO:	373 3269	DATE:	28 April 1994
COPY TO:			
FROM:	Scott Wythe	TOTAL PAGES:	2

David,

lower Murnaroo.

The extract yield for the Manya-5 sandstone sample was determined to be 461 ppm. We have run a GC of the extract and this follows for your information. Please note there will be no charge for this. Organic petrology is proceeding.

Best Regards,

Scott Wythe
Petroleum Geochemist
Petroleum Services

Manya-5
918.9 - 919.0 m
GC of whole extract

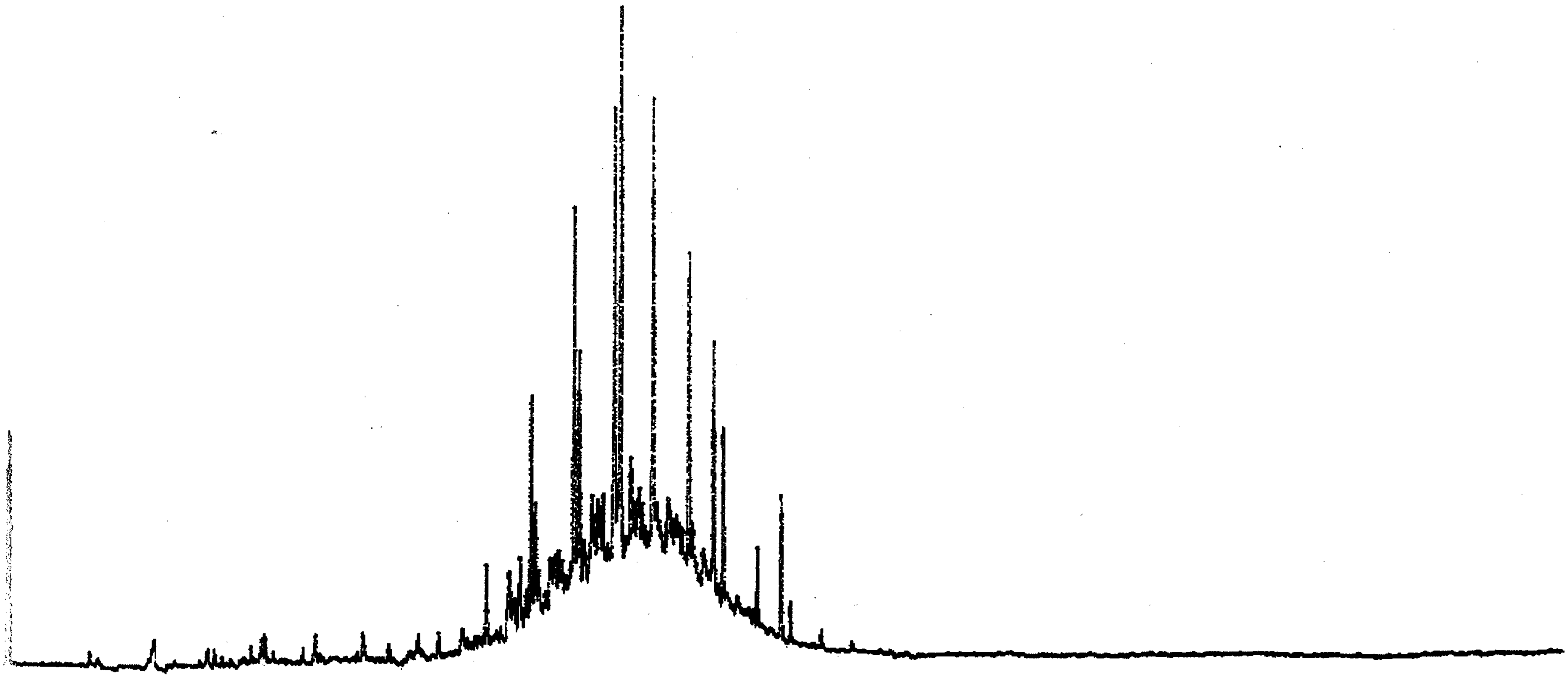

0430

amdel
A.C.N. 008 127 802

FACSIMILE TRANSMISSION FROM:

AMDEL LIMITED PETROLEUM SERVICES
35-37 STIRLING STREET, THEBARTON SA 5031
FACSIMILE NO: (08) 234 0355 or (08) 234 2760
TELEPHONE NO: (08) 416 5240

TO:	David Gravestock		
COMPANY:	SADME		
FAX NO:	373 3269	DATE:	3 May 1994
COPY TO:			
FROM:	Scott Wythe	TOTAL PAGES:	3

David,

MPI data follows as requested for the Manya-5 sandstone sample.

Best Regards,

Scott Wythe
Petroleum Geochemist
Petroleum Services

TABLE 2

AROMATIC MATURITY DATA, MANYA-5

Sample	MPI	MPR	MPDF	VR CALC (%)				
				A	B	C	E	F
918.9-919.0	0.579	0.940	0.357	0.75	1.95	0.91	0.63	0.63

KEY TO AROMATIC MATURITY INDICATORS

Methylphenanthrene index (MPI), methylphenanthrene ratio (MPR), dimethylnaphthalene ratio (DNR) and calculated vitrinite reflectance (VR_{calc}) are derived from the following equations (after Radke and Welte, 1983; Radke *et al*, (1984):

$$MPI = \frac{1.5(2\text{-}MP + 3\text{-}MP)}{P + 1\text{-}MP + 9\text{-}MP}$$

$$VR_{calc}\ (a) = 0.6\ MPI + 0.4\ (\text{for } VR < 1.35\%)$$

$$VR_{calc}\ (b) = -0.6\ MPI + 2.3\ (\text{for } VR > 1.35\%)$$

$$MPR = \frac{2\text{-}MP}{1\text{-}MP}$$

$$VR_{calc}\ (c) = 0.99\ \log_{10} MPR + 0.94 (VR = 0.5\text{-}1.7\%)$$

$$DNR = \frac{2{,}6\text{-}DMN + 2{,}7\text{-}DMN}{1{,}5\text{-}DMN}$$

$$VR_{calc}\ (d) \quad 0.46\ DNR + 0.89\ (\text{for } VR = 0.9\text{-}1.5\%)$$

Where
P = phenanthrene
1-MP = 1-methylphenanthrene
2-MP = 2-methylphenanthrene
3-MP = 3-methylphenanthrene
9-MP = 9-methylphenanthrene
1,5-DMN = 1,5-dimethylnaphthalene
2,6-DMN = 2,6-dimethylnaphthalene
2,7-DMN = 2,7-dimethylnaphthalene

Peak areas measured from m/z 156 (dimethylnaphthalene), m/z 178 (phenanthrene) and m/z 192 (methylphenanthrene) mass fragmentograms of diaromatic and triaromatic hydrocarbon fraction isolated by thin layer chromatography.

Recalibration of the methylphenanthrene index using data from a suite of Australian coals has given rise to another equation for calculated vitrinite reflectance (after Boreham *et al*, 1988):

$$VR_{calc}\ (e) = 0.7\ MPI + 0.22\ (\text{for } VR < 1.7\%)$$

The methylphenanthrene distribution ratio (MPDF) and calculated vitrinite reflectance VR_{calc} (f) is derived from the following equation (after Kvalheim *et al*, 1987):

$$MPDF = \frac{(2\text{-}MP + 3\text{-}MP)}{(2\text{-}MP + 3\text{-}MP + 1\text{-}MP + 9\text{-}MP)}$$

$$VR_{calc}\ (f) = -0.166 + 2.242\ MPDF$$

Chromatogram D:APS284 Acquired: Apr-22-1994 11:37:09
Comment: MPI SADME MANYA-5 918.9-919.0m AMDEL PETROLEUM SERVICES
Scan Range: 2000 - 2800 Scan: 2000 Int = 85 @ 33:21 100% = 1782

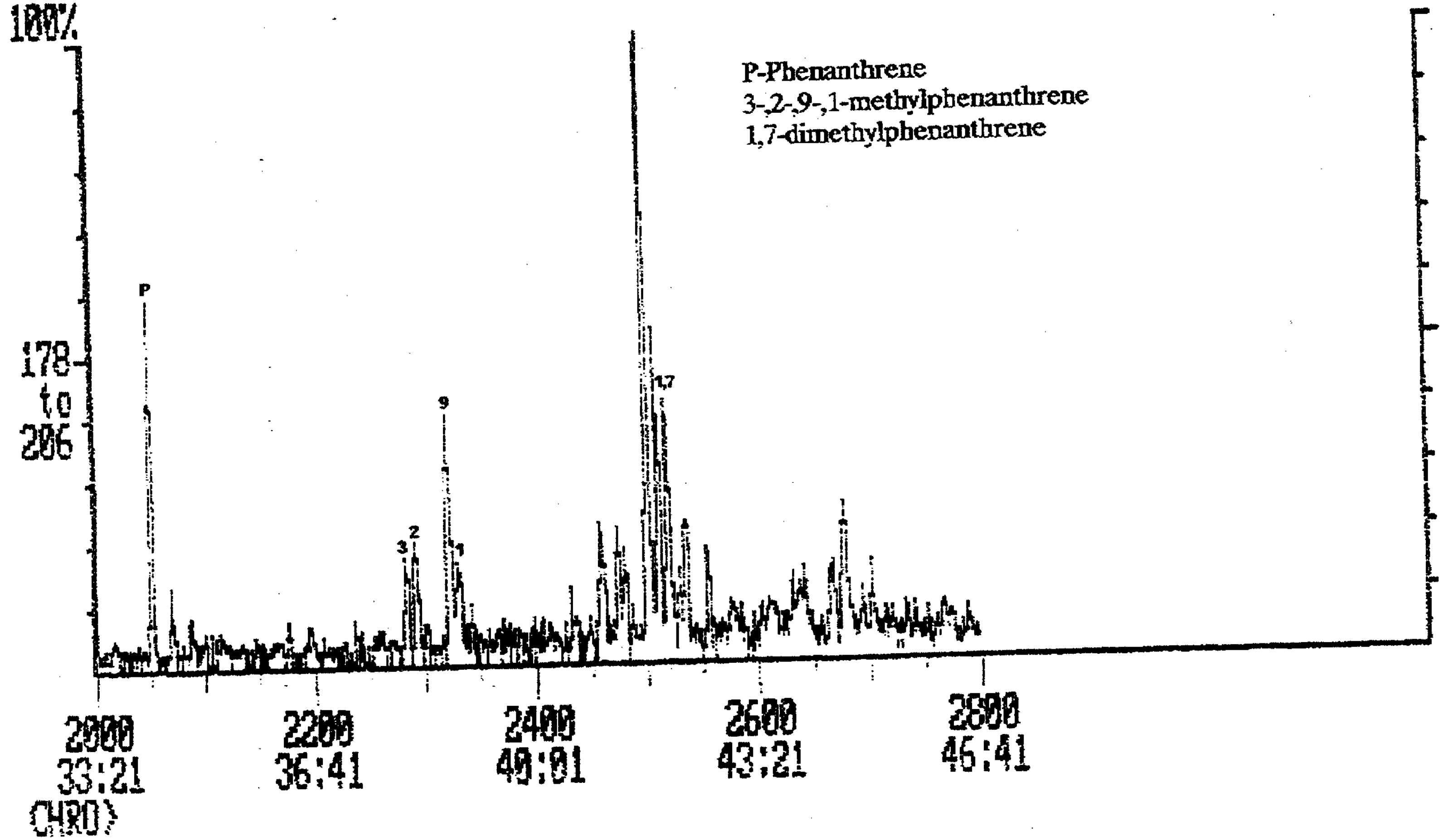

amdel

Amdel Limited
A.C.N. 008 127 802

Petroleum Services
PO Box 338
Torrensville SA 5031

Telephone: (08) 416 5240
Facsimile: (08) 234 0355

14 July 1994

Mines and Energy South Australia
PO Box 151
EASTWOOD SA 5063

Attention: Information Officer

REPORT LQ2959

CLIENT REFERENCE: 58/GR2/956

WELL NAME: KD-1 and KD-2A

MATERIAL: Rock Samples

WORK REQUIRED: Source Rock Analysis

Please direct technical enquiries regarding this work to the signatory below under whose supervision the work was carried out.

Brian Watson

Brian L. Watson
Manager
Petroleum Services

1. INTRODUCTION

Five (5) samples from KD-1 and KD-2A were received for TOC analysis and Rock-Eval pyrolysis. This report is a formal presentation of results forwarded as they became available.

2. ANALYTICAL PROCEDURE

2.1 Sample Preparation

Samples (as received) were ground in a Siebtechnik mill for 20-30 seconds.

2.2 Total Organic Carbon (TOC)

Total organic carbon was determined by digestion of a known weight (approximately 0.2 g) of powdered rock in HCl to remove carbonates, followed by combustion in oxygen in the induction furnace of a Leco WR-12 Carbon Determinator and measurement of the resultant CO_2 by infra-red detection.

2.3 Rock-Eval Pyrolysis

A 100 mg portion of powdered rock was analysed by the Rock-Eval pyrolysis technique (Girdel IFP-Fina Mark 2 instrument; operating mode, Cycle 1).

3. RESULTS

TOC and Rock-Eval pyrolysis results are presented in Table 1. Figure 1 is a plot of Hydrogen Index versus T max illustrating maturity and organic matter type. The three Rock-Eval pyrograms are shown in Figure 2.

TABLE 1

AMDEL PETROLEUM SERVICES

Rock–Eval Pyrolysis 06/06/94

Client: *MESA*

Well: *As listed below*

Depth (m)	T Max	S1	S2	S3	S1+S2	PI	S2/S3	PC	TOC	HI	OI
KD–1											
263.35	427	0.59	4.59	5.37	5.18	0.11	0.85	0.43	1.18	388	455
275.43									0.20		
KD–2A											
211.80									0.34		
285.50	427	0.49	3.20	4.76	3.69	0.13	0.67	0.30	0.73	438	652
297.95	425	0.70	2.20	3.35	2.90	0.24	0.66	0.24	0.59	372	567

FIGURE 1

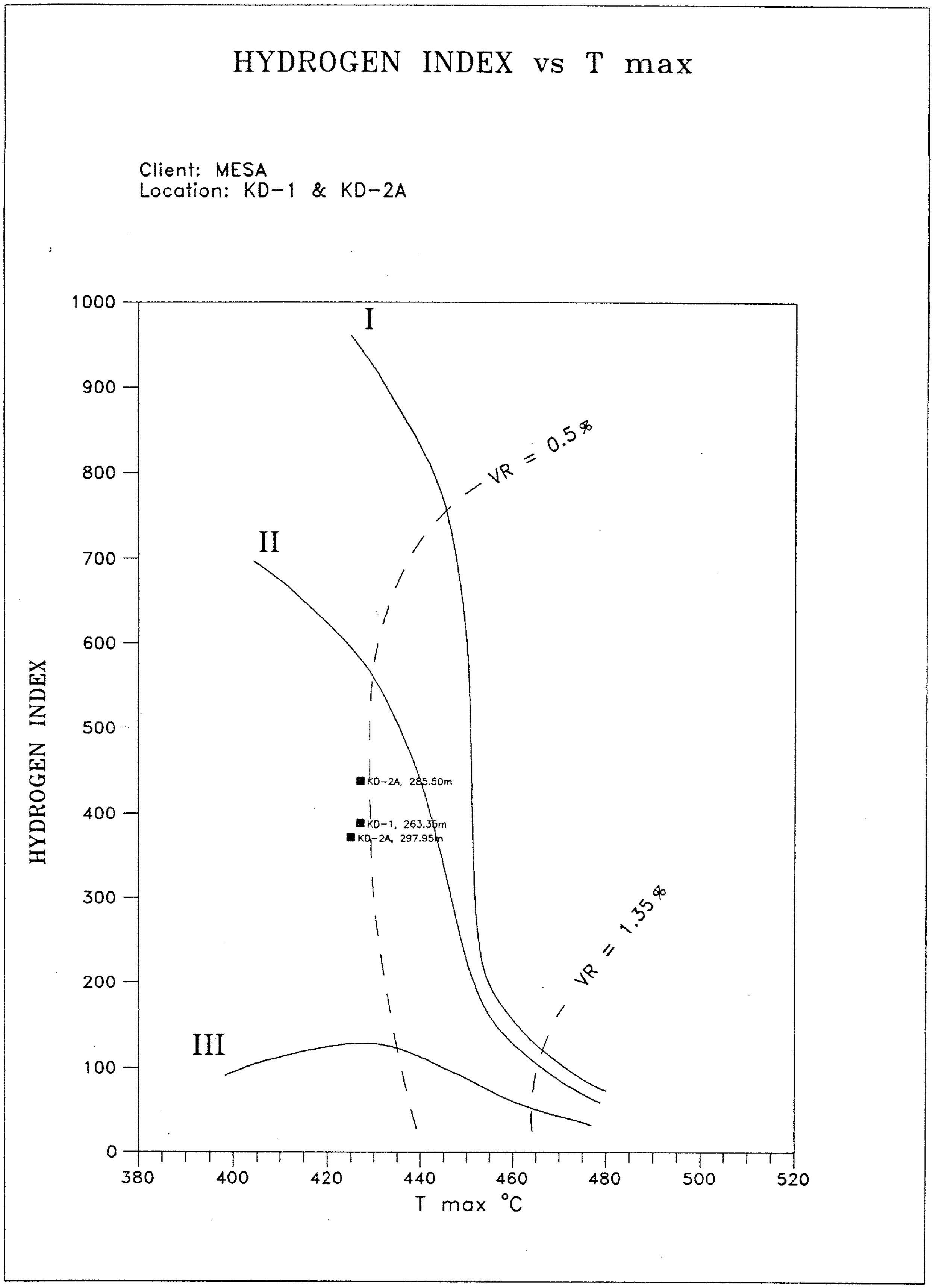

HYDROGEN INDEX vs T max
Client: MESA
Location: KD-1 & KD-2A
HYDROGEN INDEX
T max °C
I
II
III
VR = 0.5 %
VR = 1.35 %
KD-2A, 285.50m
KD-1, 263.35m
KD-2A, 297.95m
1000
900
800
700
600
500
400
300
200
100
0
380
400
420
440
460
480
500
520

FIGURE 2

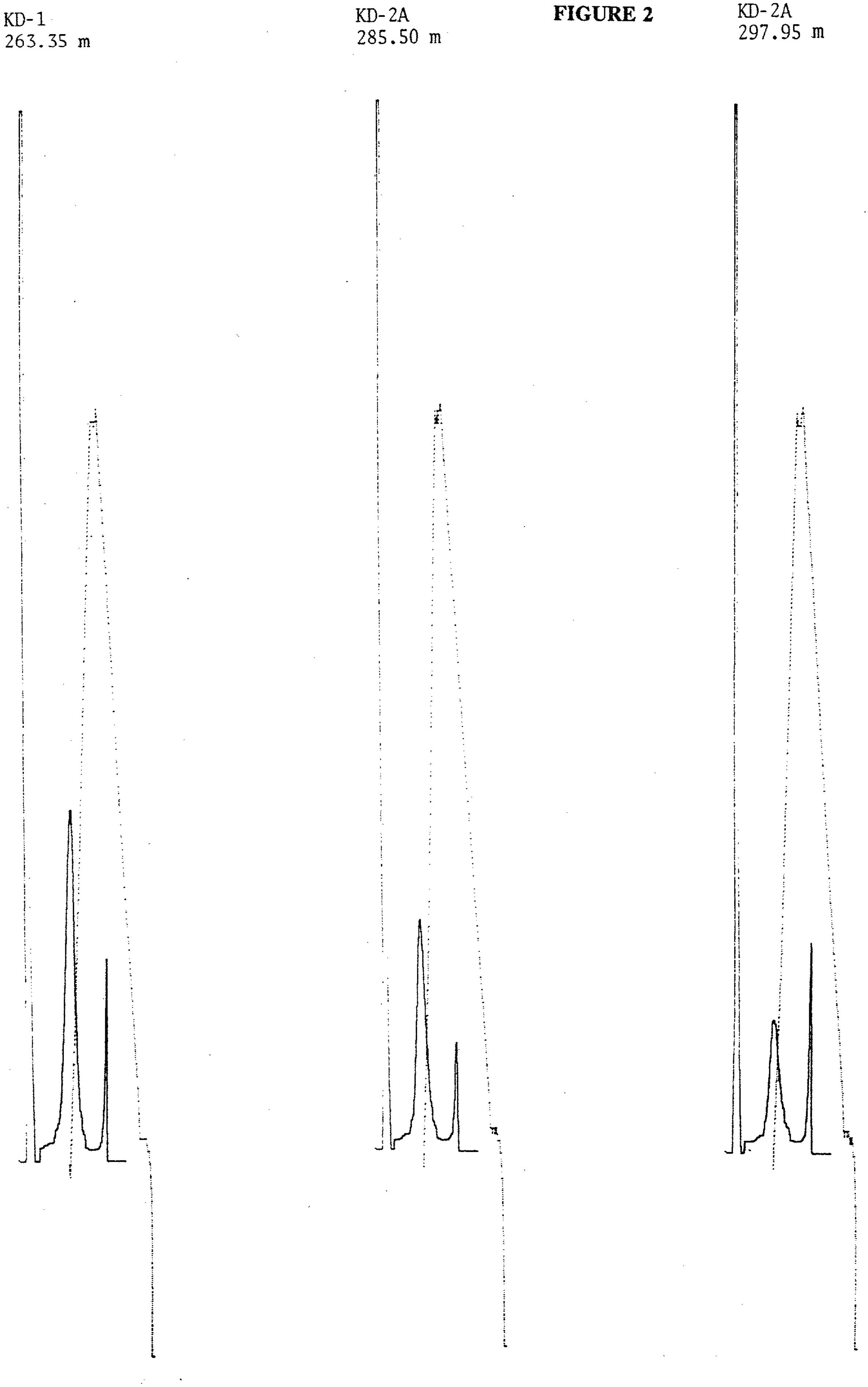

0438

Amdel Limited
A.C.N. 008 127 802

Petroleum Services
PO Box 338
Torrensville SA 5031

Telephone: (08) 416 5240
Facsimile: (08) 234 0355

14 July 1994

Mines and Energy South Australia
PO Box 151
EASTWOOD SA 5063

Attention: Information Officer

REPORT LQ2938

CLIENT REFERENCE: 58/GR2/953

WELL NAME/RE: Manya-5

MATERIAL: Core Sample

WORK REQUIRED: Geochemistry

Please direct technical enquiries regarding this work to the signatory below under whose supervision the work was carried out.

Brian L. Watson
Manager
Petroleum Services

1. INTRODUCTION

One (1) core sample from Manya-5, 918.9-919.0 metres depth was received for extraction of any organic matter present followed by GC-MS analysis to determine the oil extract maturity of the sample. This report is a formal presentation of results forwarded as they became available.

2. ANALYTICAL PROCEDURE

2.1 Isolation of Residual Oil

Core chips were extracted with dichloromethane in Soxhlet apparatus for 8 hours. Removal of solvent by careful rotary evaporation gave the oil (nominal C_{12+} fraction).

2.2 Thin Layer Chromatography (TLC)

Aromatic hydrocarbons were isolated from the extracted oil by preparative TLC using Merck GF_{254} silica plates and distilled AR grade n-pentane as eluent. Naphthalene and anthracene were employed as reference standards for the diaromatic and triaromatic hydrocarbons, respectively. These two bands, visualised under UV light, were scraped from the plate and the aromatic hydrocarbons redissolved in dichloromethane.

2.3 Gas Chromatography-Mass Spectrometry (GC-MS)

The di- and triaromatic hydrocarbons isolated from the extracted oil by thin layer chromatography were analysed by GC-MS.

GC-MS analysis of the aromatic hydrocarbons was undertaken in the selected ion detection (SID) mode. The instrument and its operating parameters were as follows:

System:	Perkin-Elmer 8420 GC coupled with an Ion Trap mass selective detector and data system
Column:	25 m x 0.2 mm I.D. HP BP5 cross-linked methylsilicone phase fused silica, interfaced directly to source of mass spectrometer
Injector:	Split injection (8:1)
Carrier gas:	Helium at 1.2 kg/cm^2 head pressure
Column temperature:	50-260°C @ 4°C/minute
Mass spectrometer conditions:	70 eV EI; 9-ion selected ion monitoring, 70 millisec dwell time for each ion

The following mass fragmentograms were recorded:

m/z	Compound Type
155 + 156	dimethylnaphthalenes
169 + 170	trimethylnaphthalenes
178	phenanthrene
191 + 192	methylphenanthrene

The area of the phenanthrene peak was multiplied by a response factor of 0.667 when calculating the methylphenanthrene index (MPI).

3. RESULTS

The extract yield for the sample was determined to be 461 mg/kg.

Table 1 lists the aromatic maturity data. Figure 1 is a gas chromatogram of the whole extract while a chromatogram showing the relevant aromatic compounds is given in Figure 2.

TABLE 1

AROMATIC MATURITY DATA, MANYA-5

Sample	MPI	MPR	MPDF	VR CALC (%)				
				A	B	C	E	F
918.9-919.0	0.579	0.940	0.357	0.75	1.95	0.91	0.63	0.63

KEY TO AROMATIC MATURITY INDICATORS

Methylphenanthrene index (MPI), methylphenanthrene ratio (MPR), dimethylnaphthalene ratio (DNR) and calculated vitrinite reflectance (VR_{calc}) are derived from the following equations (after Radke and Welte, 1983; Radke *et al*, (1984):

$$MPI = \frac{1.5(2\text{-}MP + 3\text{-}MP)}{P + 1\text{-}MP + 9\text{-}MP}$$

$$VR_{calc}\ (a) = 0.6\ MPI + 0.4\ (\text{for } VR < 1.35\%)$$

$$VR_{calc}\ (b) = -0.6\ MPI + 2.3\ (\text{for } VR > 1.35\%)$$

$$MPR = \frac{2\text{-}MP}{1\text{-}MP}$$

$$VR_{calc}\ (c) = 0.99\ \log_{10} MPR + 0.94 (VR = 0.5\text{-}1.7\%)$$

$$DNR = \frac{2{,}6\text{-}DMN + 2{,}7\text{-}DMN}{1{,}5\text{-}DMN}$$

$$VR_{calc}\ (d) \quad 0.46\ DNR + 0.89\ (\text{for } VR = 0.9\text{-}1.5\%)$$

Where
P = phenanthrene
1-MP = 1-methylphenanthrene
2-MP = 2-methylphenanthrene
3-MP = 3-methylphenanthrene
9-MP = 9-methylphenanthrene
1,5-DMN = 1,5-dimethylnaphthalene
2,6-DMN = 2,6-dimethylnaphthalene
2,7-DMN = 2,7-dimethylnaphthalene

Peak areas measured from m/z 156 (dimethylnaphthalene), m/z 178 (phenanthrene) and m/z 192 (methylphenanthrene) mass fragmentograms of diaromatic and triaromatic hydrocarbon fraction isolated by thin layer chromatography.

Recalibration of the methylphenanthrene index using data from a suite of Australian coals has given rise to another equation for calculated vitrinite reflectance (after Boreham *et al*, 1988):

$$VR_{calc}\ (e) = 0.7\ MPI + 0.22\ (\text{for } VR < 1.7\%)$$

The methylphenanthrene distribution ratio (MPDF) and calculated vitrinite reflectance VR_{calc} (f) is derived from the following equation (after Kvalheim *et al*, 1987):

$$MPDF = \frac{(2\text{-}MP + 3\text{-}MP)}{(2\text{-}MP + 3\text{-}MP + 1\text{-}MP + 9\text{-}MP)}$$

$$VR_{calc}\ (f) = -0.166 + 2.242\ MPDF$$

FIGURE 1

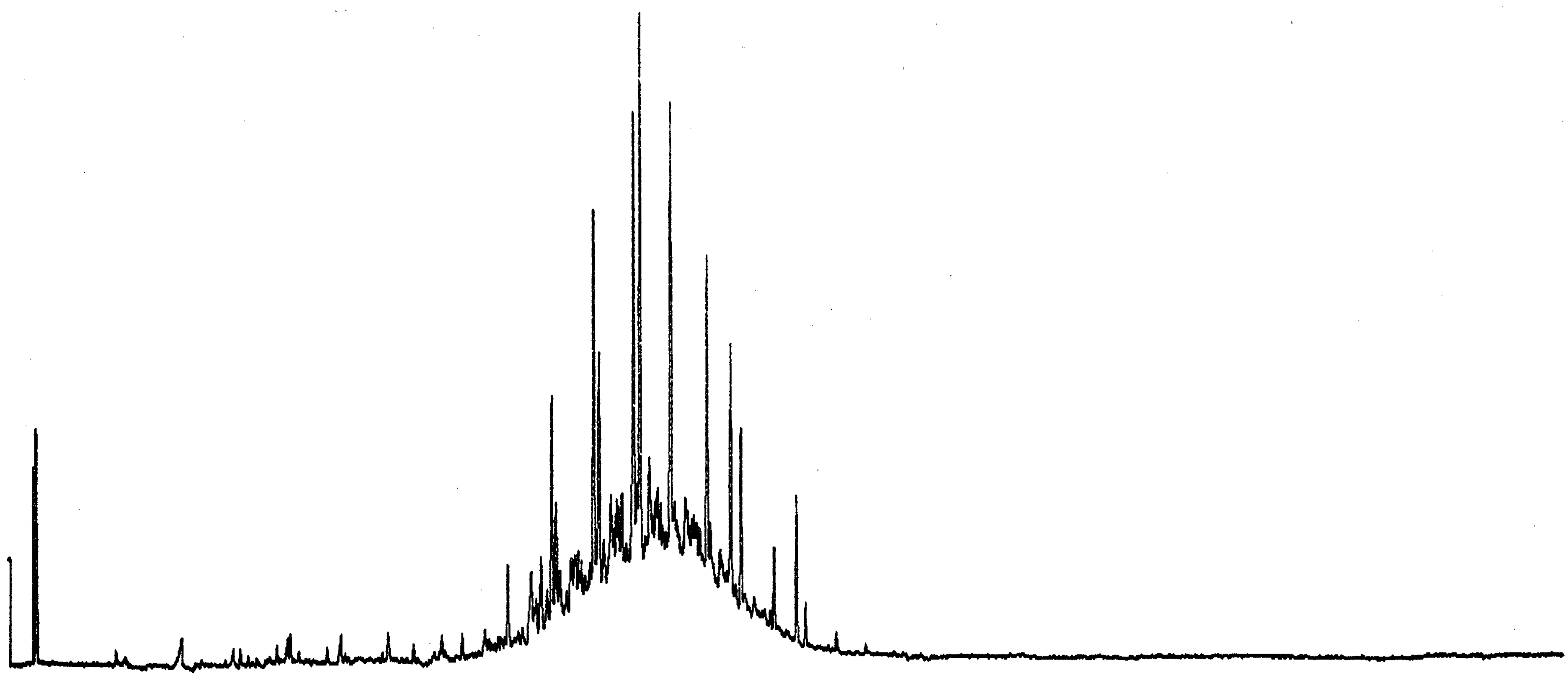

0442

Chromatogram D:APS284 Acquired: Apr-22-1994 11:37:09
Comment: MPI SADME MANYA-5 918.9-919.0m AMDEL PETROLEUM SERVICES
Scan Range: 2000 - 2800 Scan: 2000 Int = 85 @ 33:21 100% = 1782

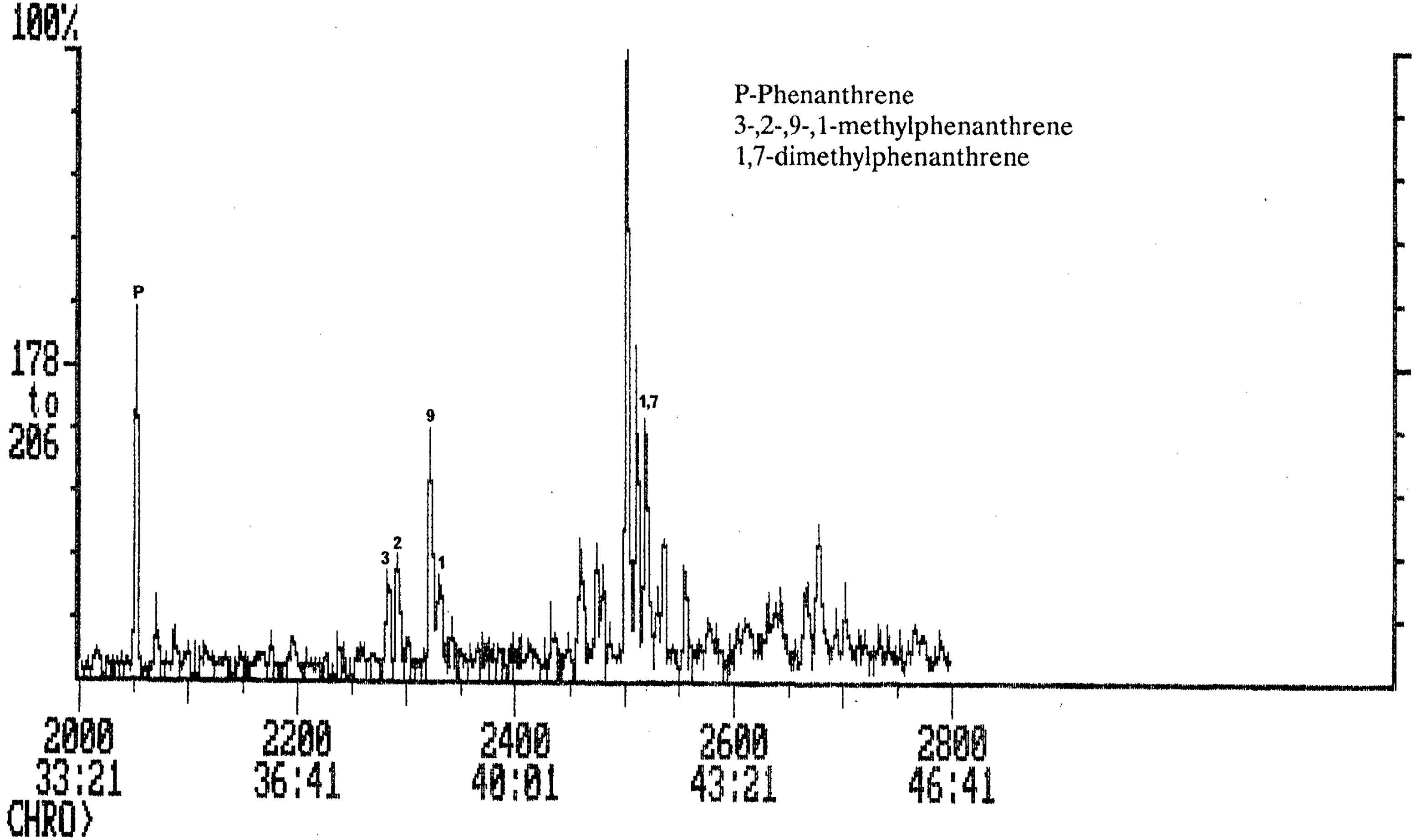

0443

amdel

Amdel Limited
A.C.N. 008 127 802

Petroleum Services
PO Box 338
Torrensville SA 5031

Telephone: (08) 416 5240
Facsimile: (08) 234 0355

14 July 1994

Mines and Energy South Australia
PO Box 151
EASTWOOD SA 5063

Attention: Information Officer

REPORT LQ3039

CLIENT REFERENCE:	58/GR2/953
WELL NAME/RE:	Marla–10
MATERIAL:	Core Sample
WORK REQUIRED:	Identification of Staining

Please direct technical enquiries regarding this work to the signatory below under whose supervision the work was carried out.

Brian Watson

Brian L. Watson
Manager
Petroleum Services

1. INTRODUCTION

One (1) core sample from Marla–10, 114.7 metres depth was received for analysis to determine the nature of a dark staining within the sample. This report is a formal presentation of results forwarded as they became available.

2. ANALYTICAL PROCEDURE

The black portion of the core piece was removed and analysed by X–Ray diffraction (XRD). A further core piece was extracted with dichloromethane in a Soxhlet apparatus for approximately 8 to 10 hours. Removal of solvent by careful rotary evaporation gave the extract (nominal C_{12+} fraction).

3. RESULTS

XRD analysis determined that the dark staining was the mineral cryptomelane (KMn_8O_{16}).

The extract yield for the sample was 129.2 mg/kg. Figures 1 and 2 are GC of the extractable organic matter shown at different attenuations.

FIGURE 1

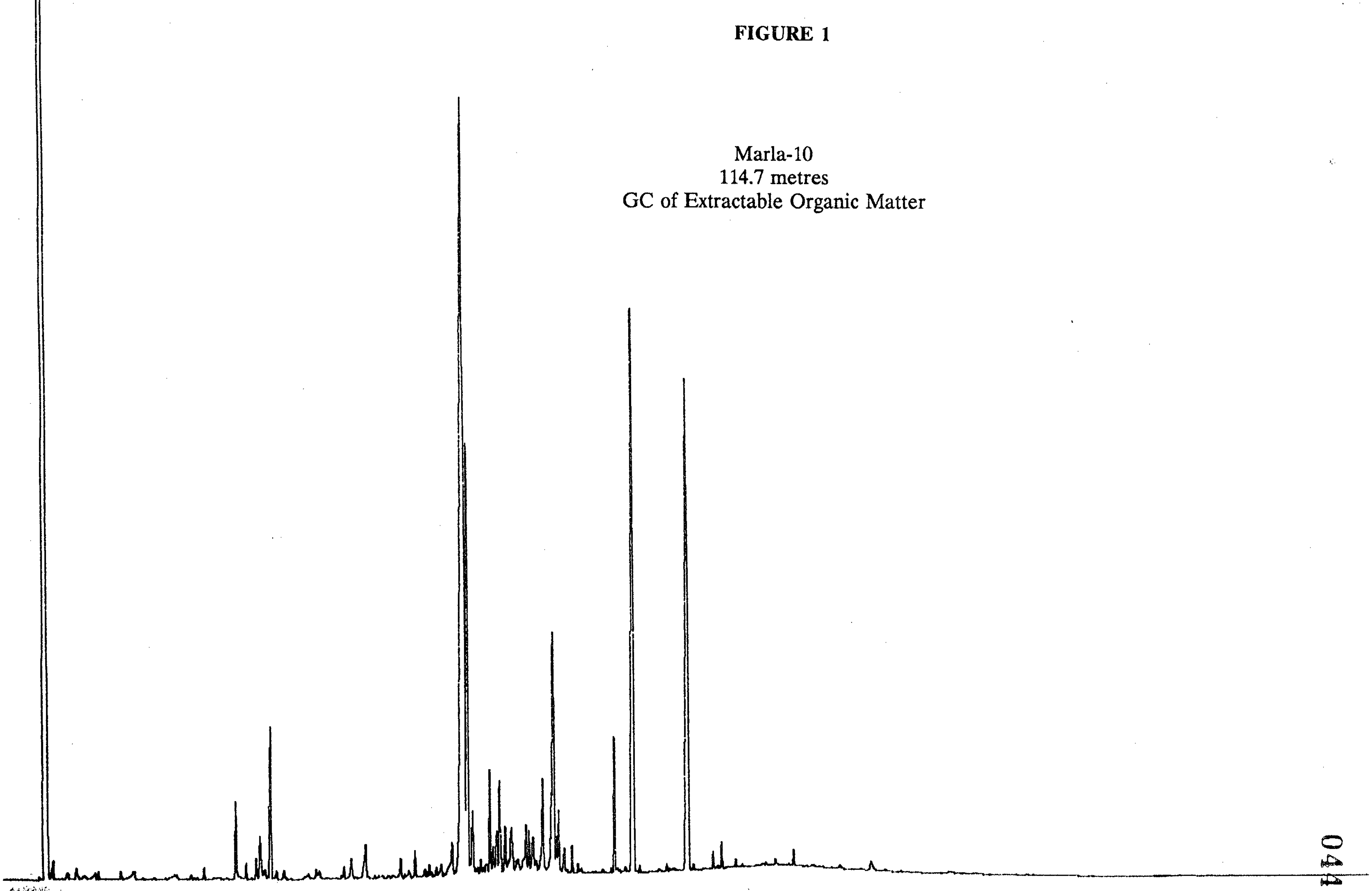

Marla-10
114.7 metres
GC of Extractable Organic Matter

FIGURE 2

Marla-10
114.7 metres
GC of Extractable Organic Matter

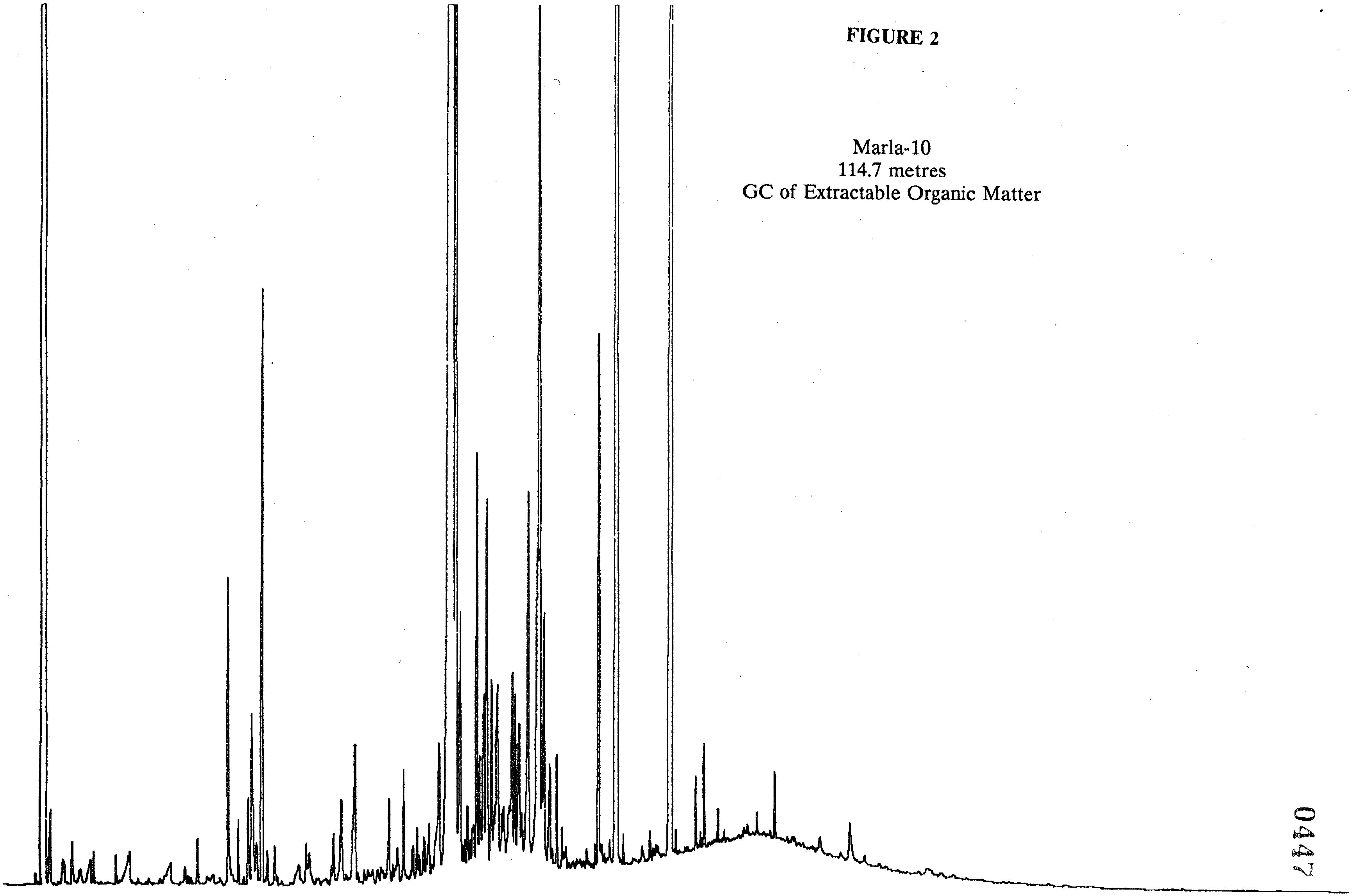

0448

amdel

Amdel Limited
A.C.N. 008 127 802

Petroleum Services
PO Box 338
Torrensville SA 5031

Telephone: (08) 416 5240
Facsimile: (08) 234 0355

24 March 1994

South Australian Department of Mines and Energy
PO Box 151
EASTWOOD SA 5063

Attention: Information Officer
Debit Code: 58/GR2/953

REPORT LQ2811

CLIENT REFERENCE: EX 1444

WELL NAME/RE: Comalco Coal Holes 3,4.

MATERIAL: Cuttings Samples

WORK REQUIRED: Petrographical and Geochemical Analyses

Please direct technical enquiries regarding this work to the signatory below under whose supervision the work was carried out.

Brian L. Watson
Manager
Petroleum Services

1. INTRODUCTION

Three (3) samples were received for vitrinite reflectance analysis and organic petrology. In addition a further sample was received for extraction and aromatic maturity determination (MPI). This report is a formal presentation of results forwarded by facsimile on 11 March 1994.

2. ANALYTICAL PROCEDURES

2.1 Organic Petrology

Representative portions of each sample (crushed to -14+35 BSS mesh) were obtained with a sample splitter and then mounted in cold setting Glasscraft resin using a 2.5 cm diameter mould. Each block was ground flat using diamond impregnated laps and carborundum paper. The surface was then polished with aluminium oxide and finally magnesium oxide.

Reflectance measurements were made with a Leitz MPV1.1 microphotometer fitted to a Leitz Ortholux microscope and calibrated against synthetic standards. All measurements were taken using oil immersion (n = 1.518) and incident monochromatic light (wavelength 546 nm) at a temperature of 23±1°C. Fluorescence observations were made on the same microscope utilising a 3 mm BG3 excitation filter, a TK400 dichroic mirror and a K510 suppression filter.

2.2 Isolation of Extract

Core chips and cuttings samples were extracted with dichloromethane in Soxhlet apparatus for 8 hours. Removal of solvent by careful rotary evaporation gave the oil (nominal C_{12+} fraction).

2.3 Gas Chromatography - Mass Spectrometry (GC-MS)

The di- and triaromatic hydrocarbons isolated from the extracted oil by thin layer chromatography were analysed by GC-MS.

GC-MS analysis of the aromatic hydrocarbons was undertaken in the selected ion detection (SID) mode. The instrument and its operating parameters were as follows:

System:	Perkin-Elmer 8420 GC coupled with an Ion Trap mass selective detector and data system
Column:	25 m x 0.2 mm I.D. HP BP5 cross-linked methylsilicone phase fused silica, interfaced directly to source of mass spectrometer
Injector:	Split injection (8:1)
Carrier gas:	Helium at 1.2 kg/cm^2 head pressure
Column temperature:	50-260°C @ 4°C/minute
Mass spectrometer conditions:	70 eV EI; 9-ion selected ion monitoring, 70 millisec dwell time for each ion

The following mass fragmentograms were recorded:

m/z	Compound Type
155 + 156	dimethylnaphthalenes
169 + 170	trimethylnaphthalenes
178	phenanthrene
191 + 192	methylphenanthrene

The area of the phenanthrene peak was multiplied by a response factor of 0.667 when calculating the methylphenanthrene index (MPI).

3. RESULTS

Vitrinite reflectance data is listed in Table 1 and histogram plots are included as Appendix 1. Tables 2 to 4 list the organic petrology data while colour plates are presented in Appendix 2. MPI calculations are given in Table 5 and mass spectra are shown in Figures 1 and 2.

TABLE 1

SUMMARY OF VITRINITE REFLECTANCE MEASUREMENTS

Depth (m)	Mean Maximum Reflectance (%)	Standard Deviation	Range	Number of Determinations
Coalhole 3 187 m	0.37	0.03	0.33-0.50	34
Coalhole 4 205 m	0.33	0.02	0.30-0.38	32
Coalhole 4 216 m	0.33	0.02	0.29-0.36	32

TABLE 2

MACERAL GROUP PROPORTIONS

Depth (m)	Percentage of		
	Vitrinite	Inertinite	Liptinite
Coalhole 3 187 m	55	35	10
Coalhole 4 205 m	25	60	15
Coalhole 4 216 m	35	50	15

TABLE 3

ORGANIC MATTER TYPE AND ABUNDANCE

Depth (m)	Relative Maceral Group Proportions	Estimated Volume of		Exinite Macerals
		DOM (%)	Liptinite	
Coalhole 3 187 m	V>I>L	>20	Ab	Spo, Cut, Res
Coalhole 4 205 m	I>V>L	>30	Ab	Lama, Cut, Lipto, Res, Spo, Tela
Coalhole 4 216 m	I>V>L	>40	Ab	Spo, Lama, Cut, Res, Tela, Lipto

TABLE 4

LIPTINITE MACERAL ABUNDANCE AND FLUORESCENCE CHARACTERISTICS

Depth (m)	Liptinite Macerals	Lithology/Comments
Coalhole 3 187 m	Spo(Ab;mY-mO), Cut(Co;mY-mO), Res(Sp;mY-mO)	Chiefly sandstone with ≈40% coal (duroclarite).
Coalhole 4 205 m	Lama(Co-Ab;mY-mO), Cut(Ra;mY-mO), Lipto(Ra;mY-mO), Res(Ra-Sp;iY), Spo(Sp;mY-mO), Tela(Sp;iG-iY)	Chiefly carbonaceous shale with ≈40% coal (duroclarite and clarodurite). Telaginite is generally *botryococcus* related with possible tasmanites algae.
Coalhole 4 216 m	Spo(Co-Ab;mY-mO), Lama(Co;mY-mO), Cut(Ra;mY-mO), Res(Ra;iY), Tela(Ra;iG-iY), Lipto(Sp;mY-mO)	Chiefly carbonaceous shale with ≈40% coal (duroclarite). Telalginite is *botryococcus* related.

TABLE 5

AROMATIC MATURITY DATA

Sample	MPI	MPR	DNR	MPDF	VR CALC (%)					
					A	B	C	D	E	F
Coalhole 3 196 m	0.745	1.871	2.221	0.565	0.85	1.85	1.21	1.91	0.74	1.10

KEY TO AROMATIC MATURITY INDICATORS

Methylphenanthrene index (MPI), methylphenanthrene ratio (MPR), dimethylnaphthalene ratio (DNR) and calculated vitrinite reflectance (VR_{calc}) are derived from the following equations (after Radke and Welte, 1983; Radke *et al*, (1984):

$$\mathrm{MPI} = \frac{1.5(\text{2-MP} + \text{3-MP})}{\text{P} + \text{1-MP} + \text{9-MP}}$$

$$VR_{calc}\ (a) = 0.6\ \mathrm{MPI} + 0.4\ (\text{for VR} < 1.35\%)$$

$$VR_{calc}\ (b) = -0.6\ \mathrm{MPI} + 2.3\ (\text{for VR} > 1.35\%)$$

$$\mathrm{MPR} = \frac{\text{2-MP}}{\text{1-MP}}$$

$$VR_{calc}\ (c) = 0.99 \log_{10} \mathrm{MPR} + 0.94(\text{VR} = 0.5\text{-}1.7\%)$$

$$\mathrm{DNR} = \frac{\text{2,6-DMN} + \text{2,7-DMN}}{\text{1,5-DMN}}$$

$$VR_{calc}\ (d) \quad 0.46\ \mathrm{DNR} + 0.89\ (\text{for VR} = 0.9\text{-}1.5\%)$$

Where
P = phenanthrene
1-MP = 1-methylphenanthrene
2-MP = 2-methylphenanthrene
3-MP = 3-methylphenanthrene
9-MP = 9-methylphenanthrene
1,5-DMN = 1,5-dimethylnaphthalene
2,6-DMN = 2,6-dimethylnaphthalene
2,7-DMN = 2,7-dimethylnaphthalene

Peak areas measured from m/z 156 (dimethylnaphthalene), m/z 178 (phenanthrene) and m/z 192 (methylphenanthrene) mass fragmentograms of diaromatic and triaromatic hydrocarbon fraction isolated by thin layer chromatography.

Recalibration of the methylphenanthrene index using data from a suite of Australian coals has given rise to another equation for calculated vitrinite reflectance (after Boreham *et al*, 1988):

$$VR_{calc}\ (e) = 0.7\ \mathrm{MPI} + 0.22\ (\text{for VR} < 1.7\%)$$

The methylphenanthrene distribution ratio (MPDF) and calculated vitrinite reflectance VR_{calc} (f) is derived from the following equation (after Kvalheim *et al*, 1987):

$$\mathrm{MPDF} = \frac{(\text{2-MP} + \text{3-MP})}{(\text{2-MP} + \text{3-MP} + \text{1-MP} + \text{9-MP})}$$

$$VR_{calc}\ (f) = -0.166 + 2.242\ \mathrm{MPDF}$$

Chromatogram E:APS200 Acquired: Feb-21-1994 13:11:50
Comment: MPI COALHOLE 3 196m AMDEL PETROLEUM SERVICES
Scan Range: 2050 - 2550 Scan: 2050 Int = 31 @ 34:11 100% = 222

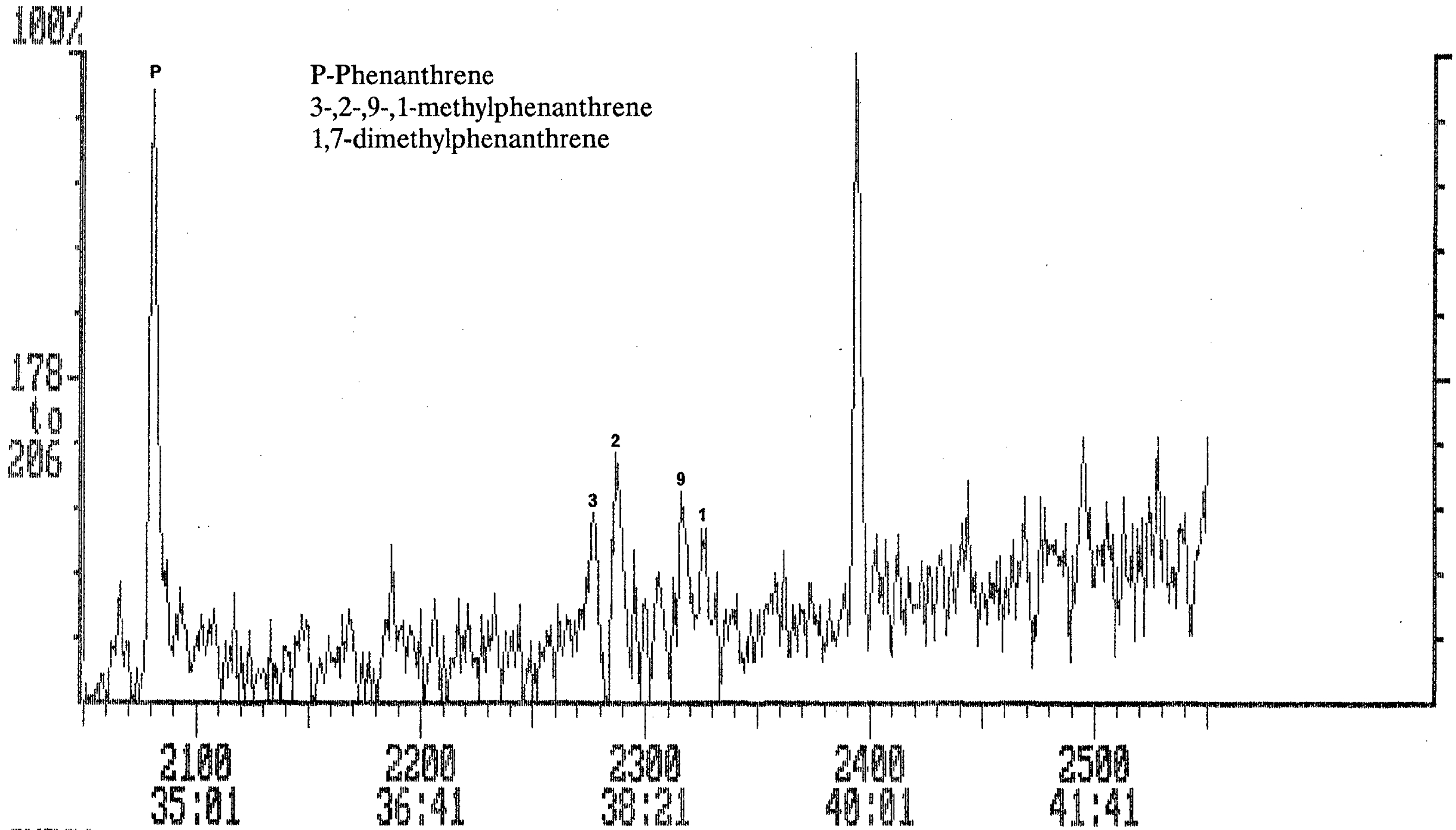

CHRO>

0454

romatogram E:APS200 Acquired: Feb-21-1994 13:11:50
mment: MPI COALHOLE 3 196m AMDEL PETROLEUM SERVICES
an Range: 1250 - 1750 Scan: 1250 Int = 0 @ 20:51 100% = 236

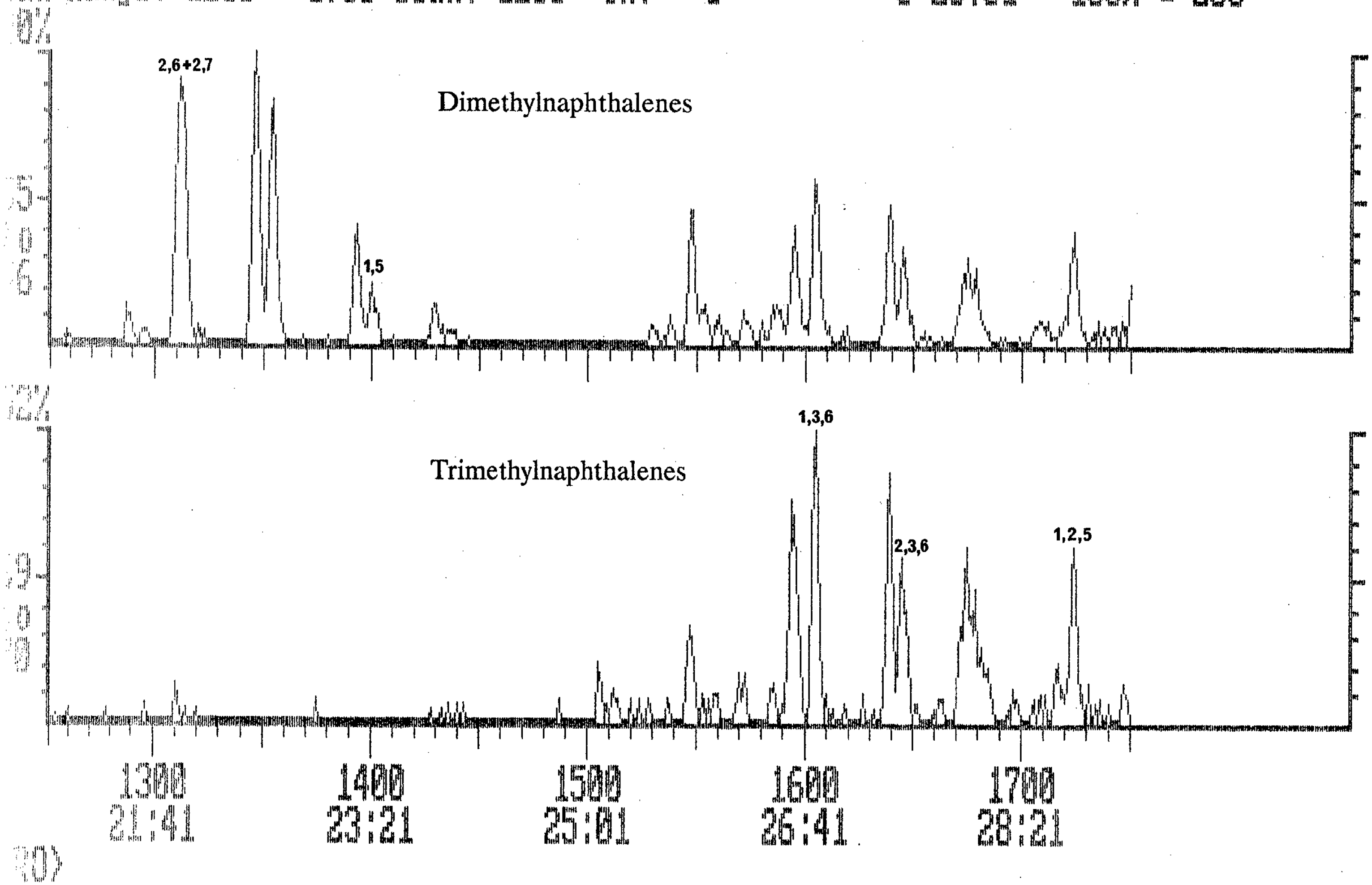

APPENDIX 1

HISTOGRAM PLOTS OF VITRINITE REFLECTANCE DETERMINATIONS

Vitrinite Reflectance Values

Well Name: *Coalhole 3*
Depth: *187 m.*

Sorted List

0.33	0.35	0.37	0.40
0.34	0.35	0.37	0.40
0.34	0.36	0.37	0.48
0.34	0.36	0.37	0.50
0.35	0.36	0.38	
0.35	0.36	0.38	
0.35	0.36	0.38	
0.35	0.37	0.39	
0.35	0.37	0.39	
0.35	0.37	0.39	

Number of values	34
Mean of values	0.37
Standard Deviation	0.03

HISTOGRAM OF VALUES
Reflectance values multiplied by 100

33–35	************
36–38	***************
39–41	*****
42–44	
45–47	
48–50	**

Vitrinite Reflectance Values

Well Name: *Coalhole 4*
Depth: *205 m.*

Sorted List

0.30	0.32	0.33	0.37
0.30	0.32	0.33	0.38
0.30	0.32	0.33	
0.30	0.32	0.33	
0.30	0.32	0.34	
0.31	0.32	0.34	
0.31	0.32	0.34	
0.31	0.32	0.35	
0.31	0.33	0.35	
0.32	0.33	0.36	

Number of values	32
Mean of values	0.33
Standard Deviation	0.02

HISTOGRAM OF VALUES
Reflectance values multiplied by 100

30–32	******************
33–35	***********
36–38	***

Vitrinite Reflectance Values

Well Name: *Coalhole 4*
Depth: *216 m.*

Sorted List

0.29	0.33	0.34	0.36
0.29	0.33	0.34	0.36
0.30	0.33	0.34	
0.30	0.33	0.34	
0.31	0.33	0.34	
0.32	0.33	0.34	
0.32	0.33	0.34	
0.32	0.33	0.35	
0.32	0.34	0.36	
0.33	0.34	0.36	

Number of values	32
Mean of values	0.33
Standard Deviation	0.02

HISTOGRAM OF VALUES
Reflectance values multiplied by 100

29–31 *****
32–34 **********************
35–37 *****

APPENDIX 2

PLATES

Fluorescence Mode Plates were deliberately over-exposed in this study to aid in the identification of dull fluorescing macerals.

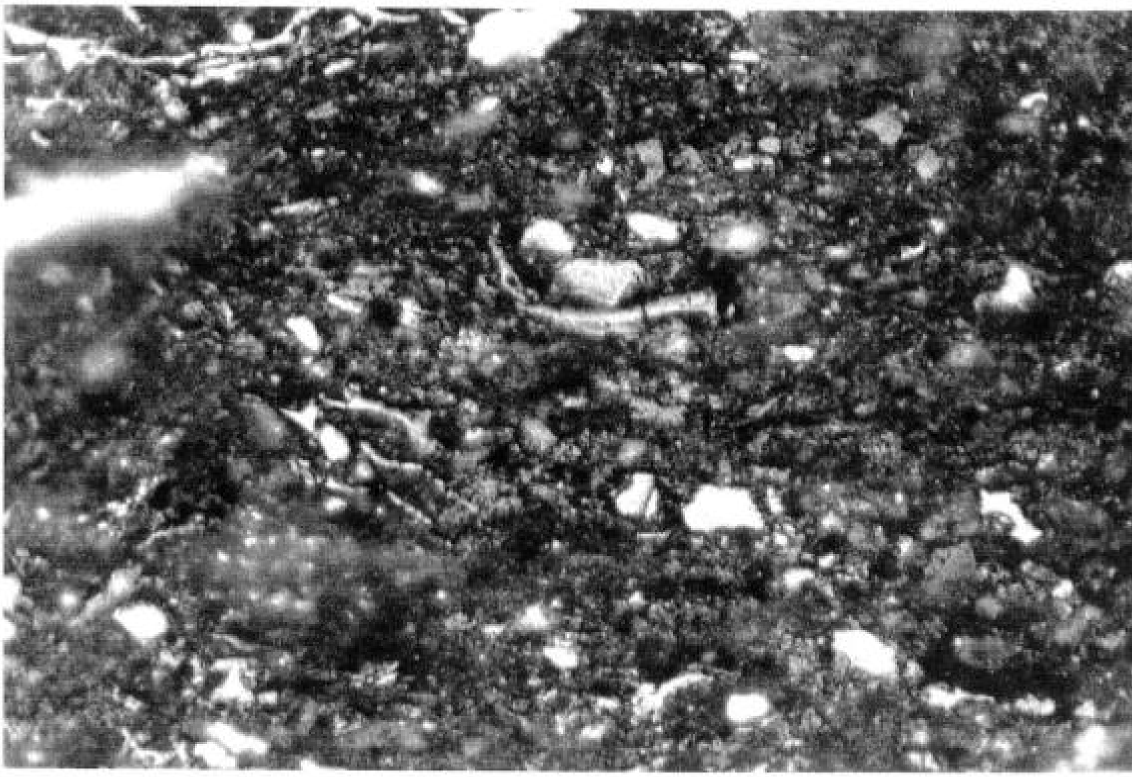

Plate 1: **Coal Hole-3 187 m** **Reflected Light**
Organic matter consists largely of inertinite (white) and liptinite (brown) in this silty coal fragment.
Field Dimensions 0.26 x 0.53 mm

Plate 2: **Same field as above** **Fluorescence Mode**
In fluorescence mode the liptinites may be identified as *botryococcus* related telalginite (intense yellow; bottom left), lamalginite (moderate yellow) and cutinite (moderate orange).

Plate 3: **Coal Hole-4 205 m** **Reflected Light**
Vitrinite (grey) and inertinite (white) occur here with liptinite (brown).
Field Dimensions 0.26 x 0.53 mm

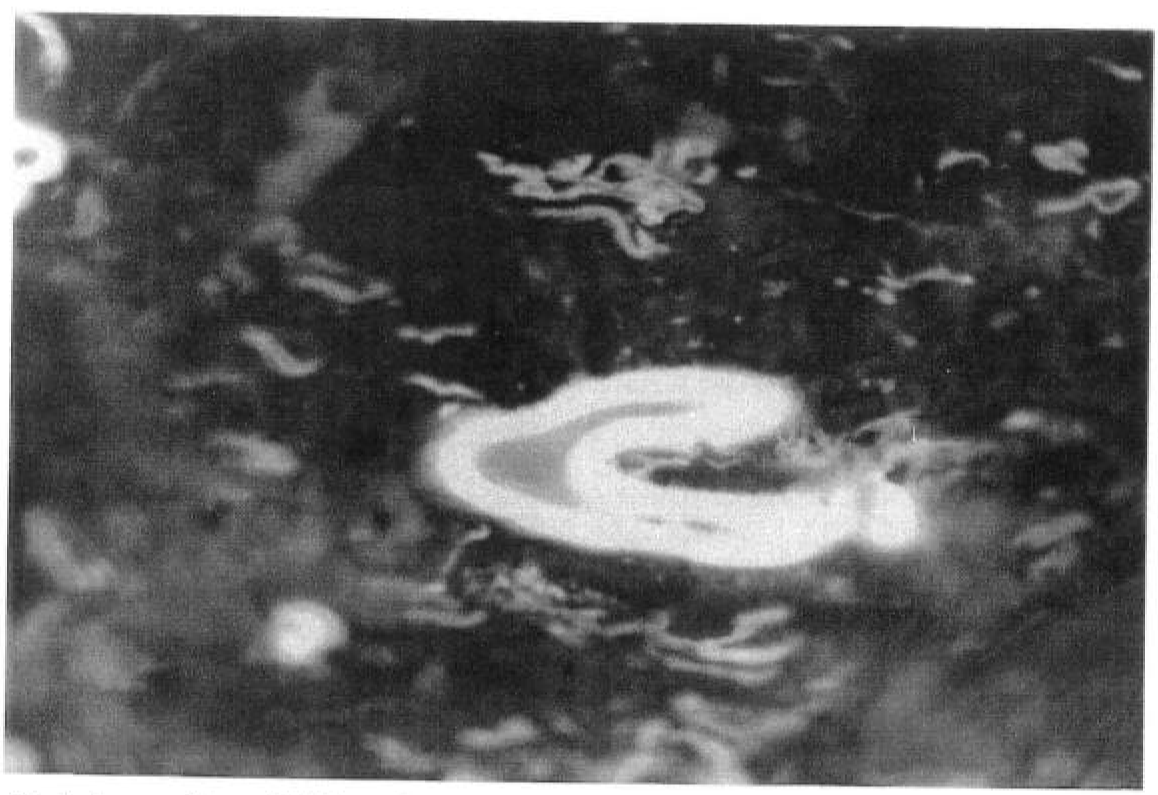

Plate 4: **Same field as above** **Fluorescence Mode**
The large intense fluorescent organism in the centre of the plate is tentatively identified as ?*Tasmanites* algae. Palynolgical identification would be more reliable. The finer fluorescent material is lamalginite.

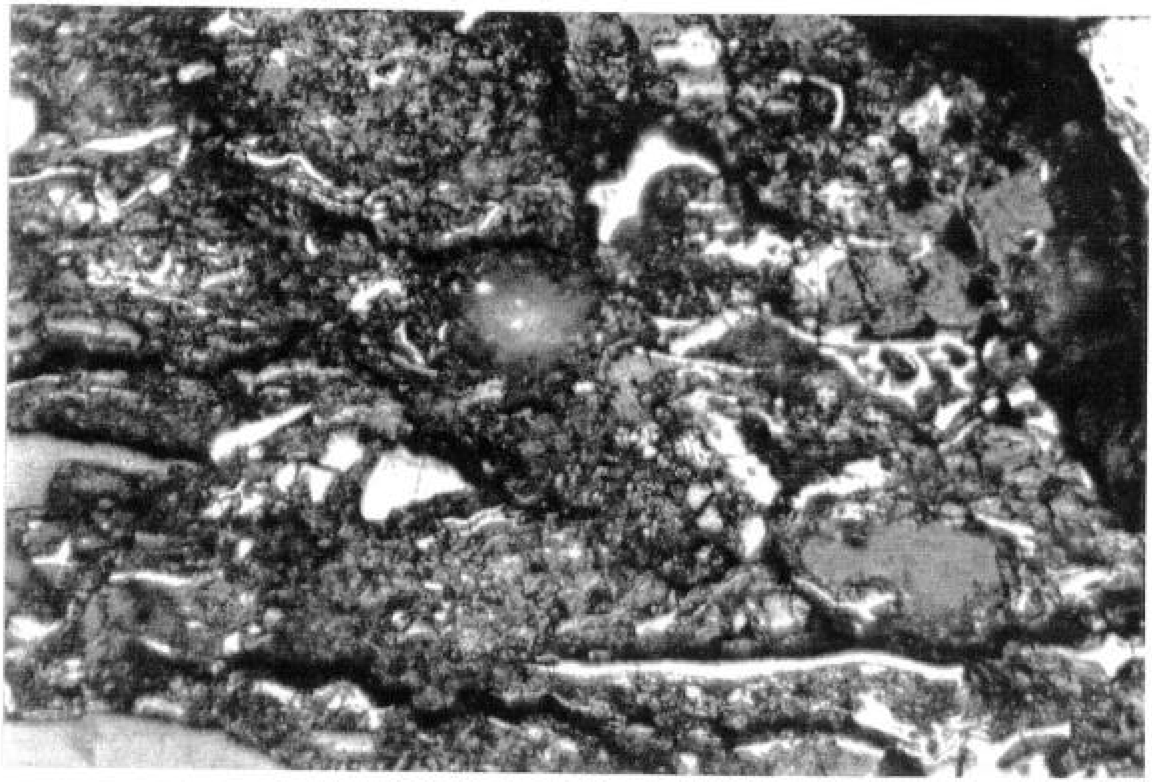

Plate 5: **Coal Hole-4 205 m** **Reflected Light**
This is a similar field of view to the previous plates (3 & 4).
Field Dimensions 0.26 x 0.53 mm

Plate 6: **Same field as above** **Fluorescence Mode**
Telalginite, lamalginite and liptodetrinite are dispersed in this coal.

Plate 7: **Coal Hole-4 216 m** **Reflected Light**

This portion of the coal is quite rich in liptinite (brown) and inertinite (white).

Field Dimensions 0.26 x 0.53 mm

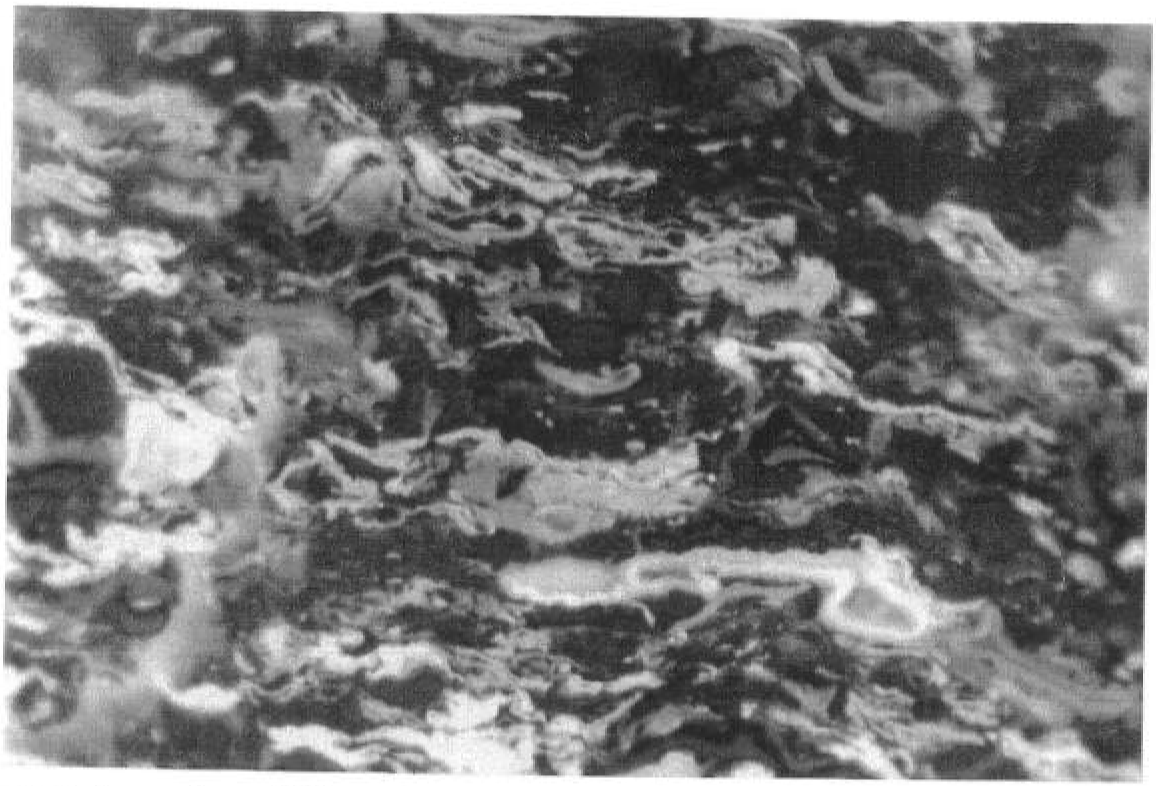

Plate 8: **Same field as above** **Fluorescence Mode**

Lamalginite, sporinite and liptodetrinite with variable fluorescence are dispersed in the coal.

Plate 9: **Coal Hole-4 216 m** **Reflected Light**
This carbonaceous shale fragment contains similar proportions of vitrinite, inertinite and liptinite as the coal in this sample.
Field Dimensions 0.26 x 0.53 mm

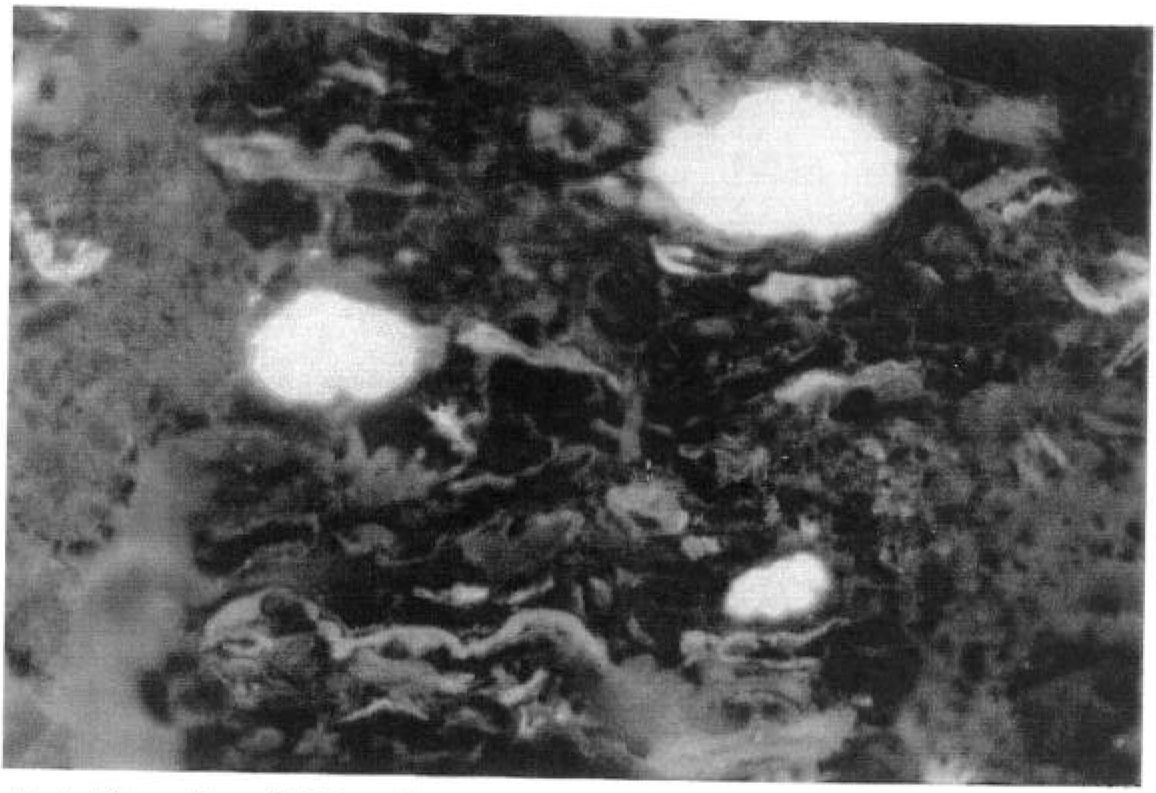

Plate 10: **Same field as above** **Fluorescence Mode**
This is the same field as above in fluorescence mode. *Botryococcus* - related telalginite, lamalginite, cutinite and liptodetrinite are present in this field.

Plate 11: **Coal Hole-4 216 m** **Reflected Light**

This portion of the coal consists largely of vitrinite (grey) and inertinite (white).

Field Dimensions 0.26 x 0.53 mm

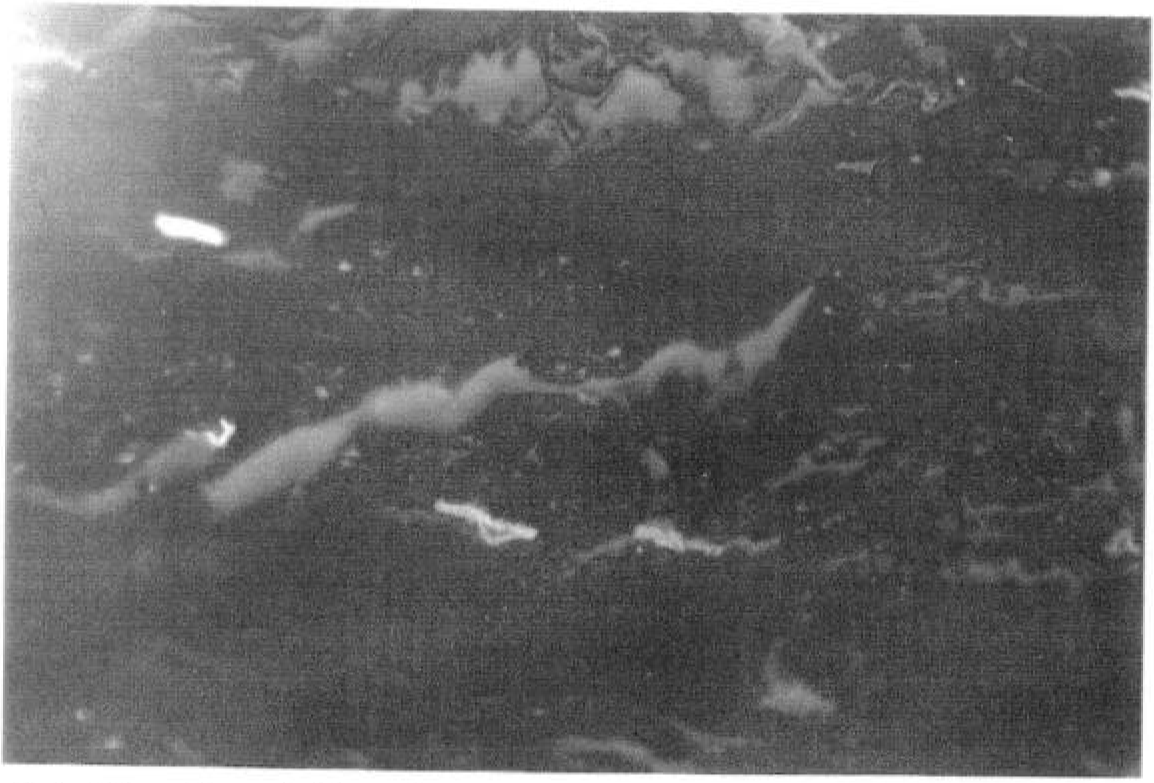

Plate 12: **Same field as above** **Fluorescence Mode**

In fluorescence mode a minor portion of liptinite (sporinite and liptodetrinite) is evident.

GEOTRACK

To: David Gravestock
Oil, Gas and Coal Division
S.A. Mines and Energy
Fax No.(08) 373 3269

Date:5th July '94

From: Patrick R Kelly, Operations Manager
FAX No. (61) 3 347 5938
(Telephone enquiries: (61) 3 344 7214)

No. of pages: 2 (including this sheet)

PROVISIONAL APATITE YIELDS *

* This is provisional data and gives an indication only of the potential of the sample for AFTA

Geotrack Report # 531

Geotrack #	Your Ref.	Apatite Yield		
		Good	Low	Zero
Manya-2				
GC531-1	245.5m - 247.7m	*		
GC531-2	492.9m - 494.3m	*		
GC531-3	510m - 516m	*		
Manya-6				
GC531-4	448.2m - 448.8m	*		
GC531-5	1699.6m - 1701.2m	*		
Manya-5				
GC531-6	455.1m - 455.5m	*		
GC531-7	459m - 459.6m	*		

Telephone:
National (03) 344 7214
International 613 344 7214
Facsimile 613 347 5938
Telex AA35185 UNIMEL

Geotrack International Pty Ltd
PO Box 4120
Melbourne University
Victoria 3052
Australia

Samples to:
Room 225
Earth Sciences Bldg
University of Melbourne
Cnr Swanston and Elgin St
Carlton Victoria 3052
Australia

GEOTRACK

Geotrack #	Your Ref.	Apatite Yield Good	Apatite Yield Low	Apatite Yield Zero
Manya-5(cont.)				
GC531-8	1054.5m - 1055.8m	*		
SMD5001				
GC531-9	217.7m - 218.7m	*		
GC531-10	488.2m - 488.8m	*		
Giles-1				
GC531-11	416.6m - 416.9m	*		
GC531-12	422.3m - 422.6m	*		
GC531-13	1063.4m - 1063.8m	*		
GC531-14	1299.1m - 1299.6m			*

Telephone:
National (03) 344 7214
International 613 344 7214
Facsimile 613 347 5938
Telex AA35185 UNIMEL

Geotrack International Pty Ltd
PO Box 4120
Melbourne University
Victoria 3052
Australia

Samples to:
Room 225
Earth Sciences Bldg
University of Melbourne
Cnr Swanston and Elgin St
Carlton Victoria 3052
Australia

APPENDIX 3

Preprint. Zang (in prep.)

Note in proof: Giles Mudstone (Sukanta, 1993) is now replaced by Meramangye Formation

EARLY NEOPROTEROZOIC SEQUENCE STRATIGRAPHY AND ACRITARCH BIOSTRATIGRAPHY, EASTERN OFFICER BASIN, SOUTH AUSTRALIA

Zang, Wenlong

ABSTRACT The early Neoproterozoic Torrensian (=latest Tonian, about 800 - 750 Ma) succession in the central and eastern Officer Basin was deposited in an intra-cratonic rift basin. The outcropping Pindyin Sandstone consists of basal lowstand conglomerate, and upward-fining transgressive sandstone and is conformably overlain by marine highstand shale of the Alinya Formation. In Giles 1 well, the Pindyin Sandstone contains aeolian to fluvial deposits and is overlain by peritidal and sabkha sediments of the Alinya Formation. Seismic interpretation suggests that the succession is thin on the Murnaroo Platform and thickens toward the Munyarai Trough. The two sedimentary provinces are separated by the Ungoolya Hinge which probably marks the southeastern margin of the Fraser-Musgrave fold belt. Highstand organic-rich shale in the Alinya Formation is probably an important petroleum source rock.

Acritarchs occur in both chert and shale in the Alinya Formation and their distribution was probably controlled by sedimentary environments. Similar assemblages from outcrop and subsurface provide a reliable evidence for regional correlation. The assemblages in Giles 1 are dominated by benthic coccoids and contain many distinct spinose acritarchs which are particularly abundant in subtidal grey shale, whereas mainly phytoplankton are present in the chert. The assemblage, represented by *Trachyhystrichosphaera vidalii* - *T. aimica* - *Cymatiosphaeroides kullingii*, can be used for global correlation in the early Neoproterozoic. The abundant microfossils from the Alinya Formation and equivalent beds around the world probably indicate a microorganism explosion at 750 - 800 Ma, prior to the Neoproterozoic glaciations.

Thirty-seven acritarchs/spheroids and seven cyanobacterial filaments are briefly described in this study, including 5 new species: *Comasphaeridium tonium, Eoentophysalis gilesis, Goniosphaeridium alinyum, Gorgonisphaeridium pindyium* and *Gorgonisphaeridium torrensium* and a newly combined species *Archaeoellipsoides karatavicus* comb. nov.

INTRODUCTION

The early Neoproterozoic Torrensian succession in the central and northeastern Officer Basin was recognised by geological mapping in the late 1960s and early 1970s (Major et al., 1971; Major and Teluk, 1973). Extensive field investigation led to recognition of the Pindyin beds which contain sandstone and shale, unconformably overlying granite gneiss basement of the Musgrave Block (Major, 1973a). This succession became better known following petroleum exploration in the eastern Officer Basin in the 1980s. One deep, fully-cored petroleum well and comprehensive seismic interpretation make correlation possible between outcrops in the central and the subsurface succession in the eastern basin. The two lithological units within this succession are Pindyin Sandstone and Alinya Formation (Zang, 1994).

The Pindyin Sandstone is widely distributed as a thin uniform sandstone blanket. It represents the basal sediments which rest unconformably the metamorphosed basement. A strong, continuous seismic reflector (reflector H) separates the sediments from basement rocks (Thomas, 1990). The Pindyin beds were named from outcrop (Major, 1973a) and have been used for subsurface logging (Stainton et al., 1988; Thomas, 1990; Lindsay et al., 1992), but correlation between the outcrops and subsurface was not attempted.

The Alinya Formation is revised from the "Alinya (= Alynia in Thomas, 1990; Lindsay et al., 1993) beds" which was first used by Stainton et al. (1988), but not formally defined nor reserved, and followed by Thomas (1990) and Lindsay et al. (1992). The formation is intersected in Giles 1 well in the eastern basin (1288.7-1231.4m), and contains mainly anhydritic siltstone, shale, minor dolomite and sandstone, representing a coastal sabkha deposit (Stainton et al., 1988). A distinct diapir structure in the Munta area was developed from this unit (Thomas, 1990). The Alinya Formation conformably overlies the aeolian Pindyin Sandstone on the Murnaroo Platform and is unconformably overlain by alluvial to deltaic sandstone of Ediacarian age. The distribution of the sabkha deposit or its equivalent can be seismically interpreted across the Murnaroo Platform and into the Munyarai Trough (Figure 1), also near outcrops at the Purndu Hills. The shale of the Alinya Formation (previously upper part of the Pindyin beds) at the North Pindyin Hills type section is weathered, whereas the uppermost part is obscured by more recent sediments.

The Torrensian succession was considered to be Sequence 1 in the eastern Officer Basin (Stainton et al., 1988), but its sedimentary environments and sequence systems tracts have not been studied. No biostratigraphic investigation was conducted for this succession.

The purpose of this study is to discuss the distribution of the Pindyin Sandstone and Alinya Formation in the central and eastern Officer Basin and undertake lithological correlation between outcrops and the subsurface. From interpretation of the core and seismic data, regional tectonics, sequence stratigraphy and acritarch biostratigraphy, a model of the sedimentary basin is presented.

TECTONIC SETTING

The Officer Basin is an intra-cratonic, east-west trending arcuate, complex of troughs and sub-basins, extending from Western Australia into South Australia. The basin is bounded by the Archean to Mesoproterozoic Gawler Craton, Musgrave Block, Yilgarn Craton and Coompana Block. Permian and Mesozoic sediments onlap the Officer Basin from the east and Cenozoic Eucla Basin sediments onlap from the south (Figure 1). The basin extends east-west about 500km and covers 350 000km^2. It is filled with Neoproterozoic to Late Devonian sediments in South Australia, although a major part of the basin is covered by the aeolian sand of the Great Victoria Desert. It is believed that the basin was probably connected with the Adelaide Geosyncline, Stuart Shelf and Amadeus Basin during the Neoproterozoic, extending to the Warburton Basin in the east and Canning Basin in the west during the Early Palaeozoic. Neoproterozoic and Cambro-Ordovician sediments in the basin crop out in a belt along the southern Musgrave Block and sporadically on the Murnaroo Platform and in the vicinity of the Wintinna opal field. Outcrops are often deeply weathered. Drilling and seismic data suggest that the sediments are at least 10km thick in the deeper part of the Munyarai Trough in the eastern basin (Ivic, 1986) and about 8km thick in the western part (Townson, 1985) with an estimated maximum of up to 12km (Jackson and van de Graaff, 1981).

The eastern Officer Basin is believed to have been strongly framed by three tectonic movements: Fraser-Musgrave (1300-1000 Ma), Paterson (750-530 Ma or its regionally-related episode Petermann Ranges Orogeny during 570-530 Ma) and Alice Springs (Devonian - Carboniferous) Orogenies. The basin might have originated when the Gawler Craton collided westerly with the older Yilgarn Craton, an event perhaps forming the Fraser-Musgrave fold belt dated at 1300 to 1000 Ma (Myers, 1990). The basin was probably much larger than its present size because it has been episodically compressed from the north by the Musgrave Block during the Petermann Ranges and Alice Springs Orogenies. Many reverse and thrust faults are present dipping northwards. Seismic line EQ indicates that there are about 10000m of sediment present towards the margin of the Musgrave Block, where the Everard Thrust, formed during the Alice Springs Orogeny, is located.

The Fraser - Musgrave fold belt trends NE-SW from the southern margin of the Yilgarn Craton to the southeastern Musgrave Block; the Munyarai Trough was probably located within this belt (Figure 2). The belt was considered to be the evidence of continental collision or amalgamation (Myers, 1990). In the southwestern belt the Albany-Fraser Province contains a broad and complex mobile zone which increases in metamorphic grade from greenschist and amphibolite facies in western greenstone belts to high grade gneiss and granulite facies in the east (Townson, 1985), possibly indicating a tectonic transport direction from the east to west. The southeastern margin of the belt is bounded by the Ungoolya Hinge, which is marked by the presence of the stable Gawler Craton rocks in the southeast and can be recognised from a linear, positive aeromagnetic anomaly (Thomson, 1970; Zang and Major, 1994). The hinge extends from Munta - Ungoolya - Cartu Hill to Ammaroodinna Hill where a porphyroblastic, muscovite-rich rock provides radiometric ages of 1104 Ma (K-Ar), 1050 Ma and 973 Ma (Rb-Sr) (Webb, 1985). This hinge zone was active during orogenesis, particularly the Petermann Ranges and Alice Springs Orogenies, and now is the site of diapirs (e.g. Munta and Ungoolya regions) and thrust faults (Ammaroodinna region) (Figure 4). The hinge zone separates the tectonically-mobile Munyarai Trough to the northwest from the relatively-stable Murnaroo Platform to the southeast, where the sediments rest unconformably on the Gawler Craton basement. Generally the Torrensian succession is thin on the platform (about 200-500m) and thicker in the trough (up to 1500m) (Figure 3).

The Musgrave Block is a distinctive tectonically-mobile province in the central Australia and consists mainly of Mesoproterozoic metamorphic and igneous rocks with ages ranging 1600(?) - 1000 Ma. It separates the Amadeus Basin to the north from the Officer Basin to the south (Figure 2). Its structural trends were mainly influenced by the Fraser-Musgrave and Paterson deformations (Thomson, 1970; Myers, 1990). Similarities in petrological features and geochronological histories between the southeastern Musgrave Block and the Albany-Fraser Province led to the suggestion that they were the same tectonic unit (Thomson, 1970; Plumb, 1979; Rutland, 1981), which perhaps were genetically linked. The Fraser-Musgrave fold belt is overlain now by thick Officer Basin sediments. The Petermann Ranges Orogeny might have substantially shaped the southern margin of the Musgrave Block. Uplift and reverse faulting on the northern margin of the Officer Basin created a series of foreland basins at the time of the Ediacarian and Palaeozoic (Myers, 1990; Preiss, 1993).

However, there is reliable evidence to suggest that prior to the Ediacarian the eastern Officer Basin may have been mildly extensional after a long post-collision lacuna (1000-850 Ma). Many graben and half-graben structures are interpreted on N-S seismic lines, e.g. seismic lines IP1-9 (Amoco, 1987) and IP1-2A. This rift event might be interpreted as an extensional "rebound" or "thinning of the crust" after collision or amalgamation. Its influence in the basin may be episodic and most faults were probably superimposed or overprinted by later major compressional events. At least two major rift episodes have been recorded in the early Neoproterozoic and this can be interpreted from the formation of the Ungoolya Hinge and Munyarai Anticline (Figure 3).

The Ungoolya Hinge zone in the Ungoolya region contains two low relief subsurface faulted-blocks which were probably originated from a pre-Torrensian graben. The graben, about 7km wide and 1300m deep, was probably formed during the first seismic-recognised episode and disconformably overlapped by the Torrensian sediments in the eastern Officer Basin. The faults of the graben structure might be active during the second Torrensian extensional episode, and then rejuvenated by major compressional and thrust events during the Petermann Ranges and Alice Springs Orogenies, creating a distinctive subsurface hinge zone high (Figure 4).

The Munyarai Anticline was the first subsurface tectonic high drilled by Munyarai 1 well. Seismic interpretation suggests that across the N-S anticline Sequences 2 and 4-6 (Figure 5) thicken towards the trough and Sequence 2 contains several half-graben structures which probably formed during the second extensional episode. The structural framework of these half-grabens is probably similar to the domino model, in terms of magnitude of footwall uplift versus hangingwall subsidence (Roberts et al., 1993). Movements along the reverse faults formed by the Petermann Ranges Orogeny probably resulted in uplift of the anticline (probably also overprinted the half-graben structures), which made Palaeozoic Sequences 7-8 thicken toward the syncline of the platform side (Figure 3).

These extensional phases are also interpreted from the widespread distribution of the doleritic Gairdner Dyke Swarm in the Musgrave Block and Gawler Craton. These dyke swarms were first recognised as extensional by Goode (1970), and probably multi-episodic in the Gawler Craton and spanning 1100-800 Ma in age (Flint, 1993). Zhao and McCulloch (1993) suggested that two distinct Proterozoic events of mafic magmatism in central Australia were related to crustal extension. The later 800Ma event of the mafic dyke swarms was correlated with the upper Gairdner Dyke Swarm in the Musgrave Block and Beda Volcanics in the Gawler Craton (Zhao et al., 1992b). To the east in the Adelaide Geosyncline a rift phase is more recognisable, where up to 8000m of Torrensian Burra Group strata were deposited (Forbes and Preiss, 1987).

In the central Officer Basin the Nurrai Ridge is a distinctive gravity and magnetic intensity high, separating the Munyarai Trough to the east from the Birksgate Sub-basin on the west (Figure 1, 15). The ridge is not parallel to the Fraser-Musgrave fold belt and there are no seismic lines across this anomaly. However, AGSO Line 93AGS.L4 shows no sediment displacement at the southern part of the ridge where gravity and magnetic intensity are normal (Lindsay et al., 1992; Lindsay, 1994, pers. comm.). On the northern margin of the Ridge the Neoproterozoic sediments crop out sporadically. The Nurrai Ridge might have been present before the deposition of the early Neoproterozoic succession, as evidenced by Sequence 2 consisting mainly of open marine deposits in the Birksgate Sub-basin whilst coastal sabkha deposits occur on the Murnaroo Platform in the east. It probably formed a sill during the early Neoproterozoic, barring or semi-barring the eastern part of the basin from the open marine environment, thus forming a giant saline basin or embayment. This saline basin is considered to be a potential petroleum province on the basis of the presence of porous and permeable sandstones and organic-rich shales. However, the framework of the sedimentary basin in the eastern Officer Basin is poorly known. A foreland basin model during the late Ediacarian was proposed for the eastern basin after studying the sedimentary features of the Rodda beds (Preiss, 1993), even though this model was previously rejected by Lambeck (1984).

SEQUENCE STRATIGRAPHY

A depositional sequence is a relatively conformable succession of genetically related lithofacies bounded by unconformities and their correlative conformities. The sequence stratigraphic approach provides a framework for analysing basin architecture and developing predictive facies models (Lindsay and Korsch, 1991). At least five Neoproterozoic second order depositional sequences are recognised from seismic, outcrop and core interpretation in the Munyarai Trough and Murnaroo Platform (Stainton et al., 1988; Sukanta et al., 1991; Sukanta, 1993), whereas another sequence or supersequences is present in the Marla region in the Manya Trough. The Pindyin Sandstone and Alinya Formation are considered to be Sequence 2. Nine sequences can be recognised in the central and eastern Officer Basin, which are mainly bounded by tectonically-generated unconformities except the boundary between Sequences 4 and 5, which is locally conformable (Figure 5).

Sequences in the eastern Officer Basin

The basement of the eastern Officer Basin is poorly known because of deep burial and shallow drilling. On the northwestern margin of the Gawler Craton some mineral exploration drillholes penetrated the metamorphosed rocks of the crystalline basement in the Nawa Ridge area. In the south-central basin Lake Maurice East 1 well (SMD 5002) intersected metamorphic granite of the Gawler Craton at the depth of 691m, where Ediacarian Tarlina Sandstone rests unconformably on the basement and pre-Ediacarian sediments were eroded or not deposited. Lake Maurice East 1 well is located on the southeastern side of the Ungoolya Hinge, probably marking the margin of the Torrensian sea in the Officer Basin. No sediments have been found or seismically interpreted underlying Sequence 2 in the Munyarai Trough and Murnaroo Platform, although in the western Officer Basin Sequence 2 equivalent unconformably overlies sediments of the Meso to Palaeoproterozoic Bangemall and Nabberu Basins (Townson, 1985), whereas in the eastern margin of the basin and hinge zone Sequence 1 was intersected.

Manya 5 in the Marla region intersected Willouran (850 - 800 Ma) succession which is unconformably overlain by the fluvial Murnaroo Sandstone, where the Torrensian sediments are absent. The succession is probably correlated with the upper siltstone of the Younghusband Conglomerate, Coominaree Dolomite and overlying mafic Cadlareena Volcanics of the Peake and Denison Inlier in South Australia (Coats and Preiss, 1987a; Preiss, 1993). The sediments in the pre-Torrensian graben in the Ungoolya Hinge are probably of similar age for similarity of the 'graben' shape and seismic signature. The upper siltstone of the Younghusband Conglomerate contains the large acritarch *Trachyhystrichosphaera*.

In the study area Sequence 2 is unconformably overlain by the younger sediments, mostly the Ediacarian sediments, and no Cryogenian tillites are found to overlie the Torrensian sequence. The Chambers Bluff Tillite (Sequence 3) crops out along the northern margin of the Gawler Craton and was probably intersected in Nicholson 2 well. Neither its lower nor upper boundaries are known and its age could be either Sturtian or Marinoan (Coats and Preiss, 1987b; Williams, 1991). The tillite in Nicholson 2 well contains glaciofluvial to glaciomarine diamictites separated by thick, probably lacustrine and peritidal siliciclastics which contain acritarchs. Tidal-influenced rhythmites are also present (Williams, 1991). In the Indulkana region the Wantapella Volcanics of unknown age overlie a bed of dolomite (Coats and Preiss, 1987b). Volcanics have not been intersected or seismically interpreted in the Munyarai Trough and Murnaroo Platform (Stainton et al., 1988; Sukanta et al., 1991; Amoco, 1987; Thomas, 1990). It is possible that the tillites in this region contain both Sturtian and Marinoan glaciogenic sediments thus Sequence 3 is considered to be a supersequence.

Sequences 4-6 are bounded by the Neoproterozoic tillites and Cambrian succession and comprise the thickest sediment accumulation in the eastern Officer Basin. Seismic interpretation indicates that the successions is up to 5000m thick near the Everard Thrust. Sequence 4 was fully penetrated and cored in Giles 1 (1231.4-584m, Figure 7) and Lake Maurice East 1 (691-117m), and partly intersected in Meramangye 1. The Tarlina Sandstone (cf. Sukanta, 1993) is red-brown, massive sandstone with a basal conglomerate and considered to have been deposited in an alluvial to deltaic environment, representing a lowstand systems tract. The sandstone passes transitionally upwards into red-brown siltstone of the Giles Mudstone in which the upper part contains interbedded green-grey shale. The mudstone is mainly thinly-bedded, but low-angle and trough cross-bedding, ripples and slump structures are not uncommon. Sedimentary features and parasequence analysis indicate that the mudstone in Giles 1 and Lake Maurice East 1 was deposited in a delta front to prodelta environment, whereas in Meramangye 1 mainly thin-bedded calcareous mudstone and limestone indicate a shelf setting. The mudstone is conformably overlain by sandstone of the Murnaroo Formation which contains estuarine, fluvial to peritidal sediments.

Sequence 5 consists exclusively of the lower and middle Rodda beds, a succession of mainly siliciclastic sediments with carbonates towards the upper part. The succession was fully intersected and cored in Munta 1, Ungoolya 1, Giles 1, Lake Maurice West 1, and in many wells only the upper part of the succession was penetrated. Seismic interpretation suggests that the beds are up to 3000m thick near the Everard Thrust. The lower unit contains mainly red-brown siltstone (Dey-Dey Mudstone, cf.

Sukanta, 1993) with basal fluvial conglomerate and sandstone. The siltstone is massive to laminated, with some low-angle cross-bedding and slump structures and thin green-grey shale interbeds are present in upper part. In its lower part the Acraman impact ejecta layer was found (Wallace et al., 1989) and in the uppermost rhythmites were observed. Sedimentary features suggest that the lower unit was rapidly deposited in a delta front to prodelta setting and a study of similar rhythmites resulted in a similar conclusion (Williams, 1991). The siltstone was probably formed in a transgressive systems tract, reaching its maximum flooding surface in the uppermost part. This siltstone is conformably overlain by the middle unit which consists mainly of highstand carbonate and siltstone. The transition between the lower and middle unit is marked by several beds of siltstone containing rip-up dolomitic intraclasts, which can be observed in the core at this level almost in every well in the eastern Officer Basin. Several hundred kilometres east in the Adelaide Geosyncline a similar transition occurs between the Bunyeroo and Wonoka Formations (Jenkins et al., 1993). However, in Giles 1, an unconformity was also observed at 584m where an angular contact between the red-brown rhythmitic siltstone and grey-green dolomitic grainstone occurs. The middle unit was probably deposited in a prodelta and shelf environment and contains abundant well-preserved, large, morphologically-complex acritarchs similar to those found in the upper Pertatataka Formation in the Amadeus Basin (Jenkins et al., 1992; Zang and Walter, 1992b; Gray in Jenkins et al., 1993; Zang, unpub. data).

Sequence 6 contains the upper unit of the Rodda beds and was probably deposited in canyons, forming a seismically recognised unconformity in the Munyarai Trough and Murnaroo Platform. The canyons often incised into the lower and middle units of the Rodda beds and occasionally into the Giles Mudstone (Sukanta et al., 1991). Up to 900m canyon deposits were intersected in wells, but seismic interpretation suggests that the canyon fill is up to 2000m thick. The canyon deposits are mainly siltstone in the lower part, silty limestone in the middle and an uppermost bed of calcareous siltstone found only in Karlaya 1 well but probably eroded in other wells. The sediments are mainly thin-bedded to laminated, but graded bedding or Bouma sequence and large slumps are not uncommon in the lower part. The lower siltstone was probably a lowstand canyon fill and the upper carbonate and calcareous siltstone were deposited as a highstand systems tract, which is supported by seismic interpretation (IP1-6) of carbonate reflectors onlapping against the canyon deposits and overlying the middle unit of the Rodda beds.

The Palaeozoic successions in the eastern Officer Basin include Cambrian (Sequence 7), Ordovician (Sequence 8) and Devonian (Sequence 9) sediments. The sedimentary basin was probably terminated by the Alice Springs Orogeny. The thrust faulting may have uplifted the sediments around the narrow "channel" between the Gawler Craton and Musgrave Block in the Bitchera Ridge and Ammaroodinna Inlier regions, isolating the Officer Basin from the eastern Australian sea. To the east and southeast the Early Permian succession of the Arckaringa Basin unconformably overlies Officer Basin sediments (Figure 5).

Description of Sequence 2

Sequence 2 contains the Pindyin Sandstone and Alinya Formation, which unconformably overlies metamorphosed basement and is unconformably overlain by Neoproterozoic tillites or Ediacarian sediments in the Munyarai Trough, Murnaroo Platform and Birksgate Sub-basin. The lower sequence boundary is present at Belundinna Hill where a lowstand fluvial conglomerate rests disconformably on granite of the Musgrave Block (Figure 6, 7:C). An upper boundary is observed at a depth of 1231.4m in Giles 1 well where lowstand red-brown alluvial to fluvial conglomerate unconformably overlies siltstone of the Alinya Formation (Figure 8). Both boundaries can be determined easily from seismic interpretation (Figure 9).

1. Lowstand deposits

Lowstand deposits were observed in the outcropping Pindyin Sandstone. At Belundinna Hill a basal 2m fluvial conglomerate and trough cross-bedded granule-sized kaolinised arkose are present. Pebbles in the conglomerate are commonly rounded and up to 30cm across. Some large-scale low-angle cross-bedding is also present. To the south, at the type section in the North Pindyin Hills, the conglomerate decreases to about 15cm thick (Major, 1973a). The southwards thinning of the conglomerate and the orientation of ripple mark and cross-bedding suggests a northern provenance (Major, 1973a). The basal conglomerate probably represents a lowstand systems tract, deposited at the beginning of Sequence 2.

The subsurface Pindyin Sandstone was intersected in Giles 1 on the Murnaroo Platform (Figure 8) where it consists mainly of quartz grains of aeolian (partly fluvial?) origin. The grains in thin section are commonly rounded with 'frosted' surface texture. Clay minerals (mainly kaolinite and smectite) form the matrix. Hematite (?turgite)-rims are very common on quartz grains (Figure 9:B). These were interpreted as fresh water (dew or rain) precipitates from iron-bearing constituents within the sand (Turner, 1980). Porosity in the sandstone is up to 20% locally. Towards the upper part of the core minor anhydrite and halite are present, probably indicating marine influence or a transgression. In Giles 1 40m of sandstone have been intersected and seismic interpretation suggests that the Pindyin Sandstone is about 100-200m thick.

2. Transgressive deposits

In outcrops the conglomerate is overlain by some 190m of medium to coarse-grained quartzitic sandstone. The sandstone is commonly red-brown, medium to coarse-grained, quartzitic, hard and brittle, strongly resistant to weathered and forming low relief hills (Figure 6:A). The sandstone is commonly well sorted with rounded to sub-rounded grains, and quartz overgrowth is common. Thin horizontal beds, low-angle cross-bedding and tidal-influenced ripple marks are not uncommon (Figure 6:F,G). Most interesting is the presence of herringbone cross-bedding at almost every outcrop (Figure 6:D,E), probably indicating a tidal influence or peritidal depositional setting. Toward the uppermost part of the sandstone some fine-grained silty sandstone beds were observed. At the type section the sandstone is conformably overlain by thinly-bedded to laminated white, weathered shale (Major, 1973a) which probably was deposited in a shelf environment, perhaps below fair-weather wave base. Thus, the upper Pindyin Sandstone was deposited in a transgressive systems tract.

Outcropping sandstone in the Birksgate Sub-basin differs from the subsurface core in Giles 1 probably because of different depositional settings. The sandstone in outcrops was probably deposited under tidal influence, as evidenced by frequent herringbone cross-bedding and asymmetrical ripple marks with mudcracks formed on the intertidal flat, whereas the sandstone in Giles 1 has no obvious bedding but erosional features and minor halite may have been formed by aeolian processes. The Pindyin Sandstone has not been intersected in the Munyarai Trough.

3. Transgressive and highstand deposits

The deposits contain the siltstone/shale, carbonate and evaporites of the Alinya Formation. About 230m of shale and minor carbonate crop out at the North Pindyin Hills type section (Figure 6:B), but elsewhere outcrops are sporadic and sand covered (Major, 1973a). The shale is white or pale-green, commonly thin-bedded to laminated, with some chert beds near the base and thin-bedded limestone and dolomite towards the top. The uppermost formation is weathered and covered by loose grains of ?arkosic sandstone, either belonging to the Alinya Formation or overlying sediments. Gypsum or anhydrite are not present. The sedimentary structures may indicate an open marine shelf environment as the sediments grade from the underlying tidal-influenced deposits of the Pindyin Sandstone.

It is interesting that in one thin section (5042RS2, Figure 5) of brownish banded chert near the base of the Alinya Formation the muscovite flakes and dolomite rhombs have been completely replaced by silica (Figure 20:G,H). Acritarchs *Trachyhystrichosphaera, Leiofusa, Asteridium, Gorgonisphaeridium, Melanocyrillium, Archaeoellipsoides karatavicus, Leiosphaeridia* and sparse cyanobacterial filaments are present and may suggest an open marine environment (Zang and Walter, 1992b).

About 57m of shale and siltstone intersected in Giles 1 can be divided into two units (Figure 8). The lower unit consists of red-brown to pale green siltstone with thin interbeds of sandstone. Anhydrite is common, either as thin beds, veins or cement (Figure 10:B). About 2m of breccia, probably karst-infill, consists of angular pebbles in an anhydrite matrix. Red-brown sandstone and sandy siltstone contains erosive sedimentary surfaces, which were probably formed under subaerial exposure, and halite is occasionally observed. The sedimentary features indicate that the lower unit was deposited on an intertidal flat. The unit conformably overlies the aeolian Pindyin Sandstone and is overlain by subtidal shale and, in turn, by the sabkha deposits, and thus represents part of a transgressive systems tract.

The upper unit of the Alinya Formation in Giles 1 comprises stacked, cyclic, 0.2-5m thick, coastal sabkha deposits (Figure 12:A, 13). Each cycle usually commences with graded bedding of aeolian sandstone and organic-rich siltstone or mudstone with a sharp, erosional base (Figure 12:B); this grades into black shale or mudstone in which most organic matter seems to be degraded; this is succeeded by a bed of grey to green-grey shale or siltstone, in which lamination and graded bedding are present, with occasional low angle cross-bedding and anhydrite, indicating that the sediments were deposited in shallower water conditions. The environment of deposition continues to shallow upwards, represented by mainly red-brown anhydrite, siltstone or shale and minor dolomite, in which laminae are formed by cyanobacterial *Eoentophysalis gilesis* mats and clay or silt. This intertidal anhydritic siltstone is overlain by supratidal evaporites in which 'chicken-wire' anhydrite fabric is common. The cycle ends with a bed of aeolian sandstone with minor anhydrite and halite and an erosional upper surface. Only two complete cycles were observed in core, the remainder being incomplete.

The depositional systems tract of Sequence 2, in brief, started with lowstand fluvial channel deposits, followed by a transgressive shoreface herringbone cross-bedded sandstone, and ended with highstand shale and carbonate of the Alinya Formation. In subsurface Giles 1, the succession begins with aeolian (? locally fluvial) sandstone and intertidal anhydritic siltstone to sabkha deposits, indicating deposition during rising sea-level. These systems tracts can be interpreted from seismic data at the margin of the Murnaroo Platform where the siltstone or shale of the lower part of the Alinya Formation onlaps Pindyin Sandstone and is offlapped by the evaporites of the uppermost Alinya Formation (Figure 14:A, 17:B). In the Munyarai Trough, halite might have been deposited as a last episode of the saline giant, which represents a lowstand deposit. The recognition of the transgressive systems tract in the upper Pindyin Sandstone in the central basin and the lower Alinya Formation in the east may suggest that the Torrensian transgression was from the west to east.

The uppermost part of Sequence 2 has been eroded before the Ediacarian sediments were deposited. The succession studied is thin (less than 500m), but in the Munyarai Trough is interpreted to be much thicker.

4. Regional distribution

Sequence 2 sediments are exposed sporadically from eastern Western Australia along the southern margin of the Musgrave Block to the Indulkana region and is deeply weathered (Major et al., 1971; Major and Teluk, 1973). Subsurface towards the depocenter of the Munyarai Trough seismic interpretation suggests a thickness from 400-500m to about 1500m near the Everard Thrust (Figure 16, 17), but no wells have yet penetrated that depth.

In the northeastern basin the Pindyin Sandstone and Alinya Formation extend from the Murnaroo Platform to Munyarai Trough, gently dipping on the platform and then sharply northwards into the trough (Figure 14, 15). The lowest interpreted seismic reflector (H mark) in the east is considered to be the sediments of the Pindyin Sandstone overlying the basement. The seismic profile indicates an increasing thickness of the succession across the Giles 1 - Munta 1 - Ungoolya 1 - Munyarai 1 section. The Alinya Formation is also distinct in the seismic profile because it contains diapiric and salt structures (Thomas, 1990). Correlation of the succession intersected on the Murnaroo Platform (Giles 1) and their equivalents in the Munyarai Trough can be easily achieved by seismic means (Figures 14, 16). To the east and southeast of the Murnaroo Platform Ediacarian sediments disconformably overlie metamorphic granite of the Gawler Craton (e.g. Lake Maurice East 1) and no Cryogenian tillites and Torrensian sediments are present in this region.

Sequence 2 sediments can be traced seismically for about 125km in the Munyarai Trough from Munyarai 1 to the eastern Trainor Hill (Figure 16, Amoco, 1987). This shows that the thickness of the Alinya Formation distinctly increases towards the Everard Thrust fault zone. Seismic interpretation suggests a rapid increase in thickness of a probable salt or evaporitic deposit along the north part of Line EQ, but for most part in the trough it is about 400-700m thick.

Subsurface sediments in the eastern part of the basin are separated by the Ungoolya Hinge and divided into platform and trough facies. Most faults in this region probably originated during the Petermann Ranges and Alice Springs Orogenies. Salt diapirs are often present near the hinge zone (Figure 14). Towards the northern margin of the basin the thick sand dune cover obscures most bedrock across the trough. However, seismic line FD indicates probable sediments well below the surface "basement" (Ivic, 1986) and the influence of the Everard Thrust fault on the northern margin of the Munyarai Trough is poorly known. A possible isopach of the Alinya Formation is illustrated in Figure 17:A, but interpretation of the distribution in the southwestern basin is not included in this study.

Sequence 2 Equivalents Elsewhere in Australia

Sequence 2 transgression can be recognised in many Neoproterozoic basins in Australia, such as the western Officer Basin in Western Australia, Adelaide Geosyncline in South Australia and Amadeus Basin in Northern Territory. Similar sequential development and the presence of evaporites and acritarchs indicate a major sea-level change prior to the later Neoproterozoic glaciations (Figure 18).

Sequence 2 equivalents in the western Officer Basin are probably the Townsend Quartzite and Lefroy beds, both units cropping out on the western and southern margin of the Musgrave Block (Jackson and van de Graaff, 1981). The two units may extend across the State border. The Townsend Quartzite consists of medium to coarse-grained, orthoquartzitic, fluvial to shallow marine sandstone, up to 370m in outcrop, overlain by fine sandstone, siltstone and grey-coloured shale of the Lefroy beds (250m) (Townson, 1985). The two units were intersected in the Yowalga sub-basin which is considered to be a foreland basin (Myers, 1990). Kanpa 1A and Yowalga 3 are deep petroleum exploration wells penetrating the thick Browne beds (?=Lefroy beds). Kanpa 1A intersected 120m of Townsend Quartzite and 1150m evaporites of the Browne beds; Yowalga 3 stopped within the Browne beds where 2300m evaporites had been intersected. According to seismic interpretation the Browne beds are probably up to 4000m thick in the depocenter of the sub-basin and consist of variegated (green, red-brown, grey and black) shale and siltstone interbedded with halite, anhydrite and dolomite, deposited in shallow marine, sabkha to playa lake environments (Townson, 1985).

The Torrensian succession is well developed and studied in the Amadeus Basin (Lindsay and Korsch, 1991; Southgate, 1991). The succession comprises lower Heavitree Quartzite and upper Bitter Springs Formation, which were deposited in shallow marine conditions (often tidal), on a platform or ramp (Lindsay and Korsch, 1991). The two units form a major depositional sequence from the relatively shallow marine tidal Heavitree Quartzite, deepening upward into the Gillen Member and then shallowing upwards to a marine, and later lacustrine carbonate, in the Loves Creek Member of the Bitter Springs Formation (Southgate, 1991). Acritarchs suggest that the Gillen Member is correlative with the Alinya Formation but the sediments of the Loves Creek Member equivalent may be absent in the eastern Officer Basin. The Loves Creek marine shale in the Amadeus Basin contains mainly spheroidal acritarchs with mainly benthic coccoids and cyanobacterial filaments in the lacustrine chert (Schopf, 1968; Schopf and Blacic, 1971; Zang and Walter, 1992b).

However, evidence from Wallara 1 well in the central Amadeus Basin suggests that there was probably a later marine transgression following deposition of the lacustrine Loves Creek Member. "Finke beds" do not crop out but were first intersected in Finke 1 well and recently the fully cored Wallara 1 intersected "Finke beds" at the depth 1424-1510m, unconformably underlying the Neoproterozoic glaciogenic Areyonga Formation (Weste, 1990). The "Finke beds" consists of dolomite, dark-grey laminated dolomitic siltstone and minor sandstone and unconformably overlie the lacustrine deposits of the Loves Creek Member. The "Finke beds" were considered to be deposited in a marine environment (Weste, 1990). A sample collected from this unit contains well preserved acritarchs, including many morphologically complex spinose forms (Zang, unpub. data).

The thickest succession of Torrensian sediments in Australia is in the Adelaide Geosyncline where the Burra Group contains up to 8000m siliciclastics and carbonate (Forbes and Preiss, 1987), from which four sequence sets were recognised (Preiss, 1993). Sequence stratigraphy and acritarch biostratigraphy of the Burra Group are yet to be systematically studied in the Geosyncline. Recent drilling suggests that the Burra Group sediments are also present at the eastern margin of the Stuart Shelf. Seismic interpretation indicates that 200 - 500m sediments are present below the Sturtian tillites; the uppermost part of the dark-grey shale, dolomite and sandstone (?Myrtle Springs Formation, upper Burra Group) was intersected in BLD 4 well. Acritarchs collected from the dark grey shale contain mainly spheroids and several spinose forms and their assemblages are probably correlative with those from the "Finke beds" (Zang, unpub. data). Schopf (in Schopf and Klein, 1992) described a group of spheroidal coccoids and cyanobacterial filaments from the chert in the Skillogalee Dolomite (middle Burra Group) and most forms resemble those from the chert of the Loves Creek Member.

Isotopic ages are consistent for the Torrensian successions in Australia. An age of 897±9 Ma (Rb/Sr on separated minerals) was obtained on dykes in the basement underlying the Heavitree Quartzite, indicating a maximum age for the sediments in the Amadeus Basin (Black et al., 1980). Recently an age of 800 Ma was suggested for the tholeiitic basalt-equivalent in the Bitter Springs Formation (Zhao et al., 1992b; Korsch, 1993). A minimum date of 830 Ma might be close to the age of the basal Callanna Group in the Adelaide Geosyncline (cf. Preiss, 1987). A thin tuff in the rift-valley succession of the upper Callanna Group yielded a concordant U/Pb age (on zircon) of 802±10 Ma, indicating a maximum age for the Torrensian, and post-Sturtian-glacial sediments provided a Rb-Sr age of 750±53 Ma (Preiss, 1987). On this evidence, Sequence 2 and its equivalent sediments in Australia probably ranges in age from 800 to 750 Ma.

ACRITARCHS AND CORRELATION

Early Neoproterozoic acritarchs and cyanobacterial microfossils are well known from Australia and around the world. A mainly benthic microfossil assemblage was found in the chert of the Loves Creek Member (Bitter Springs Formation) as early as 1965 (Barghoorn and Schopf, 1965) and received much attention in the study of Precambrian palaeobiology and early eucaryotic evolution (Schopf, 1968; Schopf and Blacic, 1971). A well-preserved Late Riphean acritarch assemblage which includes a large, spinose acritarch *Trachyhystrichosphaera aimica* Hermann and other morphologically complex forms, was described from Siberia (Timofeev et al., 1976; Jankauskas, 1989). Acritarch assemblages of similar age were also described from USA (Vidal and Ford, 1985), Spitsbergen (Knoll, 1984; Butterfield et al., 1988; Knoll et al., 1991), and Australia (Zang and Walter, 1992a). A similar diverse assemblage exists in the coastal sabkha deposits from the Alinya Formation, in which the abundance and diversity of the morphologically complex acritarchs can be used for intra and intercontinental correlation.

The biostratigraphy of the eastern Officer Basin was poorly investigated and correlation has hitherto been based on lithology and seismic interpretation (Brewer et al., 1987; Stainton et al., 1988; Sukanta et al., 1991). However, some soft-bodied fossil impressions have been reported in the sandstone of the Punkerri beds (Major, 1974). Latest Neoproterozoic acritarchs were also reported from the Rodda beds (van Niel, 1984; Amoco, 1987; Jenkins et al., 1992), but no acritarchs or other fossils have been described from the early Neoproterozoic succession in the Officer Basin.

Distribution and Preservation

Four distinct microfossil communities can be recognised from the coastal sabkha deposits of the upper Alinya Formation in Giles 1 and their distribution is probably related to environmental gradients (Figure 19). In the upper intertidal to supratidal sandstone some algal or cyanobacterial borings were found to penetrate into the aeolian sand grains, where organic matter debris often forms a matrix (Figure 21:A-D). The borings are normally elongate, 50-100*um* long and 10-15*um* in diameter, with a rounded end within the quartz grain and the other end opening to the outside of the grain. Several borings show septa-like structures, similar to those of *Oscillatoris* or *Lynbya*. Commonly surrounding these borings are abundant coccoids, probably *Eoentophysalis gilesis* sp. nov.; occasionally some relatively large envelopes of spheroidal acritarchs were found, but only rare cyanobacterial filaments. Thus the origin of these organic activities in the sandstone is not understood, but the bored sand grains are either allogenic or authigenic.

Microfossil communities from tidal flat are dominated by *Eoentophysalis gilesis* mats with rare leiosphaerids and spinose acritarchs. The mats are commonly preserved in siltstone, but can be found in the anhydrite inter-layers where microorganisms constructed stratiform-like stromatolites. Only some loose cyanobacterial filaments, probably *Siphonophycus robustum*, were found in the communities, but rare filamentous mats.

The coccoids of *Eoentophysalis gilesis* mats are generally cemented by a translucent sheath, but loose pieces can be found in aeolian sandstone and sublittoral to basinal shales, where they may be allogenic. In anhydrite, the mats are usually well-spaced, ranging from 1-8mm in thickness. On the mudflat, coccoids and siliciclastic silts form graded beds, which commonly pass from siltstone through silty mudstone to organic-rich mudstone with a sharp base. The sharp, erosional base probably indicates flood influence or a sedimentary interruption (Figure 20). This fabric is similar to that of modern *Entophysalis* mats at Hamelin Pool, Shark Bay, Western Australia and elsewhere (Logan et al., 1974; Golubic and Hofmann, 1976). On the semi-arid intertidal mudflat of Hamelin Pool, *Entophysalis* mats cover a large area. The organic matter can be eroded and transported into the basin by storms or cyclones, together with other benthic organisms, forming a 1.5m thick black "ooze" like on the southern basinal plain at the Pool, in which TOC is up to 5%. This ooze is regarded as an important potential petroleum source rock (Burne and Hunt, 1990).

Black to dark grey, laminated shale is interpreted to have been deposited below storm-wave base and is dominated by benthic communities, mainly spheroidal mats or groups, and abundant degraded organic debris. Three forms are particularly abundant: *Coniunctiophycus* sp. cf. *C. majorinum*, *Myxococcoides* sp. cf. *M. cantabrigiensis* and *Sphaerophycus* sp. Acritarchs are mainly *Leiosphaeridia* with some spinose acritarchs. In the black shale graded bedding is not uncommon (Figure 12:B) but cross-bedding is rare, suggesting stagnant water conditions.

Laminated to cross-bedded green to dark grey shale (deposited above fair-weather wave base) contains abundant phytoplanktonic spheroids and spinose acritarchs. Benthic coccoids are still dominant, but cyanobacterial filaments are sometimes particularly abundant in some samples (up to 50% of all specimens in 5341RS337). Organic debris is relatively rare compared to samples from the basinal black shale. Consistent current influence indicated by frequent cross-bedding probably favoured conditions for phytoplankton.

Diagenetic change within the Alinya Formation has not significantly damaged the organic matter in Giles 1. In sandstone no quartz overgrowth is present. In the anhydrite (part of which retains the original gypsum) *Eoentophysalis gilesis*, benthic coccoids and acritarchs were well-preserved, similar to microfossils in the microcrystalline chert/quartz. Fine-grained layers in the siltstone seem to preserve more organic matter, but some microfossils were also found in sandstone (Figure 21:D).

One thin section (5042RS2) was cut from the chert of the lower Alinya Formation collected from the type section in the North Pindyin Hills. The chert is brownish grey, irregularly banded by white colloform silica. Patchy vugs are filled with microcrystalline silica or partly with spherulitic chalcedony. Authigenic dolomite rhomb pseudomorphs are completely replaced by silica (Figure 21:G-H). Spheroidal and spinose acritarchs, filaments and vase-shaped microfossils, probably *Melanocyrillium* sp, were found in the colloform or microcrystalline silica (Figure 21:E-F), and the specimens are commonly dark grey and show some degradation. In the area of abundant dolomite rhomb pseudomorphs only organic debris was observed. The chert, which is an interbed in marine carbonate and shale, passed through dolomitization and silicification during diagenesis and its organic matter was thus partly degraded.

Acritarch Biostratigraphy

The acritarchs in this study were mainly macerated from the sublittoral green-grey to dark-grey shale, and to a lesser extent from the anhydrite, chert and dark grey siltstone thin section (Figures 23-32). The green-grey shale is interpreted to have been deposited in a sublittoral environment where the water probably circulated freely with the open sea. This is demonstrated by the usually well preserved organic matter and lack of evidence of reworking by anaerobic or sulphur bacteria. On the other hand the basinal black shale contains abundant degraded or reworked organic debris, whereas stagnant hypersaline brines in the basin provided favourable conditions for sulphur bacteria. The acritarch assemblages in the Alinya Formation, therefore, are mixed with both open marine and barred-basin communities.

The assemblage from the Alinya Formation in Giles 1, as a whole, comprises mainly benthic microorganisms, in which *Eoentophysalis gilesis* dominated the intertidal flat communities, and benthic coccoids *Coniunctiophycus, Myxococcoides* and *Sphaerophycus* dominated the subtidal to basinal substrate communities. Cyanobacterial filaments are locally abundant in some subtidal samples. The most interesting taxa in the assemblage are the large, morphologically-complex and membrane-coated spinose species which can be used for intercontinental correlation. This assemblage, named the *T. vidalii - T. aimica - C. kullingii* assemblage, defines an important biostratigraphic zone prior to the Neoproterozoic glaciations.

Trachyhystrichosphaera vidalii Knoll, 1984 and *Cymatiosphaeroides kullingii* Knoll, 1984 were first described from chert in the Upper Riphean Hunnberg Formation of Nordaustlandet, Spitsbergen (Svalbard) (Knoll, 1984). The species bear either hollow (*T. vidalii*) or solid (*C. kullingii*) processes and are surrounded by an outer membrane or membranes. The two species are also present in a Neoproterozoic tidal/lagoon complex (Draken Conglomerate Formation) in Spitsbergen (Knoll et al., 1991). *C. kullingii* was recorded in the Awatubi Member (Kwagunt Formation), Chuar Group, USA (Vidal and Ford, 1985) and *T. vidalii* was found in the Upper Riphean in Russia (Jankauskas, 1989). These collections are from Neoproterozoic pre-glacial deposits, ranging from 700 - 850 Ma. The two species are now found in the Alinya Formation of similar age, implying a global distribution (Figure 23:A-E, 24:H-K).

Trachyhystrichosphaera aimica Hermann, 1976, bearing a large vesicle with long, distinct hollow processes without an outer membrane or wall, was first described from the upper Riphean Lakhanda Formation, Khabarovsk region in Siberia (Timofeev et al., 1976; Jankauskas, 1989). About 15 similar specimens were observed in the Alinya Formation, in which the vesicles range from 50-400*um* in diameter with spines up to 70*um* long (Figure 26:B). Another interesting species, *Trachyhystrichosphaera stricta*, consisting of an excystment envelope enclosing a free-moving, spinose encysted body, is also present in the Upper Riphean and the Alinya Formation. Its size is up to 800*um* in diameter (Figure 25:H). This species was also reported from siliciclastics in the Svanbergfjellet Formation, Spitsbergen (Butterfield et al., 1988, fig.3:g), but was not found in the chert of the overlying Draken Conglomerate Formation. However, one other distinct species in the Upper Riphean, *Amadeusphaeridium (=Trachyhystrichosphaera) cyathophora* (Hermann, in Jankauskas, 1989) (Zang and Walter, 1992b), which has a large vesicle with funnel-shaped processes, has not been found in this study.

Relatively abundant specimens (about 20 vesicles) of *Vandalosphaeridium* sp. cf. *V. reticulatum* are present in the Alinya Formation. This species was defined as a spheroidal versicle bearing short sturdy processes to support an outer membrane. The type species was described from the Upper Riphean to Lower Vendian Visingso beds (Vidal, 1976). The Alinya specimens have about 8-15 short solid processes surrounded by a smooth outer membrane (Figure 23:F-H). Belonging to this group, *Vandalosphaeridium walcottii* Vidal and Ford, 1985, was described from the equivalent beds in the Chuar Group, Arizona (Vidal and Ford, 1985), and *Vandalosphaeridium (=Skiagia) pusillum* (Zang), a small vesicle with funnel-shaped processes probably surrounded with a membrane, was described from the Gillen Member (Bitter Springs Formation) in the Amadeus Basin (Zang and Walter, 1992b).

Several new spinose acritarchs are described from the Alinya Formation. *Comasphaeridium tonium* sp. nov. is characterised by its moderate size (40-85μm) and discrete and relatively short hair-like processes (Figure 24:A-G); occasionally it has a spinose protuberance structure which was found in another distinct early Neoproterozoic species *Trachsphaeridium laufeldi* (Vidal and Knoll, 1983; Vidal and Ford, 1985). Another new species, *Goniosphaeridium alinyum* (Figure 25:A-D), bears hollow triangular to blade-like processes, together with *C. tonium* seem to be morphologically advanced acritarchs in the Torrensian.

In the Alinya Formation two new species are named for their solid process structure. The development of this structure, possibly a membrane-coated spinose structure, may be related to environmental gradients: under the evaporitic conditions, acritarchs grew more resistant to salinity rather than developing the means for floating. Solid or membrane-coated process structures may prevent losing internal moisture in an arid environment. One species, *Gorgonisphaeridium pindyium* sp. nov., contains specimens which were also found in the Gillen Member (Bitter Springs Formation) in the Amadeus Basin and the Draken Conglomerate Formation, Spitsbergen; both formations were considered to have been deposited in arid coastal marine to lagoonal environments (Zang and Walter, 1992b, Knoll et al., 1991).

The Alinya Assemblages contain various spinose forms: *Germinosphaera* sp. cf. *G. unispinosa* Mikhailova, 1986 bears a single prominent, hollow, conical process; *Leiofusa bicornuta* Sin and Liu, 1973 has two processes at the apices; and *Asteridium* sp. has several solid processes. In the Gillen Member asterids are relatively abundant (Zang and Walter, 1992b).

Two large specimens with a polyhedral outline, probably belonging to *Polyhedrosphaeridium*, were found in the Alinya Formation. The vesicles are 215-275μm in diameter with several protuberances on the margin and probably belongs to *Polyhedrosphaeridium*. The type species of this genus, *P. echinatum* Zang, was described from the Ediacarian Pertatataka Formation in the Amadeus Basin, central Australia (Zang and Walter, 1992b) and bears hollow processes, probably indicating an evolutionary advance in comparison with that from the Alinya Formation.

Valeria lophostriata (Jankauskas), a distinctive species in the Upper Riphean assemblages and widely recorded from Russia (Jankauskas, 1989), USA (Vidal and Ford, 1985) and elsewhere (Vidal and Siedlecka, 1983; Vidal and Moczydlowska, 1992), is present in the Alinya Formation.

Nematode-like *Rectia costata* (Jankauskas) is characterised by its annulated tube-like structure and its type specimen was described from the Upper Riphean in Siberia (Jankauskas, 1989). From the same level in Siberia, as well as in the Alinya Formation, another species, *Annulusia annulata* (Timofeev and Hermann) Jankauskas, 1989, a rim-like acritarch, was also found. Possibly the two forms are named from same microorganism, that is, the rim-like *Annulusia annulata* is a segment of a filamentous microorganism like *Rectia costata.*

Spheroidal acritarchs in the Alinya Formation include many forms common in the Neoproterozoic elsewhere, such as *Leiosphaeridia, Synsphaeridium, Satka, Tasmanites, Simia, Sinianella, Sphaerocongregus* and *Archaeoellipsoides*. Vase-shaped microfossils *Melanocyrillium* and the square or octahedral *Octoedryxium intrarium* are also present in the Alinya assemblage.

Many early Neoproterozoic microfossil assemblages recorded seem to be, in comparison with those from the Ediacarian and Palaeozoic, dominated by benthic microorganisms and cyanobacterial filaments (Knoll, 1984; Jankauskas, 1989; Knoll et al., 1991; Zang and Walter, 1992b). In the Alinya Formation the species of the cyanobacterial and benthic mats are estimated to form 60% of the microfossil assemblage with individual specimens up to 85%. In the lacustrine chert of the Loves Creek Member (Bitter Springs Formation) about 30 to 50 species of cyanobacteria and benthic microfossils were described (Schopf, 1968; Schopf and Blacic, 1971; Knoll and Golubic, 1979). Most of these benthic species disappeared after the Neoproterozoic glaciations or were replaced by other species (Volkova et al., 1979; Vidal and Knoll, 1983; Downie, 1984; Yin, 1987; Jankauskas, 1989; Knoll and Walter, 1992; Zang, 1992; Zang and Walter 1992a,b).

The acritarch assemblage from the lower Bitter Springs Formation (Gillen Member) (Zang and Walter, 1992b) is very similar to that from the upper Alinya Formation in Giles 1. Stratigraphically the Bitter Springs and Alinya Formations overlie the basal blanket sandstone in central Australia and were probably deposited in a transgressive to highstand systems tract, with both formations containing open marine to sabkha deposits. They are commonly considered to be correlative (e.g. Stainton et al., 1988) and this is now confirmed by acritarch correlation (Figure 22).

However, there are differences between the two assemblages, which probably resulted from different sedimentary settings. More than thirty acritarch species were observed in open marine shale and limestone from core 2 in Bluebush 1 (Gillen Member, Bitter Springs Formation) in the southeastern Amadeus Basin. The assemblage is dominated by spheroids, as well as many spinose elements including *Asteridium, Comasphaeridium, Vandalosphaeridium pusillum* (Zang) and large *Trachyhystrichosphaera* and *Gorgonisphaeridium* (Zang and Walter, 1992b). Acritarchs from the Alinya Formation in the Officer Basin, like those in the Gillen Member, also contain abundant spheroids, several specimens of *Asteridium* sp., *Trachyhystrichosphaera, Gorgonisphaeridium* and *Octoedryxium intrarium* (Timofeev) Jankauskas, 1989 which is also abundant in the Gillen Member (Zang and Walter, 1992b). The Alinya assemblages are obviously more diverse than those from the Gillen Member. The sabkha deposits of the Alinya Formation also contain other distinctive species such as *Comasphaeridium, Goniosphaeridium, Trachyhystrichosphaera vidalii, T. aimica* and *Cymatiosphaeroides kullingii*, which were not found in the Gillen Member.

More than 200 microfossils have been described so far from the early Neoproterozoic sediments and most are long-ranging benthic spheroids and cyanobacterial filaments. Acritarch assemblages, represented by spinose species *T. vidalii, T. aimica* and *C. kullingii*, provide the potential for global correlation. In this study, the acritarch assemblage from the Alinya Formation is broadly correlated with that from the Gillen Member (Zang and Walter, 1992b), the Draken Conglomerate Formation (or underlying Svanbergfjellet Formation - Butterfield et al., 1988), Spitsbergen (700-800 Ma, Knoll et al., 1991), Chuar and Uinta Mountain Groups, USA (800-850 Ma, Horodyski, 1993; Vidal and Ford, 1985), and Upper Riphean (Lakhanda Formation), Siberia (Jankauskas, 1989; Schopf in Schopf and Klein, 1992, Chapter 24.2). Selected acritarchs from the known early Neoproterozoic assemblages are listed in Figure 22.

The upper Neoproterozoic successions are probably equivalent to the Qingbaikouan (800-1000 Ma) sediments on the North China Platform. The acritarchs from the sediments are poorly known (Sin Yu-sheng and Liu, 1973).

In addition to acritarchs in the Officer Basin some fossil traces, including possible horizontal and vertical bioturbation, were observed in the Pindyin Sandstone (Major, 1993, pers. comm.). Although there is some uncertainty in the identification they may resemble those vertical tubes in the Heavitree Quartzite in the Amadeus Basin (Lindsay, 1991). They may be inorganic, however, like de-watering structures.

PETROLEUM POTENTIAL

The Alinya Formation was probably deposited in a saline giant containing abundant organic matter in the early Neoproterozoic. In Giles 1 the organic matter in the black shale of the sabkha deposits on the Murnaroo Platform seems to be partly reworked by bacteria, but in the grey-green shale it has neither been excessively diluted by sediment, nor suffered complete microbial destruction during sedimentation and early diagenesis. The organic matter has the potential for diagenetic transformation into oil and gas. The Alinya Formation overlies the aeolian Pindyin sandstone and is overlain by alluvial to deltaic sandstone (Tarlina Sandstone). Both sandstones are permeable and have porosities of 5-20% (Figure 10:B); in turn the Tarlina Sandstone is overlain by the Giles Mudstone which is a thick, effective seal. This combination provides an ideal target for petroleum exploration.

The significance of the source-rock potential in marine evaporitic environments was discussed by Kirkland and Evans (1981). The organic matter would normally be transformed into microbial lipids which migrate, accumulate and finally are converted into petroleum at 50-80°C (Zhang Yi-gang, 1981). In the upper Alinya Formation, sabkha siltstone/shale on the Murnaroo Platform contains a large volume of quartz grains of aeolian origin, which would likely reduce TOC values (0.1-0.62%). The organic matter consists mainly of benthic microorganisms and reworked *Eoentophysalis gilesis* fragments. Investigation of the TOC distribution in Hamelin Pool, Shark Bay, Western Australia indicates that on the *Entophysalis*-dominated intertidal platform TOC is around 1%, in the subtidal (2-4m deep) 2-3% and in the depocenter up to 5% (Burne and Hunt, 1990). In the Alynia Formation *Eoentophysalis*-dominated red-brown sandy siltstone yields 0.1% TOC and organic matter often formed thin layers at the top of the graded-bedding (Figure 20). The organic matter from the green to grey shale (0.14% TOC) is commonly a yellow to orange colour and is dispersed among inter-granular pores. The organic matter in the black shale is often degraded and interspersed with quartz silt and sometimes aeolian sand (Figure 12:B). Rock-Eval pyrolysis on the basinal black shale (0.25-62% TOC) suggests it contains a mature gas-prone kerogen (T_{max} =439-445°C; hydrogen index = 58-106) (Zang and McKirdy, 1993).

The oldest known Siberian oil and gas reservoirs are found in Sequence 2 equivalent Upper Riphean carbonates of the Eastern Siberia. Geochemical data there suggest that the major petroleum hydrocarbons were probably sourced from Neoproterozoic carbonate-evaporite successions (Meyerhoff, 1980; Surkov et al., 1991). A recent study shows that most petroleum in the Persian Gulf area, especially in Oman, was sourced from the Neoproterozoic salt-related kerogenous rocks (Edgell, 1991). About 70% of the world's giant oil fields in carbonate rocks bear a relationship to evaporites (Zhang Yi-gang, 1981) even though evaporites constitute only 2% of the world's platform sediments (Warren, 1989). In China the largest gas pool is in late Neoproterozoic carbonates. Recent exploration in the Amadeus Basin discovered a significant gas show from the Heavitree Quartzite(?), which was probably sourced from the Gillen Member. Extensive diapir and salt structures and predicted high organic matter concentration in the Munyarai Trough implies that a potential petroleum reserve may exist in the eastern Officer Basin.

CONCLUSIONS

The Torrensian Pindyin Sandstone and Alinya Formation are considered to have been deposited during the interval of 800 - 750 Ma and comprise an early Neoproterozoic depositional sequence in the central and eastern Officer Basin. Abundant morphologically complex acritarchs in the Alinya Formation can be broadly used for intercontinental correlation and their abundance and diversity probably indicate an important evolutionary explosion of microorganisms prior to the Neoproterozoic glaciations. In the eastern basin the sabkha deposits on the Murnaroo Platform contain gas-prone organic matter; the aeolian Pindyin Sandstone is highly porous and regarded as a potential reservoir rock. The two lithological units, together with disconformably overlying porous alluvial sandstone, sealed by mudstone, may form a potential petroleum resource.

SYSTEMATIC PALAEONTOLOGY

The group Acritarcha was proposed by Evitt (1963) for phytoplankton of organic composition of unknown affinity. The microfossils described in this study were collected from shale, siltstone, anhydrite and chert of the Alinya Formation and both petrographical section and maceration techniques were applied for several samples to study the preservation and abundance. The species are listed alphabetically herein in the spheroidal and filamentous divisions.

The specimens and samples are deposited in the Core Library, Department of Mines and Energy, South Australia, Glenside, Adelaide, Australia, and marked by "RS" number. Each specimen illustrated in this study is indicated by England Finder coordinates, whereas several specimens from large petrographic sections are marked only by X+Y coordinates from Zeiss Microscope (No. 1953) at Biostratigraphy Branch, Department of Mines and Energy, South Australia.

Spheroidal microfossils

Genus *Annulusia* Timofeev and Hermann in Jankauskas, 1989

Type species. *Annulusia annulata* (Timofeev and Hermann) Jankauskas, 1989

Annulusia annulata (Timofeev and Hermann) Jankauskas, 1989

(Figure 28:A-B)

1989 *Annulusia annulata* Timofeev and Hermann, 1979, nom. nov., Jankauskas, p.135, fig.29:12.

Description. Vesicle rim-like with a large central opening, originally, probably, ring or 'cylinder'-like. Rim surface smooth to slightly shagreen, with stable width (3-15*um*) on single vesicle; central opening circular, 5-20*um* across; two specimens showing a broken thin membrane surrounding vesicle and opening. Vesicle 15-90*um* across (10 specimens).

Remarks. The diameters of photographed type specimens from the Lakhanda Formation, Siberia seem to differ between those from Jankauskas (1989, plate 29:12) and those from Schopf (in Schopf and Klein, 1992, plate 15:D). Alinya specimens are all solitary and their reproduction and colony structures are unknown. Probably *Annulusia annulata* is described from the loose septa or segments of a septate filamentous microorganism.

Genus *Archaeodiscina* Naumova, 1960

Type species. *Archaeodiscina granulata* Naumova, 1960.

Archaeodiscina sp.

(Figure 31:I)

Description. Vesicle circular, originally spheroidal, with a distinct, surficial, darker spheroidal body and radiating processes; wall shagreen to finely granular and commonly folded; darker spheroidal body 8-13*um* across, rounded with a sharp margin, 4-7 processes (3-9*um* long) radiating from a central disc and tapering towards the margin of the vesicle. Vesicle 25-60*um* in diameter (7 specimens).

Remarks. The present specimens have no distinctive characters and are more or less similar to the Cambrian species *Archaeodiscina umbonulata* Volkova, 1968.

Genus *Archaeoellipsoides* Horodyski and Donaldson, 1980

Type species. *Archaeoellipsoides grandis* Horodyski and Donaldson, 1980.

Archaeoellipsoides karatavicus (Jankauskas) comb. nov

(Figure 29:H-K)

1989 *Eosynechococcus karatavicus* (Jankauskas), Jankauskas, p.91, pl.21:7,8,10.

Description. Vesicle elongate, originally sausage-shaped; surface smooth to slightly granular and often folded; width:length ratio of the 'sausage' about 7:10 to 1:2.5; colonies in regularly linear arrangement or chain-like, with connection of long-axis apices, generally vesicle in colonies smaller; no excystment observed. Vesicle 5-25*um* wide and 8-55*um* long (20 specimens).

Remarks. The specimens in this study were collected from both chert thin section and maceration in the Alinya Formation and indicate that the size of the 'sausages' varies and the three genera (*Archaeoellipsoides*, *Eosynechococcus* and *Brevitrichoides*) are probably intergraded. *Eosynechococcus* commonly includes very small 'sausages'. Jankauskas (1989, p.91) transferred *Brevitrichoides karatavicus* Jankauskas, 1980 to *Eosynechococcus.*

Genus *Asteridium* Moczydlowska, 1991

Type species. *Asteridium lanatum* (Volkova) Moczydlowska, 1991 (=*Micrhystridium lanatum* Volkova, 1969)

Asteridium sp.

(Figure 26:J)

Description. Vesicle small, circular to irregular, originally spheroidal; surface smooth to shagreen; processes solid, relatively long (3-6*um*), variable, conical to slightly flared at tip; no excystment observed. Vesicle 10-15*um* in diameter (3 specimens).

Remarks. Moczydlowska (1991) separated *Micrhystridium* into two genera: *Asteridium* (with solid processes) and *Heliosphaeridium* (with hollow processes). Most previous Proterozoic micrhystrids, including *M. geminatum* and *M. pisinnum* Zang both in Zang and Walter, 1992b from the Bitter Springs Formation, seem to have solid processes and should be transferred to *Asteridium.* However, *Heliosphaeridium* differs very little from the original designation of *Micrhystridium* because most Palaeozoic micrhystrids are single-layered. Double-layered micrhystrids are rare and are probably preservational variations.

Genus *Comasphaeridium* Staplin, Jansonius and Pocock, 1965

Type species. *Comasphaeridium cometes* (Valensi), Staplin, Jansonius and Pocock, 1965 (= *Micrhystridium cometes* Valensi, 1948).

Comasphaeridium tonium sp. nov.

(Figure 24:A-G)

Etymology. For the age of Neoproterozoic Tonian.

Holotype. Figure 24:B, slide 5341RS308-8, Q45/4, collected from Giles 1 (1237.9m), Alinya Formation.

Description. Vesicle moderately large, circular to subcircular, originally spheroidal; wall thin, commonly folded; surface smooth to shagreen; processes hair-like, moderately thin, short to relatively long (2-9*um*), solid, numerous (up to 250 individuals at outline), unbranched and flexible; occasionally a spinose protuberance on the vesicle margin and a darker spot in the center; no excystment structure and outer membrane observed. Vesicle 40-85*um* in diameter (30 specimens measured, holotype 65*um* in diameter).

Remarks. The present species is distinguishable from Palaeozoic species of the genus by its relatively large vesicle, discrete, relatively short processes and occasional spinose protuberant structure. Most Ediacarian species in the genus are larger (Zhang, 1984; Zang and Walter, 1992b). *Comasphaeridium pollostum* from the Gillen Member (Bitter Springs Formation) has a small vesicle with very thin, villus-like processes (Zang and Walter, 1992b).

Distribution. Upper Alinya Formation.

Genus *Coniunctiophycus* Zhang, 1981

Type species. *Coniunctiophycus gaoyuzhuangense*, 1981

Coniunctiophycus sp. cf. *C. majorinum* Knoll et al., 1991

(Figure 30:A-E)

1991 *Coniunctiophycus majorinum* sp. nov., Knoll et al., p.554-557, fig.16:1-4.

Description. Specimen colony-form, elongated-ellipsoidal group to very long multi-lobate shape; single 'lobate' type consisting of about 20-50 individuals; individual wall thin, smooth to shagreen surface, 5-15*um* in diameter, tightly packed in colony, commonly with stable size in a single lobe. Lobes often interconnected in line or forming stubby 'branches'; bud-like structures very common; no outer membrane or common envelope observed. 'Lobate' colony up to 500*um* long (100 specimens).

Remarks. Alinya specimens are larger, both individuals and lobate colonies, than the Draken counterparts. Bud-like forms in colonies are probably reproductive or growing structures.

Genus *Cymatiosphaeroides* Knoll, 1984
Type species. *Cymatiosphaeroides kullingii* Knoll emend. Knoll et al., 1991
Cymatiosphaeroides kullingii Knoll emend. Knoll et al., 1991
(Figure 24:H-K)
1991 *Cymatiosphaeroides kullingii* Knoll emend., Knoll et al., p.557, fig.4:4, 4:6.
Description. Vesicle circular to subcircular, originally spheroidal; wall robust, commonly folded; numerous (up to 200 around the margin), solid, discrete, thin, hair-like processes standing to support an outer membrane; processes commonly with consistent length (5-10*um* long) in a single vesicle, blunt or slightly flared at tip; no excystment structures observed. Vesicle 50-250*um* in diameter (20 specimens).

Remarks. Most large specimens in the Alinya Formation have suffered varying degrees of damage, particularly to the outer membrane. No outer multilaminae were observed in the Alinya specimens, which is probably a preservational phenomenon between the specimens from the chert as opposed to clastic samples.

Genus *Eoentophysalis* Hofmann, 1976 emend. Mendelson and Schopf, 1982
Type species. *Eoentophysalis belcherensis* Hofmann, 1976
Eoentophysalis gilesis sp. nov.
(Figure 31:A-D)
Etymology. From the name of Giles 1 well.

Holotype. Figure 31:B, slide 5341RS339, 38 X 95.3, collected from petrographic section in Giles 1 (1242.45m), upper Alinya Formation.

Description. Mat-building colony consisting of numerous irregular spheroidal individuals; size variable in life cycle (Figure 19:A), from 3*um* to large compound form up to 40*um* in diameter; small individual vesicles enclose 1-8 smaller internal dark blebs of organic matter, whereas large compound forms contain up to 80 dark blebs arranged like a ring. Occasionally two concentric rings observed with a tightly packed bleb center; large compound usually on the top of a mat and often observed as a loose individual; individual wall membrane-like, commonly single-layered, occasionally double-layered.

Remarks. New species is distinguishable by its individual-compound structure and ontogenetic variation. This species dominated the intertidal communities in the Alinya assemblages and is abundantly preserved in anhydrite layers. The mats are usually thin in anhydrite (0.5cm) and up to 2cm in siltstone.

Distribution. Torrensian Alinya Formation.

Genus *Germinosphaera* Mikhailova, 1986
Type species. *Germinosphaera unispinosa* Mikhailova, 1986
Germinosphaera sp. cf. *G. unispinosa* Mikhailova, 1986
(Figure 26:K-L)
1989 *Germinosphaera unispinosa* Mikhailova, Jankauskas, p.143, pl.47:1.
Description. Vesicle circular to subcircular, originally spheroidal to irregularly ellipsoidal, with a distinctive, relatively long process. Wall thin to moderately thick, smooth to finely granular, commonly folded; a prominent process tapering from the vesicle to a point, process hollow, freely communicating with the vesicle cavity, 16-25*um* long. Vesicle 28-45*um* in diameter (5 specimens).

Remarks. Present specimens are relatively large, process is relatively short and not constrained between the vesicle and process in comparison with the Russian type species (cf. Jankauskas, 1989).

Genus *Goniosphaeridium* Eisenack, 1969 emend. Kjellstrom, 1971
Type species. *Goniosphaeridium polygonale* Eisenack, (1931) 1969 (=*Baltisphaeridium polygonale* Eisenack, 1931).

Goniosphaeridium alinyum sp. nov.
(Figure 25:A-D)

Etymology. From the name of the Alinya Formation.

Holotype. Figure 25:B, slide 5341RS337-6, G47/1, collected from Giles 1 (1244.2m), Alinya Formation.

Description. Vesicle moderate to relatively large in diameter, circular to subcircular, originally spheroidal; wall moderately thick, finely granular and folded; processes sparse (1-7 around the margin), variable (triangular, blunt or blade-like), very thick, relatively short (6-15*u*m long), unbranched, widened at base (9-14*u*m wide) and sharp or truncated at tip; process hollow, freely communicating with the vesicle cavity; neither external membrane nor excystment structure observed. Vesicle diameter 48-110*u*m (holotype 48*u*m in diameter) (10 specimens measured).

Remarks. Short, variable blade to triangular processes are the characteristic features for *Goniosphaeridium alinyum.*

Distribution. Torrensian Alinya Formation.

Genus *Gorgonisphaeridium* Staplin, Jansonius and Pocock, 1965
Type species. *Gorgonisphaeridium winslowii* Staplin, Jansonius & Pocock, 1965

Gorgonisphaeridium pindyium sp. nov.
(Figure 27:A-E)

1991 *Gorgonisphaeridium maximum* (Yin) comb. nov., Knoll et al., p.557, fig.21:13.
1992b *Trachyhystrichosphaera* sp., Zang and Walter, p.114, fig.59:C-D (?fig.59:A-B).
Etymology. For the type section in the North Pindyin Hills.

Holotype. Figure 27:B, 5042RS2, H42/3, from the chert thin section collected from the North Pindyin Hills, lower Alinya Formation.

Description. Vesicle of moderate to large size, circular to irregular in outline, originally spheroidal; wall moderately thin to thick (up to 2.5*u*m), flexible, shagreen to finely granular and commonly folded; processes short (3-8*u*m long), sparse to moderately abundant (12-60 around the margin), triangular to slightly conical, solid, unbranched, pointed to slightly blunt. Vesicle 50-200*u*m (holotype 100*u*m) in diameter (20 specimens).

Remarks. Short, triangular to conical and solid processes are the characteristic feature for *Gorgonisphaeridium pindyium.* Most large specimens in the Alinya Formation show some degree of diagenetic deformation and longer processes have been damaged.

One incomplete specimen with solid, blunt conical processes was collected from the early Neoproterozoic Draken Conglomerate Formation. The specimen was combined with late Ediacarian *Gorgonisphaeridium maximum* (Yin) (=*Baltisphaeridium maximum* Yin, 1987), which bears solid, slim, sharp-pointed conical processes; similar specimens were found in the late Ediacarian Rodda beds in the eastern Officer Basin (Zang, unpubl. data). The Draken specimen is tentatively considered to be conspecific with *Gorgonisphaeridium pindyium.* Also belonging to this species are two specimens from the Bitter Springs Formation, which bear probably solid processes (Zang and Walter, 1992b, p.114). *Baltisphaeridium maximum* Yin was considered to be a synonym of *Ericiasphaera spjeldnaesii* (Vidal, 1990).

Distribution. Torrensian Alinya Formation (Officer Basin), Gillen Member, Bitter Springs Formation (Amadeus Basin) and Draken Conglomerate Formation (Spitsbergen).

Gorgonisphaeridium torrensium sp. nov.
(Figure 27:F-H)

Etymology. For the age of the Torrensian.

Holotype. Figure 27:H, slide 5341RS311-10, M45/2, from Giles 1 well (1255.8m), Alinya Formation.

Description. Vesicle of small to moderate size, circular to subcircular, originally spheroidal; wall thick (up to 2*u*m), smooth to finely granular and folded; processes sparse (3-10 around the margin), relatively short (2.5-6*u*m), solid, rounded-blunt to short-cylindrical, unbranched, slightly widened at the base, tip closed and rounded; no excystment structure observed. Vesicle diameter 23-45*u*m (holotype 38*u*m) in diameter (6 specimens).

Remarks. Short, solid, rounded to blunt processes distinguish *Gorgonisphaeridium torrensium* from other species of similar morphology. In thin section solid processes seem to be filled by sponge-like material.

Distribution. Torrensian Alinya Formation.

Genus *Lakhandinia* Timofeev and Hermann, 1979

Type species. *Lakhandinia prolata* Timofeev and Hermann, 1979

Lakhandinia dilatata Hermann in Jankauskas, 1989
(Figure 29:A-G)

1989 *Lakhandinia dilatata* Hermann sp. nov., in Jankauskas, p.62, pl.49:5.

Description. Vesicle elongate, originally ellipsoidal, occasionally spheroidal to sausage-shaped; wall thin, commonly folded; surface shagreen to finely granular, large individuals occasionally with fine striae; reproduction probably by binary fission and splitting along the long axis, occasionally bud-like structures observed; colony with linear arrangement or chain-like, connected by long apices, commonly individual in the middle of the colony is largest; no excystment observed. Vesicle average width 40-90*u*m and length 50-180*u*m, whereas smaller individual at the terminals of a chain down to 10*u*m in width (80 specimens).

Remarks. This species is similar to *Leiosphaeridia atava*, particularly those loose ellipsoidal to sphaeroidal individuals, but its binary fission reproduction and distinctive chain-like colony form distinguish the two species. Commonly the colonies of *Leiosphaeridia* are spheroidally grouped or in irregular, loose associations.

Genus *Leiofusa* Eisenack, 1938

Type species. *Leiofusa fusiformis* (Eisenack) Eisenack, 1938 (= *Ovum hispidum fusiformis* Eisenack, 1934).

Leiofusa bicornuta Sin and Liu, 1973
(Figure 26:I)

Description. A single specimen in the thin section of chert from the lower Alinya Formation in the North Pindyin Hills. The vesicle is fusiform, elongate, with thick, finely granular wall. Each apex tapers to a blunt process. The processes in thin section seem solid, which is probably related to diagenetic deformation. The vesicle is 20*u*m long, 12*u*m wide and process 7*u*m long. The species was previously recorded from the Hongshuizhuang Formation (Jixian System, 1000-1400Ma), and Sinian Liulaobei and Zhaowei Formations (Zang and Walter, 1992a).

Genus *Leiosphaeridia* Eisenack, 1958 emend. Downie and Sarjeant, 1963

Type species. *Leiosphaeridia baltica* Eisenack, 1958

Leiosphaeridia atava (Naumova) Jankauskas, 1989

(Figure 28:G-H)

Description. Vesicle circular to subcircular in outline, originally spheroidal; wall robust, granular, flexible, commonly folded; occasionally a circular or medium split opening structure and a central darker bleb of organic matter observed. Colonies spheroidal or occur in irregular loose clusters. Vesicle diameter 20 - 500*um* (up to 700*um*, 100 specimens measured).

Remarks. Granular surface texture serves empirically to identify *Leiosphaeridia atava* from *Leiosphaeridia crassa* (Naumova) Jankauskas, 1989.

Leiosphaeridia crassa (Naumova) Jankauskas, 1989

(Figure 28:C-D)

Description. Vesicle circular to subcircular, originally spheroidal; occasionally with a darker bleb in the centre; wall very flexible, moderately thin, smooth, psilate, shagreen or finely granular, commonly folded; colonies spheroidal clusters or irregular loose groups. Vesicle diameter 20-450*um* (100 specimens measured).

Remarks. *L. crassa* and *L. atava* are most common forms in the Alinya Formation and present in almost every sample studied.

Leiosphaeridia holtedahlii (Timofeev) Jankauskas, 1989

(Figure 28:F)

Description. Vesicles circular or subcircular, originally spheroidal; surface smooth to finely granular; wall occasionally folded; vesicle with several large, circular, oval or irregularly shaped openings with random distribution and covered by a very thin, translucent membrane. Vesicle diameter 25-50*um* and opening diameters are 3-8*um* (5 specimens).

Remarks. Thin surrounding membrane was observed through interference microscopy and is the first recorded in *Leiosphaeridia holtedahlii*.

Leiosphaeridia ternata (Timofeev)

Mikhailova and Jankauskas in Jankauskas, 1989

(Figure 28:K-L)

Description. Vesicle circular or subcircular in outline, originally spheroidal; wall extremely robust, smooth or finely granular, usually folded; commonly margin of the vesicle exhibits several to many splits; vesicles in colony loosely associated. Vesicle diameter 20-50*um* (50 specimens measured).

Remarks. This species is described cautiously in this study because the marginal splitting structures could be deformed artefacts.

Leiosphaeridia visingsa Zang in Zang and Walter, 1992a

(Figure 28:J)

Description. Vesicle circular or subcircular in outline, originally spheroidal; wall thick (1-2*um*), smooth or psilate, velutinous (velvet-like) appearance; slits, folds and openings rarely observed. Vesicle diameter 25 - 60*um* (30 specimens measured).

Remarks. Velutinous surface texture is a characteristic feature of this species.

Genus *Lomentunella* Hermann, 1981

Type species. *Lomentunella vaginata* Hermann, 1981

Lomentunella sp. cf. *L. vaginata* Hermann, 1981

(Figure 30:G-J)

1989 *Lomentunella vaginata* Hermann, Jankauskas, p.131, pl.37:5.

Description. Specimen contained in chain-like colonies, each 'chain' enclosed by thin membrane. Individual vesicle mainly subcircular to elongate, originally ellipsoidal to sausage-shaped, width 3-6*um* and length 4-9*um*; wall thin, smooth and folded; individuals in 'chain' surrounded and connected by a thin membrane, lining up along its long axis, adjacent individuals closely connected or loosely separated, single colony including up to 25 individuals; no branch structure observed in colonies. Colony up to 180*um* long (20 specimens).

Remarks. Individual vesicles of the present specimens are much smaller than the Russian type specimens. Its reproduction was probably by means of binary fission.

Genus *Melanocyrillium* Bloeser, 1985

Type species. *Melanocyrillium hexodiadema* Bloeser, 1985

Melanocyrillium sp.

(Figure 25:E-F)

Description. Vesicle vase-shaped, rounded and closed at bottom and widely open at 'oral' end; wall moderately thick, shagreen to granular and folded; occasionally double-walled structure observed; 'oral' opening slightly constricted. Vesicle 50-80*um* long, 30-40*um* wide and 20-25*um* across the 'oral' opening (3 specimens).

Remarks. A darker, elongate structure is present in one specimen (Figure 25:E). The structure seems to connect with 'oral' margin, like an internal body, alternatively it could be degraded organic matter. In chert thin section (Figure 25:F) vesicle seems spongy.

Genus *Myxococcoides* Schopf, 1968

Type species. *Myxococcoides minor* Schopf, 1968

Myxococcoides sp. cf. *M. cantabrigiensis* Knoll, 1982

(Figure 30:F, K)

1989 *Myxococcoides cantabrigiensis* Knoll, Knoll et al., p.558, Figure 11.

Description. Vesicle circular to subcircular, originally spheroidal to ellipsoidal; vesicles clumped in colonies composed of up to hundreds of individuals and tightly packed in a mat; wall thin, psilate or smooth, folded in large vesicles; opaque inclusions observed in some vesicles; no outer membrane observed in either individuals or colonies. Vesicle diameter 4-20*um* and colony up to 1mm across (200 specimens measured).

Remarks. The species is one of the dominant benthic coccoids in the Alinya assemblages and the present specimens are commonly larger than those from the Draken Conglomerate Formation. Type specimens of this species were collected from the chert thin sections of both lagoonal and open coastal marine environments (Knoll, 1982, 1984; Knoll et al., 1991).

Genus *Octoedryxium* Rudavskaja, 1973

Type species. *Octoedryxium truncatum* Rudavskaja emend. Vidal, 1976

Octoedryxium intrarium (Timofeev) Jankauskas, 1989

(Figure 25:G)

Description. Vesicle square in outline, originally octahedral; wall spongy, porous, moderately thick (1.5*um*); square corners sharp to blunt. The sides of the square vesicle 16-23*um* across (3 specimens measured).

Remarks. The presence of a regular darker square in the centre serve to characterise *Octoedryxium intrarium.*

Genus *Paleasphaeridium* Yin, 1985

Type species. *Paleasphaeridium zonale* Yin, 1985

Paleasphaeridium zonale Yin, 1985

(Figure 31:G-H)

Description. Vesicle circular to subcircular, originally spheroidal; surface shagreen to finely granular, commonly folded, usually as a thickened rim around margin; rim 0.5 - 1.7*um* wide, commonly stable on a single vesicle; vesicle loosely sticking to a sheath or membrane and occasionally adjacent vesicles connected to each other; a darker central bleb present on most vesicles. Vesicle diameter 15 - 26*um* (20 specimens measured).

Remarks. The species is distinguishable by its loosely-associated vesicles connected by a sheath-like membrane.

Genus *Polyhedrosphaeridium* Zang in Zang and Walter, 1992b

Type species. *Polyhedrosphaeridium echinatum* Zang in Zang and Walter 1992b

Polyhedrosphaeridium sp.

(Figure 26:H)

Description. Vesicle large, polyhedral or subcircular in outline, originally probably a many-sided microorganism; wall thick, granular and folded; 5-7 protuberances and short processes on margin, protuberance rounded to irregular, each short process widens at base and truncated at tip, 3-5*um* long; no excystment structure observed. Vesicle diameter 215*um* and 275*um* (2 specimens).

Genus *Rectia* Jankauskas, 1989

Type species. *Rectia costata* (Jankauskas) Jankauskas, 1989

Rectia costata (Jankauskas) Jankauskas, 1989

(Figure 32:J)

Description. Thallus, septate, unbranched, originally annulated tubes; annuli flexible, 1-2.5*um* thick, connected by a translucent membrane; tube slightly tapering towards apex; no proboscis-like structure observed. Thallus 100-150*um* wide (2 fragments).

Genus *Satka* Jankauskas, 1979

Type species. *Satka favosa* Jankauskas, 1979

Satka compacta Zang in Zang and Walter, 1992b

(Figure 27:J)

1992b *Satka compacta* sp. nov., Zang in Zang and Walter, p.93, Fig.69:F-H.

Description. Vesicle compound, consisting of many tightly packed individuals (40-65) to form a spheroidal to subspheroidal group; vesicle of moderate size, wall finely-granular or spongy, no external membrane visible, occasionally splitting around margin; individuals in a single compound structure with consistent size. Vesicle diameter 40-100*um* and individuals 10-18*um* in diameter (5 specimens measured).

Genus *Simia* Mikhailova and Jankauskas, 1989

Type species. *Simia simica* (Jankauskas) Jankauskas, 1989;

Simia annulare (Timofeev) Mikhailova in Jankauskas, 1989

(Figure 28:E)

Description. Vesicle circular with an outer translucent rim, originally, probably, a spheroid (?pterate form) surrounded by an outer membrane or lighter organic matter; vesicle often folded; outer rim thin, shagreen to finely granular and folded; no openings observed. Vesicle diameter 25-75*um* and outer rim 8-17*um* wide (10 specimens).

Genus *Sinianella* Yin emend. Zang in Zang and Walter, 1992a

Type species. *Sinianella uniplicata* Yin emend. Zang in Zang and Walter 1992a

Sinianella uniplicata Yin emend. Zang in Zang and Walter, 1992a

(Figure 27:I)

1992a *Sinianella uniplicata* Yin emend. Zang, Zang and Walter, p.310, pl.8:A-I.

Description. Vesicle subcircular to elongate, originally bottle-shaped; wall moderately thick, surface shagreen to finely granular, often folded; one prominent process drawn out from an apex and the other apex commonly rounded; process tube-like, 4-8*um* long, 4-6*um* wide, truncated at tip and commonly open. Vesicle diameter 35-75*um* at long axis (10 specimens measured).

Genus *Sphaerocongregus* Moorman, 1974

Type species. *Sphaerocongregus variabilis* Moorman, 1974

Sphaerocongregus variabilis Moorman, 1974

(Figure 29:L-M)

Description. Vesicle compound, consisting of many (up to 70 individuals counted) tightly packed individuals; vesicle circular to subcircular, originally spheroidal or subspheroidal; individuals spheroidal, 5-14*um* across; occasionally a broken, thin, external membrane observed. Compound 20 - 90*um* across (20 specimens).

Genus *Sphaerophycus* Schopf, 1968

Type species. *Sphaerophycus parvum* Schopf, 1968

Sphaerophycus sp.

(Figure 30:L-M)

Description. Mat-building coccoid colony, consisting of numerous individuals; individual vesicle circular to irregular, originally spheroidal, wall thin, smooth to finely granular, often solitary, commonly single-celled, occasionally binary forms observed, arranged in loose cluster; individuals in cluster smaller towards center and larger on the margin (up to 34*um* in diameter); no outer membrane and excystment structure observed. Vesicle diameter average 6-25*um* and cluster up to 500*um* across.

Remarks. The unnamed species is one the main mat-building coccoids in the Alinya assemblages. It is distinguished by its loose cluster of numerous individuals and variable size range from the center to the margin in a single cluster.

Genus *Synsphaeridium* Eisenack, 1965

Type species. *Synsphaeridium gotlandicum* Eisenack, 1965

Synsphaeridium sp.

(Figure 31:E-F)

Description. Specimen consisting of many individuals to form an unstructured cluster or an irregular chain. Individual vesicle circular to subcircular, originally spheroidal; wall moderately thick, smooth to granular, often folded; vesicles in cluster loosely connected to each other; no external membrane or excystment structure observed. Vesicle 15-35*um* in diameter and cluster up to 300*um* across (50 specimens).

Remarks. This species intergrades with species of some other genera, such as *Leiosphaeridia* and *Stictosphaeridium*. *Synsphaeridium* sp. in this study includes those clusters not convincingly assigned to other genera.

Genus *Trachyhystrichosphaera* Timofeev and Hermann, 1976
emend. Hermann and Jankauskas in Jankauskas, 1989

Type species. *Trachyhystrichosphaera aimica* Hermann, 1976

Trachyhystrichosphaera sp. cf. *T. aimica* Hermann, 1976

(Figure 26:A-G)

1989 *Trachyhystrichosphaera aimica* Hermann, Jankauskas, p.46, pl.1:6,8.

Description. Vesicle moderate to large, circular to irregularly elongate, originally spheroidal; wall moderately thick, finely granular, commonly folded; processes conical, sparse to moderate (1-18 around the vesicle margin), moderately long (commonly 4-11*um* long, up to 70*um*), unbranched, slightly widened at base, tapering continuously towards a sharp tip; process hollow, freely communicating with the vesicle cavity; no excystment structure observed. Vesicle diameter commonly 50-215*um* (up to 480*um*) (15 specimens measured).

Remarks. Most specimens in the Alinya assemblages were damaged in situ or by laboratory processing, particularly those large vesicles often with broken processes on the vesicle margin. The type specimen of *T. aimica* seems to have cylindrical, hollow processes with blunt to truncated tip. The processes in the Alinya specimens often have a sharp tip.

Trachyhystrichosphaera stricta Hermann in Jankauskas, 1989
(Figure 25:H-J)

1988 Unnamed specimen, Butterfield, Knoll and Swett, Fig.3:g.
1989 *Trachyhystrichosphaera stricta* Hermann sp. nov., Jankauskas, p.47, pl.2:4, 7 (?Fig.2:8).
1989 *Trachyhystrichosphaera vidalii* Knoll, Jankauskas, p.48, pl.2:1.

Description. Vesicle moderate to very large, circular to subcircular, originally spheroidal; wall moderately thick, robust, finely granular and often folded; encystment structure containing a spinose darker circular or spheridal body; process on encyst spherid from short to very long (6-170*um*, average 10-40*um*), free or connecting the outer wall, probably related to the size of external envelope; process cylindrical to conical, sharp to slightly blunt tip, probably hollow and freely communicating with the encystment cavity, 5-10 spines counted around the margin of the encystment body. Vesicle diameter commonly 50-120*um* (4 specimens measured, with another specimen, Figure 25:H, reaching 800*um* in diameter).

Remarks. A robust, unornamented outer wall enclosing a spinose encystment structure serves to distinguish *T. stricta* from the other species in the genus. It is possible that the living *T. stricta* probably had a sac-like excyst envelope and an enclosed freely moving spinose encyst. In *T. vidalii* the processes are always supporting and connected to the outer membrane. The specimen (in Jankauskas, 1989, pl.2:1) seems to have an outer wall and free processes and here is regarded as a lectotype or paratype specimen of *T. stricta,* because of the preservation and photograph quality of the type specimen (Jankauskas, 1989, pl.2:4).

The assignment of the species is of temporary expedience because of poor preservation of the holotype which is similar to those of *T. vidalii.*

Trachyhystrichosphaera vidalii Knoll, 1984
(Figure 23:A-E)

1984 *Trachyhystrichosphaera vidalii* sp. nov., Knoll, p.154, fig.8:A-F, H-J.

Description. Vesicle circular to subcircular, originally spheroidal; wall moderately thick, often folded; processes sparse to moderately abundant (11-20 around margin), cylindrical to conical, relatively short (3-18*um* long), widened at base and blunt or slightly flared at tip; process hollow, freely communicating with the vesicle cavity; process supporting an outer, thin translucent membrane, membrane has porous appearance. Vesicle diameter 35-250*um* and membrane rim 4-18*um* wide (18 specimens).

Remarks. The type specimen of *T. vidalii* was described from a thin section of chert from the Hunnberg Formation and is commonly large (Knoll, 1984). In the Alinya Formation, 13 of the 18 specimens counted are less than 100*um* in diameter whereas the large specimens are damaged.

Genus *Valeria* Jankauskas, 1982

Type species. *Valeria lophostriata* (Jankauskas) Jankauskas, 1982

Valeria lophostriata (Jankauskas) Jankauskas, 1982
(Figure 28:I)

Description. Vesicle circular to irregular, originally spheroidal; wall moderately thick, finely granular and often folded; surface ornamented with very fine, uni- or bi-directional striae; no excystment structure observed. Vesicle 150-250*um* (6 specimens).

Remarks. Striae were generally observed by interference microscopy, otherwise *V. lophostriata* is similar to *Leiosphaeridia crassa.*

Genus *Vandalosphaeridium* Vidal, 1981

Type species. *Vandalosphaeridium reticulatum* (Vidal) Vidal, 1981 (=*Peteinosphaeridium reticulatum* Vidal, 1976)

Vandalosphaeridium sp. cf. *V. reticulatum* (Vidal) Vidal, 1981

(Figure 23:F-H)

1976 *Pteinosphaeridium reticulatum* sp. nov., Vidal, p.27, fig.14.

Description. Vesicle circular to subcircular, originally spheroidal; wall moderately thick and sometimes folded; processes moderately long (4-10*um*), conical slim, solid, commonly sharp-pointed, relatively sparse (8-15) around the margin, unbranched and supporting an outer, finely granular, translucent membrane; membrane connected with neighbouring processes to form a shallow curve on the margin and forming a network in plane view. Vesicle diameter 30-72*um* (15 specimens measured).

Remarks. Alinya specimens have relatively long, sharp-pointed processes in comparison to the type specimens.

Skiagia pusilla Zang in Zang and Walter, 1992b was described from the Gillen Member (Bitter Springs Formation); it probably bears solid processes flaring at tip, and should be transferred to *Vandalosphaeridium pusillum*.

Unnamed Acritarchs

Unnamed specimen A

(Figure 27:K)

Remarks. A single specimen from the upper Alinya Formation. Vesicle is broken, originally spheroidal. A distinctive spheroidal bud-like structure is drawn out from the vesicle and connected to it by a long, narrow 'neck'. Vesicle is 52*um* in diameter, bud-like spheroid 12*um* in diameter and 'neck' 5*um* long and 2*um* wide.

Unnamed specimens B

(Figure 31:J-L)

Remarks. Several spheroids (55-65*um* in diameter) from the upper Alinya Formation with irregular, low-ridged surface network and surrounded by thin membrane.

Filamentous Microfossils

Genus *Cephalophytarion* Schopf, 1968

Type species. *Cephalophytarion grande* Schopf emend. Schopf and Blacic, 1971

Cephalophytarion sp.

(Figure 32:D-E)

Description. Thallus relatively thick, uniseriate, unbranched, septate, tapering gradually towards a blunt apex; septate joint slightly constrained; no external membrane observed. Septa average 12*um* wide and 5*um* long, broken trichome up to 150*um* long (5 specimens).

Genus *Clavitrichoides* Mikhailova in Jankauskas, 1989

Type species. *Clavitrichoides rugosus* Mikhailova, 1989

Clavitrichoides rugosus Mikhailova, 1989

(Figure 32:I)

Description. Thallus moderately thick, tubular, cylindrical, probably septate, unbranched and with rounded apices; wall smooth to finely granular, very thick, septa sometimes visible, but very obscure; thallus with one apex broad and the other constrained. Thallus averages 6-9*um* width and is up to 140*um* long (5 specimens).

Genus *Heliconema* Schopf, 1968

Type species. *Heliconema australiensis* Schopf, 1968

Heliconema fidicularis Zang in Zang and Walter, 1992b

(Figure 32:H)

Description. Thallus thin, tubular, nonseptate, unbranched, irregularly coiled like a cord; wall moderately thick, finely granular; thallus commonly sinuous, sometimes with an angular bend; no apical or reproductive structure observed. Thallus 2-5*u*m wide, up to 200*u*m long (7 specimens).

Genus *Oscillatoriopsis* Schopf, 1968

Type species. *Oscillatoriopsis obtusa* Schopf, 1968

Oscillatoriopsis spp.

(Figure 32:K)

Description. Thallus moderately thick, septate, tubular, unbranched; thallus with a consistent width on a single filament, not constricted at the septate joint and apical structures not observed. Thallus 5-12*u*m with, up to 200*u*m long (30 specimens).

Genus *Quaestiosignum* Zang in Zang and Walter, 1992b

Type species. *Quaestiosignum filum* Zang in Zang and Walter, 1992b

Quaestiosignum filum Zang in Zang and Walter, 1992b

(Figure 32:A-C)

Description. Thallus compound; individual very thin, unseptate, unbranched, scores of individuals combined by sheath-like membrane to form a thick ribbon; ribbon straight, curved, circular, sickle-shaped to irregular. Ribbon 3-15*u*m wide, up to 800*u*m long; individual 0.5-1.5*u*m wide (20 specimens).

Genus *Siphonophycus* Schopf, 1968 emend. Knoll et al., 1991

Type species. *Siphonophycus kestron* Schopf, 1968

Siphonophycus sp. cf. *S. kestron* Schopf, 1968

(Figure 32:F-G)

Description. Thallus broad, tubular, nonseptate, unbranched, straight to irregularly curved; solitary, occasionally several individuals interwoven; wall thick, finely granular, and folded; width commonly consistent at a single thallus; neither apical nor reproductive structures observed. Thallus 13-24*u*m wide, up to 200*u*m long (30 specimens).

Siphonophycus robustum (Schopf) Knoll et al., 1991

(Figure L-M)

1991 *Siphonophycus robustum* comb. nov., Knoll et al., p.565, fig.10:3, 10:5.

Description. Thallus tubular, unbranched, nonseptate, solitary to scores of individuals interwoven to form mat; wall smooth to finely granular; width consistent for a single thallus; no apical or reproductive structures observed. The filaments are 2-8*u*m wide and up to several hundred microns long (80 specimens).

ACKNOWLEDGMENTS

This study was funded by the South Australian Exploration Initiative and undertaken in the Biostratigraphy Branch, Mineral Exploration Division, Department of Mines and Energy, South Australia. N. Alley and D. I. Gravestock critically and constructively read this report and contributed many valuable suggestions. R. B. Major kindly allowed use of his field notes and photos. Ms. Lyn Broadbridge, Tina Nezic and Paula Benz assisted with the laboratory work and photography. B. van der Stelt helped to print out aeromagnetic image. B. Logan and his colleagues helped with sampling in the Core Library. The figures were drafted by A. Francis, M. Ross and E. R. Calabio. R. Gates and D. Grigg helped to prepare the bromide copies. S. Daly and G. Krieg contributed valuable discussions. D. I. Gravestock and L. P. Hough helped to re-process the seismic line IP1-2A. W. V. Preiss and C. Gatehouse constructively reviewed the manuscript. I extend my sincere appreciation to all these individuals.

REFERENCES

Amoco, 1987. Technical evaluation of PEL 29, East Officer Basin, Australia. *South Australia. Department of Mines and Energy. Open file Envelope*, 6843 and 6766.

Barghoon, E. S. and Schopf, J. W., 1965. Microorganisms from the Late Precambrian of central Australia. *Science*, 150, 337-339.

Black, L. P., Shaw, R. D. and Offe, L. A., 1980. The age of the Stuart Dyke Swarm and its bearing on the onset of late Precambrian sedimentation in central Australia. *Journal of the Geological Society of Australia*, 27, 151-155.

Brewer, A. M., Dunster, J. N., Gatehouse, C. G., Henry, R. L. and Westes, G., 1987. A revision of the stratigraphy of the eastern Officer basin. *South Australia. Geological Survey. Quarterly Notes*, 102, 15p.

Burne, R. V. and Hunt, G. (compilers), 1990. The geobiology of Hamelin Pool - Research reports of the Baas Becking Geobiological Laboratory's Shark Bay Project. *Australia. Bureau of Mineral Resources, Geology and Geophysics. Record* 1990/89.

Butterfield, N. J., Knoll, A. H. and Swett, K., 1988. Exceptional preservation of fossils in an Upper Proterozoic shale. *Nature*, 334, 424-427.

Coats, R. P. and Preiss, W. V., 1987a. Chapter 5. Stratigraphy of the Callanna Group. *In*: Preiss, W. V. (compiler). The Adelaide Geosyncline - late Proterozoic stratigraphy, sedimentation, palaeontology and tectonics. *South Australia. Geological Survey. Bulletin* 53, 43-71.

Coats, R. P. and Preiss, W. V., 1987b. Chapter 7. Stratigraphy of the Umberatana Group. *In*: Preiss, W. V. (compiler). The Adelaide Geosyncline - late Proterozoic stratigraphy, sedimentation, palaeontology and tectonics. *South Australia. Geological Survey. Bulletin* 53, 125-209.

Drexel, J. F., Preiss, W. V. and Parker, A. J. (Editors)., 1993. The geology of South Australia. Vol. 1, The Precambrian. *South Australia. Geological Survey. Bulletin* 54, 242p.

Downie, C., 1984. Acritarchs in British stratigraphy. *Geological Society, London, Special Report*, 17, 26pp.

Edgell, H. S., 1991. Proterozoic salt basins of the Persian Gulf area and their role in hydrocarbon generation. *In*: Walter, M. R. (editor), Proterozoic petroleum. *Precambrian Research*, 54, 1-14.

Evitt, W. R., 1963. A discussion and proposals concerning fossil dinoflagellates, hystrichospheres, and acritarchs, I. *National Academy of Sciences, Proceedings*, 49, 158-164.

Flint, R. B., 1993. Mesoproterozoic. *In*: Drexel, J. F., Preiss, W. V. and Parker, A. J. (Editors). The geology of South Australia. Vol. 1, The Precambrian. *South Australia. Geological Survey. Bulletin* 54, 107-169.

Forbes, B. G. and Preiss, W. V., 1987. Chapter 6. Stratigraphy of the Burra Group. *In*: Preiss, W. V. (compiler). The Adelaide Geosyncline - late Proterozoic stratigraphy, sedimentation, palaeontology and tectonics. *South Australia. Geological Survey. Bulletin* 53, 73-123.

Golubic, S. and Hofmann, H. J., 1976. Comparison of Holocene and Mid-Precambrian Entophysalidaceae (Cyanophyta) in stromatolitic algal mats: cell division and degradation. *Journal of Paleontology*, 50, 1074-1082.

Goode, A. D. T., 1970. The petrology and structure of the Kalka and Ewarara layered basic intrusions, Giles Complex, central Australia. University of Adelaide. Ph.D. thesis (unpublished).

Hibburt, J. (compiler), 1993. Petroleum exploration and development in South Australia. *South Australia. Department of Mines and Energy. Report Book*, 93/9, 9th edition.

Horodyski, R. J., 1993. Paleontology of Proterozoic shales and mudstones: examples from the Belt Supergroup, Chuar Group and Pahrump Group, western USA. *In*: B. Nagy, J. S. Leventhal and R. F. Grauch (Editors), Metalliferous black shales and related ore deposits. *Precambrian Research*, 61, 241-278.

Horodyski, R. J. and Donaldson, J. A., 1980. Microfossils from the Middle Proterozoic Dismal Lakes Group, Arctic Canada. *Precambrian Research*, 11, 125-159.

Ivic, D., 1986. Summary of geological interpretations of the Everard Thrust, northeast Officer Basin, South Australia. *South Australia. Department of Mines and Energy. Report Books*, 86/78.

Jackson, M. J. and van de Graaff, W. J. E., 1981. Geology of the Officer Basin. *Australia. Bureau of Mineral Resources, Geology and Geophysics, Bulletin*, 206.

Jankauskas, T. V. (editor), 1989. Mikrofossilii Dokemkriya SSSR (Precambrian microfossils of the USSR). Trudy Institut Geologii ee Geokhronologii SSSR Akademii Nauk, Leningrad, 191p.

Jenkins, R. J. F., McKirdy, D. M., Foster, C. B., O'Leary, T. and Pell, S. D., 1992. The record and stratigraphic implications of organic-walled microfossils from the Ediacaran (terminal Proterozoic) of South Australia. *Geological Magazine*. 129, 401-410.

Jenkins, R. J. F., Lindsay, J. F. and Walter, M. R., 1993. Field Guide the the Adelaide Geosyncline and Amadeus Basin, Australia. *Australian Geological Survey Organisation. Record* No. 1993/35, 133p.

Kirkland, D. W. and Evans, R., 1981. Source rock potential of evaporitic environments. *American Association of Petroleum Geology, Bulletin* 65, 181-190.

Knoll, A. H., 1982. Microfossils from the late Precambrian Draken Conglomerate, Ny Friesland, Svalbard. *Journal of Paleontology*, 56, 755-790.

Knoll, A. H., 1984. Microbiotas of the late Precambrian Hunnberg Formation, Nordaustlandet, Svalbard. *Journal of Paleontology*, 58, 131-162.

Knoll, A. H. and Golubic, S., 1979. Anatomy and taphonomy of a Precambrian algal stromatolite. *Precambrian Research*, 10, 115-151.

Knoll, A. H., Swett, K. and Mark, J., 1991. Paleobiology of a Neoproterozoic tidal flat/lagoon complex: the Draken Conglomerate Formation, Spitsbergen. *Journal of Paleontology*, 65, 531-570.

Knoll, A. H. and Walter, M. R., 1992. Latest Proterozoic stratigraphy and earth history. *Nature*, 356, 673-678.

Korsch, R. J., 1993. Structural and tectonic framework of the Amadeus Basin, with some deep seismic examples. *In*: Alexander, E. M. and Gravestock, D. I. (eds.), Central Australian basins workshop, Alice Springs, September 13-14, 1993, Programme and Abstracts. 22-28.

Lambeck, K., 1984. Structure and evolution of the Amadeus, Officer and Ngalia Basins of central Australia. *Australian Journal of Earth Sciences*, 31, 25-48.

Lindsay, J. F., 1991. New evidence for ancient metazoan life in the Late Proterozoic Heavitree Quartzite, Amadeus Basin, central Australia. *In*: Korsch, R. J. and Kennard, J. M. (editors), Geological and geophysical studies in the Amadeus Basin, central Australia. *Australia. Bureau of Mineral Resources, Geology and Geophysics, Bulletin* 236, 91-96.

Lindsay, J. F. and Korsch, R. J., 1991. The evolution of the Amadeus Basin, central Australia. *In*:Korsch, R. J. and Kennard, J. M. (eds.), Geological and geophysical studies in the Amadeus Basin, central Australia. *Australian Bureau of Mineral Resources , Geology and Geophysics, Bulletin* 236, 7-32.

Lindsay, J. F., Leven, J. and Krieg, G., 1992. Central Officer Basin, South Australia - Seismic data acquisition 1993. *Canberra. Australian Geological Survey Organisation. Record* 1992/91.

Logan, B. W., Hofmann, P. and Gebelein, C. D., 1974. Algal mats, cryptalgal fabrics and structures, Hamelin Pool, Western Australia. *American Association of Petroleum Geology, Memoir*, 13, 38-84.

Major, R.B., 1973a. The Pindyin beds. *South Australia. Geological Survey. Quarterly Geological Notes*, 46: 1-5.

Major, R.B., 1973b. The Wright Hill beds. *South Australia. Geological Survey. Quarterly Geological Notes*, 46: 6-10.

Major, R.B., 1974. The Punkerri beds. *South Australia. Geological Survey. Quarterly Geological Notes*, 51: 2-5.

Major, R. B., Johnson, J. E. and Teluk, J. A., 1971. BIRKSGATE map sheet, Geological Atlas of South Australia, 1:250 000 series. *Geological Survey of South Australia.*

Major, R. B. and Teluk, J. A., 1973. LINDSAY map sheet, Geological Atlas of South Australia, 1:250 000 series. *Geological Survey of South Australia.*

Meyerhoff, A. A., 1980. Geology and petroleum fields in Proterozoic and Lower Cambrian strata, Lena-Tunguska petroleum province, Eastern Siberia, USSR. *American Association of Petroleum Geology, Memoir* 30, 225-252.

Moczydlowska, M., 1991. Acritarch stratigraphy of the Lower Cambrian and the Precambrian - Cambrian boundary in southeastern Poland. *Fossil and Strata*, 29. 1-127.

Myers, J. S., 1990. Precambrian tectonic evolution of part of Gondwana, southwestern Australia. *Geology*, 18, 537-540.

Plumb, K. A., 1979. The tectonic evolution of Australia. *Earth Science Review*, 14. 205-249.

Preiss, W. V. (compiler), 1987. The Adelaide Geosyncline. *South Australia. Geological Survey. Bulletin*, 53, 438p.

Preiss, W. V., 1993. Neoproterozoic. *In*: Drexel, J. F., Preiss, W. V. and Parker, A. J. (Editors). The geology of South Australia. Vol. 1, The Precambrian. *South Australia. Geological Survey. Bulletin* 54, 171-202.

Roberts, A. M., Yielding, G. and Badley, M. E., 1993. Tectonic and bathymetric controls on stratigraphic sequences within evolving half-graben. *In*: Williams, G. D. and Dobb, A. (eds.), Tectonics and sequence stratigraphy. *Geological Society Special Publication* 71, 87-121.

Rutland, R. W. R., 1981. Structural framework of the Australian Precambrian. *In*: Hunter D. R. (ed.), Precambrian of the Southern Hemisphere. *Developments in Precambrian Geology*, 2, 1-32.

Schopf, J. W., 1968. Microflora of the Bitter Springs Formation, late Precambrian, central Australia. *Journal of Paleontology*, 42, 651-688.

Schopf, J. W. and Blacic, J. M., 1971. New microorganisms from the Bitter Springs Formation (late Precambrian) of the north-central Amadeus basin, Australia. *Journal of Paleontology*, 46, 925-959.

Schopf, J. W. and Klein, C. (editors), 1992. Evolution of the Proterozoic biosphere - a multidisplinary study. Cambridge University Press, New York, 1348p.

Sin (Xing) Yu-sheng and Liu, K., 1973. On Sinian microflora in the Yenliao region of China and its geological significance. *Acta Geologica Sinica*, 1, 1-52 (in Chinese).

Southgate, P. N., 1991. A sedimentary model for the Loves Creek Member of the Bitter Springs Formation, northern Amadeus Basin. *In*:Korsch, R. J. and Kennard, J. M. (eds.), Geological and geophysical studies in the Amadeus Basin, central Australia. *Australian Bureau of Mineral Resources, Geology and Geophysics, Bulletin* 236, 113-126.

Stainton, P.W., Weste, G. and Cucuzza, G., 1988. Exploration of PEL 23 and PEL 30, eastern Officer Basin, SA, 1983-1988. *South Australia. Department of Mines and Energy. Open file Envelope*, 5073: 1243-1321.

Sukanta, U., 1993. Sedimentology, sequence stratigraphy and palaeogeography of Marinoan sediments in the eastern Officer Basin, South Australia. Ph.D thesis, The Flinders University of South Australia (unpulished).

Sukanta, U., Thomas, B., von der Borch, C. C., Gatehouse, C. G., 1991. Sequence stratigraphic studies and canyon formation, South Australia. *Petroleum Exploration of South Australia, Journal*, 19, 68-73.

Surkov, V. S., Grishin, M. P., Larichev, A. I., Lotyshev, V. I., Melnikov, N. V., Kontorovich, A. Eh., Trofimuk, A. A. and Zolotov, A. N., 1991. The Riphean sedimentary basins of the Eastern Siberia Province and their petroleum potential. *In*: Walter, M. R. (editor), Proterozoic petroleum. *Precambrian Research*, 54, 37-44.

Thomas, B., 1990. Summary of seismic interpretation in the eastern Officer Basin. *South Australia. Department of Mines and Energy. Report Book*, 90/58.

Thomson, B. P., 1970. A review of the Precambrian and Lower Palaeozoic tectonics of South Australia. *Transactions of Royal Society, South Australia*, 94, 193-221.

Timofeev, B. V., Hermann, T. N. and Mikhailova, N. S., 1976. Mikrofitofossilii dokembriya, kembriya, i ordovika (Microfossils from the Precambrian, Cambrian and Ordovician) Trudy Institut Geologii i Geokhronologii Dokembri, Leningrad, 106p.

Townson, W.G., 1985. The subsurface geology of the western Officer Basin - results of Shell's 1980-1984 petroleum exploration campaign. *Australian Petroleum Exploration Journal*, 25: 34-51.

Turner, P., 1980. Continental red beds. *Developments in Sedimentology*, 29, 562p.

van Niel, J. 1984. Palynology of Upper Proterozoic and Cambrian samples from 11 wells in South Australia, for Shell Development (Australia) Pty Ltd. (Birksgate-1, Byilkaoora-1, Emu-1, Marla-1B, Munyarai-1, Murnaroo-1, Wallira West-1, Wilkinson-1). *South Australia. Department of Mines and Energy. Open file Envelope*, 6846: 3-17.

Vidal, G., 1976. Late Precambrian microfossils from the Visingsö Beds in southern Sweden. *Fossils and Strata*, 9, 57p.

Vidal, G., 1990. Giant acanthomorph acritarchs from the upper Proterozoic in southern Norway. *Palaeontology*, 33, 287-298.

Vidal, G. and Ford, T. D., 1985. Microbiotas from the Late Proterozoic Chuar Group (northern Arizona) and Uinta Mountain Group (Utah) and their chronostratigraphic implications. *Precambrian Research*, 28, 349-389.

Vidal, G. and Knoll, A. H., 1983. Proterozoic plankton. *Geological Society of America, Memoir*, 161, 265-277.

Vidal, G. and Moczydlowska, M., 1992. Patterns of phytoplankton radiation across the Precambrian-Cambrian boundary. *Journal of the Geological Society*, London. 149, 647-654.

Vidal, G. and Siedlecka, A., 1983. Planktonic, acid-resistant microfossils from the Upper Proterozoic strata of the Barents Sea region of Varanger Peninsula, East Finnmark, northern Norway. *Norges Geologiske Undersokelse, Bulletin*, 382, 45-79.

Volkova, N. A., Kirjanov, L. V., Piscun, L. V., Paskeviciene, L. T. and Jankauskas, T. V., 1979. Plant microfossils. *In*: Upper Precambrian and Cambrian palaeontology of the East European Platform - Contribution of the Soviet - Polish working group on the Precambrian - Cambrian boundary problem. Academy of Sciences, USSR, Geological Institute. Nauka. (English Translation - Urbanek, A. and Rozanov, A. Yu. (editors), 1983. Wydawnictwa Geologiczne, Warszawa, 7-46.0

Wallace, M. W., Gostin, V. A. and Keays, R. R., 1989. Discovery of the Acraman impact ejecta blanket in the Officer Basin and its stratigraphic significance. *Australian Journal of Earth Sciences*, 36, 585-587.

Warren, J. K., 1989. Evaporite sedimentology: its importance in hydrocarbon accumulations. Prentice Hall, Englewood Cliffs, New Jersey, 285p.

Webb, A. W., 1985. Geochronology of the Musgrave Block. *South Australia. Mineral Resources Reviews*, 155, 23-37.

Weste, G., 1990. EP20 Wallara No.1 well completion report. (unpublished report for Indigo Oil Pty. Ltd.). *Northern Territory. Geological Survey*, Alice Springs, *Open File.*

Williams, G. E., 1991. Upper Proterozoic tidal rhythmites, South Australia: sedimentary features, deposition, and implications for the earth's paleorotation. *In*: Smith, D. G., Reinson, G. E., Zaitlin, B. A. and Rahmani, R. A. (eds.), Clastic tidal sedimentology. *Canadian Society of Petroleum Geologists, Memoir* 16, 161-178.

Yin Lei-ming, 1987. Microbiotas of the latest Precambrian sequences in China. *In*: Stratigraphy and palaeontology of systemic boundaries in China, Precambrian - Cambrian boundary, 1, Nanjing, China, 415-494.

Zang, Wen-long, 1992. Sinian and Early Cambrian floras and biostratigraphy on the South China Platform. *Palaeontographica B*, 224, 75-119.

Zang, Wen-long and McKirdy, D., 1993. Microfossils and molecular fossils from the Neoproterozoic Alinya Formation - a possible new source rock in the eastern Officer Basin. *In*: Alexander, E. M. and Gravestock, D. I. (eds.), Central Australian basins workshop, Alice Springs, September 13-14, 1993, Programme and Abstracts. 62-63.

Zang, Wen-long, 1994. Torrensian Pindyin Sandstone and Alinya Formation in the eastern Officer Basin, South Australia. *South Australia. Geological Survey. Quarterly Geological Notes* (in press).

Zang, Wen-long and Walter M.R., 1992a. Late Proterozoic and Cambrian microfossils and biostratigraphy, Amadeus Basin, central Australia. *Memoir of the Association of Australasian Palaeontologists*, 12, 1-134.

Zang, Wen-long and Walter M.R., 1992b. Late Proterozoic and Early Cambrian microfossils and biostratigraphy, northern Anhui and Jiangsu, central eastern China. *Precambrian Research*, 57, 243-323.

Zhang Yi-gang, 1981. Cool shallow origin of petroleum - microbial genesis and subsequent degradation. *Journal of Petroleum Geology*, 3, 427-444.

Zhang Zhongying, 1984. A new microphytoplankton species from the Sinian of the western Hubei Province. *Acta Botanica Sinica*, 26, 94-98.

Zhao, J. X. and McCulloch, M. T., 1993. Sm-Nd mineral isochron ages of Late Proterozoic dyke swarms in Australia: evidence for two distinctive events of mafic magmatism and crustal extension. *Chemical Geology*, 108 (in press).

Zhao, J. X., McCulloch, M. T. and Bennett, V. C., 1992a. Sm-Nd and U-Pb zircon isotopic constraints on the provenance of sediments from the Amadeus Basin, central Australia: evidence for REE fractionation. *Geochimica et Cosmochimica Acta*, 56, 921-940.

Zhao, J. X., McCulloch, M. T., Warren, R. G., Rudnick, R., Camacho, A. and Ellis, D. J., 1992b. Geochemical and isotopic studies of Proterozoic mafic dyke swarm in central Australia. *The Australian National University, Research School of Earth Sciences, Annual Report* 1991, 103-105.

FIGURE CAPTIONS

Figure 1. Index maps of the study area. A. Location of the Officer Basin and surrounding region, showing major structural elements of central Australian basins. B. Central and eastern Officer Basin in South Australia, showing well localities and major tectonic elements (modified from Hibburt, 1993). C. Outcrops of the early Neoproterozoic sediments in the central basin (modified from Major, 1973a).

Figure 2. Tectonic framework of southern Australia, showing that the eastern Officer Basin was strongly shaped by the Fraser-Musgrave and Paterson fold belts (combined from Thomson, 1970; Myers, 1990; Preiss, 1987; Drexel et al., 1993).

Figure 3. Interpretation of the Munyarai Trough, showing early Neoproterozoic Torrensian extensional faults superimposed and modified by later reverse faults during the Petermann Ranges Orogeny (discuss with Dr. S. N. Apak, 1993).

Figure 4. Interpretation of the Ungoolya Hinge structure (discuss with Dr. S. N. Apak, 1994).

Figure 5. Stratigraphic column of the eastern Officer Basin (revised from Hibburt, 1993).

Figure 6. Stratigraphy of the type section of the Pindyin Sandstone and Alinya Formation in the North Pindyin Hills (after Zang and Major, 1994).

Figure 7. Sedimentary structures in the Pindyin Sandstone and Alinya Formation (photographs by R. Major). A. Landscape of the Pindyin Sandstone at Belundinna Hill. B. Thin-bedded shale of the Alinya Formation in the North Pindyin Hills. C. Unconformity between basal conglomerate of the Pindyin Sandstone and weathered granite of the Musgrave Block at Belundinna Hill. D-E. Herringbone cross-bedded Pindyin Sandstone, D - Belundinna Hill, C - the South Pindyin Hills. F. Tidal-influenced ripple marks in the upper part of the Pindyin Sandstone in the North Pindyin Hills. G. Asymmetrical ripple marks and mudcracks from the upper part of the Pindyin Sandstone at Belundinna Hill.

Figure 8. Detailed lithological description of the Pindyin Sandstone and Alinya Formation in comparison with wireline logs for Giles 1. Arrows indicate the samples for maceration. "*" indicates thin-section studied.

Figure 9. Close-up of the seismic line (101A) across Munyarai 1, showing sequence stratigraphy from seismic interpretation (combined and revised from Ivic, 1986; Amoco, 1987; Thomas, 1990). LST - lowstand systems tract, TST - transgressive systems tract, and HST - highstand systems tract. A - Palaeozoic, B - Neoproterozoic, E - reflector of basal Palaeozoic sediments, F - basal canyon, F_5 - top of the Murnaroo Formation, G - top of the evaporite (?salt) in the Alinya Formation, G_2 - ?top of the Pindyin Sandstone, and H - basal Pindyin Sandstone. Interpretation of the systems tracts in SQ2 and 4 is based on the core observation in Giles 1, Karlaya 1, Munta 1 and Meramangye 1.

Figure 10. Core and thin section photograph of the Pindyin Sandstone in Giles 1. A. Part of core at depth 1324.5-1326.9m (aeolian sandstone with evaporite pseudomorphs). Scale bar is 1cm for each black and white grid. B. Aeolian quartz grains evenly coated by hematite/turgite. Frosted grain surface texture is probably due to capillary activity. Qz - quartz grain, Po - intergranular pore, and Hm - hematite rim. Scale as indicated. Thin section 5341RS235, 1291.36m, plane-polarised light.

Figure 11. Core and thin section photograph of the lower Alinya Formation in Giles 1. A. Part of core at depth 1277.4-1280.6m, showing red-brown sandstone and grey-green siltstone interbeds. Angular breccia pebbles in anhydrite are probably a karst-fill. Scale bar is 1cm for each black and white grid. B. Quartz grains cemented by anhydrite. Qz - quartz grain and An - anhydrite. Thin section 5341RS233, 1279.9m, cross-nicols.

Figure 12. Core and thin section photograph of the upper Alinya Formation in Giles 1. A. Part of core at depth 1242-1245m, showing grey-green shale and red-brown siltstone, anhydrite is common. Scale bar is 1cm for each black and white grid. B. Thin section showing graded bedding. Thin section 5341RS340, 1243m, cross-nicols.

Figure 13. Idealised complete cycle of the coastal sabkha deposits of the upper Alinya Formation in Giles 1 well.

Figure 14. Seismic profile across Giles 1 - Munta 1 - Ungoolya 1 - Munyarai 1 section. A-B. Seismic interpretation of the section (modified from Thomas, 1990). A is the composite seismic lines from Giles 1, Munta 1 to Ungoolya 1. C. Vertical-exaggerated lithological distribution from the seismic and drilling interpretations (modified from Hibburt, 1993).

Figure 15. Block diagram showing Torrensian sequence in the central and northeastern Officer Basin in South Australia. Top figure - total magnetic intensity image of the eastern basin; bottom - cross section (Giles 1 - Ungoolya 1 - Munyarai 1 - Birksgate 1) showing possible palaeogeographic provinces.

Figure 16. Seismic interpretation of the sedimentary sequences across the Munyarai Trough (combined and revised from Ivic, 1986; Amoco, 1987; Thomas, 1990). Seismic reflectors are referred to Figure 9. Velocity was calculated by Ivic (1986).

Figure 17. Idealised original distribution of the Alinya Formation in the Munyarai Trough and Murnaroo Platform. A - Possible restored isopach of the Alinya Formation. B - Possible depositional basin of Sequence 1, figure at the lower left corner showing sedimentary onlap wedge of the lower Alinya Formation on the Murnaroo Platform, (referring fig.14:A for seismic line), 1. Pindyin Sandstone, 2. lower Alinya Formation, 3. upper Alinya Formation. C - Schematic section of sedimentary sequences across section A-A', based on drillhole intersections and seismic lines 84-0020, 85-0019, 86-0104, IP1-2, IP1-2A, EQ, FD and IP1-8.

Figure 18. Correlation chart of the Pindyin Sandstone and Alinya Formation and their equivalent beds in Australia.

Figure 19. Microfossil distribution in the sabkha deposits of the upper Alinya Formation in Giles 1 well. All thin sections, marked with RS numbers, were cut perpendicular to bedding.

Figure 20. Reconstruction of *Eoentophysalis gilesis* sp. nov. from the Alinya Formation. A. Life cycle; B. Mat-building processes; C. Photomicrograph of thin section 5341RS341 from intertidal mudflat, showing graded bedding and stratiform mat structures, plane-polarised light.

Figure 21. A-D: Cyanobacterial borings in the quartz framework of the upper Alinya Formation in Giles 1. E-H: Preservation of the acritarchs in the chert of the Alinya Formation in the North Pindyin Hills.

A-B. Cyanobacterial borings, B is close-up of A, 5341RS342, Z28/2.

C. Cyanobacterial boring with septa-like structure, 5341RS342, C24/1.

D. Organic matter preservation within framework and in the intergranular cavities, showing coccoids and a relatively large specimen of *Leiosphaeridia crassa*. 5341RS342, W31/1.

E-F. Preservation of a group of *Gorgonisphaeridium pindyium* sp. nov. in very fine-grained quartz, E - plane-polarised light, F - cross-nicols, 5042RS2, H42/3.

G-H. Dolomite rhombs and complete silicification, most organic matter in this sample was degraded, G - plane-polarised light, H - cross-nicols, 5042RS2.

Scale bar in E is 65*u*m for B, C; 100*u*m for D; 165*u*m for A; and 300*u*m for E-H.

Figure 22. Distribution of selected acritarchs in Australia and other known localities.* Generic name has not been redescribed after *Trachysphaeridium* was considered to be congeneric with *Leiosphaeridia* (Jankauskas, 1989). ** *Vandalosphaeridium pussillum* (Zang) = *Skiagia pussilla* Zang in Zang and Walter, 1992b

Figure 23. Acritarchs from the upper Alinya Formation in Giles 1.

A-E. *Trachyhystrichosphaera vidalii* Knoll, 1984

A-B. 5341RS309.

C. 5341RS311-10, Y45.

D. 5341RS311-10, Y45/1.

E. 5341RS318-3, G34/4.

F-H. *Vandalosphaeridium* sp. cf. *V. reticulatum* (Vidal) Vidal, 1981

F. 5341RS337-5, S49/2.

G. 5341RS309-10, K40/4.

H. 5341RS337-5, R49.

Scale in C is 20*u*m for C, D, F, G, H; and 32*u*m for E. SEM A and B scale as indicated.

Figure 24. Acritarchs from the upper Alinya Formation in Giles 1.

A-G. *Comasphaeridium tonium* sp. nov.

A. 5341RS311-10, X50/4.

B. 5341RS308-8, Q45/4, holotype.

C. 5341RS311-10, K44/1.

D. 5341RS311-10, R35/1.

E. 5341RS318-3, J37/1.

F. 5341RS311-10, W39/1, note a spinose protuberance structure.

G. 5341RS311-10, U37/3.

H-K. *Cymatiosphaeroides kullingii* Knoll emend. Knoll et al., 1991

H. 5341RS309-8, T37-4.

I. 5341RS309-8, R37/1.

J. 5341RS309-9, Q50.

K. 5341RS308-8, Q45.

Scale bar in E is 20*u*m for C, D, E, F, H, J, K; 25*u*m for A, B, G; and 32*u*m for I.

Figure 25.	Acritarchs from the Alinya Formation in Giles 1 (A-E, G-J) and at the North Pindyin Hills section (F).
A-D.	*Goniosphaeridium alinyum* sp. nov.
A.	5341RS312.
B.	5341RS337-6, G47/1, holotype.
C.	5341RS311-6, L45/2.
D.	5341RS309-10, H33/2.
E-F.	*Melanocyrillium* sp.
E.	5241RS337-6, K48.
F.	5042RS2, O25.
G.	*Octoedryxium intrarium* (Timofeev) Jankauskas, 1989 5341RS341, 28.6X130.5.
H-J.	*Trachyhystrichosphaera stricta* Hermann in Jankauskas, 1989
H-I.	5341RS309-10, M25/3.
J.	5341RS337-6, F45/1.
	Scale bar in D is 20*um* for B, C, G, J; 25*um* for D, E; 32*um* for F; 80*um* for I; and 200*um* for H. In A as indicated.

Figure 26.	Acritarchs from the Alinya Formation in Giles 1 (A-H, K-L) and at the North Pindyin Hills section (I-J).
A-G.	*Trachyhystrichosphaera* sp. cf. *T. aimica* Hermann, 1976
A-B.	5341RS311. Note a loose fragment of *S. robustum* (Schopf) Knoll et al., 1991 on the vesicle (examed under Zeiss Microscope).
C-D.	5341RS337-4, Y41/1.
E.	5341RS309-9, F53.
F.	5341RS318-3, K54/3.
G.	5341RS337-6, R57-1.
H.	*Polyedrosphaeridium* sp. 5341RS309-1, F32/2.
I.	*Leiofusa bicornuta* Sin and Liu, 1973 5042RS2, T28/1.
J.	*Asteridium* sp. 5042RS2, W38-2.
K-L.	*Germinosphaera* sp. cf. *G. unispinosa* Mikhailova, 1986
K.	5341RS309-10, N44-1.
L.	5341RS309-8, F33.
	Scale bar in I is 20*um* D, G, I, J, K, L; 32*um* for E, F; 80*um* for C; and 125*um* for H. In A and B as indicated.

Figure 27.	Acritarchs from the Alinya Formation in Giles 1 (C-F, H-K) and at the North Pindyin Hills section (A, B, G).
A-E.	*Gorgonisphaeridium pindyium* sp. nov.
A-B.	5042RS2, H42/3, B - holotype.
C.	5341RS308-7, V36/2.
D.	5341RS309-3, S43/1.
E.	5341RS311-10, Y45/3.
F-H.	*Gorgonisphaeridium torrensium* sp. nov.
F.	5341RS337-1, O35/4.
G.	5042RS2, R53/3.
H.	5341RS311-10, M45/2, holotype.
I.	*Sinianella uniplicata* Yin emend. Zang in Zang and Walter 1992a 5341RS308-7, V40.
J.	*Satka compacta* Zang in Zang and Walter, 1992b

5341RS309-1, T45-4.
K. Unnamed specimen A, note bud-like structure.
5341RS311-10, S49.
Scale bar in H is 20*u*m for E, F, G, H, I, K; 25*u*m for C, D; 32*u*m for B; 40*u*m for J; and 200*u*m for A.

Figure 28. Acritarchs from the upper Alinya Formation in Giles 1.
A-B. *Annulusia annulata* (Timofeev and Hermann) Jankauskas, 1989
A. 5341RS311.
B. 5341RS311-2, F37-1.
C-D. *Leiosphaeridia crassa* (Naumova) Jankauskas, 1989
C. 5341RS309-8, F46/2.
D. 5341RS310-5, R35/1.
E. *Simia annulare* (Timofeev) Mikhailova in Jankauskas, 1989,
5341RS309-2, H37-4.
F. *Leiosphaeridia holtedahlii* (Timofeev) Jankauskas, 1989
5341RS365-4, K42/2.
G-H. *Leiosphaeridia atava* (Naumova) Jankauskas, 1989
G. 5341RS310-5, L40/4.
H. 5341RS337-6, Y35-1.
I. *Valeria lophostriata* (Jankauskas) Jankauskas, 1982
5341RS308-8, O46/4.
J. *Leiosphaeridia visingsa* Zang in Zang and Walter, 1992a
5341RS339, P54/2.
K-L. *Leiosphaeridia ternata* (Timofeev) Mikhailova and Jankauskas in Jankauskas 1989
K. 5341RS318-3, M38.
L. 5341RS337-4, V44/1.
Scale bar in J is 20*u*m for F, H, K, L; 25*u*m for B; 32*u*m for J; 80*u*m for E, I; and 100*u*m for C, D, G. In A as indicated.

Figure 29. Acritarchs from the Alinya Formation in Giles 1 (A-G, I-M) and at the North Pindyin Hills section (H).
A-G. *Lakhandinna dilatata* Hermann in Jankauskas, 1989
A. 5341RS308-7, K40/1.
B. 5341RS311-10, X46/3.
C. 5341RS308-7, E35/2.
D. 5341RS311-10, S35.
E. 5341RS308-8, J35.
F. 5341RS311-10, R44/4.
G. 5341RS311-10, E46.
H-K. *Archaeoellipsoides karatavicus* (Jankauskas) comb. nov.
H. 5042RS2, T31.
I. 5341RS312-2, K27/1.
J. 5341RS312-1, U28/3.
K. 5341RS311-9, V51-2.
L-M. *Sphaerocongregus variabilis* Moorman, 1974
L. 5341RS310-5, N34.
M. 5341RS309-1, R44-4.
Scale bar in K is 20*u*m for F, H, I, J, K; 32*u*m for A, B, D, L; 50*u*m for G; 80*u*m for C, E, M.

Figure 30. Microfossils from the upper Alinya Formation in Giles 1.
A-E. *Coniunctiophycus* sp. cf. *C. majorinum* Knoll et al., 1991
A. 5341RS311-1, X26/2.
B. 5341RS309-1, T42/1.
C. 5341RS309-1, Q42/3.
D. 5341RS313-2, E36.
E. 5341RS309.
F,K. *Myxococcoides* sp. cf. *M. cantabrigiensis* Knoll, 1982
F. 5341RS309-8, W40/2.
K. 5341RS309-1, F31.
G-J. *Lomentunella* sp. cf. *L. vaginata* Hermann, 1981
G. 5341RS308-1, M36/3.
H. 5341RS308-1, H51.
I. 5341RS308-7, X36/1.
J. 5341RS308-8, L36/3.
L-M. *Sphaerophycus* sp.
L. 5341RS309-2, Z33.
M. 5341RS309-1, L34-3.
Scale bar in F is 20*um* for J; 25*um* for F, G, H; 32*um* for I; 40*um* for D, L; and 100*um* for A, B, C, K, M. In E as indicated.

Figure 31. Microfossils from the upper Alinya Formation in Giles 1.
A-D. *Eoentophysalis gilesis* sp. nov.
A. 5341RS341, M43.
B. 5341RS339, 38 X 95.3, holotype.
C. 5341RS339, W24/4.
D. 5341RS339, 35 X 127.
E-F. *Synsphaeridium* sp.
E. 5341RS308-1, B43.
F. 5341RS309-3, V49/4.
G-H. *Paleasphaeridium zonale* Yin, 1985
G. 5341RS309-8, P36/4.
H. 5341RS309-1, T42.
I. *Archaeodiscina* sp.
5341RS318-3, V46/1.
J-L. Unnamed specimens B.
J. 5341RS337-6, M58/2, note the surface network structure and surrounded by thin membrane.
K-L. 5341RS337-6, G21/1, two focus levels, note the irregular framework and surrounding membrane.
Scale bar in E is 20*um* for G, J; 25*um* for E, F, H; 32*um* for I, K, L; 40*um* for B, C, D; and 160*um* for A.

Figure 32. Filamentous microfossils from the Alinya Formation in Giles 1 (A-D, F-M) and at the North Pindyin Hills section (E).
A-C. *Quaestiosignum filum* Zang in Zang and Walter, 1992b
A. 5341RS337-5, K34/3.
B. 5341RS337-4, M47/4.
C. 5341RS313-2, Y47/1.
D-E. *Cephalophytarion* sp.
D. 5341RS312-1, P48-4.
E. 5042RS2, E54.
F-G. *Siphonophycus* sp. cf. *S. kestron* Schopf, 1968

F. 5341RS309-1, S47/4.

G. 5341RS311-1, K45/4.

H. *Heliconema fidicularis* Zang in Zang and Walter, 1992b
5341RS308-8, R45.

I. *Clavitrichoides rugosus* Mikhailova in Jankauskas, 1989
5341RS308-1, T51.

J. *Rectia costata* (Jankauskas) Jankauskas, 1989
5341RS310-3, V33.

K. *Oscillatoriopsis* sp.
5341RS337-1, U30/2.

L-M. *Siphonophycus robustum* (Schopf) Knoll et al., 1991

L. 5341RS318-3, P51.

M. 5341RS337-1, V32/2.

Scale bar in H is 20*u*m for D, E; 25*u*m for G, I, K; 32*u*m for A, B, H; 40*u*m for C, F, M; 80*u*m for J, L.

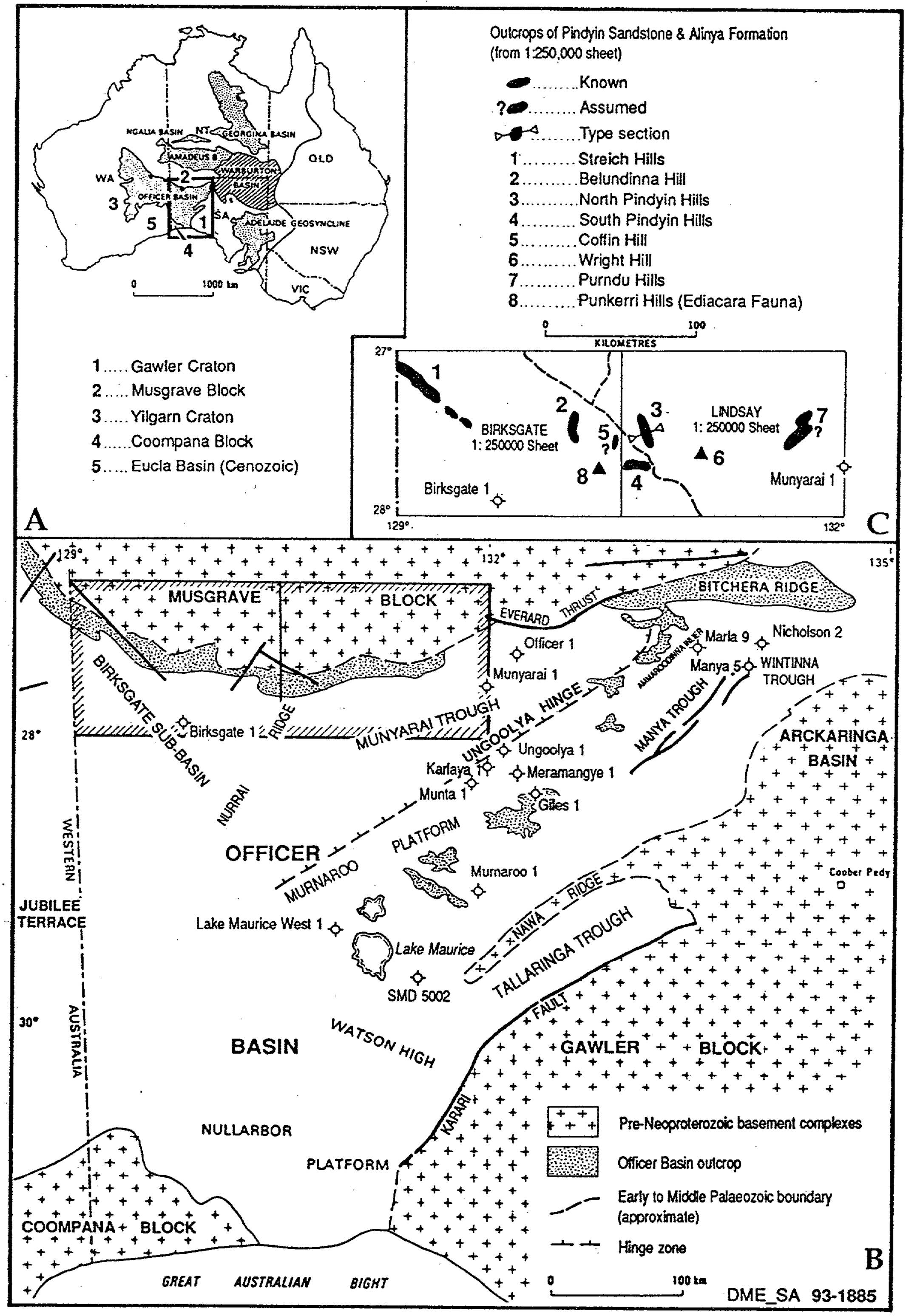

Figure 1. Index maps of the study area, eastern Officer Basin

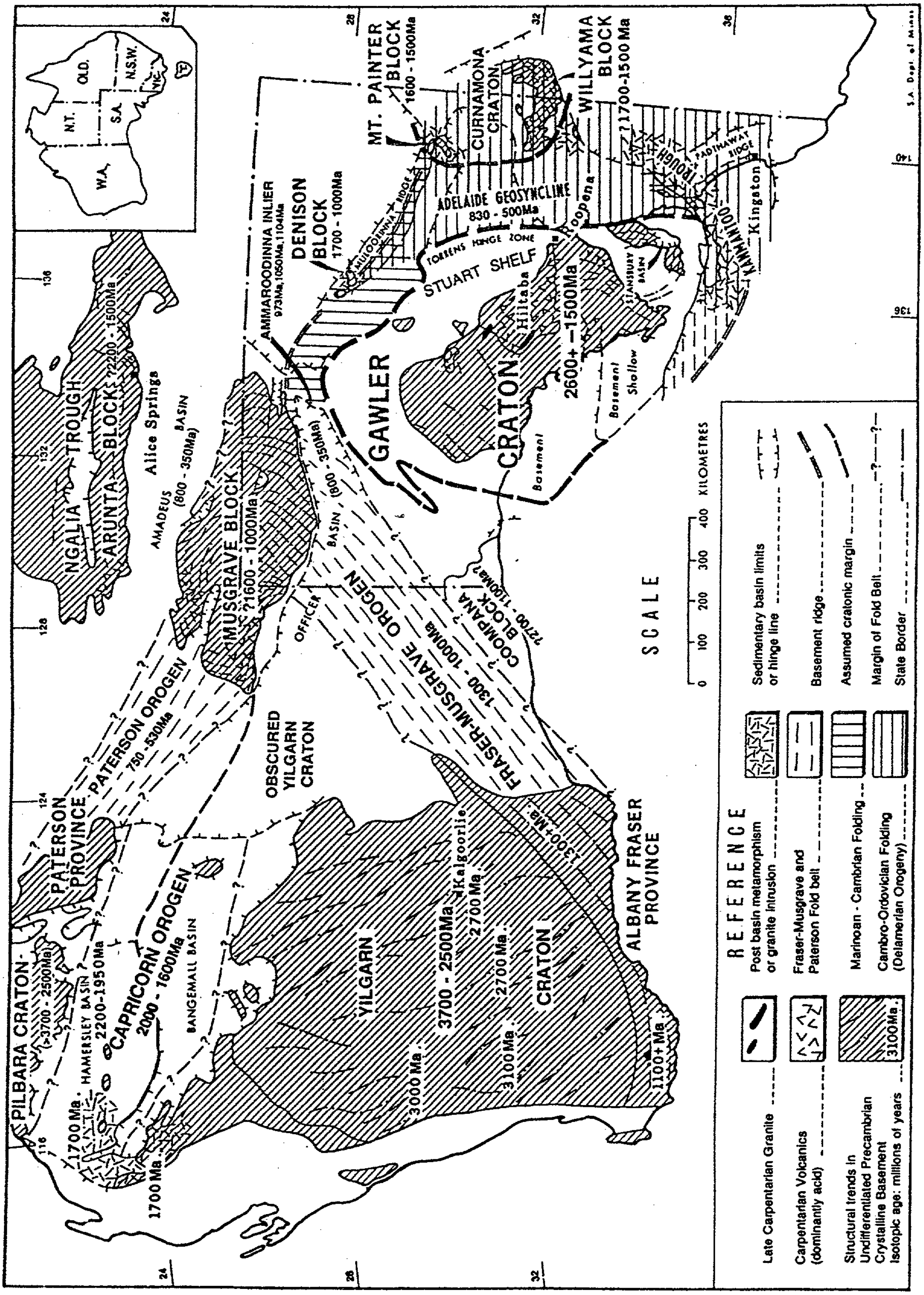

Figure 2. Tectonic framework of southern Australia

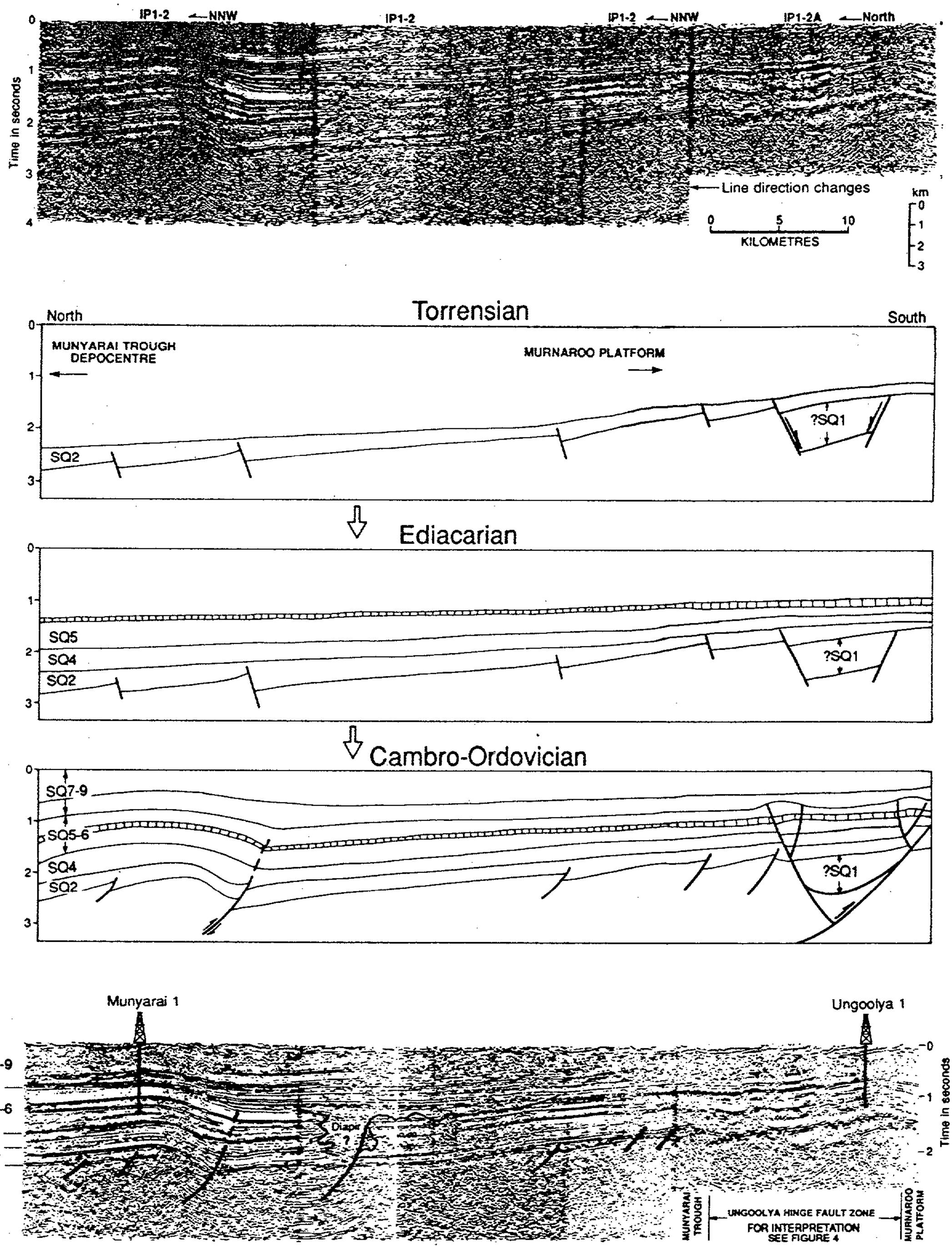

DME_SA **93-1887**

Figure 3. Interpretation of the structure of the Munyarai Trough

0514

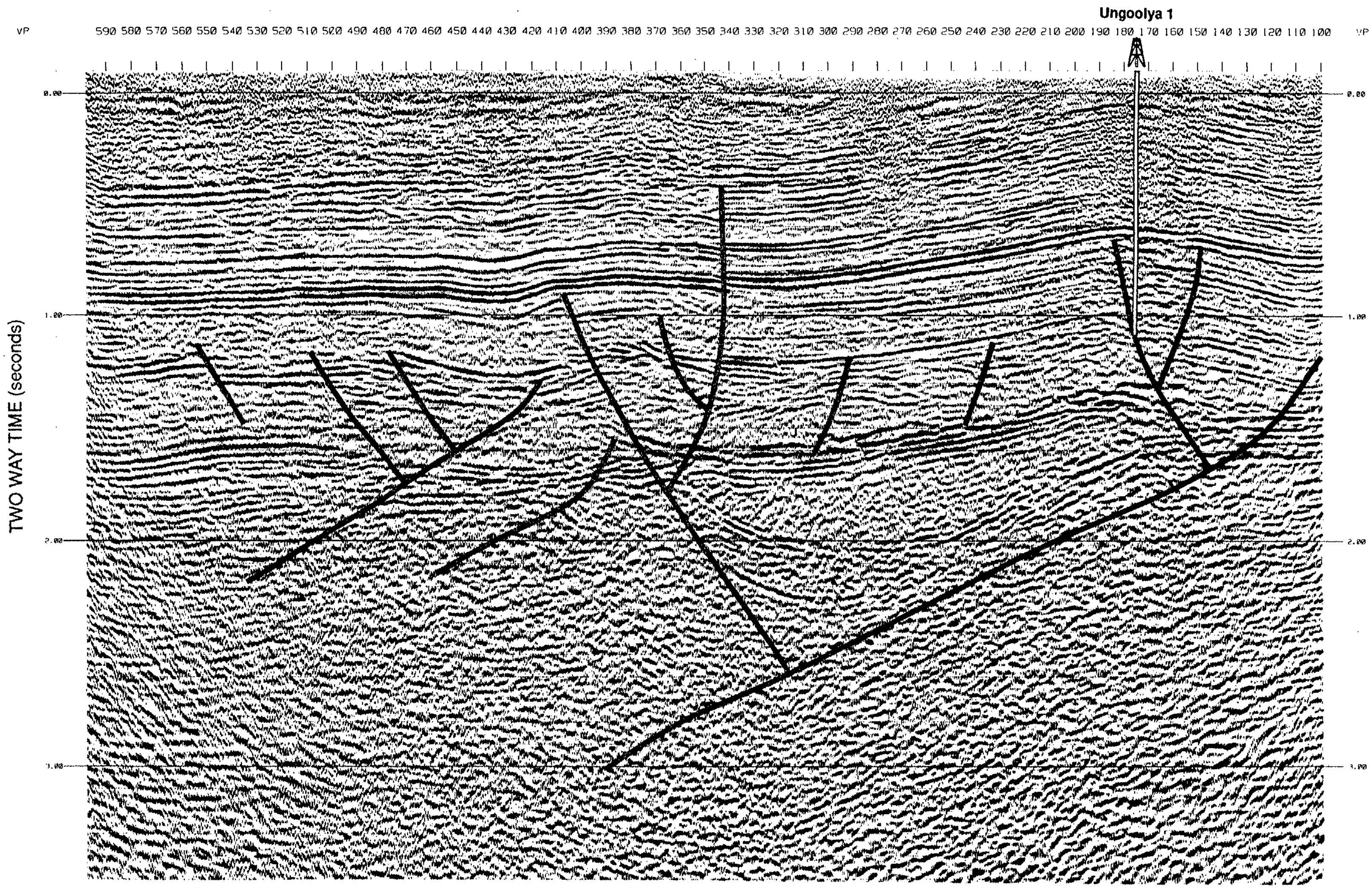

MINES AND ENERGY
SOUTH AUSTRALIA

Figure 4 Interpretation of the Ungoolya Hinge

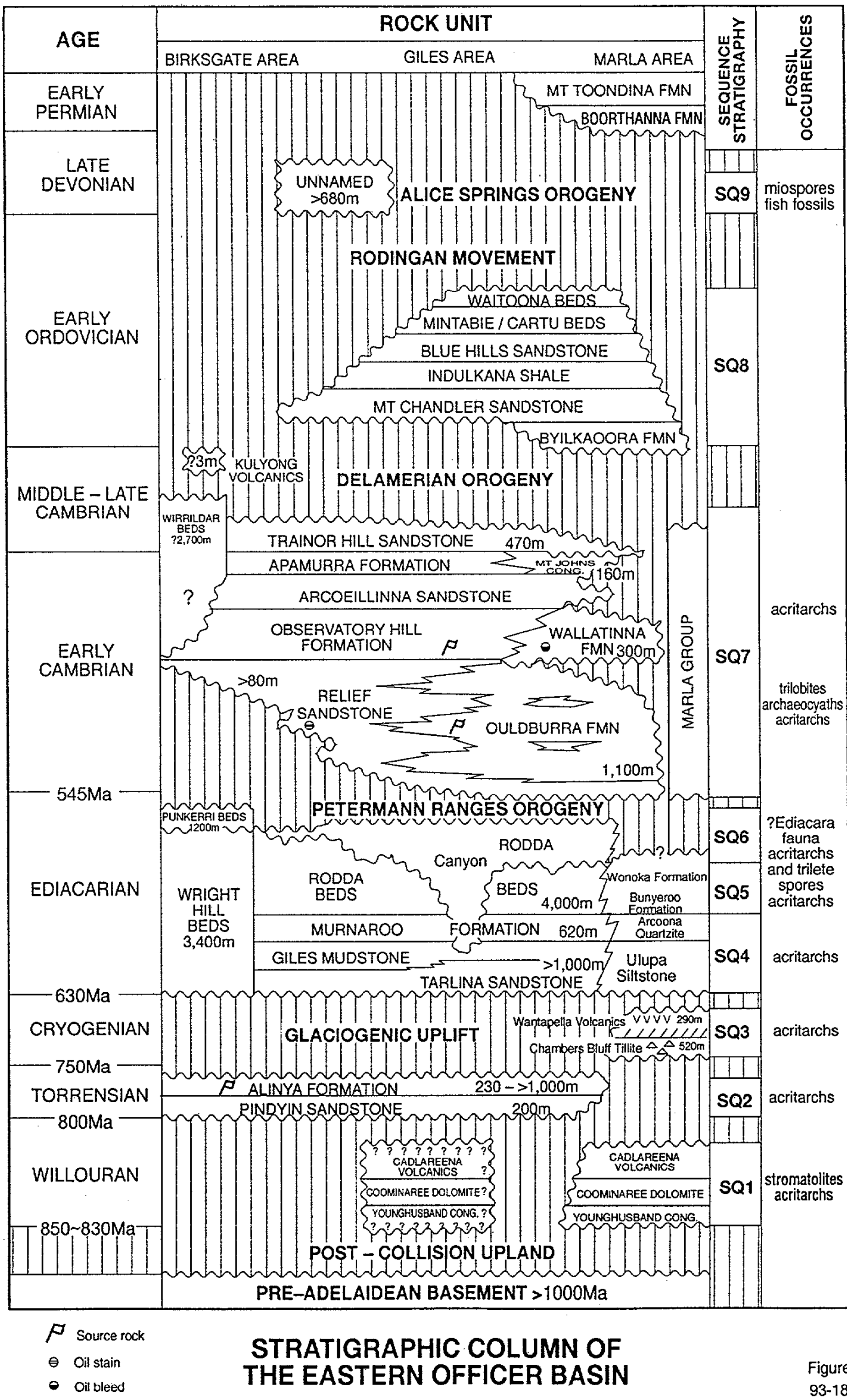

STRATIGRAPHIC COLUMN OF THE EASTERN OFFICER BASIN

Figure 5
93-1888

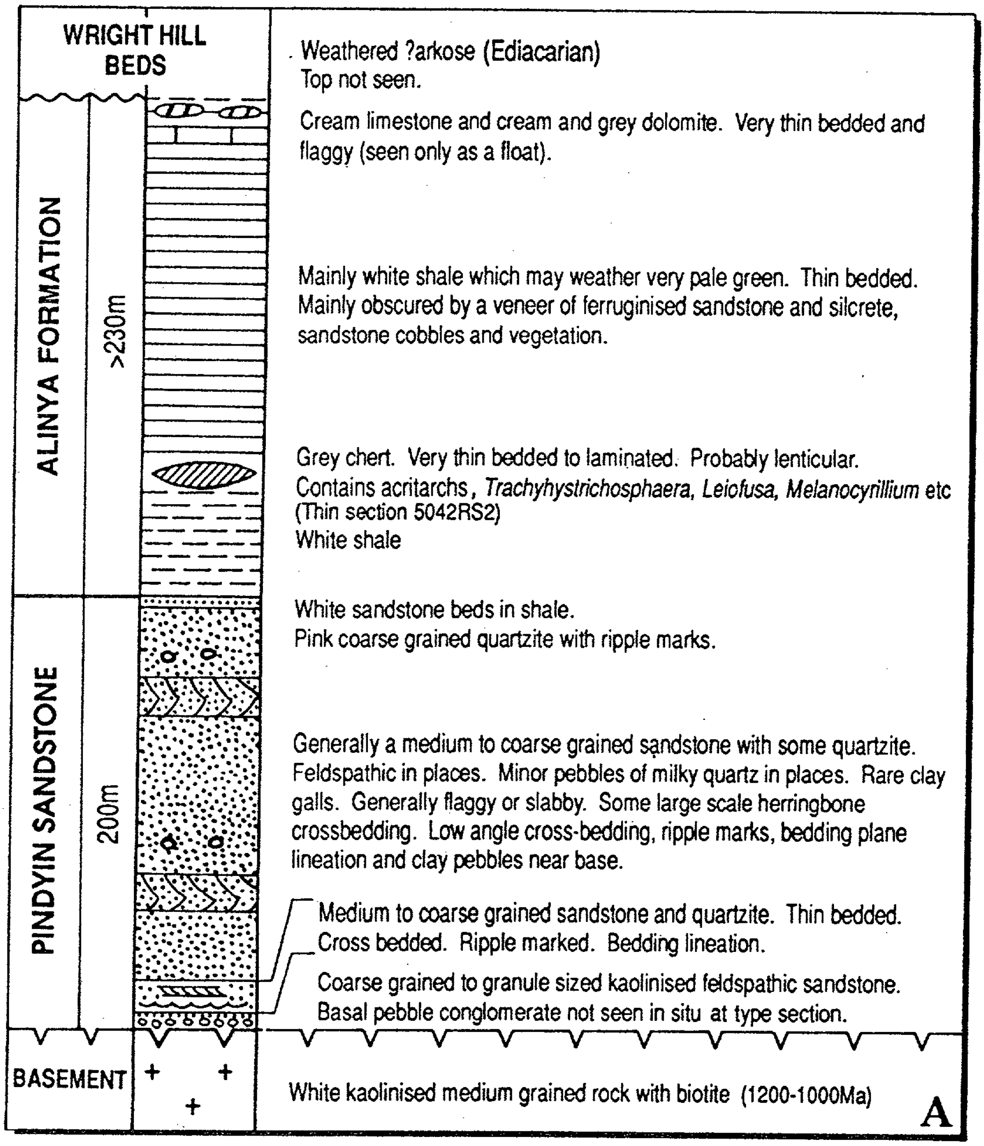

Figure 6 Stratigraphy of the type section of the Pindyin Sandstone and Alinya Formation

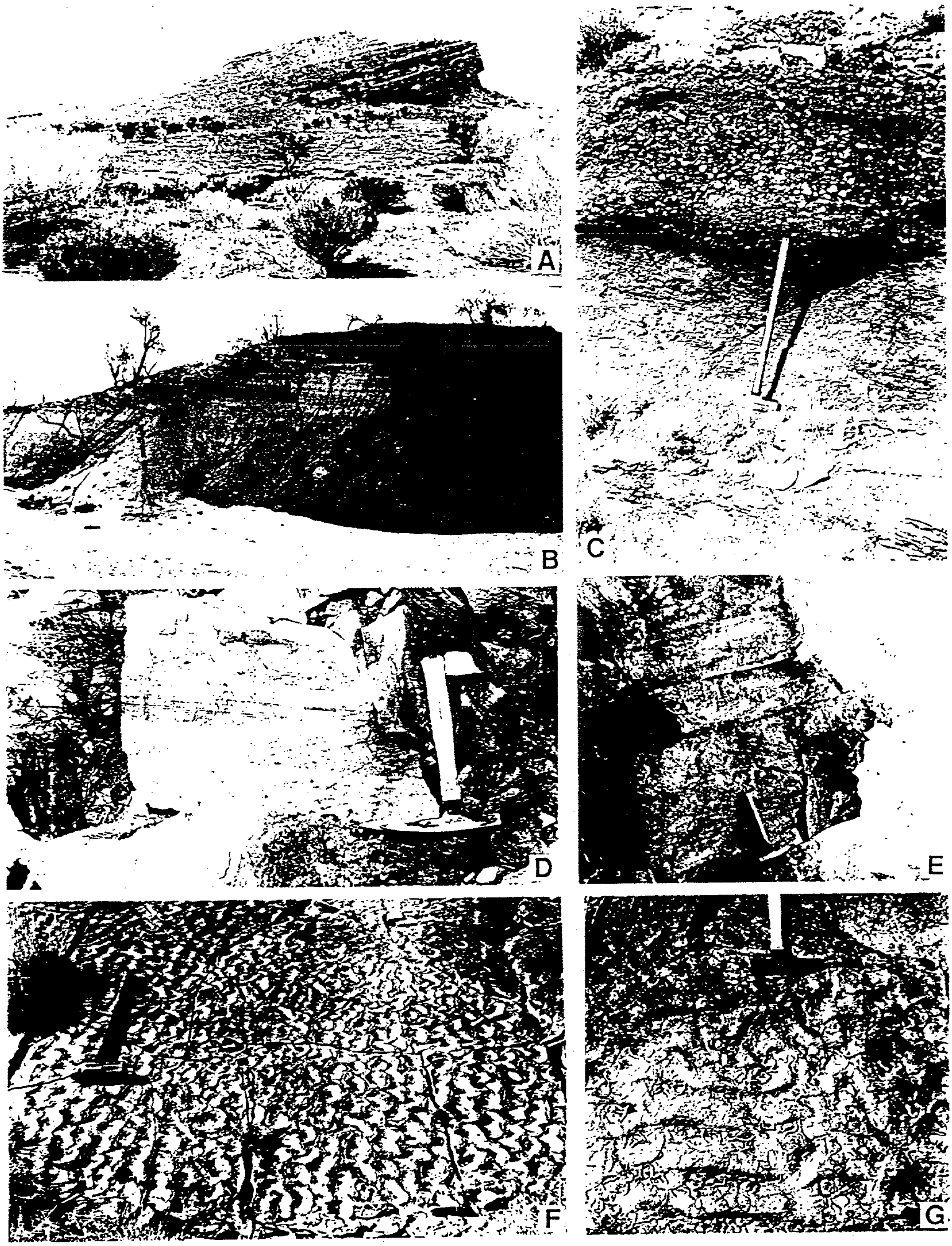

Figure 7

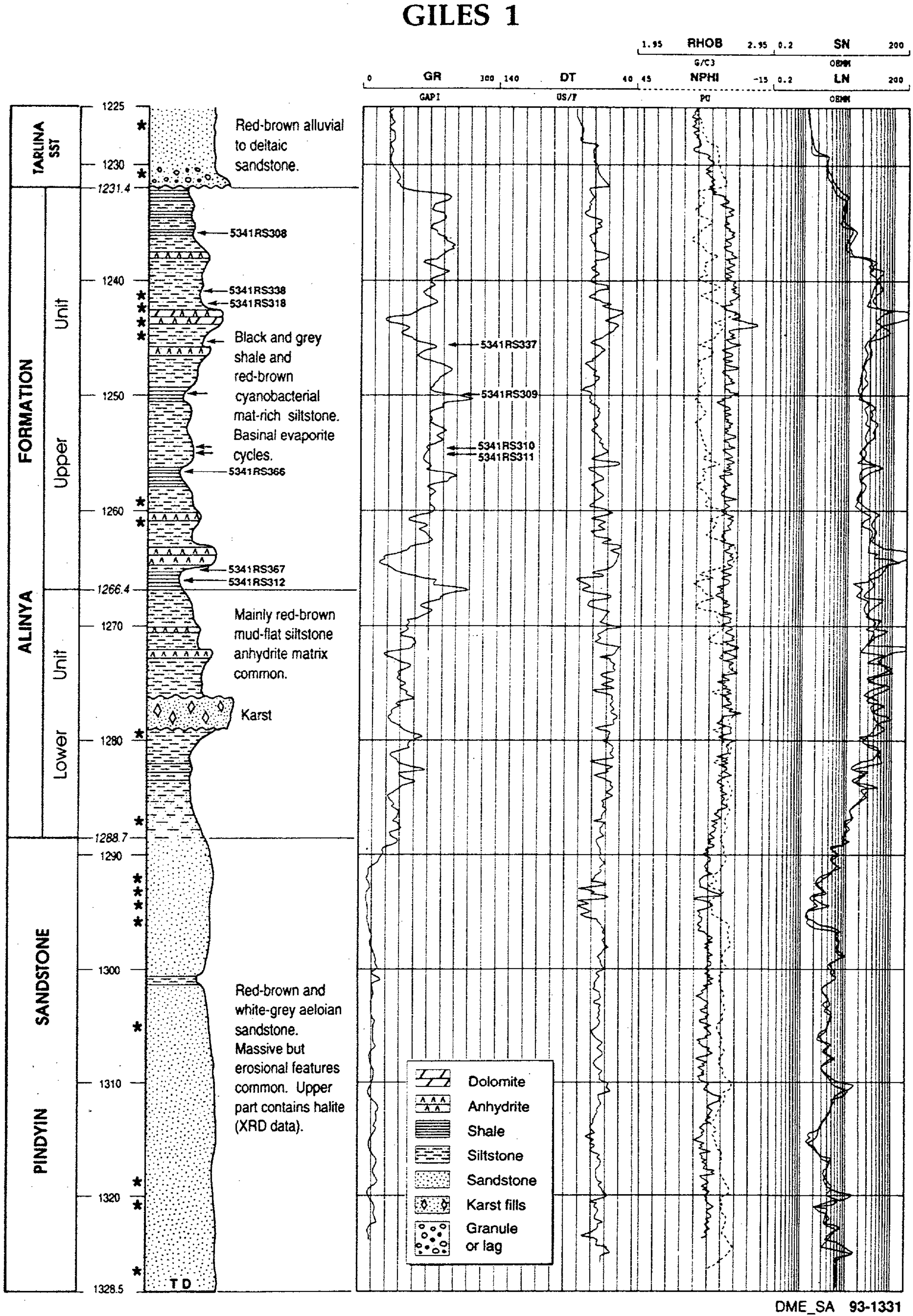

Figure 8. Detailed lithological description of the Pindyin Sandstone and Alinya Formation

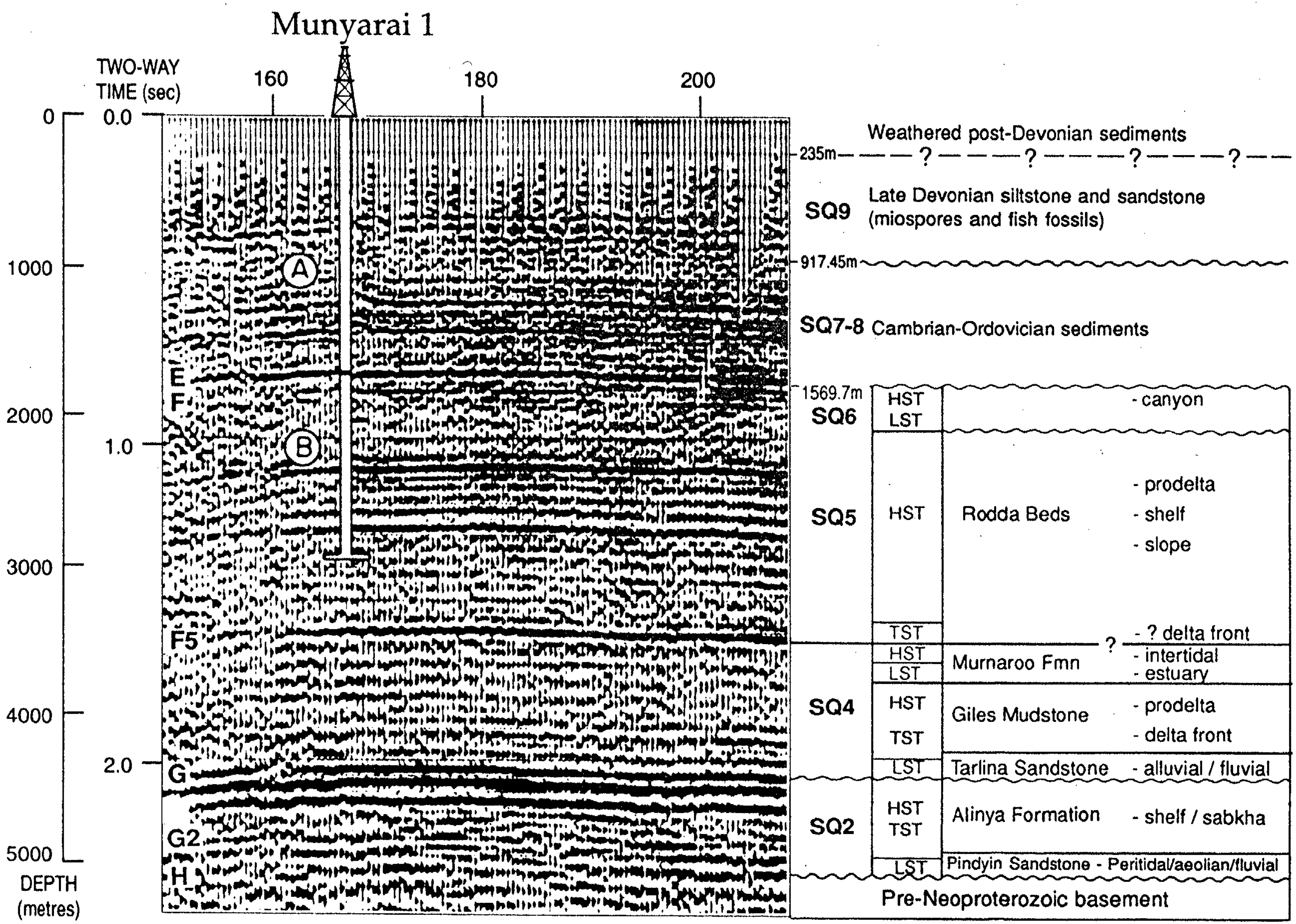

Figure 9. Close-up of the seismic line (101A) across Munyarai 1

DME_SA 93-1334

0519

Figure 10.

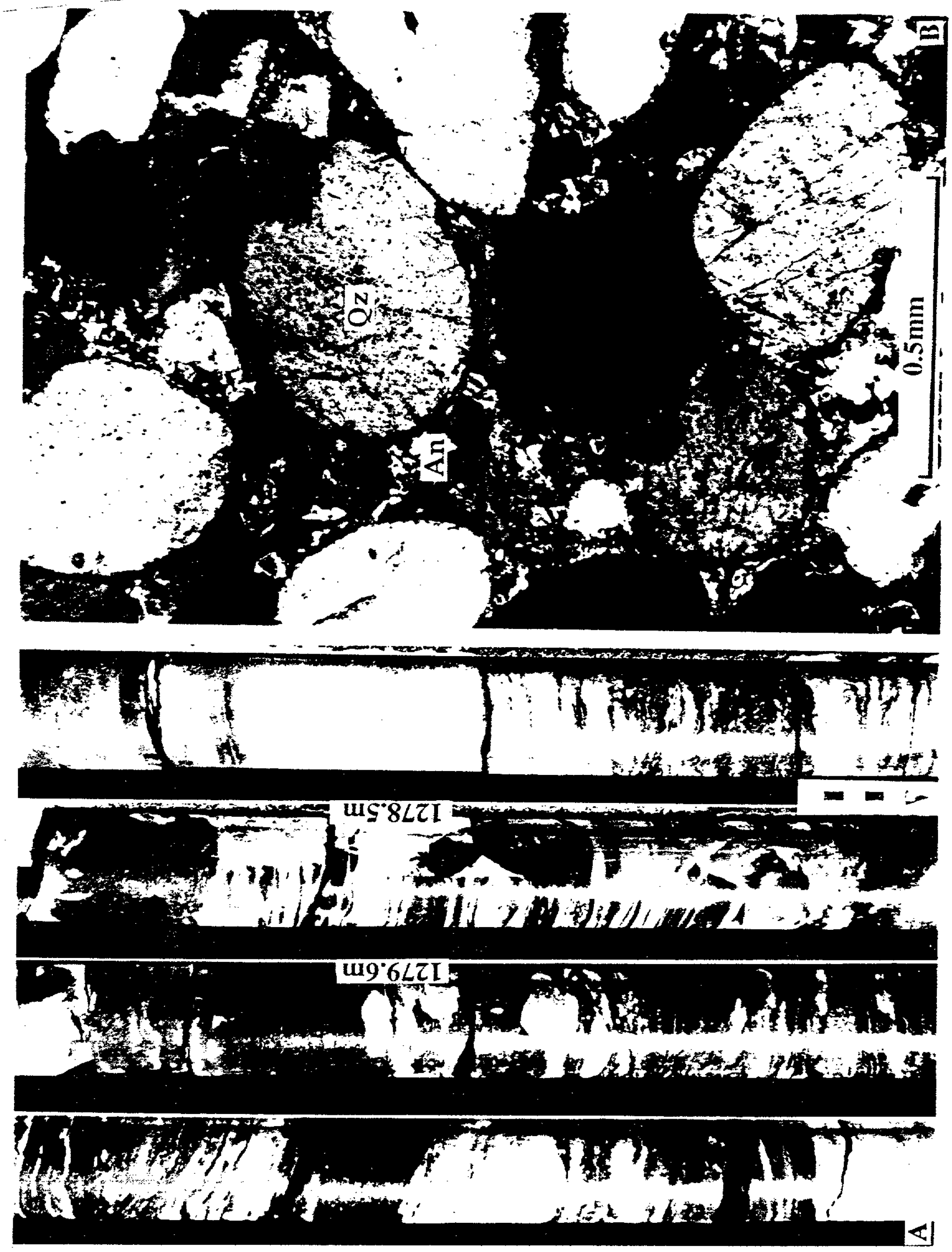

Figure 11.

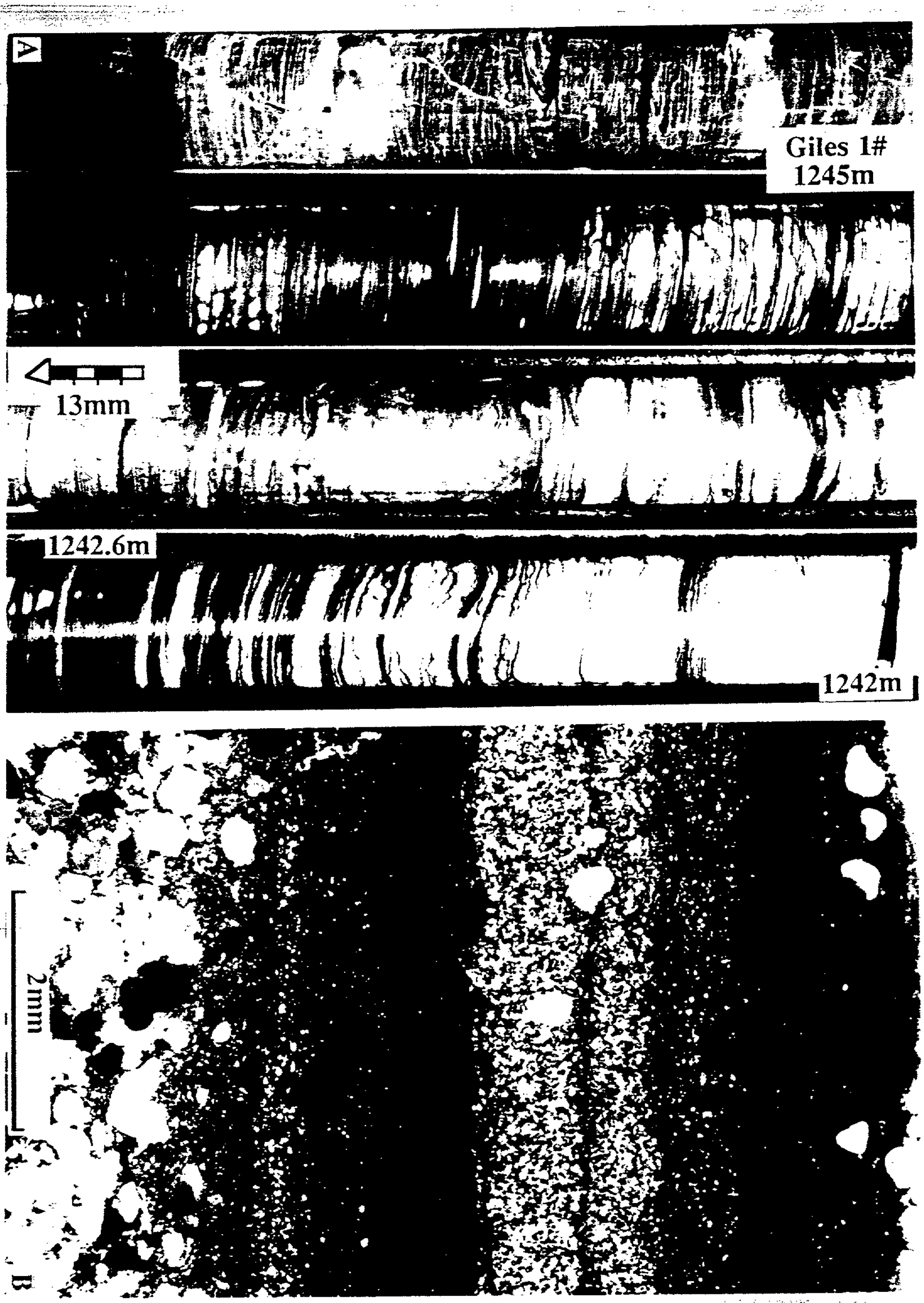

Figure 12.

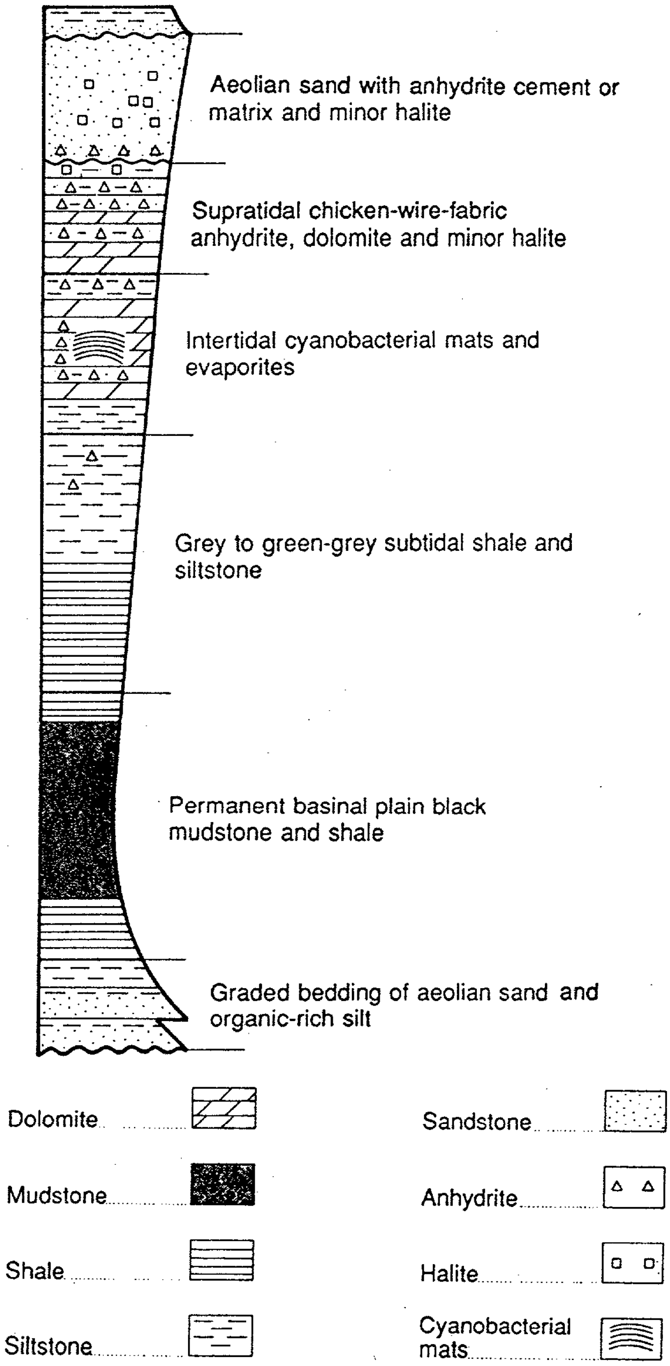

Figure 13. Idealised complete cycle of the coastal sabkha deposits of the upper Alinya Formation in Giles 1 well

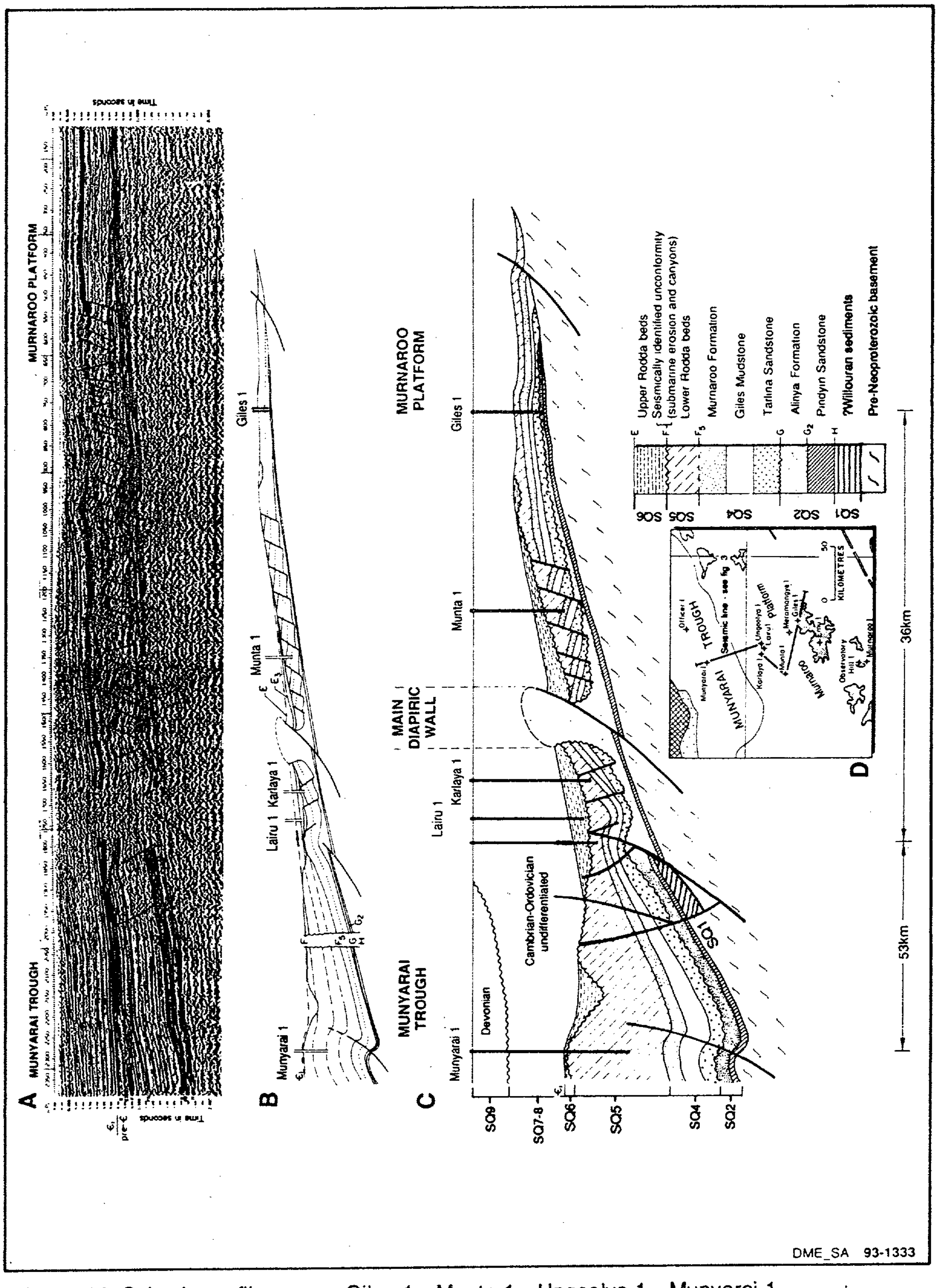

Figure 14. Seismic profile across Giles 1 - Munta 1 - Ungoolya 1 - Munyarai 1

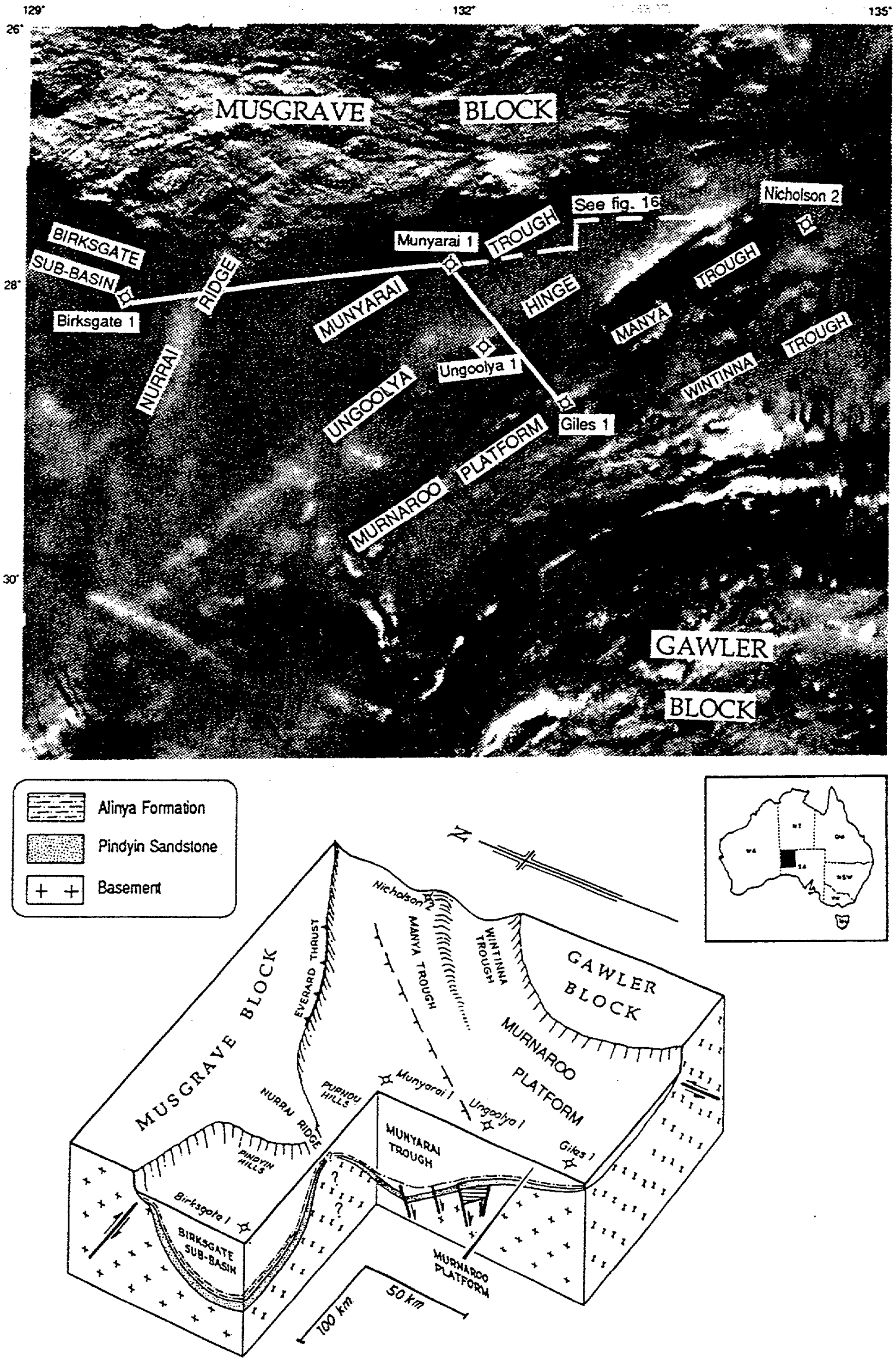

Figure 15. Section showing Torrensian sequence in the central and northeastern Officer Basin

DME_SA **93-1889**

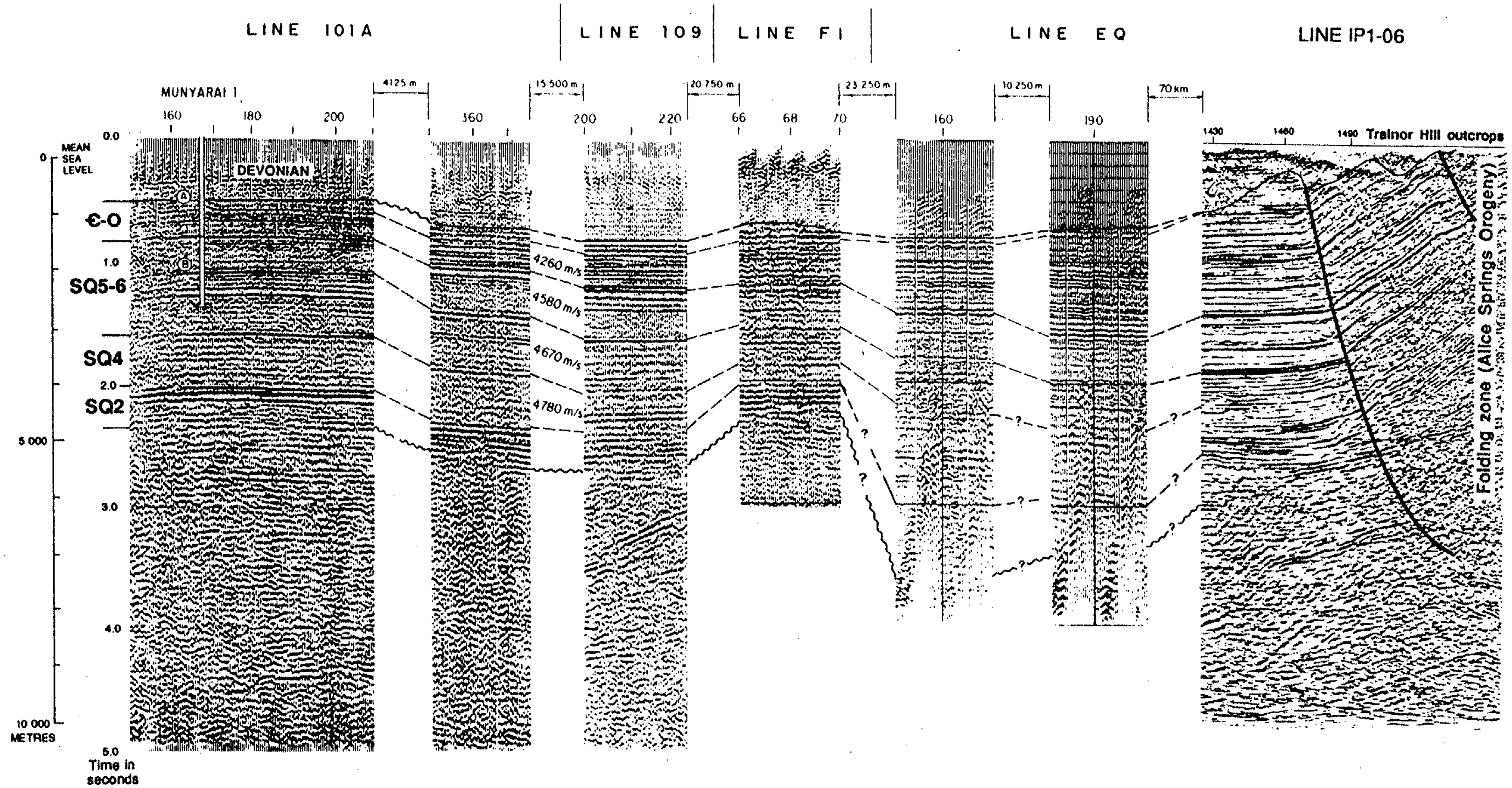

Figure 16. Seismic interpretation of the sedimentary sequences across the Munyarai Trough

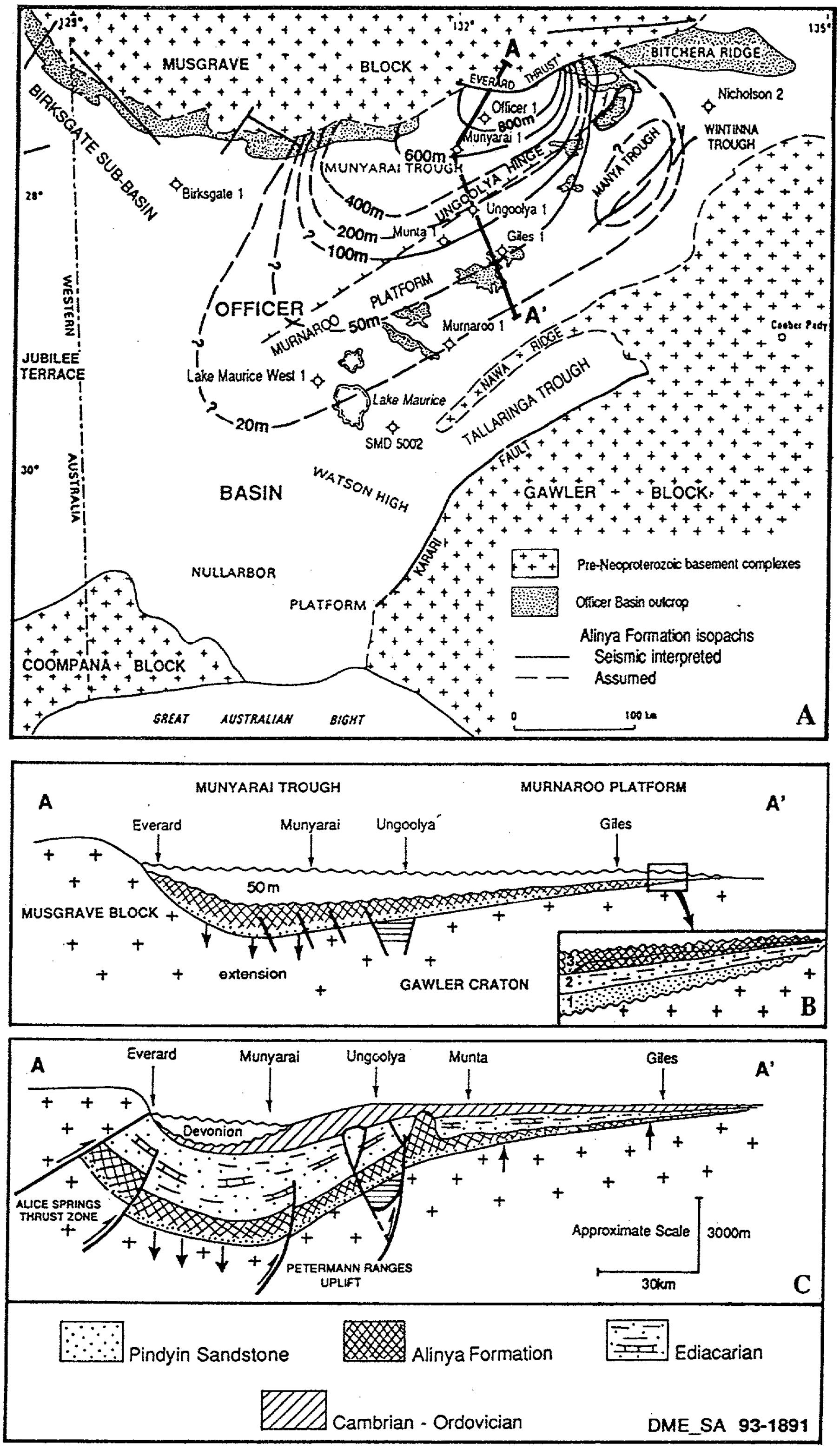

Figure 17. Idealised sedimentary basin and distribution of the Alinya Formation in the Munyarai Trough and Murnaroo Platform

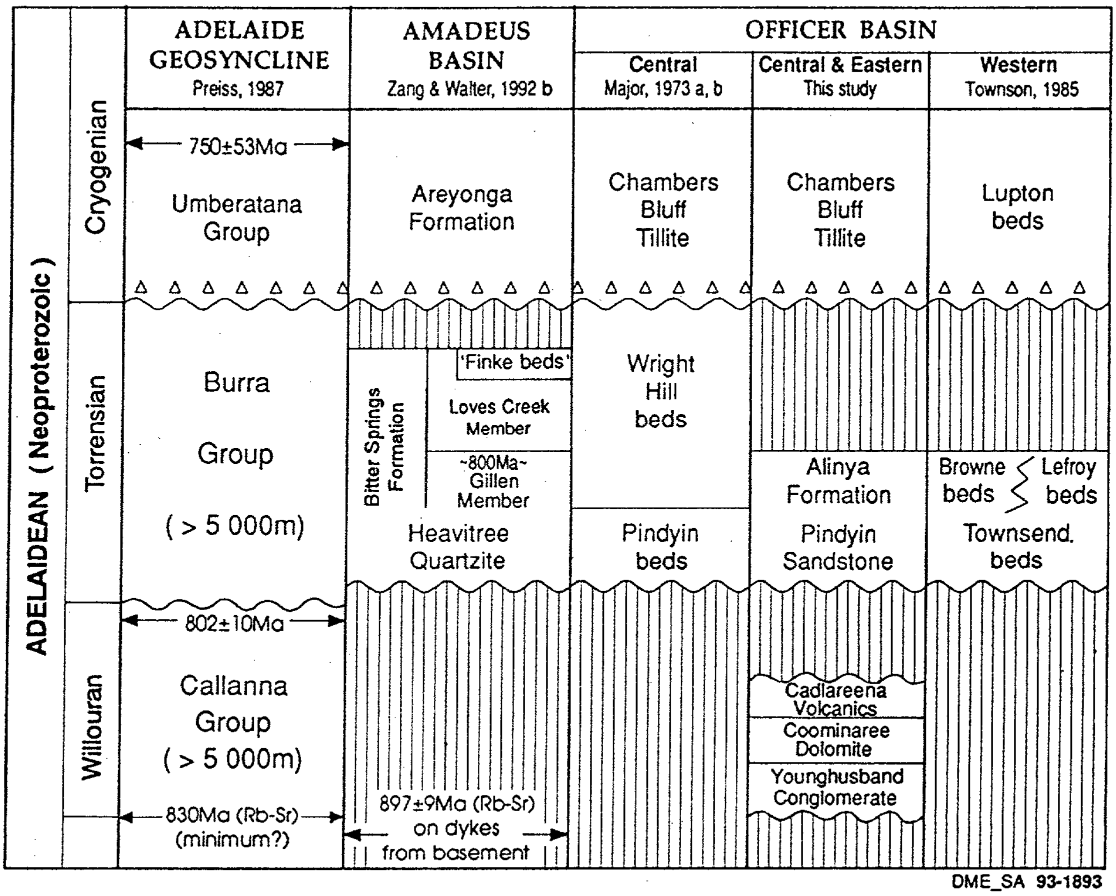

Figure 18 Correlation chart of the Pindyin Sandstone and Alinya Formation and their equivalent beds in Australia

→ *increasing water depth or distance from shore*

ORGANIC-RICH MUD CEMENTED SAND	INTERTIDAL SILTSTONE	SUBLITTORAL GREY or GREEN-GREY SHALE	BASINAL PLAIN BLACK to DARK-GREY SHALE
Cyanobacterial (filament?) borings and allogenic? *Eoentophysalis* sp., rare *Leiosphaeridia* sp. and other coccoids.	Cyanobacterial mats of *Eoentophysalis* sp. rare *Siphonophycus robustum*, *Leiosphaeridia* sp.	Benthic cyanobacterial coccoids - **50%**. Cyanobacterial filaments (mainly *Siphonophycus robustum*) - **20%** Phytoplankton - **30%** (which consists of: 80% spheroids and 20% spinose acritarchs)	Benthic cyanobacterial coccoids - **80%** Cyanobacterial filaments - **10%** Phytoplankton - **10%** Degraded organic debris is particularly abundant.
5341RS342 (1259.0m)	5341RS339 (1242.45m) 5341RS341 (1245.30m)	5341RS338 (1241.8m)	5341RS340 (1243.0m)
		Also 10 samples in maceration	

Figure 19. Microfossil distribution in the sabkha deposits of the upper Alinya Formation in Giles 1 well

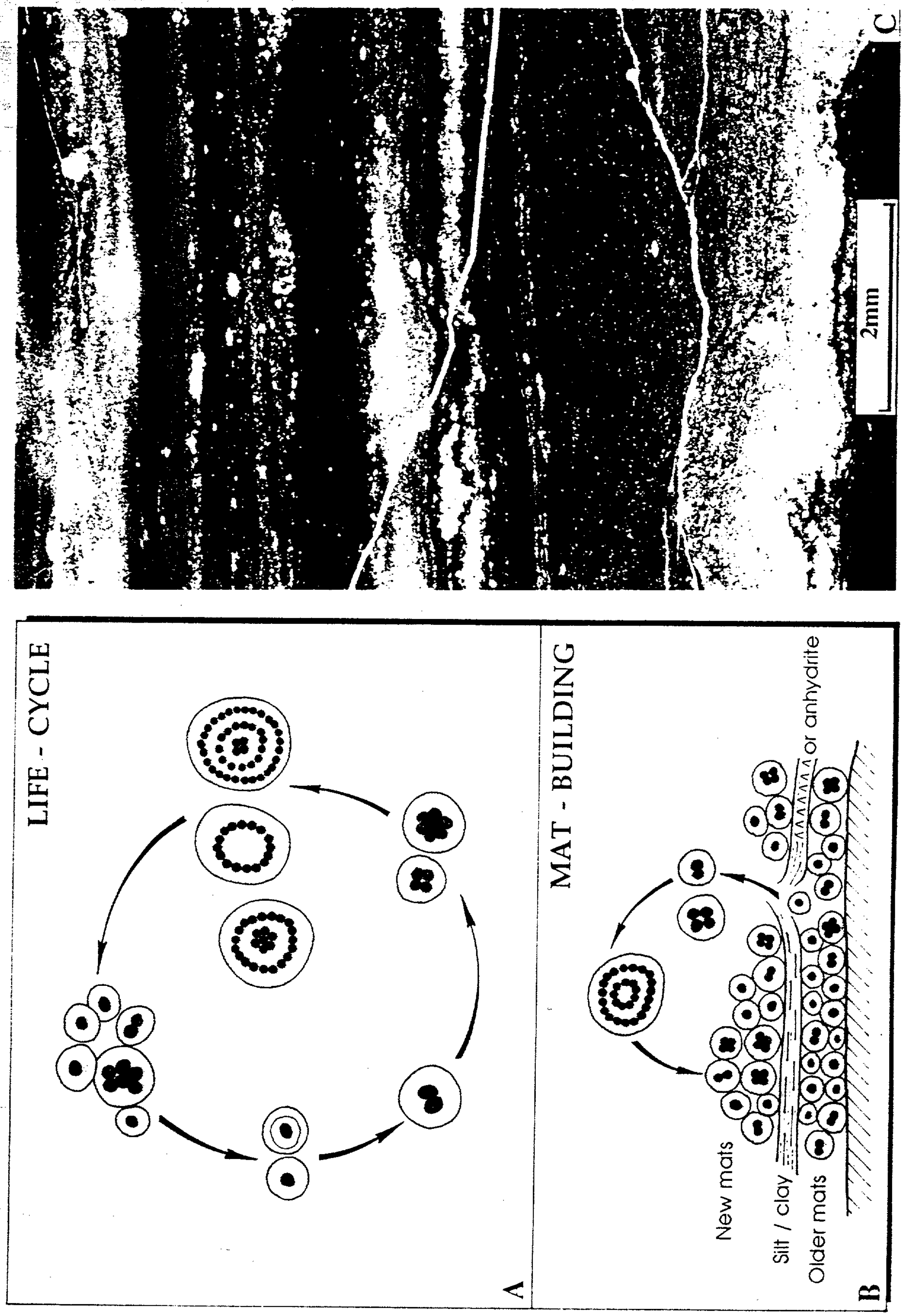
C
2mm
LIFE - CYCLE
A
MAT - BUILDING
New mats
Silt / clay
or anhydrite
Older mats
B

Figure 20

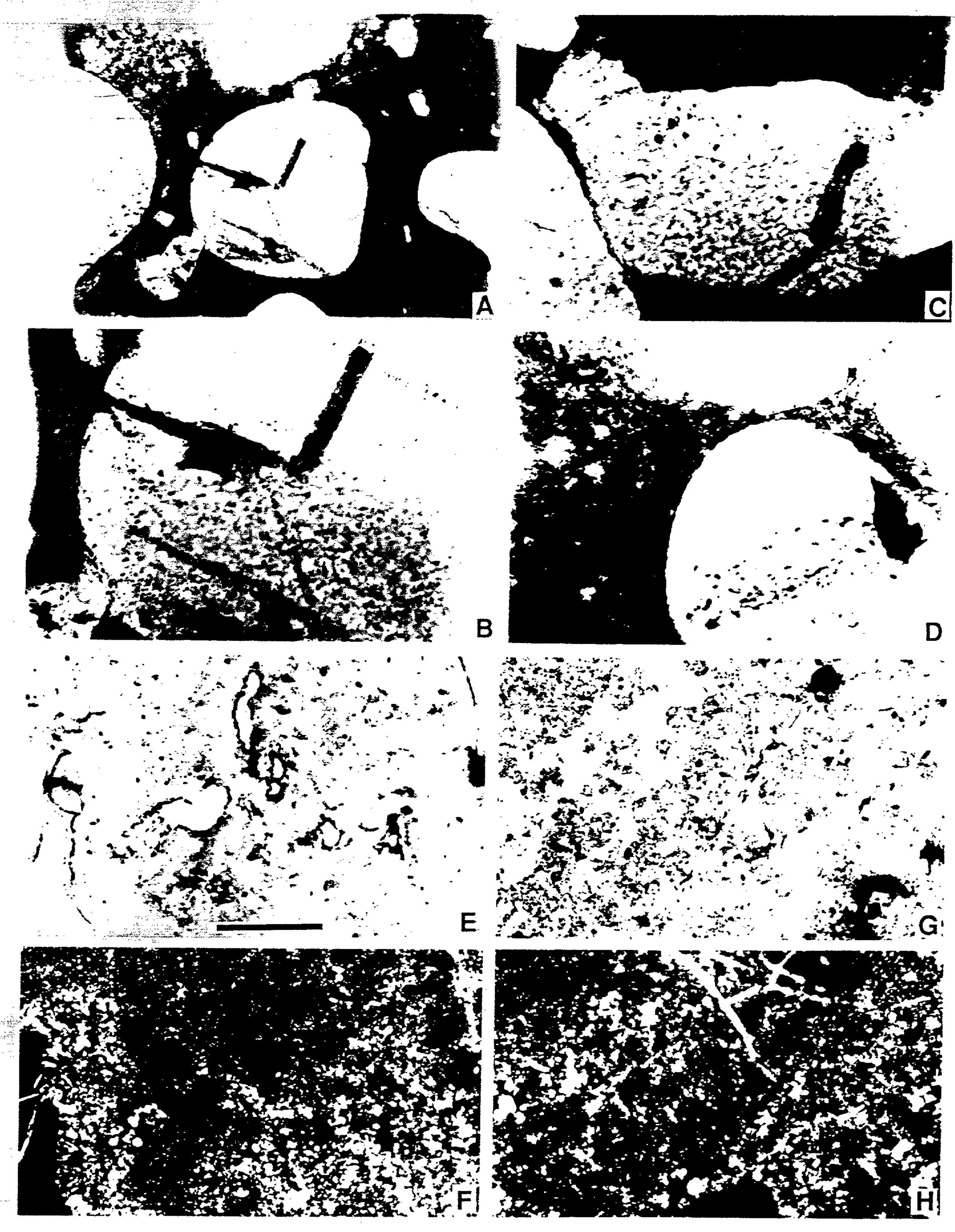

Figure 21

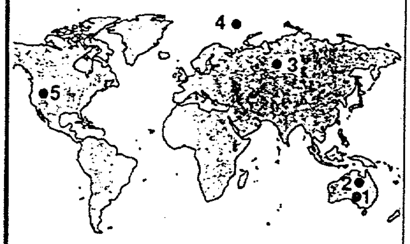

LOCALITY	1. Alinya Fmn, Officer Basin South Australia - This Study	2. Bitter Springs Fmn (Gillen) Amadeus B.-Zang & Walter, 1992b	3 Upper Riphean Siberia Jankauskas, 1989	4. Draken Conglomerate Fmn Spitsbergen-Knoll *et al.* 1991	5. Kwagunt Fmn, Chuar Group USA - Vidal & Ford, 1985
Annulusia annulata	●		●		
Archaeodiscina sp.	●				
Archaeoellipsoides karatavicus	●	?	●		
Asterdium sp.	●				
Asteridium geminatum		●			
Asteridium pissinum		●			
Comasphaeridium tonium	●				
Comasphaeridium pollostum		●			
Coniunctiophycus majorinum	●			●	
Cymatiosphaeroides kullingii	●		●	●	●
Dasysphaeridium glaessneri		●			?
Eoentophysalis gilesis	●				
Germinosphaera unispinosa	●		●	?	
Goniosphaeridium alinyum	●				
Gorgonisphaeridium pindyium	●	●		●	
Gorgonisphaeridium torrensium	●				
Lakhandinia dilatata	●		●		
Leiofusa bicornuta	●				
Leiosphaeridia atava	●	●	●	●	●
Leiosphaeridia crassa	●	●	●	●	●
Leiosphaeridia holtedahlii	●	●	●		●
Leiosphaeridia ternata	●	●	●	●	●
Leiosphaeridia visingsa	●	●	●		●
Lomentunella vaginata	●			●	
Melanocyrillium sp.	●	●	●	●	●
Myxococcoides cantabrigiensis	●			●	
Octoedryxium intrarium	●	●			
Octoedryxium truncatum			●		
Paleasphaeridium zonale	●	●			
Polyedrosphaeridium sp.	●				
Rectia costata	●		●		
Satka compacta	●	●		?	?
Simia annulare	●	●	●		
Sinianella uniplicata	●	●	?		
Sphaerocongregus variabilis	●	●	●	●	●
Sphaerophycus sp.	●			●	
Tasmanites rifejicus		?			●
Trachyhystrichosphaera aimica	●		●		
Trachyhystrichosphaera stricta	●		●		
Trachyhystrichosphaera vidalii	●		●	●	?
*Trachysphaeridium laufeldi**					●
Valeria lophostriata	●		●		●
*Vandalosphaeridium pusillum***		●			
Vandalosphaeridium reticulatum	●				
Vandalosphaeridium walcottii					●

Figure 22. Distribution of selected acritarchs in Australia and other known localities

DME_SA 93-1892

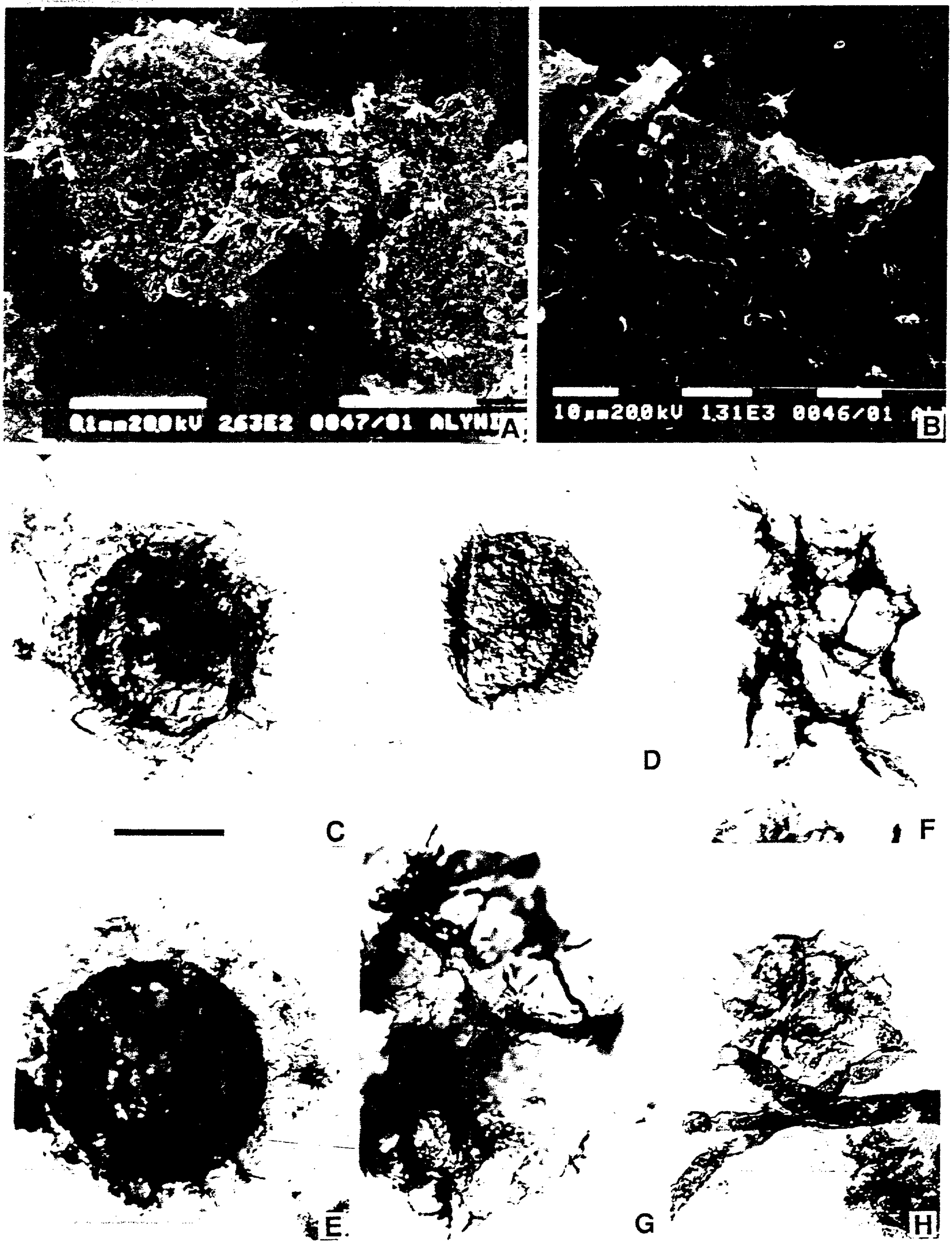

Figure 23

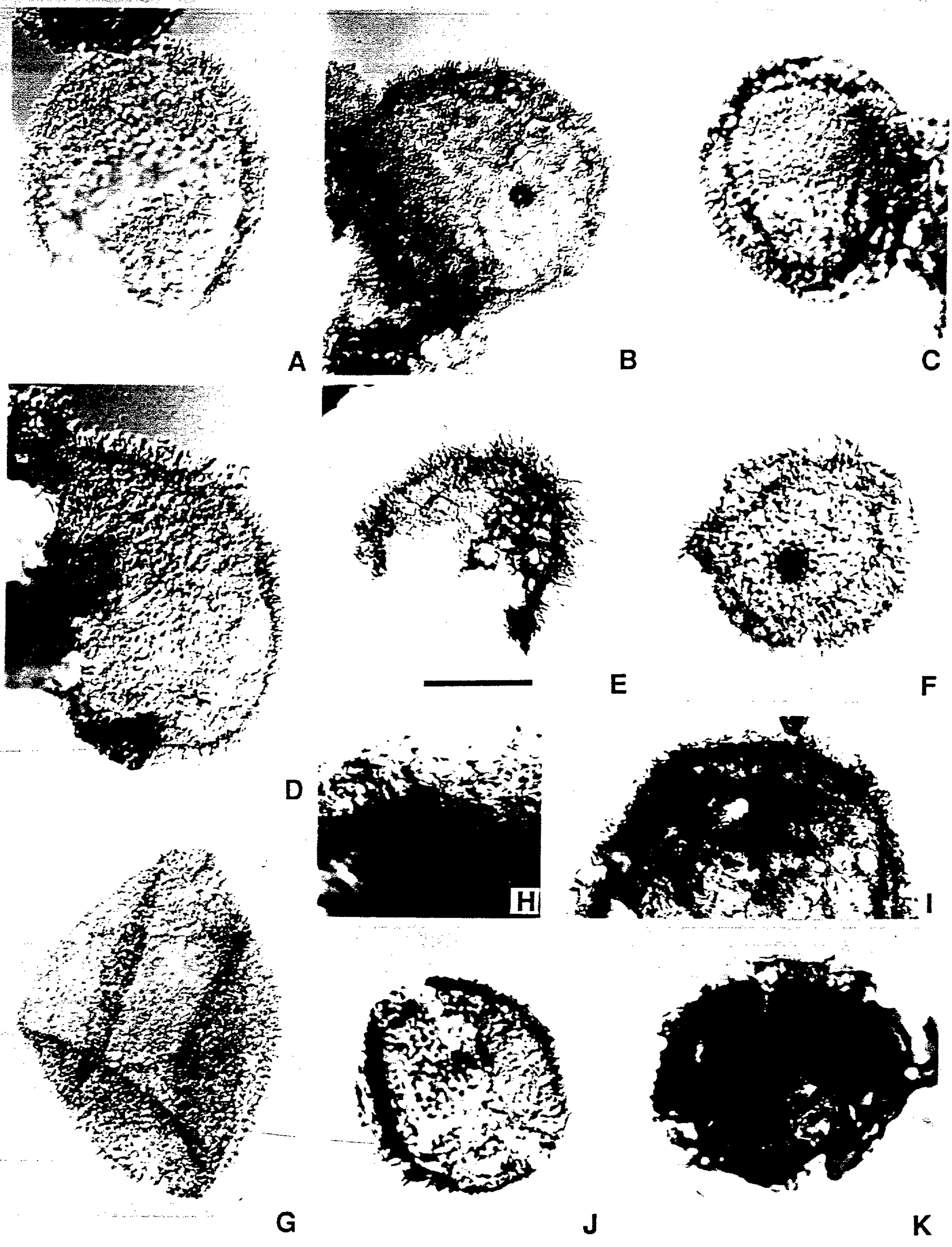

Figure 24

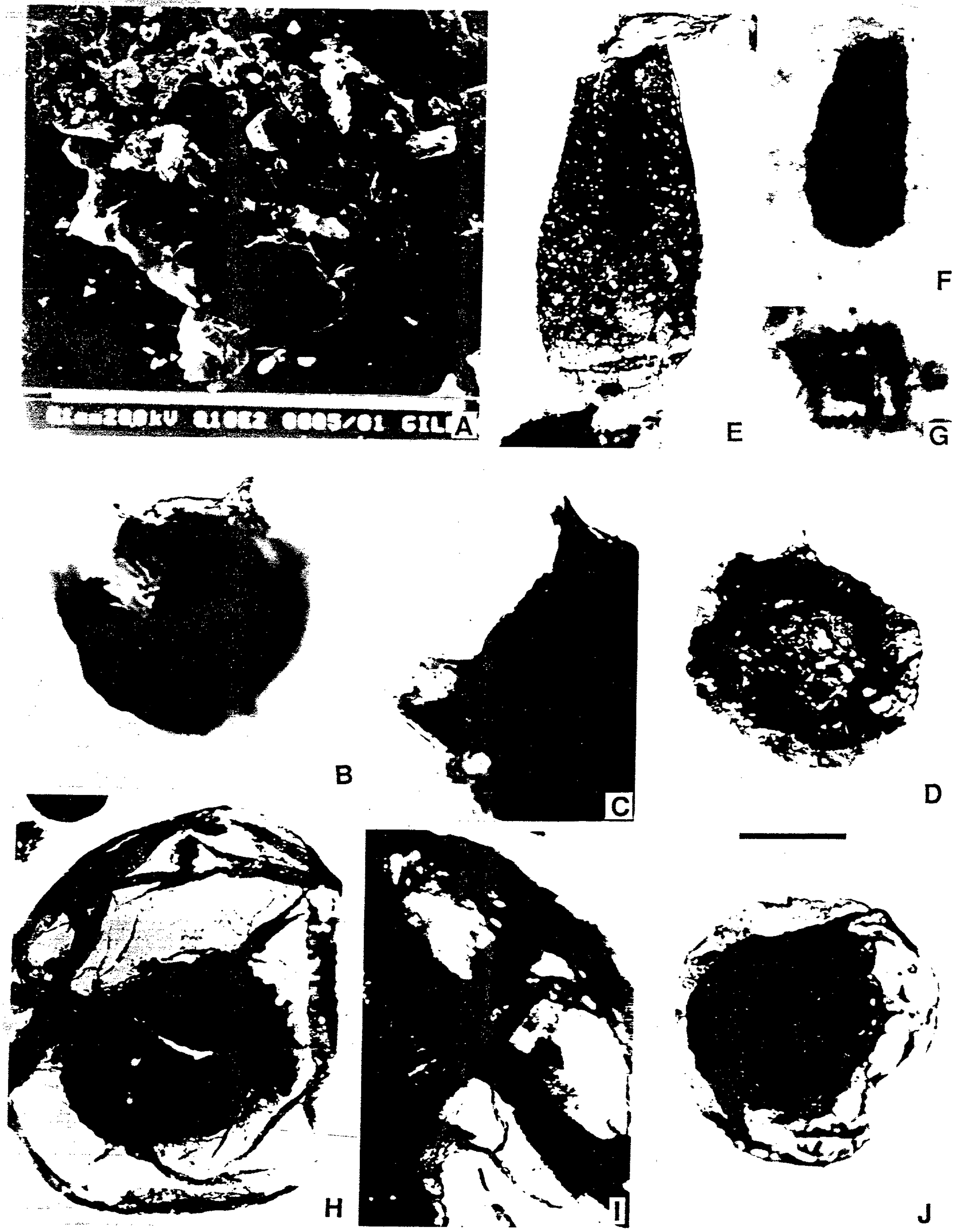

Figure 25

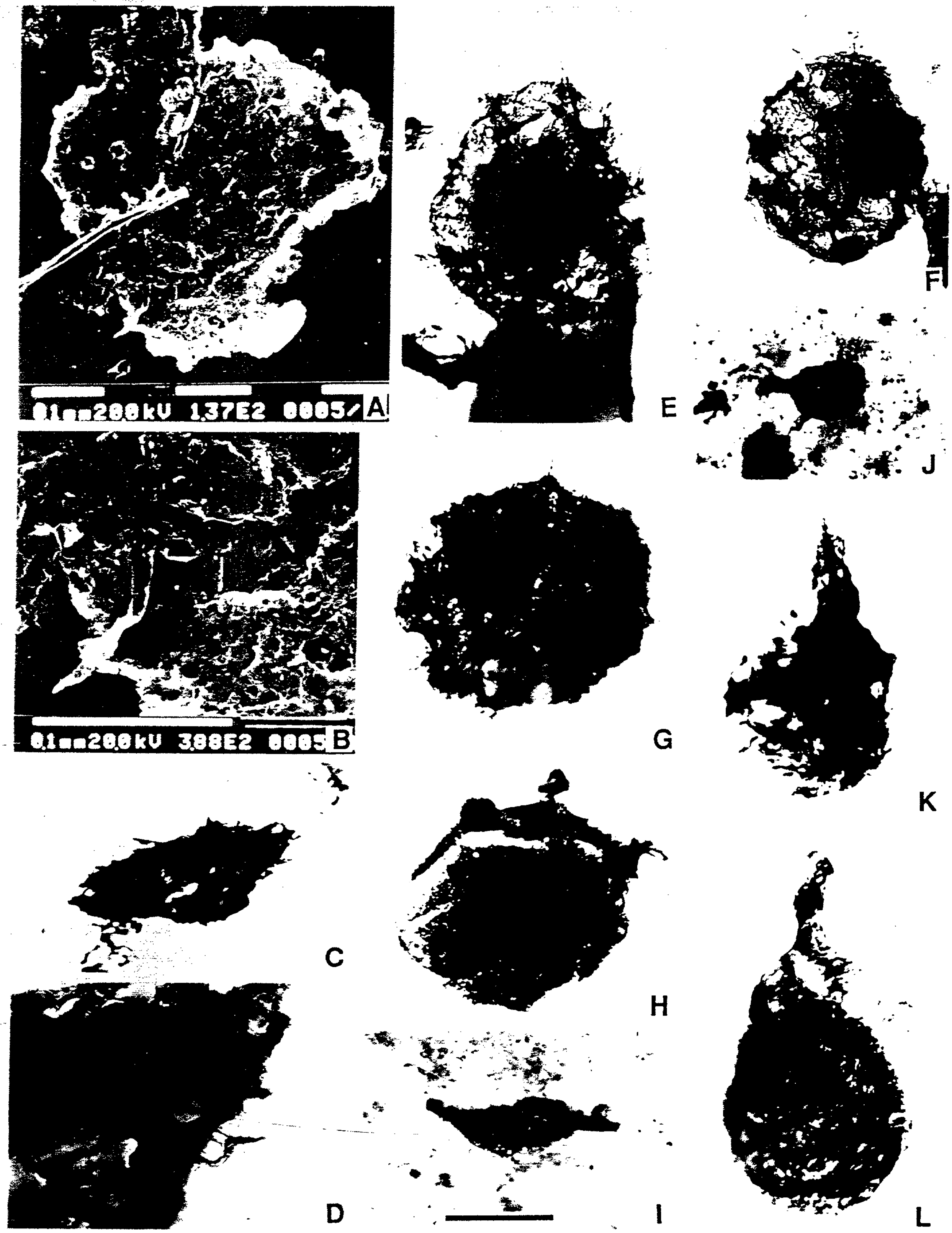

Figure 26

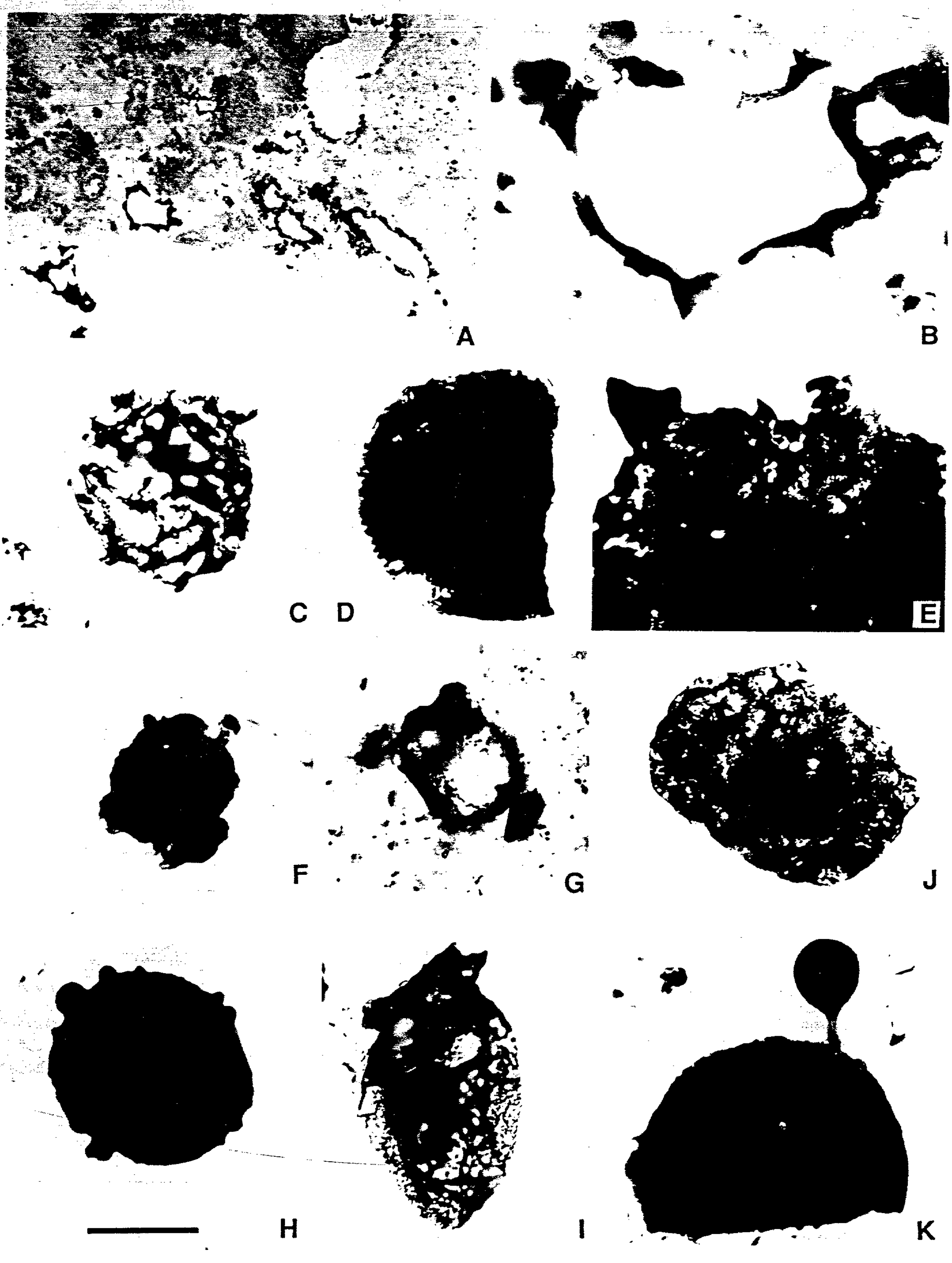

Figure 27

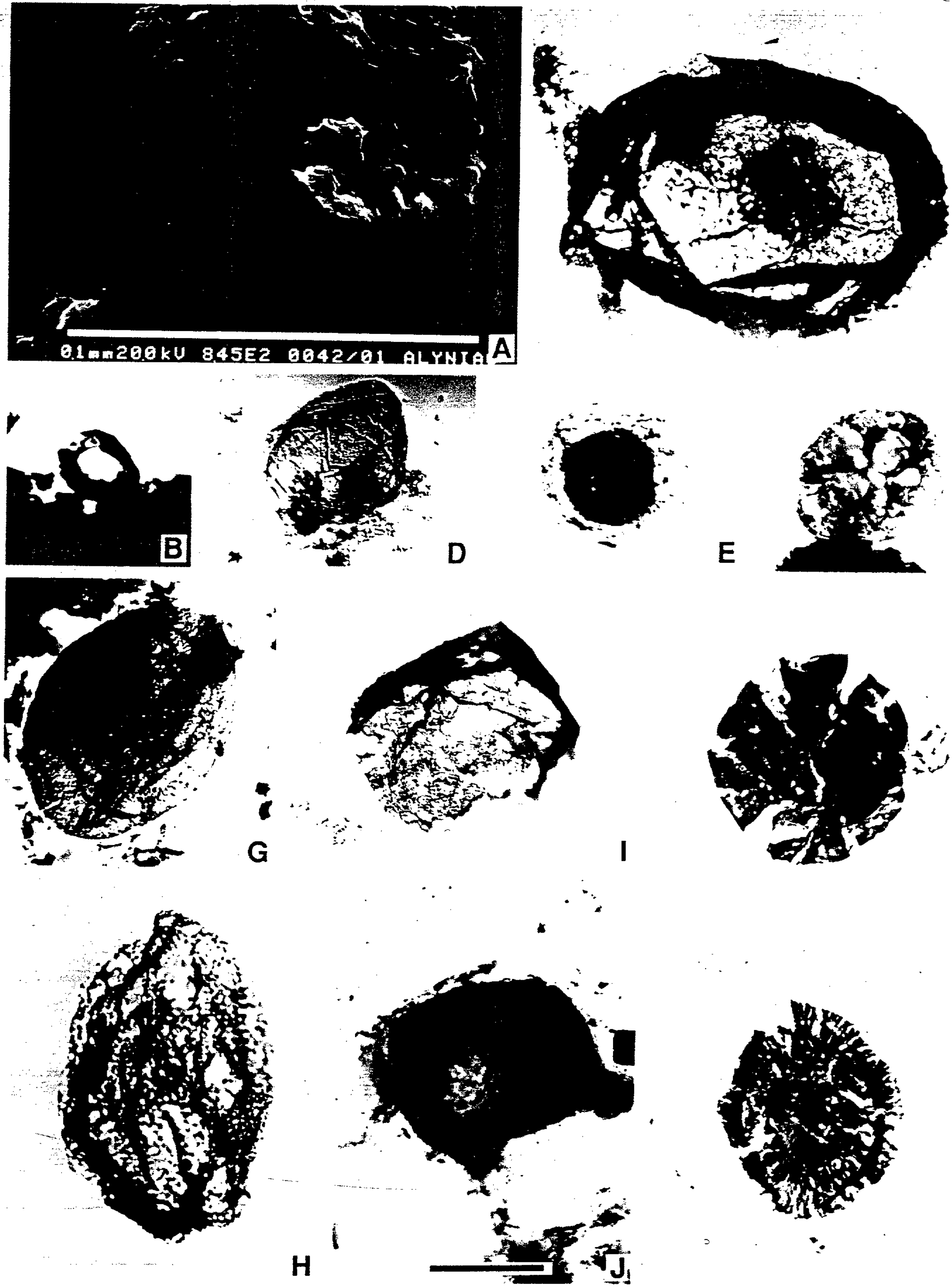

Figure 28

Figure 29

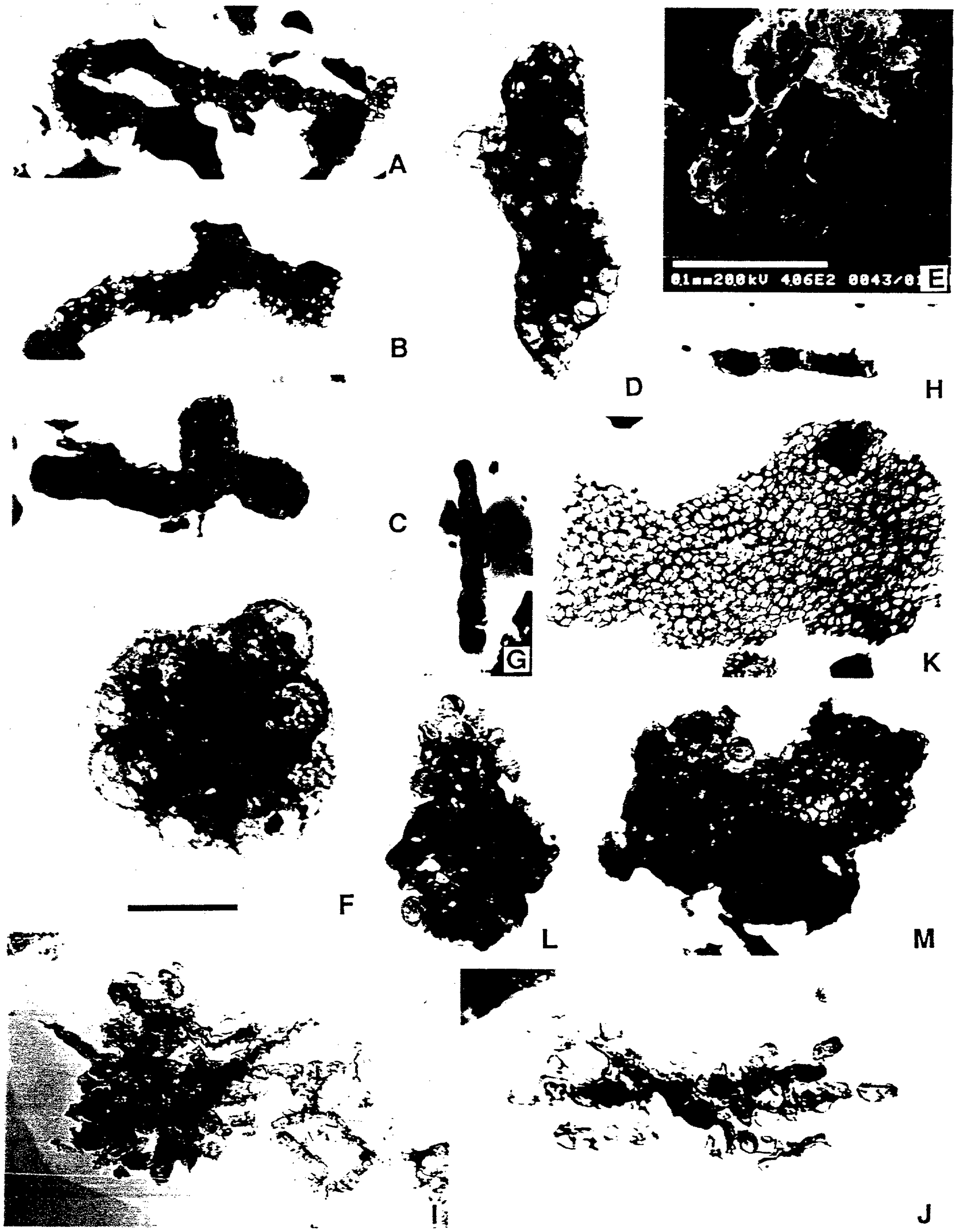

Figure 30

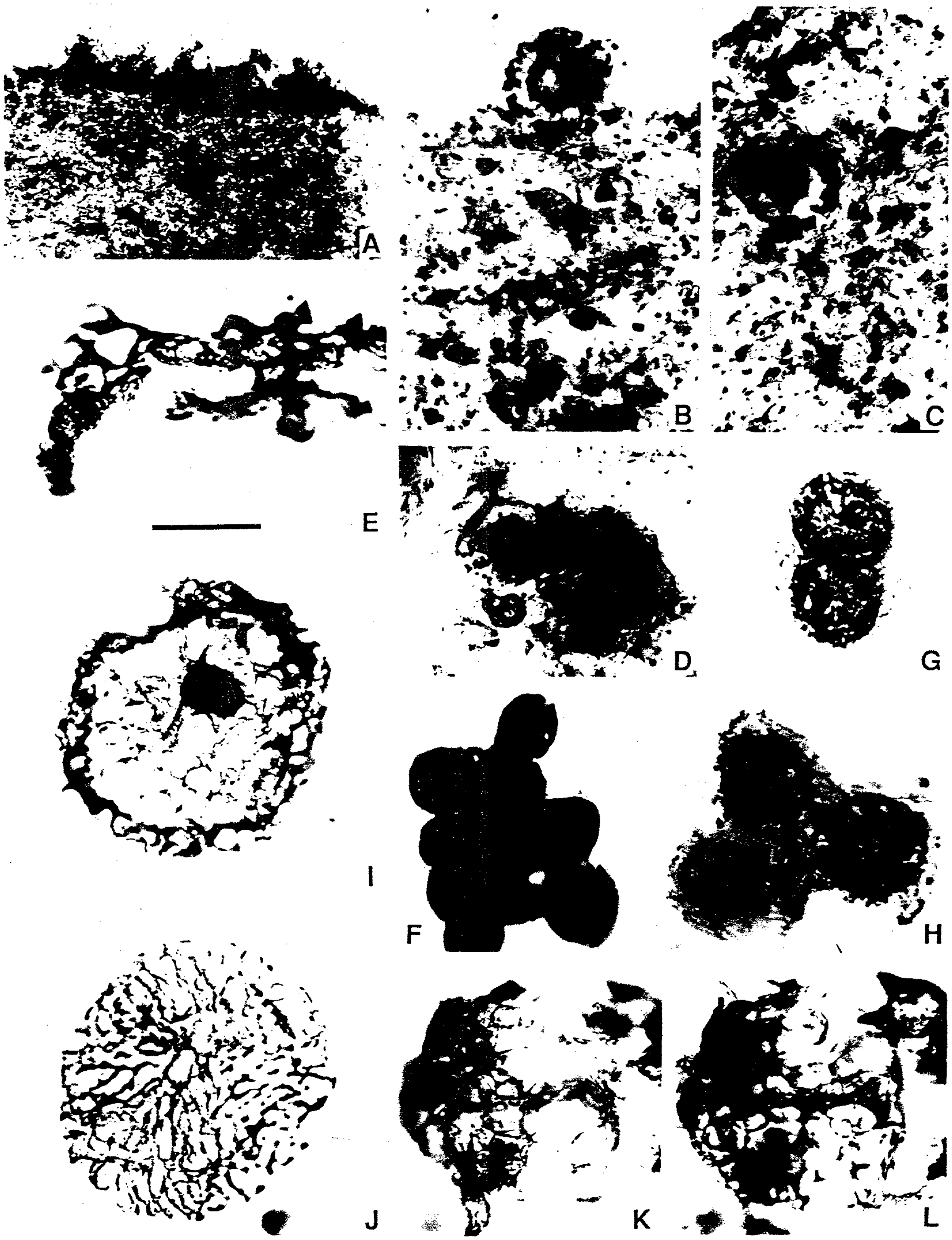

Figure 31

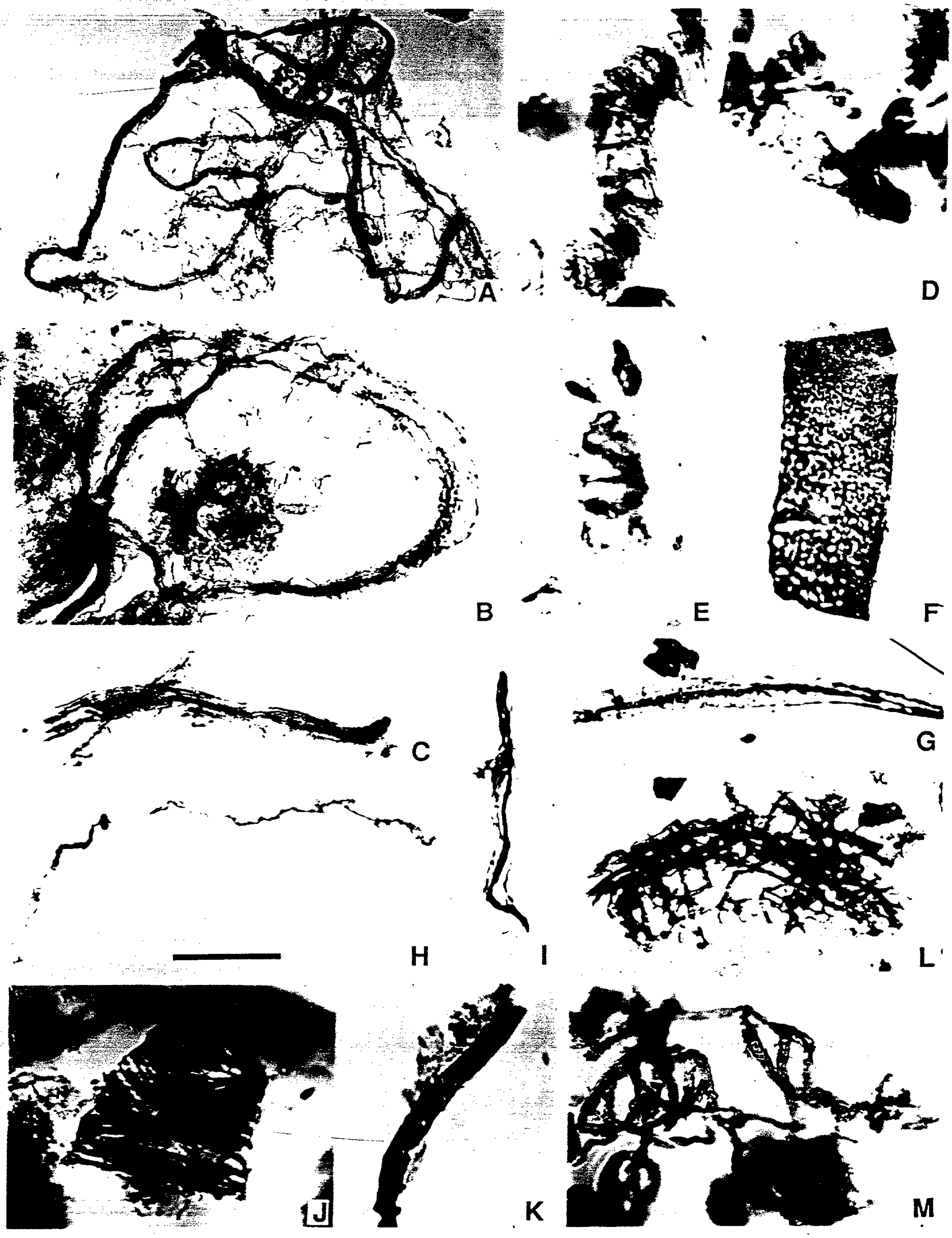

Figure 32

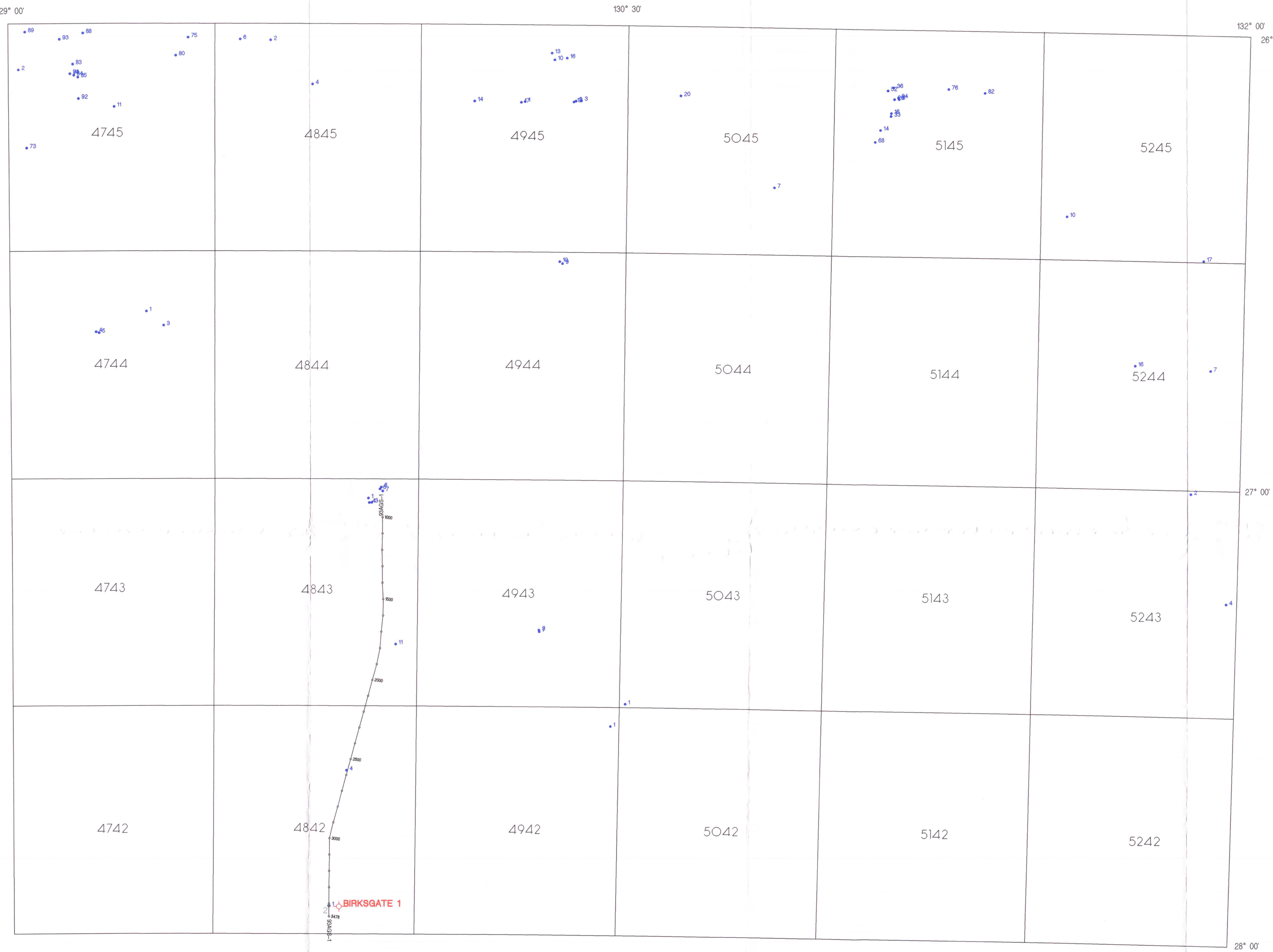

LOCALITY

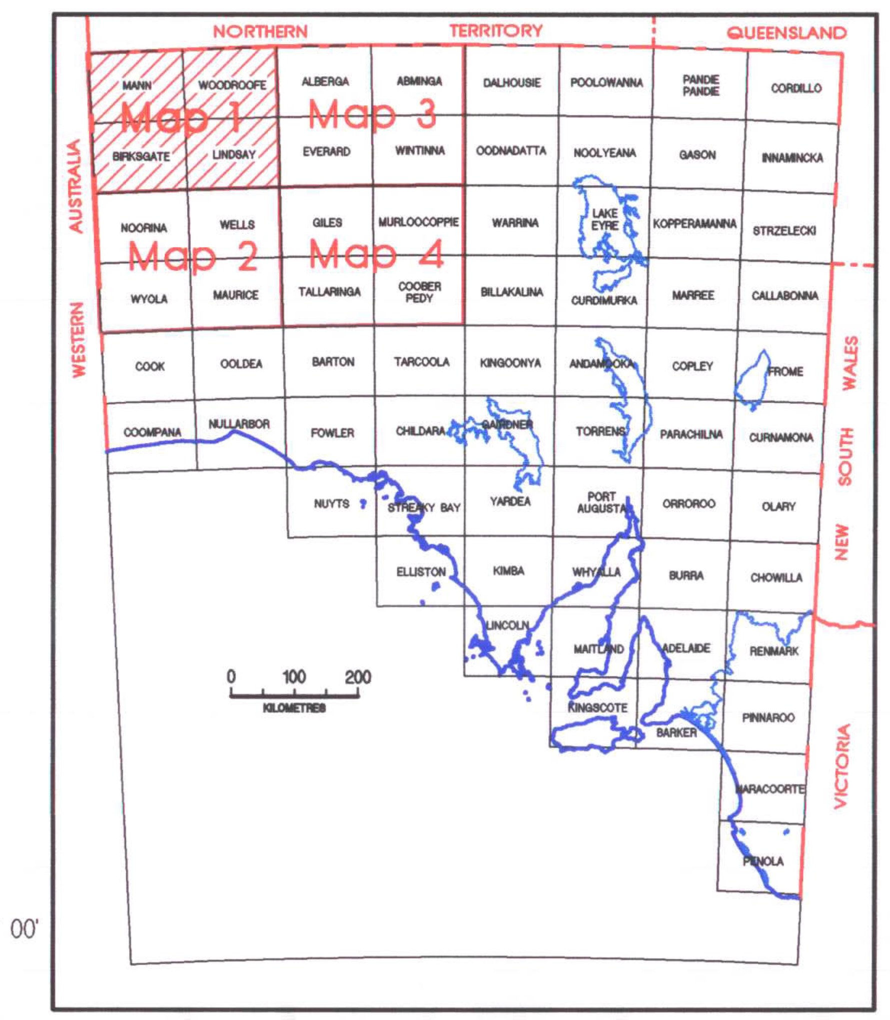

Water well > 40m

Mineral well

MUNTA 1 Petroleum well

Stratigraphic well

NOTE
Prefix well numbers with 1:100 000 sheet number to obtain full unique number

Seismic line

8591-19

0 50 100
KILOMETRES

MINES and ENERGY RESOURCES SOUTH AUSTRALIA

Enclosure 1A

OFFICER BASIN - Map 1, AMG Zone 52

SEISMIC LINES & WELL LOCATIONS

MESA 94-821

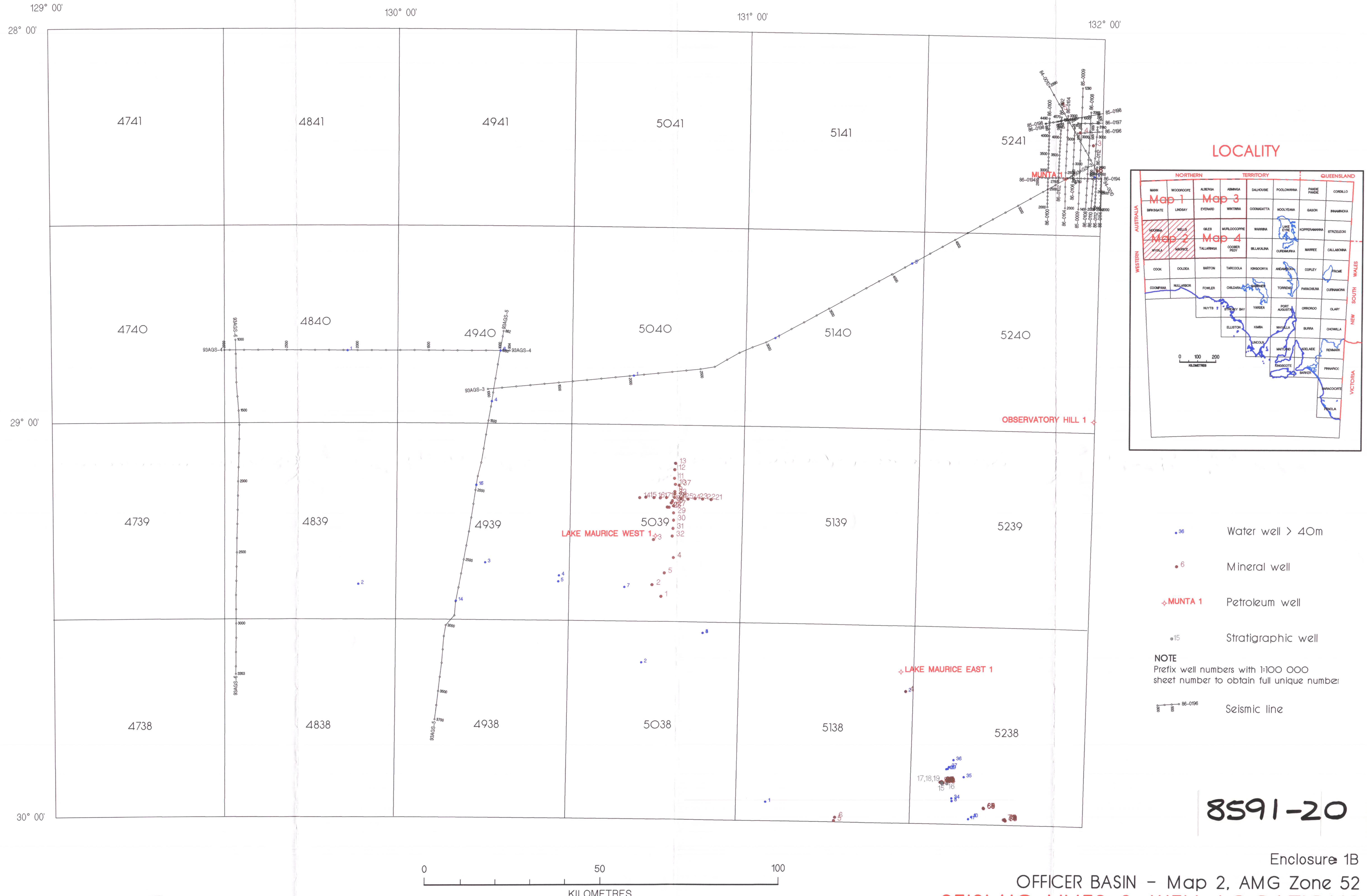

Enclosure 1B

OFFICER BASIN - Map 2, AMG Zone 52

SEISMIC LINES & WELL LOCATIONS

MESA 94-822

MINES and ENERGY RESOURCES SOUTH AUSTRALIA

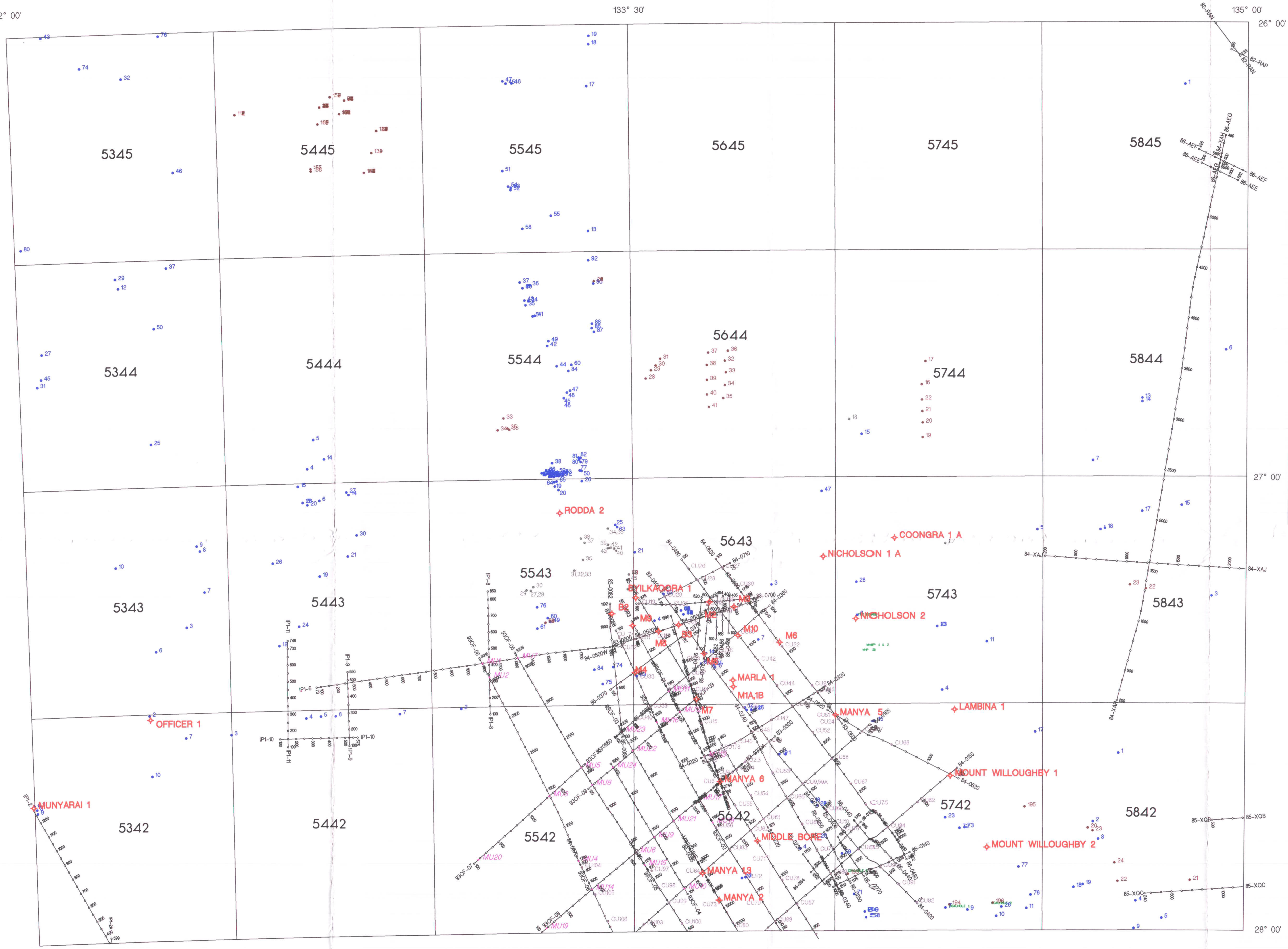

LOCALITY

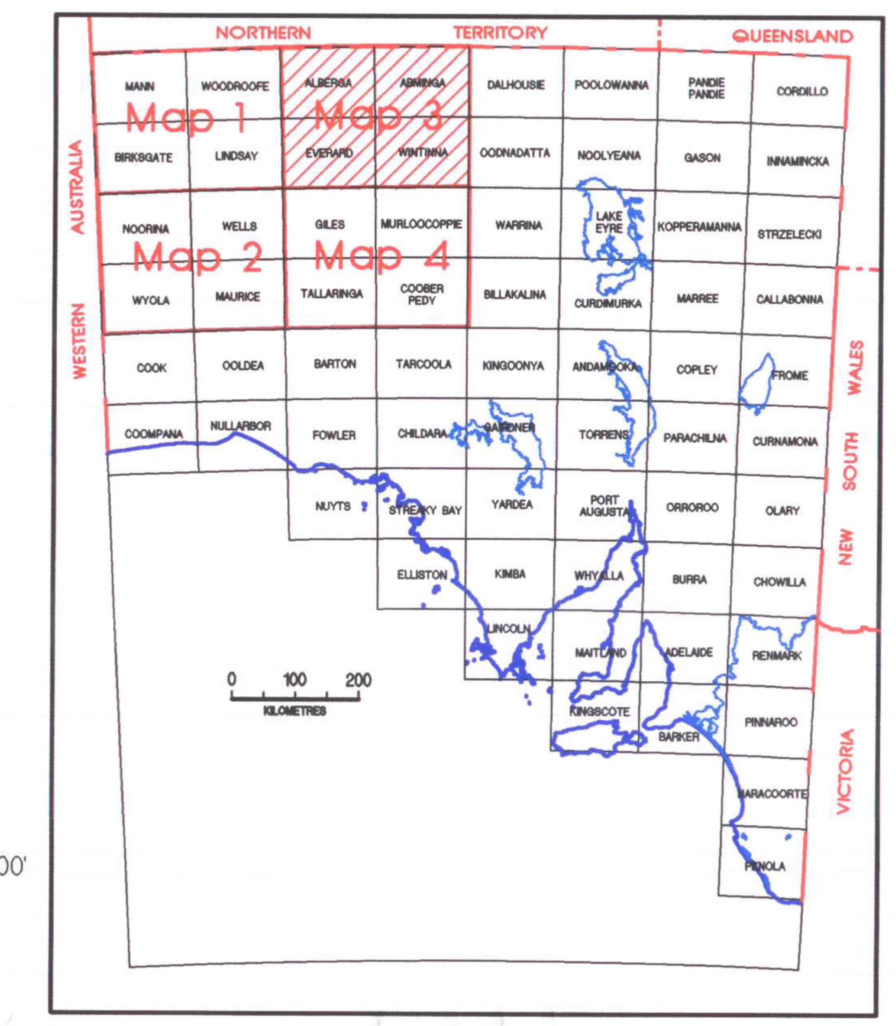

MU20 MESA uphole

CU22 Comalco uphole

3 Water well > 40m

6 Mineral well

MUNTA 1 Petroleum well

15 Stratigraphic well

NOTE
Prefix well numbers with 1:100 000 sheet number to obtain full unique number

86-0196 Seismic line

8591-21

0 50 100
KILOMETRES

Enclosure 1C

OFFICER BASIN – Map 3, AMG Zone 53

SEISMIC LINES & WELL LOCATIONS

MESA 94-823

MINES and ENERGY RESOURCES SOUTH AUSTRALIA

QD-DORA 60790G.DTA PLAN2-52

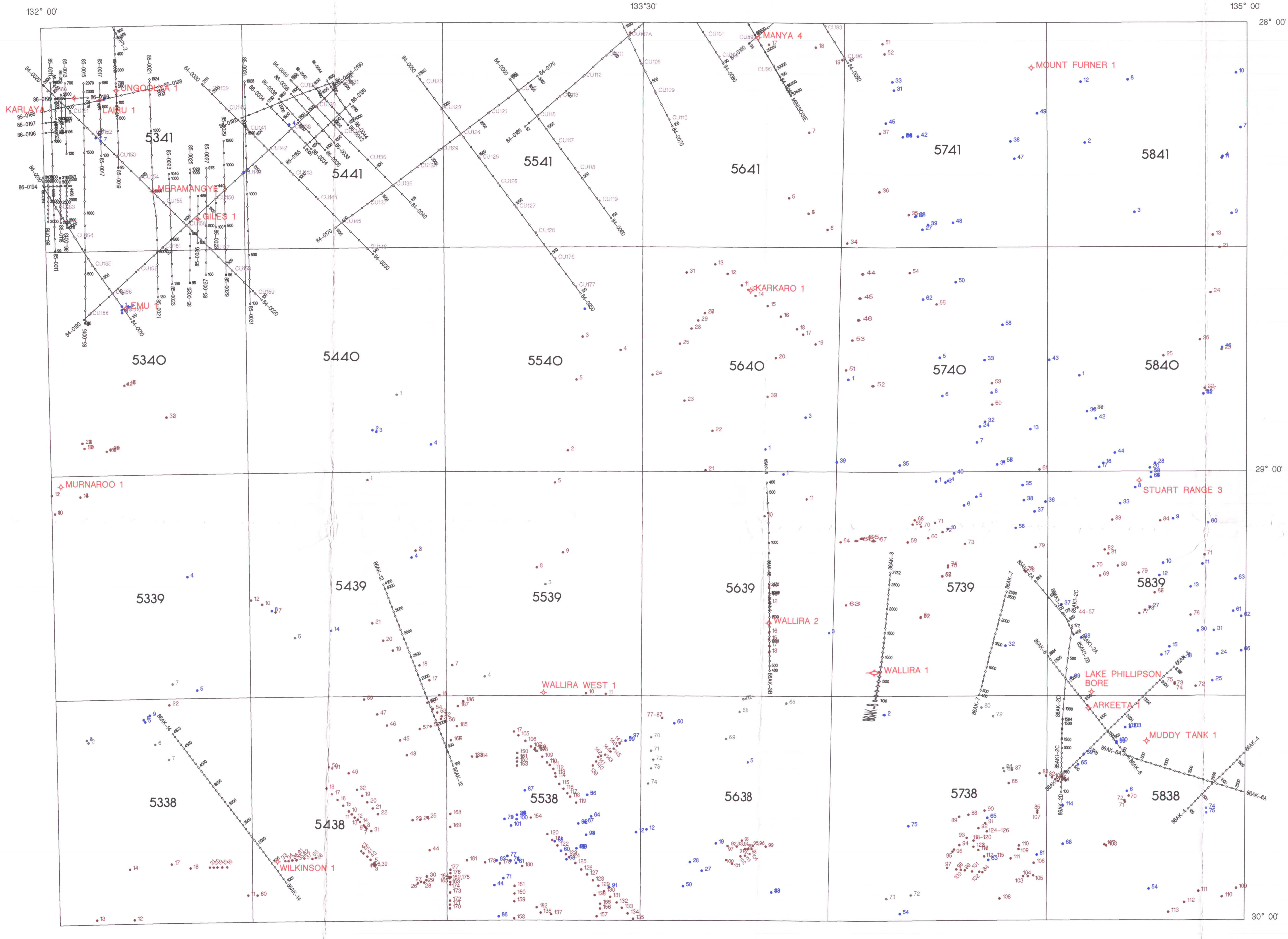

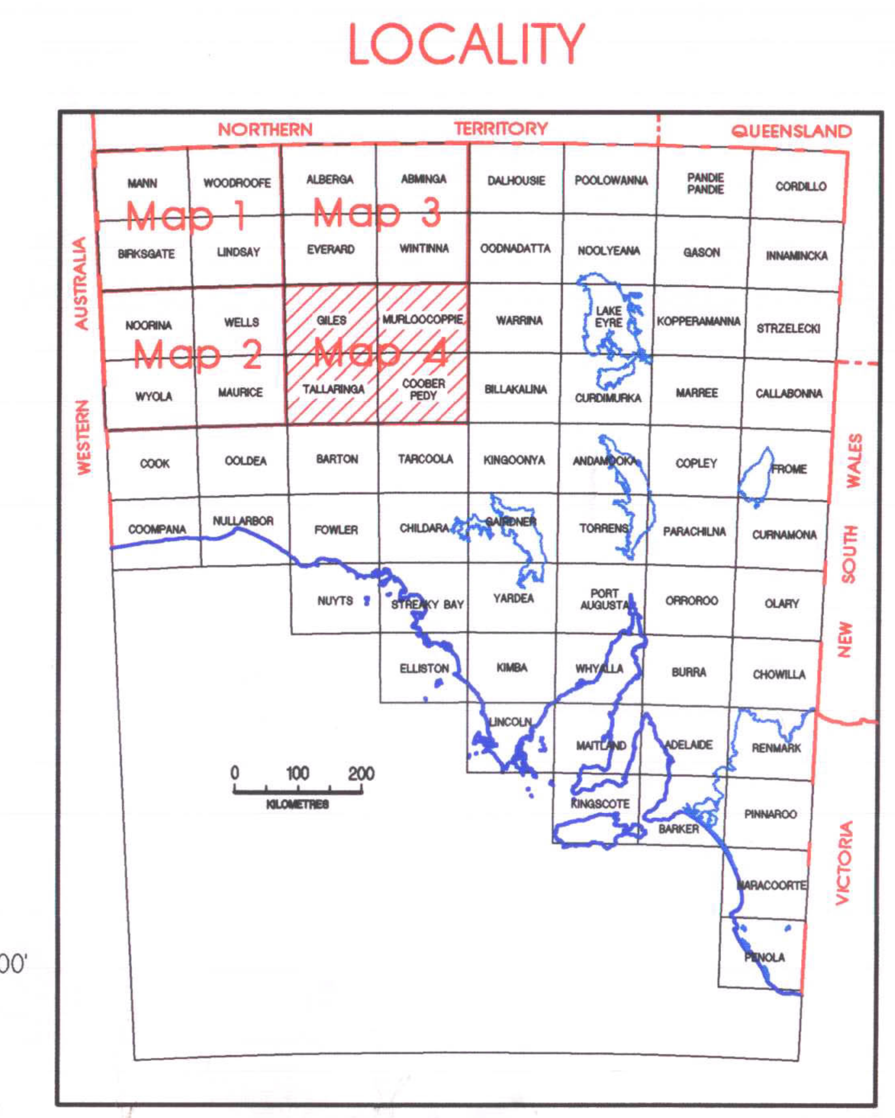

CU22 Comalco uphole

3 Water well > 40m

6 Mineral well

MUNTA 1 Petroleum well

15 Stratigraphic well

NOTE
Prefix well numbers with 1:100 000 sheet number to obtain full unique number

86-0196 Seismic line

0 50 100
KILOMETRES

8591-22

Enclosure 1D

OFFICER BASIN - Map 4, AMG Zone 53

SEISMIC LINES & WELL LOCATIONS

MESA 94-824

MINES and ENERGY RESOURCES SOUTH AUSTRALIA

QD-DOBA 6078DG.DTA PLAN2-53